Water Main Failure Prediction by Integration of Statistical Data and Physical Processes

By

LI CHUEN CHIK

A Thesis
Submitted in Fulfilment of the Requirements for the
Degree of Doctor of Philosophy

Department of Civil Engineering
Monash University
Melbourne, Australia

February 2018

ABSTRACT

The ageing and the change in operating conditions (e.g. higher water pressure) of water mains in the water distribution network have led to the increase in unplanned interruptions in recent years. These interruptions can reduce the service level of the network, disrupt the community (e.g. traffic delays) and have economic consequences (e.g. flooding damage). Pipe failure prediction models have been developed to assist water utilities in managing their network. They can be broadly classified as physical models and statistical models. The Phd aims to develop a framework that integrates the physical modelling approach with statistical failure data. The integrated approach may combine the advantage of the two modelling methods and assist the rehabilitation (including replacement) of water mains.

The Bayesian Simple Model (BSM) was first developed and compared with the Non-homogenous Poisson process (NHPP) and Hierarchical Beta Process (HBP). It was found that the BSM and HBP can be used to identify water mains that are more likely to fail in the short-term future. The NHPP is suitable for long-term rehabilitation planning as it captures the average deterioration of the water main over time.

The NHPP was studied in further detail to consider the time dependent factor, the minimum monthly antecedent precipitation index (MMAPI) with time-lag. The performance of the model reduces as the length of time-lag in the MMAPI increases. However, the model with a 1-month and 2-month time-lag can still predict the number of monthly failures with reasonable accuracy. This allows water utilities to arrange their resources to satisfy the demand for repairs ahead of time.

The number of known past failures (NOKPF) was also studied using the NHPP for failure prediction. The NOKPF is unknown in the future as it is pipe and time dependent. The expected number of failures in the future is simulated on the basis of the Poisson process and used to update the NOKPF each year. Based on the dataset studied, the NHPP without the NOKPF may under-predict the failures in the long-term future as the reduction in time to failure is not captured in the model (without the NOKPF).

After examining some of the current statistical modelling approaches, a framework was developed to integrate the physical model with statistical failure data for pipe failure prediction in cast iron pipes subjected to longitudinal split and broken back failures. The Monash Pipe Failure Prediction (MPP) model first estimates the condition of the pipe using a physical model. The result is compared with the failure data to update the corrosion parameters. Further adjustments are applied to the corrosion parameters to account for failure clustering that may be present. For longitudinal failures, the number of failures predicted by the MPP model matches well with the failure data, and its ranking performance is also comparable to the BSM and NHPP. The current framework of the MPP model performs poorly for broken back failures and requires further developments. This may involve refining

the updating of the corrosion parameters to account for the uncertainty during the updating process.

Finally, the NHPP and MPP models were both applied in water main rehabilitation. Although it is impossible to consider all future scenarios, several scenarios (e.g. no intervention) based on suggestions from the asset manager was considered to estimate the level of investment required to maintain the service level of the network. The results from these analyses can provide valuable insights for budget estimation and water renewal planning, which are being used in the next water plan of the water utility.

DECLARATION

This thesis describes my research carried out in the Department of Civil Engineering at Monash University in Australia during the candidature period from February 2014 to February 2018. The thesis is submitted to Monash University in total fulfilment of the requirements for the degree of Doctor of Philosophy.

The thesis contains no material which has been accepted for the award of any other degree or diploma in any university or institution and no material which has been previously written or published by another person except where due reference is made in the text of the thesis.

[redacted]

Li Chuen Chik,

February 2018

LIST OF PUBLICATIONS

Rathnayaka, S., Keller, R., Kodikara, J. and Chik, L. 2016. "Numerical Simulation of Pressure Transients in Water Supply Networks as Applicable to Critical Water Pipe Asset Management". *Journal of Water Resources Planning and Management,* 142**,** 04016006, doi: 10.1061/(ASCE)WR.1943-5452.0000636.

Chik, L., Albrecht, D., and Kodikara, J. 2017. "Estimation of the Short-Term Probability of Failure in Water Mains." *Journal of Water Resources Planning and Management*, 143(2), 10.1061/(ASCE)WR.1943-5452.0000730. (Chapter 3)

Chik, L., Albrecht, D., and Kodikara, J. 2018. "Modeling Failures in Water Mains Using the Minimum Monthly Antecedent Precipitation Index." *Journal of Water Resources Planning and Management,* 144(2)**,** 10.1061/(ASCE)WR.1943-5452.0000926. (Chapter 4)

ACKNOWLEDGEMENTS

I would like to express my sincerest gratitude to my main supervisor, Professor Jayantha Kodikara, and co-supervisor, Dr David Albrecht. They provided me with valuable support, guidance, suggestions, and encouragements throughout this PhD journey. Furthermore, I would like to thank our admin staffs, team members, and colleagues for the help and support that they have given me.

I wish to thank my family for their love that accompanied me during my PhD study. I would also like to give special gratitude to my wife, Zhen Lin. Her support, encouragement, and care throughout this journey was invaluable.

Finally, I would also wish to express my special appreciation to South East Water for giving me the opportunity to take part in their Water Plan, providing me with practical experience from the industry closely related to my research that cannot be gained elsewhere.

This research was supported by an Australian Government Research Training Program (RTP) Scholarship.

TABLE OF CONTENTS

LIST OF FIGURES

LIST OF TABLES

ABBREVIATIONS

AC	Asbestos Cement
ANN	Artificial Neural Network
API	Antecedent Precipitation Index
BB	Broken Back
BSM	Bayesian Simple Model
CI	Cast Iron
CI3	Number of Customers with 3 or more unplanned interruptions
CICL	Cement Lined Cast Iron
Conc	Concrete
CU	Copper
DI	Ductile Iron
HBP	Hierarchical Beta Process
LR	Log-likelihood Ratio
LS	Longitudinal Split
NHPP	Non-homogeneous Poisson Process
MAE	Mean Absolute Error
MCMC	Monte Carlo Markov Chain
MMAPI	Minimum Monthly Antecedent Precipitation Index
MPP	Monash Pipe Failure Prediction
MS	Mild Steel
NOKPF	Number of Known Past Failures
PCI	Pit Cast Iron
PE	Polyethylene
PVC	Polyvinyl Chloride

RMSE	Root Mean Squared Error
ROC	Receiver Operating Characteristic
SCF	Stress Concentration Factor
SCI	Spun Cast Iron
WDN	Water Distribution Network
WI	Wrought Iron

CHAPTER 1: INTRODUCTION

1.1. Background

Water mains in the water distribution network (WDN) transport fresh water from reservoirs into local households and businesses. In the United States, an annual maintenance cost of $29 billion is required to maintain about 2 million km of water mains that are valued over $2.1 trillion. By comparison, the total value of water mains is approximately A$71.1 billion in Australia. It was estimated that more than A$1.4 billion was spent to maintain 163,000km of water mains in 2012 (Bureau of Infrastructure, Transport and Regional Economics, 2014).

In metropolitan Melbourne, the WDN is managed by four water utilities. One of them is a distributor that supplies water to the other three retailers, which delivers water to customers in their network area. The distributor looks after the source of the water (e.g. reservoirs), while the retailers ensure that the demands from their customers are satisfied with minimal interruptions. However, since the age for part of the WDN in Melbourne is more than 100 years old (e.g. cast iron (CI) pipes), a significant portion of water mains in the network is approaching or have passed their original design life, leading to an increase in unplanned interruptions and impacting on the level of service to customers. In addition, the severity of recent climate events, such as the millennium drought in Australia, and the rapid growth of the populations imposes further threats to the structural integrity of the water mains. Therefore, it is crucial that water utilities managing the WDN can estimate the condition and maintain the performance of the growing network with their limited resources.

1.2. Modelling Condition of Water Mains

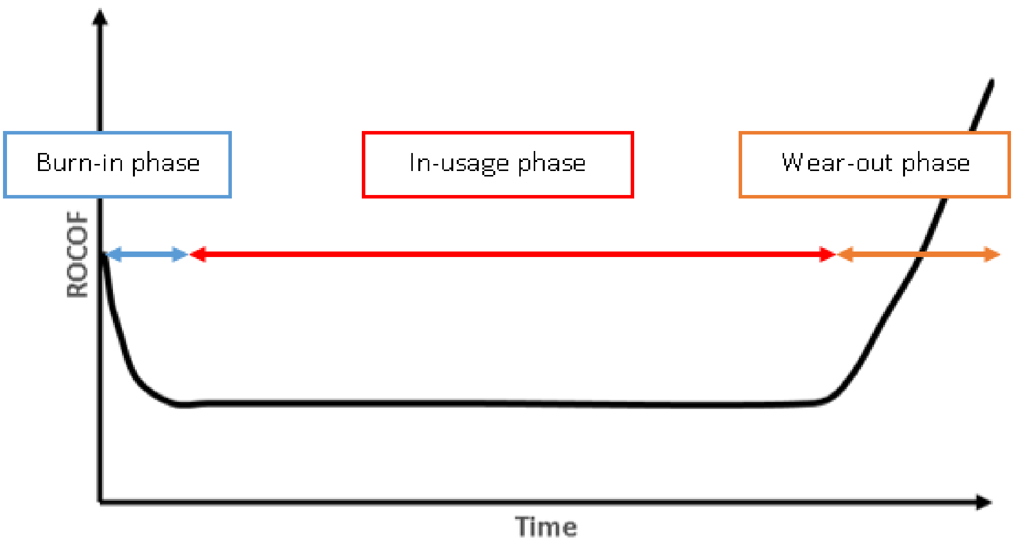

Figure 1-1: Rate of occurrence of failure for the water main.

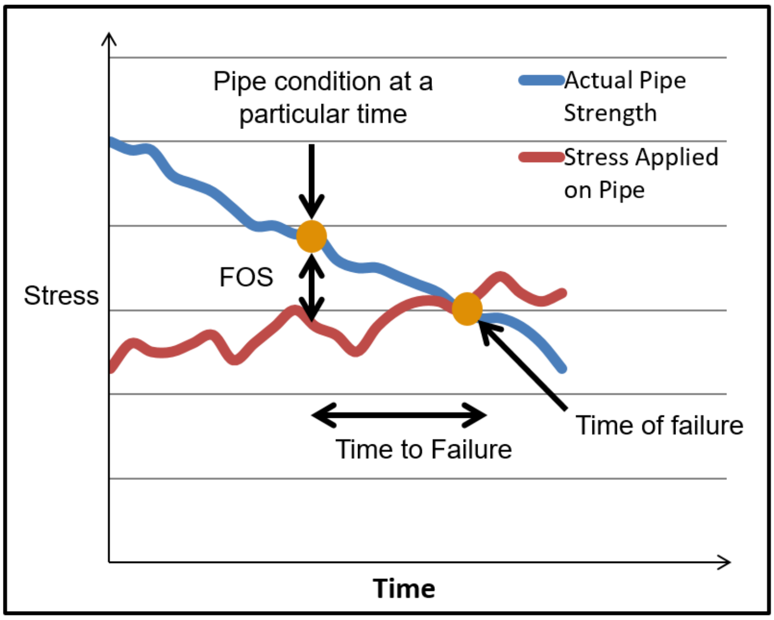

Figure 1-2: The strength of the water main, and the stress applied over time (shown deterministically).

Models have been developed by researchers to estimate and predict the condition of water mains. The condition of the pipe over its service life can be characterised using a bathtub curve (Figure 1-1). The curve describes the rate of occurrence of failure for the pipe under three phases. The first phase is called the "burn-in" phase and failures in the pipeline are mainly due to poor manufacturing or construction work. The pipeline then moves into the second "in-usage" phase, where the frequency of failure is low and will remain at this rate for most of its life. The final phase is the "wear-out" phase, the failure frequency of the pipeline increases rapidly due to the degradation of the pipe (Kleiner and Rajani, 2001).

Failure prediction models can be broadly classified into physically based models and statistically based models. The physical models consider the physical deteriorating process of the pipe material and the stress from the surrounding environments. Figure 1-2 demonstrates the degradation and the variation in stress experienced by the pipe in service. The strength of the pipe decreases over time as a result of degradation (e.g. corrosion for metallic pipes). The stress experienced by the pipe can fluctuate as the customer demands and surrounding environments change over time. The water main will fail once the applied stress is higher than the strength of the pipe (Time of Failure in Figure 1-2). The physical model will try to estimate the current condition of the pipe and the rate of deterioration to predict the time of failure. However, these types of models are very complex, and the input parameters are usually obtained through condition assessments that can be very costly if applied to the entire WDN.

Statistical models rely heavily on the availability of recorded failure data from the WDN. The failure history is used to calibrate the model to identify the general relationship between the input variables (e.g. pipe length and pipe age) and pipe burst events. After learning from the failure data, the models can be used to estimate and predict the condition of the water main (e.g. failure probability or expected number of failures) by assuming that the patterns identified in the failure data will continue into the future (Kleiner and Rajani, 2001).

The two types of models can be used for different purposes. Physical models can provide a detailed analysis of the condition of each pipe. They are suitable for analysing large diameter pipes (pipe diameter≥300mm) that adopt a proactive replacement approach (replace before failure) due to the high failure consequence associated with the failure events. Statistical models are preferred to assess the average condition of a group of reticulation pipes in the network. They represent the majority of the WDN, but the consequences of failure are much lower with respect to large diameter pipes. Therefore, a reactive approach is usually taken (replace after a certain number of failures). The predictions from the statistical models can be combined with a consequence model and used for operational, tactical and strategic planning.

1.3. Objective and Scope of Research

This research aims to develop a pipe failure prediction model for the WDN based on the physical deterioration process of the pipe (physical model approach) and utilise the failure history that has been collected by the water utility (statistical model approach). It tries to merge together the benefit of the two approaches and provides a more accurate pipe failure prediction model that can assist the rehabilitation (including replacement) of water mains. The objectives of this thesis are to:

- Review pipe failure prediction models and water main rehabilitation models that have been developed.
- Investigate statistical models that are currently used and identify possible improvements.
- Develop a framework that can integrate statistical failure data with the physical deterioration process of the pipe for failure prediction.
- Demonstrate the pipe failure prediction models developed in the thesis by applying them in rehabilitation planning.

1.4. Thesis Outline

The outline of the thesis is as follows:

- Chapter 2: An in-depth review of the literature to identify research gaps in pipe failure predictions.
- Chapter 3: The newly developed Bayesian Simple Model (BSM) for ranking pipes in the WDN will be introduced. The BSM will be compared with statistical models from the literature review (Non-homogeneous Poisson Process (NHPP) and Hierarchical Beta Process (HBP)). The results of the comparison, its implications and limitation will be discussed.

- Chapter 4: The NHPP is modified to incorporate time dependent covariates and pipe and time dependent covariates. The performance of the models with different covariates set up is investigated, and the results are discussed.
- Chapter 5: The chapter will discuss the development of the framework for integrating the physical deterioration of the pipe with failure data. The performance of the models with different initial conditions is compared with the NHPP and BSM.
- Chapter 6: This chapter will apply the failure prediction models discuss in the previous chapters for renewal planning. Several different renewal scenarios will be compared, and part of this work has been used in the development of the water plan for a water utility.
- Chapter 7: Provides a summary of the project. The strengths and weaknesses of the models that have been compared are discussed, along with recommendations for future research in the area.

CHAPTER 2: LITERATURE REVIEW

2.1. Introduction

This chapter will present a detailed review on some of the physical and statistical models that have been used to model pipe failures. The first section will cover physical models for pipe materials that are in the WDN. This is followed by a review of different statistical methods that have been developed to model water main failures. Finally, rehabilitation (including replacement) models for water main renewal planning are also discussed to provide a complete picture in the usage of the pipe failure prediction models.

2.2. Physical Models

Physical models estimate pipe failure by modelling the deterioration process of the pipe and the stress generated from the external and internal environments. The physical probabilistic model introduces uncertainty into the input parameters of the physical model. One or more of the physical input parameters (e.g. deterioration rate) are represented using a probability distribution instead of a fixed value. The resulting probability of failure is usually estimated using a Monte-Carlo simulation method (Mooney, 1997).

In a Monte-Carlo simulation, the random variables are assigned with a probability distribution (e.g. Weibull distribution). In each iteration of the simulation, a random number is drawn from the distribution using methods such as the inverse transformation method and the acceptance-rejection method (Mooney, 1997). The number drawn is used to estimate the output of the model (e.g. applied stress) and to determine whether the failure criterion is satisfied.

The following section will discuss some of the physical models and physical probabilistic models that have been used to model pipe failure in various materials.

2.2.1 Cast Iron Pipes

CI pipes are among the oldest pipes in the WDN in Australia. Rajani and Makar (2000) investigated the remaining service life of grey CI pipes under both axial and hoop stress using one or multiple corrosion measurements. The failure criterion of CI pipes for longitudinal failures was based on the work of Schlick (1940) (Equation (2-1)). The CI pipe will operate without failure under internal pressure and external three-edge ring load if the following equations are satisfied:

$$\left(\frac{w}{W}\right)^2 + \left(\frac{p}{P}\right) \leq 1$$

(2-1)

$$W = \frac{\pi h^2 \sigma_r}{3(D+h)}$$

(2-2)

$$P = \frac{2h\sigma_t}{D}$$

(2-3)

where w is the applied external load; p is the applied internal pressure; W is the external load that will cause the pipe to fail without any internal pressure; P is the internal pressure that will cause the pipe to fail in the absence of external load; h is the pipe wall thickness; D is the internal pipe diameter; σ_r is the rupture modulus; and σ_t is the tensile strength of the pipe. Rajani and Makar (2000) amended the failure criterion (Equation (2-1)) to include the effect of corrosion-pits in CI pipes and stresses induced from thermal effects and frost loads. A circumferential failure criterion was also included to incorporate circumferential failures in the model. Let σ_x and σ_t be the axial stress and the tensile strength, respectively, the failure criterion for circumferential failure can be expressed as:

$$\frac{\sigma_x}{\sigma_t} \leq 1$$

(2-4)

The study proposed two methods for estimating the remaining life of the CI pipe. A one-time corrosion-pit measurement and a multiple-time corrosion-pit measurement. The one-time corrosion-pit measurement can provide a rough estimate of the growth rate in the corrosion-pit. The multiple-time corrosion-pit measurement will give the actual growth rate of the corrosion-pit by comparing the characteristic of the pit between the first and second measurement. The growth rate of the corrosion-pit can be coupled with a corrosion model to predict the time the safety factor of the pipe falls below the desired level.

Rajani and Tesfamariam (2004) developed a physical model for pipe-soil interaction using the Winkler model for partially supported water mains. The study attempted to determine the response of the axial stress, flexural stress and hoop stress from the influence of soil elastoplasticity and length of pipe without soil support (e.g. loss of soil under the pipe due to leakage) under external loading, internal water pressure, frost loads and thermal effects. The sensitivity analysis indicated that an increase in the length of the pipe without soil support increased the flexural stress but not the axial stress. The effect of soil elastoplasticity was minor in both cases and can be ignored in practical situations.

Seica and Packer, (2006) conducted section analysis to estimate the strength of CI pipes subjected to bending in the longitudinal direction and uniform corrosion. Using non-linear analysis, the stress in the pipe was expressed as a function of strain in terms of a four parameter, double exponential function. The study found that the non-linear section analysis was capable of estimating the failure load for pipes with no or uniform corrosion. However, the method tends to overestimate the failure load for pipes that have localised corrosion pits.

Fahimi et al. (2016) evaluated the residual strength of CI water mains by combining the loss-of-section analysis with failure mechanic theory. The study developed a combined failure envelope for vertical loads and internal water pressure using the loss-of-section analysis (assuming uniform corrosion) and failure mechanics theory. The failure envelop showed a reduction in strength capacity as the corrosion depth increases on the pipe's outer surface. The loss-of-section failure envelop was the critical failure envelop in the absence of internal water pressure (only vertical load). It was the dominant failure envelop when the depth of corrosion was less than 10% of the pipe wall thickness. On the other hand, the failure envelop based on fracture mechanics theory was the critical failure envelop if only internal water pressure (without vertical load) was present. It was also the dominant failure envelop after the corrosion depth exceeds 30% of the total wall thickness.

Sadiq et al. (2004) performed a probabilistic risk analysis (without considering consequence) for CI water pipes subjected to corrosion. The depth of the corrosion-pit was assumed to grow exponentially at the start, followed by a slow linear phase. The study calculated the failure probability for both longitudinal and circumferential failures. The probability of failure was determined by finding the probability that the factor of safety (FOS) will be less than 1. Let σ_y be the residual tensile strength of the pipe; σ_x is the axial stress and σ_θ is the hoop stress. The FOS is given as:

$$FOS = \min\left(\frac{\sigma_y}{\sigma_x}, \frac{\sigma_y}{\sigma_\theta}\right)$$

(2-5)

The input parameters for the physical model were described using probability distributions. Monte Carlo simulation was used to estimate the failure probability of the pipe. The uncertainty in the FOS was found to be approximately log-normal, and the sensitivity analysis showed that the parameters in the corrosion model were the main contributors to the variation in the time to failure of a pipe.

Davis et al. (2004) developed a physical probabilistic model to estimate the failure probability of a CI pipe using corrosion rate information retrieved from condition assessments. The failure criterion has been shown in Equation (2-1). P and W were calculated as shown in Equation (2-6) and (2-7), respectively.

$$P = \frac{2\sigma_t h_0}{D}$$

(2-6)

$$W = \frac{1048\sigma_y h_0^2}{D}$$

(2-7)

$$\sigma_y = \sigma_t - 120\left(\frac{Age * \delta}{h_0}\right)$$

(2-8)

where h_0 is the initial pipe wall thickness and δ is the maximum corrosion rate of the pipe. Definitions for the other parameters are the same as those in Equation (2-1), (2-2) and (2-3)

The study fitted a Weibull distribution to the collected corrosion rate data. Then Monte Carlo simulation was used to estimate the failure probability of the pipes. The result of the simulation was found to be well represented by another Weibull distribution.

In addition to the stochastic corrosion rates in Davis et al. (2004), Moglia et al. (2008) made further exploration by introducing uncertainty into other physical parameters. The study was able to achieve a reasonable match between the failure rates estimated from the physical probabilistic model and the observed failure data after exploring various assumptions. The assumptions included stochastic corrosion rate, stochastic loads, stochastic pipe thickness, a reduction in the lower limit of the pipe tensile strength, stochastic pressure surge and truncation of the stochastic corrosion rate. Introducing uncertainty into the pressure surge was found to provide the most significant improvement to the physical probabilistic model.

Tesfamariam et al. (2006) and Rajani and Tesfamariam (2007) built upon their previous work (Rajani and Tesfamariam, 2004) by considering a possibilistic approach to account for the uncertainties in estimating the structural capacity of CI pipes and time to failure of CI pipes, respectively. The stresses in both studies comprised the external load, internal pressure, temperature differential, and longitudinal bending. Uncertainty in the input parameters was modelled using fuzzy set theory, and the failure criterion was based on the biaxial distortion energy failure criterion.

Sensitivity analysis conducted by Tesfamariam et al. (2006) showed that the pipe factor of safety decreased as the depth of the corrosion pit, length of pipe without soil support, and the stress applied on the pipe (e.g. frost load) increased. On the other hand, the factor of safety increased as the input parameters related to the structural capacity of the pipe increased (e.g. fracture toughness). Factors such as the modulus of elasticity of the soil, internal pressure, and transient pressure were found to have little influence on the factor of safety.

Rajani and Tesfamariam (2007) investigated the change in the factor of safety with the growth of the corrosion pit and the increase in unsupported bedding length. They then conducted a sensitivity analysis with all the input parameters. The analysis suggests that the long-term performance of CI pipe is mainly determined by the corrosion rate, unsupported bedding length, fracture toughness, and temperature differential on the basis of the model they assumed to apply to field scenarios.

Rajani and Abdel-Akher (2012) used Monte Carlo simulation to examine the influences of uncertainties in the input parameters for the factor of safety. They considered a large diameter pipe (48”) and a small diameter pipe (16”) under two load cases. In load case 1, the pipe was subjected to earth loads, internal water pressure, and transient pressure. In load case 2, the pipe was subjected to traffic load, earth load, and internal water pressure. Without any corrosion, both pipes were found to have a very low probability of failure. Under the uniform corrosion, load case 2 was found to be the critical load case when a significant amount of the pipe wall has been uniformly corroded. In terms of the effect of corrosion pits on the safety factor of the pipe, the study found that a combination of corrosion pits and uniform corrosion on the external surface of the pipe were required to reduce the factor of safety drastically.

Li and Mahmoodian (2013) modelled the failure probability of CI pipes subjected to hoop stress with internal and external corrosion on the pipe wall. The corrosion of the internal and external surface of the pipe was modelled using the power law model. The probability of pipe failure was defined on the basis of fracture mechanics using the following limit state function:

$$g(t) = K_c - K(t) \tag{2-9}$$

where K_c is the critical stress intensity factor; $K(t)$ is the time dependent stress intensity factor of the pipe. The pipe is at its limit state when $g(t) = 0$, a failure is observed if $g(t) < 0$, while the pipe is safe if $g(t) > 0$.

The study found that external corrosion was more likely to cause a pipe to fail compared to internal corrosion, and pipes with a higher fracture toughness had a lower failure probability. Pipes with a larger diameter were estimated with a higher failure probability due to the higher hoop stress in larger pipes.

Ji et al. (2015) estimated the time dependent failure probability of large diameter CI pipes with a circular corrosion patch. The maximum stress of a uniformly corroded pipe was calculated using a closed form expression developed by Robert et al. (2016). A bi-linear corrosion model based on the work of Petersen and Melchers (2012) was used in the study to estimate the depth of the localised corrosion-pit. The study developed an equation to estimate the stress concentration factor (SCF) for circular corrosion patch in a large diameter pipe by fitting a non-linear regression model to results from finite element models.

To account for the variability of the physical input parameters, Ji et al. (2015) introduced uncertainty into the model by assuming a probability distribution for each physical parameter. The limit state function was specified as:

$$g(\boldsymbol{x}, t) = \sigma_t - \sigma(\boldsymbol{x}, t) \tag{2-10}$$

where σ_t is the pipe tensile strength and $\sigma(\boldsymbol{x}, t)$ is the time dependent stress acting on the pipe. The pipe is at its limit state when $g(\boldsymbol{x}, t) = 0$, a failure is observed if $g(\boldsymbol{x}, t) < 0$, while the pipe is safe if $g(\boldsymbol{x}, t) > 0$.

The pipe failure probabilities were computed in two steps. A first-order reliability method was first used to locate the design point for the Monte Carlo simulation. Then the failure probability around the design point was assessed by Monte Carlo simulation. The expected failure probability from the simulation was fitted with a three-parameter Weibull distribution. A sensitivity analysis conducted on the physical parameters found that the influence of pipe geometry was most significant for young pipes. On the other hand, the pipe tensile strength, static water pressure, and the corrosion behaviour of the pipe become more significant as the age of the pipe increases over time.

2.2.2 Other Metallic Pipes

Ahammed and Melchers (1995) and Ahammed and Melchers (1997) evaluated the contribution of various parameters to pipe failure for uncoated steel pipes subjected to pitting corrosion. The limit state function for the two studies was expressed using leakage and distortion energy theory, respectively. Ahammed (1998) conducted a similar study on pressured steel pipe subjected to longitudinally oriented surface corrosion. The limit state function was expressed in terms of pipe failure pressure and the pressure applied to the pipe. The studies found that the corrosion rate was the main contributing factor to pipe failures in old pipes.

De Silva et al. (2002) estimated the failure probability of mild steel pipes by modelling the corrosion rate using condition assessment data. Ten condition assessments were conducted on four sections of a pipe laid in two different soils. A Weibull distribution was fitted to test samples in each soil type to model the maximum corrosion rate. The estimated parameters for the Weibull distributions were extrapolated to describe the corrosion rates in the pipe. They were then used to estimate the pipe failure probability using Level II First-Order-Second-Moment reliability techniques.

2.2.3 Asbestos Cement Pipes

Davis et al. (2008) explored the optimal time of inspection and replacement for asbestos cement (AC) pipes. The AC pipe samples were tested to determine the residual strength of the pipe. A Weibull distribution was fitted to the test results to model the uncertainty of the degradation rate in AC pipes. Monte Carlo simulation was used with the failure criterion shown in Equation (2-1) to estimate the expected time to failure of AC pipes.

2.2.4 Plastic Pipes

Davis et al. (2008) used measured crazed strength to predict the time to failure of Polyethylene (PE) pipes under combined pressure and deflection load. They followed the work of Duan and Williams (1998) and extended it to PE pipes buried underground under in-service loading conditions. The predictions from the simplified approach provided a good match to the test results. However, the study also identified possible improvements that can be made to the model.

Davis et al. (2007) developed a physical probabilistic model for buried polyvinyl chloride (PVC) pipes subjected to brittle and ductile failure. The defect sizes from the failures in un-plasticised polyvinyl chloride pipes were fitted to a Weibull distribution to establish the initial maximum defect size in the PVC pipes for Monte Carlo simulation.

2.3. Statistical Models

Statistical model uses failure data to identify a general relationship between influential variables (e.g. pipe length and pipe age) and pipe failure events. The combination of factors used in the models can vary significantly between datasets due to the variations in the surrounding environment and operating conditions of the water mains. This section of the literature review will provide an overview on some of the statistical models that have been used for pipe failure prediction.

2.3.1 Regression Models

One of the early work on forecasting the failure rates of the WDN was the time-exponential model proposed by Shamir and Howard (1978). The model assumed the failure rate (failure per unit length) of a pipe (or a group of pipes with similar characteristics) increases exponentially over time. The rate of failure at time t is expressed as:

$$FR(t) = FR(t_0)e^{A(t-t_0)} \tag{2-11}$$

where t is time in years; t_0 is the base year of analysis (installation year or the first year that data are available); $FR(t)$ is the number of breaks per unit length of pipe (failure/length) in year t; and A is the growth rate coefficient.

The model itself is simple and can be easily applied to the WDN. The main limitation of the model is that only pipe age is used in predicting the failure rate. Other significant covariates that influence the breakage rate of the pipe, such as pipe diameter, should also be included in the model if they are available.

The time-exponential model has been used by other researchers with modifications (Walski and Pelliccia, 1982; Kleiner and Rajani, 2000; Kleiner and Rajani, 2002; and Kutylowska, 2015) and without modifications (Kleiner et al., 2001; and Roshani and Filion, 2013). Walski and Pelliccia (1982) added two correction factors to the time-exponential model to account for the effect of past failures and pipe diameter on water main failures. Kleiner and Rajani (2000) and Kleiner and Rajani (2002) generalised the time-exponential model into a multivariate time-exponential model. The model incorporated time-varying operational factors (change in length of pipe with cathodic protection) and environmental factors (change in temperature and soil moisture). The multivariate time-exponential model is expressed as:

$$N\left(\underline{\boldsymbol{\phi}(\boldsymbol{T})}\right) = N\left(\underline{\boldsymbol{\phi}(\boldsymbol{T_0})}\right) e^{\underline{\boldsymbol{\phi}(\boldsymbol{T})\boldsymbol{a}}} \tag{2-12}$$

where $\underline{\boldsymbol{\phi}(\boldsymbol{T})}$ is the vector of time dependent covariates at time t; $N(\underline{\boldsymbol{\phi}(\boldsymbol{T})})$ is the number of breaks due to the covariates in $\underline{\boldsymbol{\phi}(\boldsymbol{T})}$; $\underline{\boldsymbol{a}}$ is the vector of coefficients associated with $\underline{\boldsymbol{\phi}(\boldsymbol{T})}$; and $\underline{\boldsymbol{\phi}(\boldsymbol{T_0})}$ is the vector of the baseline covariates at the reference year t_0.

Other types of regression models have also been explored by researchers. Dandy and Engelhardt (2001); Dandy and Engelhardt (2006); and Shin et al. (2016) used non-linear regression models to predict failures in the WDN for pipe rehabilitation programs. Kettler and Goulter (1985) investigated the effect of pipe age and pipe diameter using a linear regression model. By analysing the failure data in detail, they found that large diameter CI pipes were less likely to fail because of the better structural integrity and joint reliability. Wang et al. (2009) divided the pipe data into five material groups and modelled the log failure rate (base 10) of the pipes in the WDN. A number of independent variables were tested for each material group, including first-order interaction terms.

2.3.2 Survival Models

Survival models estimate the expected time to failure (or death) of an item. The model is generally used for non-repairable systems. However, WDNs are repairable systems, and the failure of a pipe will often lead to a repair job until it is no longer economical or practical to repair the pipe.

Andreou et al. (1987a) and Andreou et al. (1987b) applied the proportional hazard model developed by Cox (1972) to predict failures in the WDN. They divided the water mains into the early stage of deterioration and the late stage of deterioration based on their preliminary statistical analysis using the failure data. In the early stage of deterioration, the time to failure was considered to be quite long. Therefore, they model the probability of failure using the proportional hazard model. The hazard function takes the following form:

$$h(t) = h_0(t)e^{\underline{\boldsymbol{z}}\underline{\boldsymbol{A}}}$$

(2-13)

where $h(t)$ is the hazard function of the water main at time t; h_0 is the baseline hazard function; $\underline{\boldsymbol{z}}$ is a vector of covariates; and $\underline{\boldsymbol{A}}$ is the vector of coefficients corresponding to $\underline{\boldsymbol{z}}$. The baseline hazard function was estimated using the non-parametric regression model.

In the fast-breaking stage, the authors estimated the expected break rate using the Poisson regression model. The model can be expressed as:

$$P(x) = \frac{(\mu t)e^{-\mu t}}{x!} \quad x = 0,1,2 \dots$$

(2-14)

$$\mu = e^{\underline{\boldsymbol{z}}\underline{\boldsymbol{A}}} + error$$

(2-15)

where $P(x)$ is the probability of having x failures; t is the length of the time period; and μ is mean of the Poisson distribution.

Many independent variables were analysed to uncover the most suitable covariates for the datasets. It was found that the internal water pressure, land development (possible surrogate for external loads), pipe age at the time of the second break, installation period, number of previous breaks, corrosive soil, and the length of pipe to be the most significant variables.

Park (2011) and Park et al. (2011) followed a similar approach to Andreou et al. (1987a,b). They constructed multiple hazard functions to represent the different deterioration rate of water mains depending on the number of past failures. Li and Haimes (1992) used a semi-Markov process to model the deterioration of water mains. The transition probabilities were estimated utilising the work of Andreou et al. (1987a,b). Pipes with less than three failures were modelled using the proportional hazard model, while pipes with three or more failures were modelled using the Poisson distribution. The steady-state probabilities were calculated and used to optimise the system by finding the optimal action at each state.

Røstum (2000) explored both the Weibull proportional hazard model (or accelerated lifetime model) and the Non-homogeneous Poisson Process (NHPP) (discuss in Section 2.3.5). The author stratified the dataset depending on the number of previous failures a pipe has experienced in the failure data. When a failure occurs, the pipe moves to the next stratum and follows a new hazard function. It will stay in the stratum until another failure occurs or till the pipe is censored. The baseline hazard function of the Weibull proportional hazard model ($h_0(t)$) is specified as:

$$h_0(t) = \lambda\kappa(\lambda t)^{\kappa-1}$$

(2-16)

where λ ($\delta > 0$) is the scale parameter and κ ($\kappa > 0$) is the shape parameter.

The proportional representation of the hazard function ($h(t)$) and the survival function ($S(t)$) are:

$$h(t) = \lambda\kappa(\lambda t)^{\kappa-1}e^{\underline{\boldsymbol{zA}}}$$

(2-17)

$$S(t) = \exp\left[-(\lambda t)^{\kappa}\, exp\left(\underline{\boldsymbol{zA}}\right)\right]$$

(2-18)

The results of the case study were given based on the accelerated lifetime model. This is a modification of the survival function in Equation (2-18). Let $\alpha = \ln\lambda$, $\gamma = 1/\kappa$ and $\underline{\boldsymbol{A}}^{*} = -\gamma\underline{\boldsymbol{A}}$, the modified equation can be expressed as:

$$S(t) = \exp\left[-t^{\frac{1}{\gamma}}\, exp\left(\frac{\left(-\alpha - \underline{\boldsymbol{zA}}^{*}\right)}{\gamma}\right)\right]$$

(2-19)

Martins et al. (2013) compared the Weibull accelerated lifetime model with the Poisson model and the Linear Extended Yule Process. The study found that the Weibull accelerated lifetime model was the best out of the three. Kimutai et al. (2015) compared the proportional hazard model, Weibull proportional hazard model, and the Poisson model. They recommend that it would be more appropriate to use a combination of models rather than a single model to represent the constantly changing complex WDN. Malm et al. (2012) modelled the residual pipe length in the network using the Hertz distribution, Weibull distribution and a straight-line model. The Hertz distribution and Weibull distribution provided a better fit to the data.

2.3.3 Weibull-Exponential Models

The Weibull-Exponential model is a mixture model for pipe failure prediction. The underlying assumption of the model is that the ageing of the pipe is represented by at least two distinct periods. The early slow breaking stage was represented using the Weibull distribution, while the late fast breaking stage was modelled by the exponential model.

Mailhot et al. (2000) investigated the Weibull-Exponential model by considering different transition time from the Weibull ageing period to the Exponential ageing period. This study found that the Weibull distribution was generally better at modelling the time to the first break. Scheidegger et al. (2013) combined a pipe replacement model with the Weibull-Exponential model to account for the survival selection bias that might be present in the dataset. The study used a simulated dataset to demonstrate the correction for survival selective bias and a real dataset to demonstrate the inclusion of covariates (e.g. construction period) in the model.

The Weibull-Exponential model has been used as the failure prediction model in Dridi et al. (2005) and Dridi et al. (2009). One of the main planning objectives was to improve the overall structural integrity of the WDN by minimising the total cost associated with the WDN. Another pipe rehabilitation study compared 18 different replacement strategies using the Weibull-Exponential model (Scholten et al., 2014). The renewal strategies were coupled with four development scenarios in a multi-criteria decision analysis framework.

2.3.4 Artificial Neural Network

Artificial neural network (ANN) is inspired by the interconnected neurons in the biological system (Mitchell, 1997). The usual set up of the ANN consists of an input layer that feeds the input information to the hidden layer. This information is processed in the hidden layer(s) using transform functions and is then passed to an output layer, which is connected to the outside world. ANN has an extensive range of applications due to its ability in identifying patterns and relationships between a set of input and output variables.

Al-Barqawi and Zayed (2006) constructed an ANN to assess the condition of the water mains in the WDN. A supervised ANN using the back-propagation algorithm was constructed. There were eight, twelve and one neurons in the input layer, hidden layer and output layer, respectively. The authors discovered that there was an inverse relationship between the breakage rate and the condition rating from the ANN. A noticeable difference was also present in the quality of CI pipes manufactured before and after World War II. Geem et al. (2007) also applied the ANN to estimate the condition of the water mains. The ANN consists of thirteen input variables, but the number of neurons in the hidden layer was not specified.

Achim et al. (2007) and Asnaashari and Shahrour (2007) compared the multilayer perceptron back-propagation ANN with other statistical models. They found that the results from the ANNs were generally better than the models they compared. The back-propagation ANN was also applied to other WDNs. Ho et al. (2010) developed a seismic-based ANN using "the number of magnitude 3^+ earthquakes" as an input variable. Bubtiena et al. (2011) modelled the breakage rate of a WDN in the city of Benghazi. Jafar et al. (2010) estimated the number of failures in a WDN and investigated the performance of the ANN under different stratification criteria. Harvey et al. (2014) studied the time to failure for individual pipes in a WDN using the ANN for three different pipe materials. The most influential factor was the number of past failures the pipe has experienced in the past.

Nishiyama and Filion (2014) built a pattern recognition ANN to model pipe failures in a WDN. The model consists of four nodes in the input layer, twenty-five nodes in the hidden layer and two nodes in the output layer. The two output nodes classify the pipes into "pipe break" or "no pipe break". The overall prediction rate was 40.3% when considering the training, validation and testing stage together.

2.3.5 Non-homogeneous Poisson Process

The Poisson process can be used to estimate the expected number of failures in the WDN. In the homogeneous Poisson process, the rate of occurrence of failure (μ) is constant. The probability of having x failures can be estimated using Equation (2-14) and the constant parameter μ can be a function of covariates that influence pipe failures (Asnaashari and Shahrour, 2007 and Martins et al., 2013). The homogeneous Poisson Process can be considered as a special case of the non-homogeneous Poisson process (NHPP). In the NHPP, the rate of occurrence of failure is time dependent ($\mu(t)$) and can reflect the change in the rate of failure over time in the WDN.

Røstum (2000) modelled the failure events in the WDN using the NHPP. The author specified a power law model (or Weibull intensity) for the baseline intensity function and allowed the different covariates to act multiplicatively on it. The general form of the intensity function is:

$$\mu(t) = \delta t^{\delta-1} e^{\underline{\boldsymbol{z}}\underline{\boldsymbol{A}}}$$

(2-20)

where δ ($\delta > 0$) is the shape parameter of the power law model; $\underline{\boldsymbol{z}}$ is a vector of covariates; and $\underline{\boldsymbol{A}}$ is the vector of coefficients corresponding to $\underline{\boldsymbol{z}}$. The coefficients in $\underline{\boldsymbol{A}}$ and δ were estimated using the method of Maximum Likelihood.

The NHPP was able to estimate the total number of failures accurately for each year in the calibration period. The author obtained a r^2 value of 0.86. Røstum (2000) also compared the performance of the NHPP with the Weibull proportional hazard model.

The Weibull proportional hazard model tends to overestimate the number of failures compared to the NHPP. However, the author believed that the performance of the Weibull proportional hazard model will be site specific.

Kleiner and Rajani (2008) applied the NHPP with pipe dependent (pipe diameter and pipe length), time dependent (cumulative rainfall deficit, snapshot rainfall deficit and freezing index), pipe and time dependent (hotspot cathodic protection and previous number of failures) covariates, a group level constant and a pipe level constant. The set-up allowed the covariates to have a different impact on pipes in separate groups. This type of time dependent model was further explored by Rajani et al. (2012) to investigate the relationship between pipe failure rate and temperature covariates. They analysed the air and water temperature using different time steps. The author found the average air temperature, maximum air temperatures change, and the rate of change of air temperature over the time step were consistently significant. The ranking performance of the NHPP with time dependent covariates was also compared with a heuristic model, the naïve Bayesian classification model and the logistic regression model (Kleiner and Rajani, 2012). The result of the study showed that no one model was consistently better than the other in terms of pipe ranking.

Economou et al. (2009) extended the idea of zero-inflated Poisson model to the NHPP. The zero-inflated NHPP assumed that failures were generated by a NHPP with probability *p*, while a different process generates the results for pipes with no failures with probability $1-p$. The zero-inflated Poisson model can be expressed as:

$$P(x) = \begin{cases} (1-p) + pe^{-\mathrm{M}} & for\ x = 0 \\ p\left(\dfrac{e^{-M}M^{x}}{x!}\right) & for\ x = 1,2 \ldots \end{cases}$$

(2-21)

$$M = E[N(T_b) - N(T_a)] = \int_{T_a}^{T_b} \mu(t)dt$$

(2-22)

where $P(x)$ is the probability of having x failures; $M = E[N(T_b) - N(T_a)]$ is the expected number of failures between time T_a; and T_b ($T_b > T_a$); and $\mu(t)$ is the intensity of the NHPP.

The model parameters were estimated using the Bayesian method and results were summarised in a confusion matrix. The zero-inflated NHPP was found to be slightly better during the calibration period. However, the performance of the zero-inflated NHPP and NHPP was similar for the validation period.

The NHPP was also used as the failure prediction models in pipe renewal planning and optimisation models (Li et al., 2015; and Nafi and Kleiner, 2009). They will be discussed in Section 2.4.

2.3.6 Linear Extended Yule Process

The Yule process is a birth process, where each individual is assumed to give birth at a constant rate. The Linear Extended Yule Process is a modification of the Yule process. In the context of pipe failure, the intensity function is a function of the age of the pipe, and the number of known past failures (NOKPF) recorded for the pipe (Le Gat, 2009 and Martins et al., 2013). The intensity function can be expressed as:

$$\mu(t) = \big(1 + \alpha N(t-)\big)\delta t^{\delta-1} e^{\underline{\boldsymbol{zA}}}$$

(2-23)

where α is the coefficient that accounts for the number of past failures the pipe has experienced; $N(t-)$ is the number of failures the pipe has experienced before time $(t-)$.

Martins et al. (2013) compared the Linear Extended Yule Process with the Poisson regression and the Weibull accelerated lifetime model. The Linear Extended Yule Process and the Weibull accelerated lifetime model both perform better than the Poisson regression in terms of pipe ranking and estimating the number of failures in the network. However, the Linear Extended Yule Process tends to overestimate the number of failures in the network.

Claudio et al. (2014) integrated the Linear Extended Yule Process with time dependent covariates. A comparison of the time dependent Linear Extended Yule Process with the original Linear Extended Yule Process (no time dependent covariates) showed a minor difference in the long-term estimation for the fitting period. However, the monthly variations were much better accounted for by the time dependent Linear Extended Yule Process. The study identified that the major limitation of the time dependent Linear Extended Yule Process was that future climate data are not available as input. Forecasting future climate scenarios will be required for the model to make predictions.

2.3.7 Bayesian Inference Models

The Bayesian theorem can be used to update the failure probability of a pipe given that new information is available. It can be expressed mathematically as:

$$P\big(F\big|\underline{\boldsymbol{Z}}\big) = \frac{P\big(\underline{\boldsymbol{Z}}\big|F\big)P(F)}{P\big(\underline{\boldsymbol{Z}}\big)}$$

(2-24)

where $P(F|\underline{\boldsymbol{Z}})$ is the probability of observing a pipe failure given a set of information $\underline{\boldsymbol{Z}}$; $P(\underline{\boldsymbol{Z}}|F)$ is the probability of observing the set of information $\underline{\boldsymbol{Z}}$ given the pipe failure record; $P(\underline{\boldsymbol{Z}})$ is the probability of observing the set of information $\underline{\boldsymbol{Z}}$; and $P(F)$ is the failure probability of the pipe.

Wang et al. (2010) estimated the deterioration rate of a pipe using Bayes inference. The study considered several factors and the weight of the factors were determined using Bayes inference. Singh (2011) studied the failure probability of a specific type of pipe given specific attributes. In the prior analysis, the authors established prior probabilities and the probability of finding a specific pipe material based on the collected data. They applied Bayes theorem to compute the posterior failure probabilities of a pipe material given the cause of break, pipe age, pipe diameter and soil type (each factor was used individually). The posterior failure probability showed that CI pipes were most susceptible to failure in the dataset.

Bayesian Model Averaging accounts for the uncertainty in the model selection process that is ignored in classical regression models. Bayesian Model Averaging takes the weighted average of the posterior distribution from the models considered, where the weights are the posterior probability of the model (Hoeting et al., 1999).

Kabir et al. (2015d) used Bayesian Model Averaging for water main failure prediction. The study found that the Bayesian Model Averaging approach was able to capture the variables that influence pipe failure more effectively in contrast to the classical regression method, where p-values are generally used to determine the significance of a variable. The Bayesian Model Averaging approach can also provide better interpretability to the selection of variables as it estimates the probability that the variable is associated with the failure of the water main.

Kabir et al. (2015c) extended the study of Kabir et al. (2015d). They used Bayesian Model Averaging to identify influential variables that influenced pipe failures while accounting for the uncertainties of the model. Then, the Weibull proportional hazard model is applied to estimate the failure rate of the network using Bayesian Inference. The study found that the time to failure for a pipe with no past failure history is longer than those that have failed in the past. The performance of the Weibull proportional hazard model was also found to be better than the Cox proportional hazard model.

The study (Kabir et al., 2015c) was further enhanced by introducing Bayesian updating to the Weibull proportional hazard model (Kabir et al., 2016). The authors calibrated the Weibull proportional hazard model using the past data. They then updated the parameters of the model using new data that become available over time. The author believed that this updating process would be highly beneficial to small and medium water utilities that have limited failure data. It would allow them to continuously improve their prediction model as they collect more data in the future.

A Bayesian Belief Network is a directed acyclic graphical model. The nodes in the network are generally stochastic variables, and the dependency between the variables are represented using an arc (Korb and Nicholson, 2010). For example, A is the parent of B if there is an arc directly from A to B. The dependency of the variables in the Bayesian Belief Network can be expressed as conditional probability tables for all possible state of the node and its parents. A node without any parents is expressed with the unconditional prior probabilities (Korb and Nicholson, 2010).

Kabir et al. (2015b) constructed a Bayesian Belief Network to determine the failure risk of a pipe in the WDN. Four groups of factors were examined in the Bayesian Belief Network, including water quality index (e.g. turbidity), hydraulic capacity index (e.g. pressure), structural integrity index (e.g. pipe diameter), and consequence index (e.g. population). The total number of nodes in the Bayesian Belief Network was 38, and the conditional probability tables were learned from the data. The study conducted a sensitivity analysis using the variance reduction method. The age of the pipe was found to have the most significant impact of variance reduction, followed by pipe diameter, population, and turbidity. Kabir et al. (2015a) proposed a data-fusion model using the Bayesian Belief Network to combine two Bayesian regression models into one. Model 1 was developed using pipe characteristics and soil resistivity, while model 2 was developed using pipe characteristics and soil corrosion index. The fusion model allowed similar type of information gathered from different sources to be integrated together.

2.3.8 Hierarchical Beta Process

The Hierarchical Beta Process (HBP) proposed by Thibaux and Jordan (2007) is a Bayesian non-parametric method that can be used to analyse sparse data. The HBP is defined using Equation (2-25). The Beta distribution is defined using concentration (c) and mean (q) instead of the two common parameters, α $(\alpha = cq)$ and β $\left(\beta = c(1-q)\right)$. The concentration is similar to the inverse of the variance in the Normal distribution, it accounts for the spread of the Beta distribution. A Beta distribution with a small concentration will have a larger spread than a Beta distribution with a large concentration.

$$q_k \sim Beta\left(c_0 q_0, c_0(1-q_0)\right), \qquad k = 1,2,\dots,K$$

$$\pi_{k,i} \sim Beta\left(c_k q_k, c_k(1-q_k)\right), \qquad i = 1,2,\dots,n$$

$$z_{k,i,j} \sim Ber\left(\pi_{k,i}\right), \qquad j = 1,2,\dots,m_{k,i}$$

(2-25)

where K is the number of groups; n is the number of pipes; $m_{k,i}$ is the number of observation years for the *i-th* pipe in group k; c_0 and q_0 are the parameters for the concentration and the mean of the Beta distribution for q_k, respectively. Similarly, c_k is the concentration and q_k is the mean of the Beta distribution for all the pipes in group k; $\pi_{k,i}$ is the probability of failure for the *i-th* pipe in group k; and $z_{k,i,j} = 1$ if a failure is observed for the *i-th* pipe in the *j-th* observation year, otherwise $z_{k,i,j} = 0$.

Li et al. (2014) applied the HBP to estimate the failure probability of critical water mains in a water network. The result of the HBP was compared with the Cox and Weibull model. It was found that the HBP was better at ranking the pipes, the model was more likely to give a higher ranking to pipes that are going to fail compared to the Cox and Weibull model. Lin et al. (2015) explored a mixture model involving the HBP, called the Dirichlet Process Mixture of Hierarchical Beta Process. The mixture model improves upon the HBP by integrating the groupings of the pipe assets with the inference process. The Dirichlet Process Mixture of Hierarchical Beta Process was compared with several statistical models, including the HBP grouped by pipe size, material, and construction year. The study found that the DPBHBP was the most accurate model for the three regions considered in the study.

2.4. Water Main Rehabilitation Models

It is essential for water utilities to forecast the investments needed to maintain the performance of their WDN at the desired level of service. The forecast can provide many useful insights, such as the expected future condition of the network, the allocation of resources, and the pricing of water to provide the level of service set out for the WDN. This section of the literature review will provide a brief overview on some of the studies that have used the failure prediction models discussed in the previous sections to investigate the rehabilitation (including replacement) of water mains in the WDN.

Minimising the total cost (replacement cost + repair cost + failure consequences) of the WDN has always been considered as one of the prime objectives of water main rehabilitation models. Shamir and Howard (1978) developed one of the first models to determine the optimal replacement time of a water main. The failures in the WDN were predicted using the time-exponential model they proposed in the same study. By considering only the replacement cost (C_R) and direct repair cost (C_m) associated with each failure, the total cost (C_{TOT}) of the pipe can be expressed as (assuming no failures in the new pipe):

$$C_{TOT} = \frac{C_R}{(1+r)^{t_r}} + \sum_{j=1}^{t_r} \frac{C_m}{(1+r)^{j-t_r}}$$

(2-26)

where r is the discount rate and t_r is the time to replacement.

The optimal replacement time was found by searching for t_r that minimised Equation (2-26). The study also analysed the effect of failures occurring in new pipes, but it had little influence on the optimal replacement time of the pipes. This framework developed by Shamir and Howard (1978) was also adopted by Walski and Pelliccia (1982) and Mailhot et al. (2003).

Kim and Mays (1994) and Kleiner et al. (1998) applied an enumeration scheme to optimise the replacement of water mains. In addition to minimising the total cost of the network, they added constraints in the model to ensure that other requirements, such as pressure demands, are satisfied while the objective was minimised. However, due to the limitation of computational power at the time of the study, it was only suitable for small networks because the dimensionality of the problem increased rapidly as the number of pipes under analysis increased.

Other than minimising the total cost, the availability of the WDN was maximised subjected to funding constraint (Li and Haimes, 1992) and the hydraulic reliability of the network (Luong and Nagarur, 2005) using a semi-Markov model. The transition probability between each state in Li and Haimes (1992) was calculated based on the work of Andreou et al. (1987a,b). Scholten et al. (2014) combined Multi-Criteria Decision Analysis with four future development scenarios to evaluate the performance of 18 rehabilitation alternatives based on three objectives (low cost, high reliability and high degree of rehabilitation). The failures in the network were predicted using a Weibull-Exponential model.

With the advance in computational power, genetic algorithms have become one of the most common techniques for optimising the replacement of water mains. The genetic algorithm is an optimisation method that simulates the evolution of living organism to solve complex problems that are sometimes too difficult for conventional methods. The search begins with an initial population that satisfies the boundary and constraint of the problem. Each individual (chromosome) represents a possible solution in the search field. During each iteration (generation), the individuals are evaluated using a fitness function. A new generation is created using a crossover function or mutating the individual. The type of initial population, fitness function, crossover function, and mutation function used will depend on the problem at hand (Gen et al., 2010). After sufficient generations, the most optimal or suboptimal solution(s) will be selected by the algorithm.

Halhal et al. (1997) constructed a structured messy genetic algorithm to maximise the total benefit of performing a specific action on a pipe (e.g. replacement or reline) while minimising the total cost of intervention to the network. The optimal replacement time of water mains was determined by Dandy and Engelhardt (2001) using genetic algorithm. The study minimised the total cost of the network subjected to several constraints. Dridi et al. (2008) compared three types of genetic algorithm and recommended the Non-Dominated Sorting Genetic Algorithm-II for large WDN based on the results of their study.

Instead of considering a single-objective function with multiple constraints, multi-objective optimisation was performed using multi-objective genetic algorithms to select water mains for rehabilitation (Dandy and Engelhardt, 2006; Berardi et al., 2009a; Berardi et al., 2009b; Dridi et al., 2009; and Giustolisi and Berardi, 2009). Nafi and Kleiner (2009), Li et al. (2015), and Rokstad and Ugarelli (2015) integrated group replacement strategies into the multi-objective genetic algorithm. The water mains that satisfy specific requirements, such as those within a selected distance (Li et al., 2015), can form potential renewal groups. Those that are in the same group will be renewed in one replacement job at the same time, providing savings to the water utility as the fixed cost associated with each replacement event is reduced (e.g. one machinery transportation cost instead of many). Nafi and Kleiner (2009) also identified possible savings from coordination with roadworks and discount in variable cost (e.g. replace length) when the replacement length exceeds a specific limit.

2.5. Conclusion

An extensive literature review has been conducted for the physically based pipe failure prediction models, statistically based pipe failure prediction models, and water main rehabilitation models. Table 2-1 compares some of the advantages and disadvantages of the failure prediction models discussed in the chapter.

The physically based models reviewed have investigated different degradation rates (e.g. bi-linear corrosion rates (Ji et al., 2015)), operating conditions (e.g. frost loads (Rajani and Tesfamariam, 2004)), and failures modes (e.g. brittle or ductile (Davis et al., 2007)). The input parameters in the different studies are retrieved from a number of sources, including water main reports (Ji et al., 2015), pipe samples (Seica and Packer, 2006), condition assessments (Davis et al., 2004) or are derived subjectively (Tesfamariam et al., 2006). However, in terms of the entire WDN, information on some of the inputs, such as the degradation rate, is rarely available for all the water mains. In most cases, it is only cost-effective for water utilities to collect the information for a small number of water mains that is critical in the network. Therefore, the application of physically based models in practice is generally limited to large transmission mains with high failure consequences. In addition, the estimated condition of the pipe is based on data that are collected at a single point in time, but the operating condition or the surrounding environment can change over time (e.g. degradation rate might change after data collection), and therefore, increasing the error in the result predicted.

Table 2-1: Advantages and disadvantages of pipe failure prediction models.

Models	Advantages	Disadvantages
Physical Model	• Captures the physical failure mechanism. • Can account for the different pipe properties and operating environment of the pipe, given that the model has been developed and the relevant data are available.	• Model is only applicable to the failure mechanism and pipe material it is designed for. • Difficult to apply at the network level as the input parameters are generally unknown. • The model returns a deterministic result ("Failure" or "No Failure" status).
Physical Probabilistic Model	• Captures the physical failure mechanism. • Stochastic distribution is used to capture the uncertainty in the input parameters. • The model can estimate the failure probability of the pipe.	• The appropriate distribution of the input needs to be selected by the user. • The parameters of the distribution may need to be estimated based on experience when there are insufficient data.
Regression Model	• The model is easy to use.	• Assumes normally distributed errors. • Oversimplifies the problem by assuming a simple relationship between the dependent and independent variables.
Survival model	• Based on the well-established proportional hazard model developed by Cox (1972). • Covariates act multiplicatively on the hazard function which is used to model the deterioration of the pipe.	• Multiple survival functions are needed for repairable systems such as the WDN. This number of hazard functions needs to be determined by the user.
Weibull-Exponential Model	• Two different models are used to model the deterioration of the pipe. They can capture the deterioration characteristics of the pipe at different stages of their life. • Weibull model is used to model the early deterioration phase of the pipe. • The Exponential model is used to model the late fast breaking stage.	• The transition from the Weibull model to the Exponential model needs to be determined. • The Exponential model assumes a constant rate of deterioration over time. This might not be true during the wear out phase (Figure 1-1) of the pipe.
Artificial Neural Network	• Data-driven non-parametric model. • Artificial Neural network can model the time to failure, the number of failures, or used for pipe classification ("Failure" or "No Failure" status) depending on the type of neural network selected.	• Requires an in-depth understanding of the model as well as the problem to set up the structure of the neural network. • May require many trials to determine the optimal network structure.
Non-homogeneous Poisson Process	• The intensity function captures the average deterioration trend of the pipes in the network. • Covariates act multiplicatively on the intensity function. • The failure history of the pipe can be included as covariates to adjust the underlying ageing trend.	• If the failure history of the pipe is used in the model to predict failures, a modification must be made to the variable (for example, assuming the variable to be constant after the training period) because it is unknown in the future.
Linear Extended Yule Process	• The intensity function captures the average deterioration trend of the pipes in the network. • Covariates act multiplicatively on the intensity function. • The effect of the pipe's failure history on future pipe failures is captured in the intensity function.	• The failure history of the pipe is unknown in the future. This may impact the model performance as it is used in the intensity function.
Bayesian Inference Model	• Utilises prior information that may be available. • All calculations are based on Bayes Theorem. • Given sufficient data, the Bayesian Belief network can learn causal relationships between variables.	• The selection of the prior distribution can heavily influence the posterior distribution. Therefore, an appropriate prior must be selected for the posterior distribution to be meaningful. • In complex models, such as large Bayesian networks, it can be computationally expensive to estimate the posterior distributions
Hierarchical Beta Process	• The model is based on Bayes Theorem with a hierarchical structure. • Data-driven model.	• The model is not time-dependent. Therefore, the model is not suitable for making long-term predictions

Statistical models can be applied to the entire WDN given that sufficient failure data are available. They can provide predictions for individual pipes, which are useful for rehabilitation planning if coupled with a failure consequence model. However, the predictions for individual water mains are generally unreliable. This is because the water mains must be grouped into cohorts with homogeneous properties before calibration. Therefore, the estimations/predictions from the models will be tailored to the cohort of pipes rather than the individual pipes.

With studies identifying correlation between water main failures and climate events (Walski and Pelliccia, 1982; Habibian, 1994; Gould et al., 2009; Gould et al., 2011; and Fuchs-Hanusch et al., 2013), time dependent factors have been introduced into some statistical models (Kleiner and Rajani, 2002; Kleiner and Rajani, 2008; Kleiner and Rajani, 2012; Rajani et al., 2012; and Claudio et al., 2014). The results for the fitting period have shown to improve in comparison to the models without the time dependent factors (Claudio et al., 2014). However, these types of models are limited by their ability to predict future events because the time dependent factors are unknown in the future.

The rehabilitation model for water mains attempts to optimise the performance of the WDN depending on the selected objectives. Conventional methods, such as the one developed by Shamir and Howard (1978), are easy to apply to the network. However, they have limited power in dealing with multi-objective optimisation problems. More advanced techniques, such as genetic algorithm, can easily handle multi-objective problems, but it requires the user to have a greater understanding of the method to adjust the parameters in the algorithms properly. In addition, these methods (e.g. genetic algorithm) are generally computationally costly and applying it to a large WDN might not return the optimal solution.

The prediction of water main failure remains as an open field of research. The following research gaps have been identified on the basis of the literature review:

- Statistical models are generally poor in making predictions for individual pipes. Ranking pipes based on the probability of failure or expected number of failures can be considered as an alternative in identifying pipes at risk of failing. The HBP has shown to be accurate in terms of ranking high-risk pipes compared to other models. Therefore, ranking models could be an alternative in locating pipes that are more likely to fail.
- Past studies incorporating time dependent factors in statistical models have shown improvements in estimating the number of failures during the training period. However, little work has been undertaken to try and predict future failures with time dependent factors because their values are unknown in the future.

- The integration of the physical model with statistical failure data to predict water main failures has not yet been investigated. The physical model can account for the physical deterioration process. However, they may be difficult to be applied to all pipes due to the lack of deterioration data (or other information that could only be obtained through condition assessments). In addition, the collected data for the physical model generally provides information for a specific point in time but cannot represent the change in condition over time. The statistical models can use failure data that have been collected to estimate the condition of the water main. However, the estimations are usually unreliable for individual pipes. Therefore, integrating the two approaches together has the potential to produce promising results because the physical deterioration process can be supported by the failure data that have been collected. This could overcome the issue with the input data for the physical models and the poor estimation for individual water mains from the statistical models.

CHAPTER 3: THE BAYESIAN SIMPLE MODEL

3.1. Introduction

Most statistical models can be used to estimate the number of failures or the failure probability of a water main. The models are often trained using the data from a homogeneous group of pipes (e.g. same material and diameter) due to the lack of failures for individual pipes. In most cases, the estimation at the network level is reasonably accurate when compared to the recorded failure data. However, individual water mains are often overestimated or underestimated by a large degree because the model has been calibrated using the data at a group level. Therefore, the model does not have sufficient information to capture the variability of water main failures in a single pipe.

An alternate way to identify pipes with a high chance of failure is to compare the ranking of the water mains. Kleiner and Rajani (2012) compared the ranking performance of four different statistical models, including the NHPP. The NHPP is a well-established model that can account for the pipe deterioration and factors that influence the breakage of water mains. The authors ordered the pipes in descending order based on their probability of failures (or rankings depending on the model used) Their study found that none of the four models was consistently better than the other three models in the 37 scenarios they analysed. Li et al. (2014) also compared the result of their machine learning approach that is based on the HBP, with the Cox model and the Weibull model. They were able to demonstrate that their recently developed approach can provide superior results with respect to the Cox model and the Weibull model. However, the model is complex and cannot account for the deterioration of the pipe.

This chapter will introduce the Bayesian Simple Model (BSM) that has been developed to identify pipes prone to failure. It is a simple method that utilises Bayes theorem to estimate the failure probability of a pipe using the pipe failure history. The BSM will be compared with the well-established NHPP (Kleiner and Rajani, 2012; Lawless, 1987; and Røstum, 2000) and the HBP (Li et al., 2014) for short-term failure prediction. The performance of the three methods in terms of their ability to rank pipes using the prediction curve, and the accuracy in predicting the number of failures in the dataset will be investigated.

Section 3.2 provides a description on the dataset used for analysis, followed by a detail explanation of the NHPP, HBP and BSM. Section 3.4 introduces the prediction curve for pipe ranking. Section 3.5 discusses, compares and analyses the results from the three models to determine their possibilities and limitations.

3.2. Pipe Asset and Failure Data

The three models are compared using the failure data of 100mm diameter CI pipes. Other pipe sizes were not considered in the study, but the influence of pipe diameter can be incorporated by introducing additional pipe diameter covariates.

In this thesis, an individual pipe is a specific length of pipe in the network that is identified with the same "Pipe ID" by the water utility, they are usually defined between valves or pipe intersections. In the case where a small segment of the pipe is replaced, a new "Pipe ID" will be generated for the new pipe put in the network.

A pipe failure event is any bursts or leak events that are reported and recorded by the water utility. They mainly consist of broken back failures, longitudinal split failures and joint failures. The different failure modes are all included in the analysis as the statistical model does not require them to be differentiated. As a result of this, it must be kept in mind that the failure modes will not be identifiable from the model estimations. This is usually sufficient for a statistical model because they are used for planning purposes. Therefore, it is more important for the model to predict the total number of failures to estimate the condition of the network. However, if it is required to estimate the number of failures for a specific failure mode, then the model should only be trained using failure data corresponding to that specific failure mode. Note that failure caused by third-party damage and tree roots have been removed when cleaning the dataset.

Both the pipe asset data and pipe failure data have been filtered to ensure that the inputs for the models are at their best possible quality. Water mains that have been removed from the network are not included. A description of the dataset (will be referred to as dataset A) under investigation is shown in Table 3-1. The CI pipes have been laid in the ground from 1860 to 1929. The failure data have been recorded for 17 years, from 1997 to 2013. The failure data before 2012 will be used to calibrate the models and the last year, 2013, will be used as a validation year to validate and compare the results from the three models.

Since the HBP and the BSM estimate the probability of failure, they are only interested in whether the pipe has failed or not and not how many times the pipe failed in the year. Therefore, the failure data are converted into binary format, where 1 represents that the pipe failed in the year (can be more than 1 failure) and 0 means that the pipe operated without any interruptions. The NHPP will also use the same binary format for the failure data to maintain consistency in the input data between the three models.

Several covariates have been considered to model the breakage of pipes in the NHPP. Figure 3-1 plots the failure rate of the network over the observation period. An increasing trend can be observed from the graph, suggesting that the water mains have been deteriorating over the years. Note that the recorded data show the total number of failures in a year, but they are plotted as lines in the figures in the chapter instead of discrete points for better visualisation.

The effect of pipe length, static water pressure and the time to next failure are also examined using Figure 3-2, Figure 3-3 and Figure 3-4, respectively. The figures show water mains that are longer and have been operating in a high static water pressure environment have a higher failure rate. The time to subsequent failures also becomes shorter as the water main experiences more failures over the years.

Table 3-1: Description of cast iron dataset (dataset A).

Data Properties	Range of data
Number of assets	5443
Number of failures	1636
Construction period	1860 to 1929
Observation period	1997 to 2013

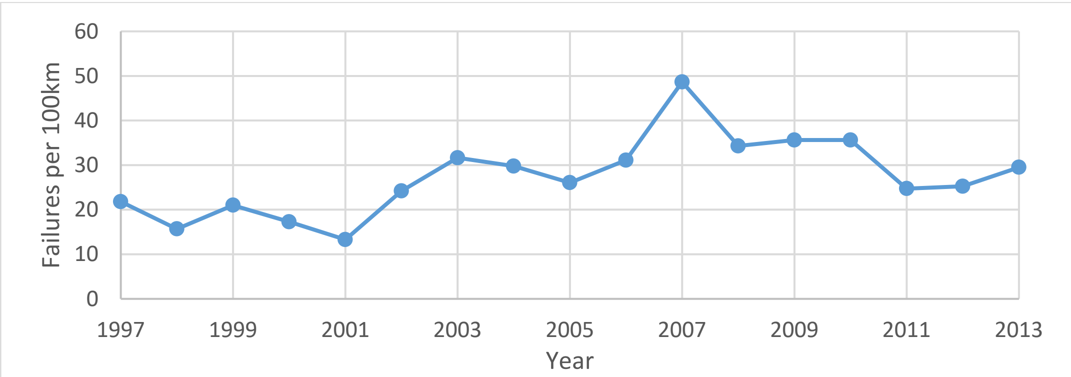

Figure 3-1: Failures per 100km for CI dataset.

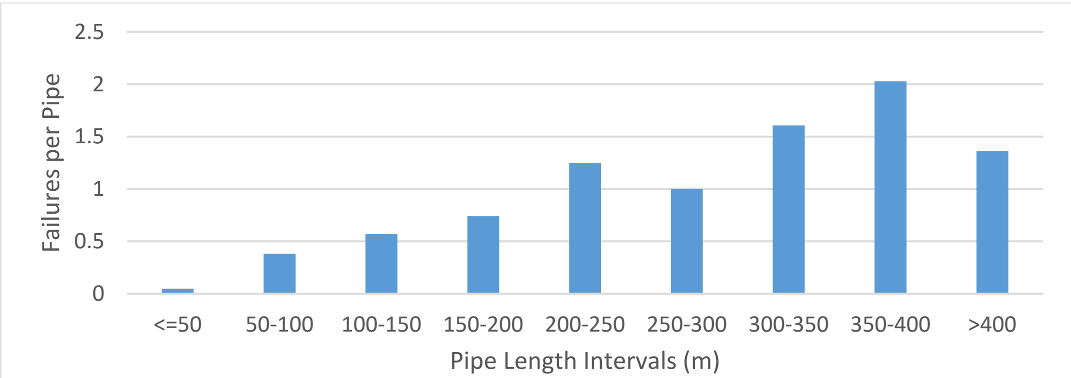

Figure 3-2: Failures for different pipe length intervals.

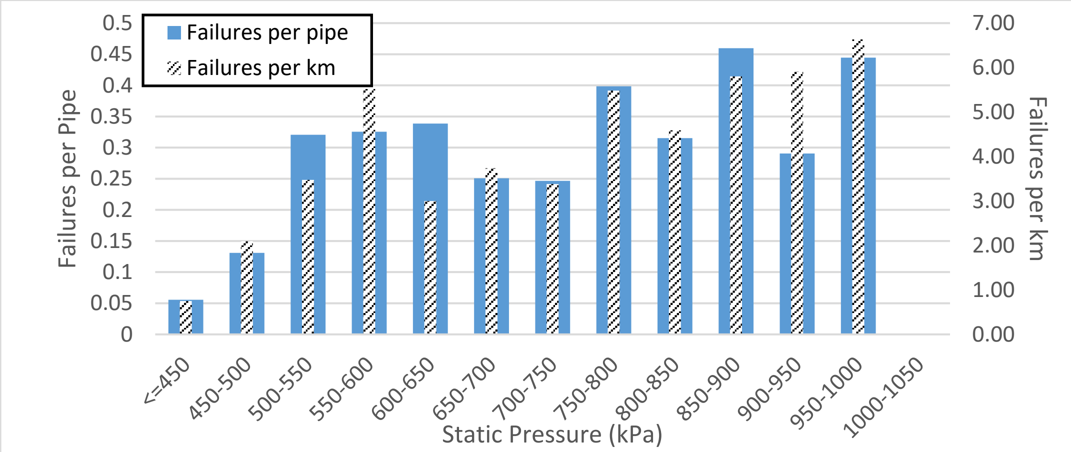

Figure 3-3: Breakages in different pressure intervals.

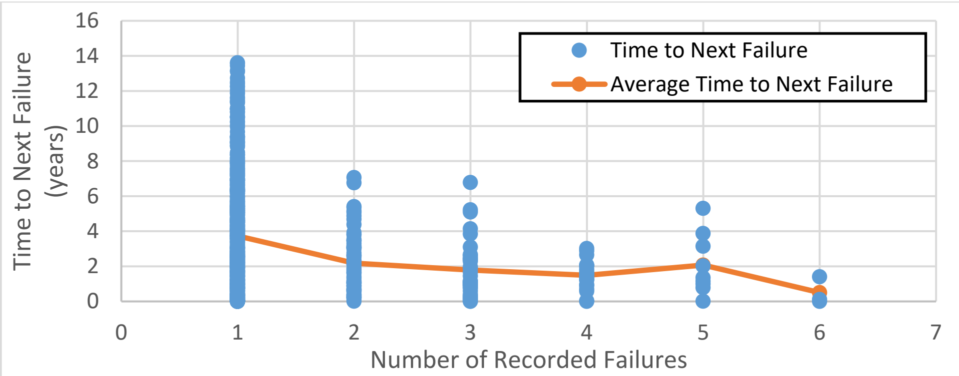

Figure 3-4: Time to next failure based on the number of failures recorded.

3.3. Model Descriptions

3.3.1 Non-homogeneous Poisson Process (NHPP)

The NHPP is a well-establish process that has been used to model trends in a repairable system. As indicated in Chapter 2, numerous studies (Economou et al., 2009; Kleiner and Rajani, 2008; Kleiner and Rajani, 2012; Nafi and Kleiner, 2009; Rajani et al., 2012; and Røstum, 2000) have used the NHPP for water main failure predictions. It is capable of capturing the underlying ageing trend of the WDN, as well as the influence from other covariates on water main breakages.

A random process,$\{N(t), t \in [0, \infty)\}$, is a counting process if (Ross, 1996):

1. $N(t)$ is an integer.
2. $N(t) \geq 0$, the number of failures cannot be negative at any time t.
3. $N(t) \geq N(s)$ given $t > s$, the number of events at time t is equal to or greater than the number of events at time s.
4. $[N(t) - N(s)]$ is the number of events occurred between time t and s.

A counting process, $\{N(t), t \in [0, \infty)\}$, with the following properties is said to be a NHPP with the intensity function $\mu(t)$:

1. $N(0) = 0$, there are no failures in a new system.
2. $N(t)$ has independent increments.
3. $N(t)$ has a Poisson distribution with mean $\Lambda(t) = \int_0^t \mu(s)ds$.

Based on the proportional intensity assumption, the intensity function of the NHPP takes the following form (Lawless, 1987):

$$\mu(t) = \mu_0(t)g(\underline{\boldsymbol{z}}; \underline{\boldsymbol{A}})$$

(3-1)

where $\mu_0(t)$ is the baseline intensity function and $g(\underline{\boldsymbol{z}}; \underline{\boldsymbol{A}})$ is a function that accounts for the covariates ($\underline{\boldsymbol{z}}$) and its coefficients ($\underline{\boldsymbol{A}}$).

Assuming that the baseline intensity function follows a power law model and $g(\underline{\boldsymbol{z}}; \underline{\boldsymbol{A}})$ takes an exponential form, the intensity function becomes:

$$\mu(t) = \delta t^{\delta-1} e^{\underline{\boldsymbol{zA}}}$$

(3-2)

where $e^{\underline{\boldsymbol{zA}}} = e^{z_0 A_0 + z_1 A_1 \cdots}$; δ is the shape factor and the scale factor are incorporated into $\underline{\boldsymbol{z}}$ as $z_0 = 1$.

The cumulative intensity function between time T_a and T_b ($T_b > T_a$) corresponds to the expected number of failures between time T_a and T_b:

$$E[N(T_b) - N(T_a)] = \int_{T_a}^{T_b} \mu(t)dt = \left(T_b^\delta - T_a^\delta\right) e^{\underline{\boldsymbol{zA}}}$$

(3-3)

The coefficients ($\underline{\boldsymbol{A}}$) and the shape factor ($\delta$) are estimated by maximising the log-likelihood function using the method of Maximum Likelihood (Yang and De Angelis, 2013). The log-likelihood function for a WDN with m pipes can be expressed as:

$$l(\delta, \underline{\boldsymbol{A}}) = \sum_{i=1}^{n} n_i \ln \delta + (\delta - 1) \sum_{i=1}^{n} \sum_{j=1}^{m_i} \ln t_{ij} + \sum_{i=1}^{n} n_i \underline{\boldsymbol{zA}} - \sum_{i=1}^{n} \left(T_{i,b}^\delta - T_{i,a}^\delta\right) e^{\underline{\boldsymbol{zA}}}$$

(3-4)

where $T_{i,a}$ and $T_{i,b}$ ($T_{i,b} > T_{i,a}$) is the pipe age at the start and end observation period, respectively; n is the number of pipes; m_i is the number of failures in pipe i observed in the period; and t_{ij} is the j-th failure of the *i-th* pipe.

The power law model has been chosen as the baseline intensity function because of its ability in modelling the changing condition of the network. If $\delta > 1$, it is suggesting that the average condition of the network is deteriorating and the failure rate of the

WDN increases over time. if $\delta < 1$, it is suggesting that the average condition of the network is improving and the failure rate of the WDN decreases over time. If $\delta = 1$, it is suggesting that there is no change in the average condition of the network and the failure rate of the WDN stays constant over the period of analysis. The NHPP also becomes the homogeneous Poisson process when $\delta = 1$.

3.3.2 Hierarchal Beta Process (HBP)

The HBP is a Bayesian non-parametric approach proposed by Thibaux and Jordan, (2007) (Equation (3-5)). Li et al. (2014) and Lin et al. (2015) applied the HBP to estimate the failure probability of critical water mains in a water network. The failure of a water main is assumed to follow a Bernoulli distribution with failure probability π_i. The failure probability of each pipe, π_i, is drawn from a Beta distribution with mean q_1 and concentration c_1. The mean of the Beta distribution is modelled using another Beta distribution with mean q_0 and concentration c_0. Figure 3-5 shows the structure of the HBP in a generalised form where the water mains are split into K groups (K is taken as 1 in this case and is explained below).

q_1 and c_1 control the distribution of π_i. q_1 and c_1 can be updated with failure data from any pipe and modifies the distribution for π_i. This process draws upon the failure from a particular water main and passes the influence of a failure onto other pipes in the same group.

The model defines the Beta distribution using the mean (q_0, q_1) and concentration (c_0, c_1) parameters instead of the common shape parameters α ($\alpha_0 = c_0 q_0$) and β ($\beta_0 = c_0(1 - q_0)$). The concentration parameter is similar to the inverse of the variance in the normal distribution, a larger concentration suggests that the spread of the Beta distribution is smaller. The k parameter in Equation (2-25) represents the number of homogenised pipe cohorts in the dataset. In the current dataset, all the water mains have been homogenised into a cohort of pipes with the same material (i.e. cast iron) and diameter (i.e. 100mm). Therefore, the parameter k has been dropped in Equation (3-5) as $k = 1$.

$$q_1 \sim Beta\big(c_0 q_0, c_0(1 - q_0)\big)$$

$$\pi_i \sim Beta\big(c_1 q_1, c_1(1 - q_1)\big), \;\; i = 1,2, \dots, n$$

$$z_{i,j} \sim Ber(\pi_i), \qquad j = 1,2, \dots, m_i$$

(3-5)

$$p(q_1 | z_{1:n}) \propto q_1^{c_0 q_0 - 1}(1 - q_1)^{c_0(1-q_0)-1}$$

$$\times \prod_i \frac{\Gamma\left(c_1 q_1 + \sum_j z_{i,j}\right)\Gamma\left(c_1(1-q_1) + m_i - \sum_j z_{i,j}\right)}{\Gamma(c_1 q_1)\Gamma\left(c_1(1-q_1)\right)}$$

(3-6)

$$p(\pi_i | q_1, z_{1:\mathrm{n}}) \sim Beta\left(c_1 q_1 + \sum_j z_{i,j}\,, c_1(1-q_1) + m_i - \sum_j z_{i,j}\right)$$

(3-7)

where n is the number of pipes; m_i is the number of observation years for the *i-th* pipe; c_0 and q_0 are the parameters for the concentration and the mean of the Beta distribution for q_1, respectively. Similarly, c_1 is the concentration and q_1 is the mean of the Beta distribution for all the pipes in the network; $\Gamma(\cdot)$ is the gamma function; π_i is the probability of failure for the *i-th* pipe; $z_{1:n} = (z_{i,j} | i = 1,2, \dots n, j = 1,2, \dots m_i)$; and $z_{i,j} = 1$ if a failure is observed for the *i-th* pipe in the *j-th* observation year, otherwise $z_{i,j} = 0$.

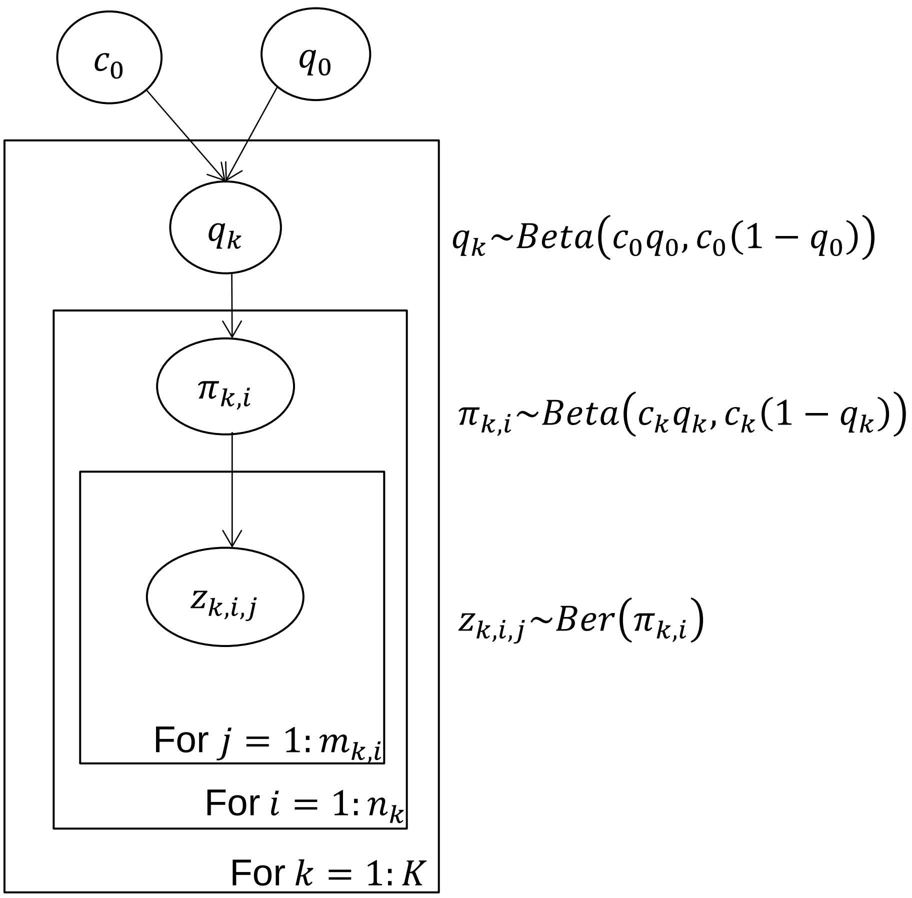

Figure 3-5: Structure of the HBP.

Using Bayes theorem, the probability of q_1 given $z_{i,j}$ can be sampled using Equation (3-6), given that the pipe failure history is known ($z_{i,j}$). The Beta distribution is a conjugate distribution to the Bernoulli distribution, therefore the posterior distribution is still a Beta distribution (Gelman et al., 2000). The probability of failure given the observed failure history and the mean of the Beta distribution prior, $Pr(\pi_i|q_1, z_{1:n})$, can be calculated using Equation (3-7). A complete definition of the HBP can be found in Thibaux and Jordan (2007) and Thibaux (2008).

Before the model can be trained using Markov Chain Monte Carlo (MCMC) methods, the values for c_0, c_1 and q_0 must be defined. c_0 and c_1 are taken as 1 ($c_0 = 1$ and $c_1 = 1$) because it provides the Beta distribution with a large spread. The average failure probability from a dataset similar to the one that is going to be analysed is used for q_0 and is equal to 0.0061. 5000 samples were taken to ensure convergence of the posterior distribution and the software WinBUGS (Lunn et al., 2000) was used to implement the HBP model.

3.3.3 Bayesian Simple Model (BSM)

A number of studies have utilised Bayes theorem to estimate the failure probability of water mains (Kabir et al. ,2015c; Kabir et al., 2015d; and Kabir et al. 2016). Kabir et al. (2015d) used Bayes Model Averaging to select significant covariates that influenced pipe failure while accounting for the uncertainties of the model. Kabir et al. (2015c) estimated the survival curve for water mains based on the Weibull proportional hazard model with Bayes inference. Kabir et al. (2016) then accounted for new data that become available over time in the Weibull proportional hazard model by developing a framework that updates the survival curve using Bayes inference.

In this chapter, the Bayesian Simple Model (BSM) is originally developed. The model utilises Bayes theorem for short-term failure predictions and is designed to identify groups of water mains that are more likely to fail in the next time period (e.g. next year). This is different from the Bayesian Weibull proportional hazard model (Kabir et al. (2015c) and Kabir et al. (2016)) that aims to predict the number of breaks in the future.

The failure history of the water mains used to calibrate (up to time T_c) the BSM is split into two parts as shown in Figure 3-6. Failure data before time $T_c - 1$ (green period) are used to divide the pipes into groups. Then, the probability of failure for each group is calculated using Bayes theorem with the failures observed between time $T_c - 1$ and T_c.

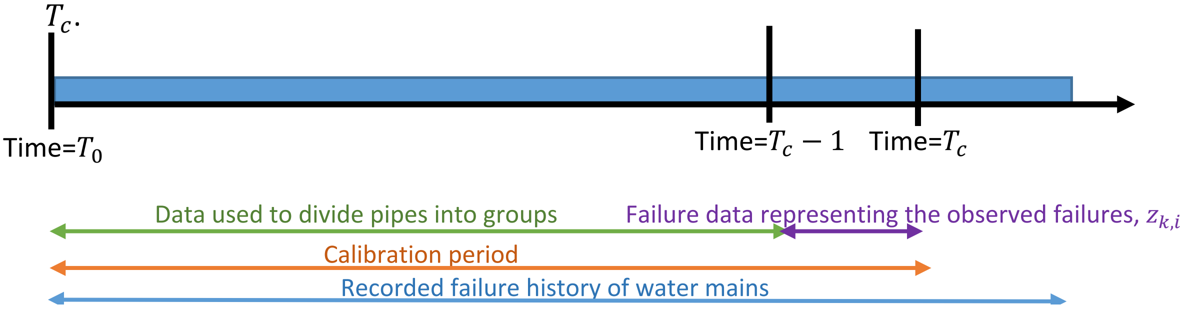

Figure 3-6: Failure data timeline.

Assuming that the failure events in the WDN are independent and identically distributed[1], and the failure probabilities of water mains with k failures follow a Bernoulli distribution (Ross, 2010), the probability of observing a set of outcomes for the pipes with k failures given the failure probability θ_k is (Equation (3-8)):

$$P\left(z_{k,1}, z_{k,2} \dots z_{k,n_k} \middle| \theta_k\right) = \prod_{i=1}^{n_k} \theta_k^{z_{k,i}} (1-\theta_k)^{1-z_{k,i}} = \theta_k^{\sum_{i=1}^{n_k} z_{k,i}} (1-\theta_k)^{n_k - \sum_{i=1}^{n_k} z_{k,i}}$$

(3-8)

$$P(\theta_k|\alpha,\beta) = \frac{\theta_k^{\alpha-1}(1-\theta_k)^{\beta-1}}{B(\alpha,\beta)}$$

(3-9)

$$P\left(\theta_k \middle| \alpha, \beta, z_{k,1}, z_{k,2} \dots z_{k,n_k}\right) \propto P\left(z_{k,1}, z_{k,2} \dots z_{k,n_k} \middle| \theta_k\right) P(\theta_k|\alpha,\beta)$$
$$\propto \theta_k^{\alpha + \sum_{i=1}^{n_k} z_{k,i} - 1} (1-\theta_k)^{n_k - \sum_{i=1}^{n_k} z_{k,i} + \beta - 1}$$

With normalisation for Beta distribution:

$$P\left(\theta_k \middle| \alpha, \beta, z_{k,1}, z_{k,2} \dots z_{k,n_k}\right) = \frac{\theta_k^{\alpha + \sum_{i=1}^{n_k} z_{k,i} - 1} (1-\theta_k)^{n_k - \sum_{i=1}^{n_k} z_{k,i} + \beta - 1}}{B\left(\alpha + \sum_{i=1}^{n_k} z_{k,i}, n_k - \sum_{i=1}^{n_k} z_{k,i} + \beta\right)}$$

(3-10)

$$E\left[\theta_k | \alpha = \frac{1}{2}, \beta = \frac{1}{2}, z_{k,1}, z_{k,2} \dots z_{k,n_k}\right] = \frac{\sum_{i=1}^{n_k} z_{k,i} + \alpha}{n_k + \alpha + \beta} = \frac{\sum_{i=1}^{n_k} z_{k,i} + 0.5}{n_k + 1}$$

(3-11)

where $P(\cdot)$ is the probability; n_k is the total number of pipes with k failures; $z_{k,i}$ represents whether the *i-th* pipe with k failures failed ($z_{k,i} = 1$) between $T_c - 1$ and T_c (Figure 3-6); and θ_k is the prior distribution that represents the failure probability of pipes with k failures. The prior distribution, θ_k, is assumed to follow a Beta distribution (Ross, 2010) with parameters α and β (Equation (3-9)) and $B(\alpha, \beta)$ is the beta function with parameter α and β.

It is unlikely that the failure data are truly independent and identically distributed because the failure events are likely to be correlated. For example, water mains that have failed more often in the past tend to have a higher chance of failure in the future. However, due to the lack of failure data, it is extremely difficult to construct the covariance matrix to model the relationship of failure events between pipes and within pipes. Later in Chapter 5, the Monash Pipe Failure Prediction Model attempts

---

[1] Failure events do not influence each other and they all follow the same distribution (Bernoulli distribution in the BSM).

to capture part of the dependency between failure events using another approach. At the current stage, the results from the BSM can be considered as a first approximation.

The failure probability (posterior distribution) of the pipes with k failures can be estimated easily due to the conjugacy of the Beta and Bernoulli distribution. The probability of failure is another Beta distribution (Equation (3-10)) (the normalising constant of the denominator can be obtained without any calculation because the nominator shows that it has a Beta distribution). Since no information is given on the condition of the pipes, the non-informative Jeffreys Prior is used to assign the parameters in the Beta distribution ($\alpha = 0.5, \beta = 0.5$) (Gelman et al., 2000). The expected failure probability of the water main in group k can be estimated by substituting the Jeffreys Prior into Equation (3-11).

The estimation of the water main's failure probability using the BSM is demonstrated using dataset A. Table 3-2 shows that all the water mains have been split into 8 groups, based on the number of failures they have experienced between time 1997 and 2011 ($T_c - 1$). The probability of failure can be estimated by substituting the number of pipes in each group (n_k), the number of failures in 2012 (T_c) ($\sum_{i=1}^{n_k} z_{k,i}$) and the Jeffreys Prior ($\alpha = 0.5, \beta = 0.5$) into Equation (3-11). For example, in Group #1, there are 4529 pipes ($n_0 = 4529$) and 31 of them failed in 2012 ($\sum_{i=1}^{n_0} z_{0,i} = 31$). The expected probability of failure for the pipes in Group #1 are (31+0.5)/(4529+1)=0.7%.

The result of the BSM suggests pipes that have experience more failures in the past are more likely to fail again. This coincides with an approach used by some water utilities, where the number of failures is used as a trigger for pipe replacement. If a certain threshold (e.g. 3 failures) is reached for a water main in a short period of time, the water main will be given a high replacement priority because of the disruptions it is causing to the customers in the area.

Table 3-2: Failure probability of dataset A using Bayesian Simple Model.

Group #	Number of failures between 1997 and 2011	Number of pipes in the group	Number of failures in 2012	Probability of failure
1	0	4529	31	0.7%
2	1	582	22	3.9%
3	2	202	15	7.6%
4	3	88	10	11.8%
5	4	25	4	17.3%
6	5	8	3	38.9%
7	6	7	2	31.3%
8	7	2	0	16.7%

3.4. Prediction Curve

The prediction curve is a graphical plot that can be used to compare the ranking performance of different statistical models. The curve shows the percentage of failures that can be predicted (or avoided) in the network if a certain percentage length of pipe with the highest probability of failure is replaced. Using the results from the BSM in Table 3-2, Table 3-3 demonstrates the process of constructing the prediction curve using the steps described below. Examples will be given in some places to help explain the calculations for part of the table:

1. Order the pipes' (or pipe group for BSM) failure probability in descending order.
2. Calculate the pipe length and number of failures in 2013 for each pipe (or pipe group).
3. Calculate the cumulative pipe length and cumulative number of failures. For example, the cumulative pipe length in group 7 (row 2) is the total pipe length of group 6 and 7 (1996+1838=3834). The cumulative number of failures in group 7 (row 2) is the total number of failures in group 6 and 7 (1+3=4).
4. The % pipe length considered for renewal = the cumulative pipe length/(total pipe length in the network (376233m)).
5. The % failures predicted = observed cumulative number of failures/(total number of failures in the network in 2013 (103)).

The prediction curve assumes that the model predictions are the only information used to determine the pipe renewal process. Pipes with the highest probability of failure (BSM and HBP) or expected number of failures (NHPP) will be given the highest priority for replacement. Each of the three models has their own prediction results for each pipe. Therefore the rankings of the pipes are unlikely to be the same (e.g. pipe A might be rank 1 in NHPP but rank last in the HBP). It must be noted that Table 3-3 only has 8 rows because the results for the pipes in the BSM are the same if they are in the same group. The models such as the HBP and the NHPP can have a unique failure probability for each pipe, leading to a much larger table.

The prediction curve based on the result in Table 3-3 is shown in Figure 3-7. Since the BSM does not differentiate pipes with the same failure history, the points in the prediction curve can only be determined at a group level (blue markers in Figure 3-7). By assuming that the pipes in the same group are randomly selected without any selection preference, it is expected that the percentage of failures predicted increases linearly between two points. The percentage length of the network considered for pipe replacement is shown in the x-axis, and the percentage of failures that the model can predict (or avoid) is shown in the y-axis. The percentage length of the network is used instead of the percentage of pipes in the network for the x-axis because the variation in pipe length can cause bias interpretations.

Based on the prediction from the BSM and assuming that new pipes are free from breakages, the curve (Figure 3-7) shows that 10% of the failures in 2013 can be found in the first 2.3% of pipe length that is considered for renewal (2.3% of pipe length with the highest failure probability). If the percentage of length considered for renewal is increased to 10%, it is expected to find about 32% of the failures in 2013. If the percentage of length considered for renewal is increased to 100% (i.e. replacing all pipes in the network), it is expected to find all the failures in 2013.

Table 3-3: BSM Prediction Table.

Group # (refer to Table 3-2)	Probability of failure (refer to Table 3-2)	Total pipe length (m)	Cumulative pipe length (m)	% Pipe length considered for renewal	Observed number of failures in 2013	Observed cumulative number of failures in 2013	% Failures predicted
6	38.9%	1996	1996	0.5%	1	1	1.0%
7	31.3%	1838	3834	1.0%	3	4	3.9%
5	17.3%	4830	8664	2.3%	7	11	10.7%
8	16.7%	239	8903	2.4%	0	11	10.7%
4	11.8%	16249	25153	6.7%	18	29	28.2%
3	7.6%	32099	57252	15.2%	10	39	37.9%
2	3.9%	74376	131628	35.0%	25	64	62.1%
1	0.7%	244606	376233	100.0%	39	103	100.0%

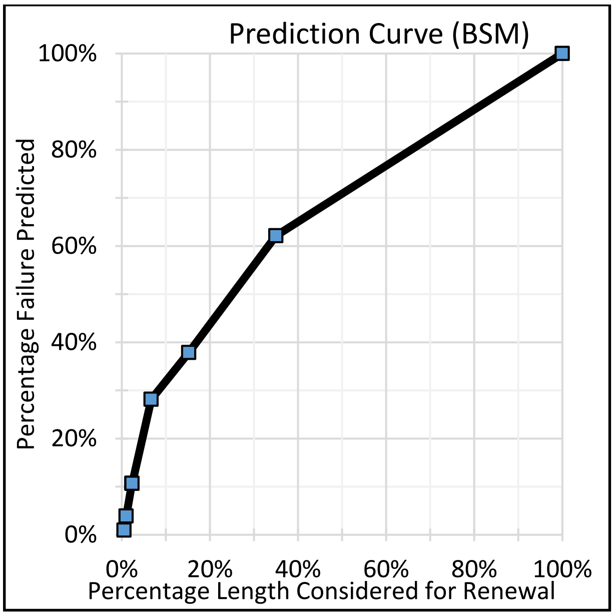

Figure 3-7: Prediction curve for the BSM.

3.5. Results and Discussions

This section first analyses the failure probability of the models and the coefficients estimated for the covariates in the NHPP. Then the ranking performances are examined using the prediction curve and the receiver operating characteristic (ROC) curve, followed by a comparison of the number of failures predicted for the network, and the influence on the models' performance by grouping the water mains into pressure cohorts. Finally, the three models are applied to four additional datasets to check for the consistency of the models' performance.

The estimated failure probability for the BSM have already been discussed in Table 3-2, a summary of the results for the HBP is shown in Table 3-4. Similar to the BSM, the results for the HBP are shown in groups, based on the failure history of the pipe. However, unlike the BSM, the pipes in the same group do not have the same probability of failure. Therefore the maximum and minimum probability of failure for the pipes in each group are shown in the table. The results suggest that the failure probability from the HBP is highly dependent on the pipe's failure history. Water mains that have experienced more failures in the past are estimated with a higher probability of failure. It is likely that the difference in results for the pipes in the same group is due to the sampling of Equation (3-6) using MCMC methods.

The estimated coefficients for the NHPP are shown in Table 3-5. The Log-likelihood ratio tests were applied to the covariates in the NHPP to ensure that they are significant in the model. The results indicate pipes that are longer, operating with higher pressure and has experienced more failures in the past (higher NOKPF) are more likely to fail. The estimated ageing factor suggests that the failure rate of the network will increase as the CI pipes deteriorate over time.

Table 3-4: Results of the HBP.

Number of failures between 1997 and 2011	Number of pipes	Probability of failure
0	4498	0.0026-0.0034
1	591	0.060-0.063
2	209	0.119-0.122
3	93	0.178-0.182
4	31	0.236-0.240
5	9	0.296-0.299
6	8	0.355-0.358
7	4	0.414-0.417

Table 3-5: Estimated coefficients for the NHPP.

Variables	Coefficients
Constant	-16.92
ln(pipe length)	0.97
Pressure	0.77
NOKPF	0.38
Ageing factor	2.57

3.5.1 Prediction Curve

The ranking performance of the models is first compared using the prediction curve. The interpretation and construction of the prediction curve have already been discussed in Section 3.4.

The prediction curves for the three models are shown in Figure 3-8. The ground truth curve (for selected past failures) represents the ideal situation, where all the pipes that are going to fail in 2013 are selected to be replaced first, followed by the ones that operate without any interruptions. A model is considered to be better in terms of pipe ranking if it is closer to the ground truth, or if it can predict more failures in the network by replacing fewer pipes. When using the prediction curve for model comparison, It is also essential to take into account of the percentage of water mains the water utility can practically replace in a year, which is generally a small percentage of their network (e.g. less than 15%). Therefore, a prediction curve focusing on the first portion of pipe length considered for pipe renewal is shown in Figure 3-9.

A substantial difference between the ground truth curve and the results from the three models can be observed from both figures. The ground truth curve shows that all failures in 2013 can be found in 5% of the total pipe length in the network. However, if the same percentage of pipe length is replaced on the basis of the model predictions, the best model can predict about 20% of the breakage that will occur in 2013.

Comparing the prediction curves (Figure 3-8 and Figure 3-9) between the three models, the performance of the HBP and the BSM are generally better than the NHPP. For example, the prediction curves show that 31% and 32% of failures in 2013, can be found in the first 10% of pipe length in the network with the highest chance of failure based on the HBP and BSM, respectively. However, the NHPP can only predict (or avoid) 26% of failures in 2013 by renewing 10% of pipe length with the highest chance of failure. This is similar to the findings in Kleiner and Rajani (2012), where the NHPP did not dominate the other models they compared with in terms of pipe ranking.

The NOKPF is a major contributing factor to the ranking performance of the models. Figure 3-10 has been plotted to compare the NHPP with and without the NOKPF. The performance of the NHPP with the NOKPF is consistently better than the one without the NOKPF. An improvement up to 15% can be observed from Figure 3-10 (at 20% of total pipe length). Furthermore, the HBP and BSM are purely data-driven models that estimate the probability of failure based on the pipes' failure history. Their ranking performance has shown to be better than the NHPP that has incorporated additional factors (e.g. pipe length) in the model. The NOKPF can be considered as an indicator of the operating condition and environment of a water main. A water main that has experienced many failures in the past are likely to be operating in a harsh environment, leading to a higher chance of failure.

The ranking performance of the HBP, BSM and NHPP have been compared using the prediction curve. The significant difference between the ground truth and the results of the models indicate that there are still rooms for improvements in the pipe failure prediction models. Although the result from the BSM is similar to the HBP and only slightly better than the NHPP, the major advantage of the BSM lies in its simple nature. The failure probability can be easily estimated for a group of pipe given sufficient data, making it an ideal desktop screening tool to identify groups of pipes that are at risk of failure.

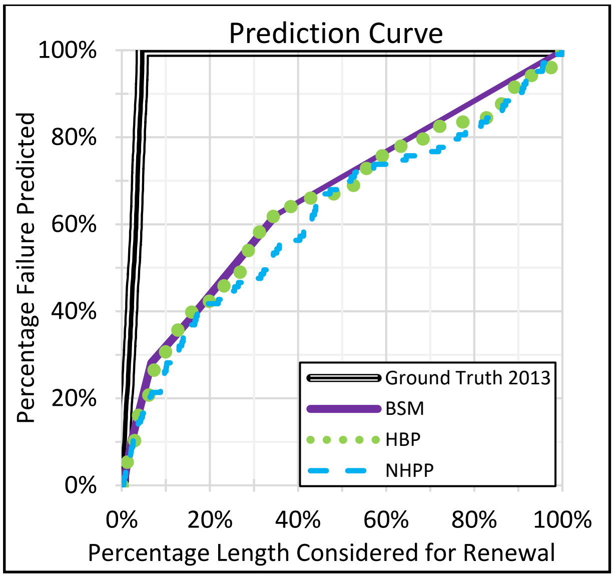

Figure 3-8: Prediction curves for the entire network.

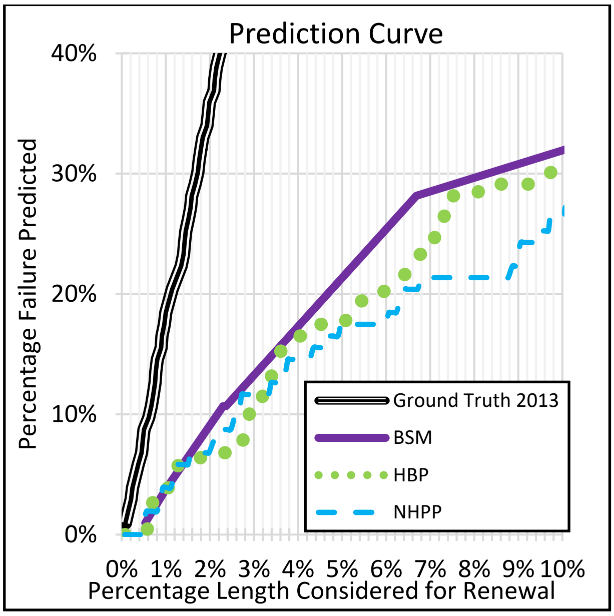

Figure 3-9: Prediction curves for 10% of total pipe length in the network.

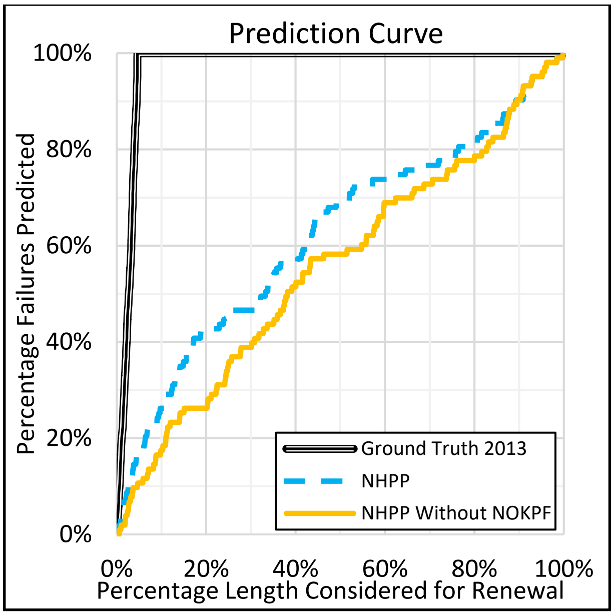

Figure 3-10: Prediction curves comparing the NHPP with and without the NOKPF.

3.5.2 ROC Curve

The ROC curve has been widely used in areas such as signal detection and diagnostic testing (Fawcett, 2006). The curve examines the model's ability in classifying binary data, which is applicable to the current dataset because the failure data have been converted into binary format. The ROC curve is constructed by plotting the sensitivity (true positive rate) against 1-specificity (false positive rate) at various probability thresholds. The calculation of the sensitivity and specificity can be found in Equation (3-12) and (3-13).

$$Sensitivity = \frac{Num\ TP}{P}$$

(3-12)

$$Specificity = \frac{Num\ TN}{N}$$

(3-13)

where $Num\ TP$ is the number of true positive, which represents the number of pipes with a failure in the dataset and also predicted to fail by the model; P is the number of observed failures; $Num\ TN$ is the number of true negatives, which is the number of pipes without any interruptions in the network and also predicted to operate normally by the model; and N is the number of pipe without any interruptions in the failure data.

The probability threshold can be considered as a probability value that divides the water main into "Failure" and "No Failure". A pipe with a higher failure probability than the threshold value is put into the “Failure” group, while a pipe with a lower failure probability than the threshold value is put into the “No Failure” group.

A confusion matrix (Table 3-6) is used to demonstrate the calculation of a point in the ROC curve. The table shows the classification performance of the results from the BSM (Table 3-2) with a probability threshold of 10%. The columns of the matrix represent the observed failure data in 2013. Pipes that have failed are considered as “Failure”, and pipes that operated without any interruptions are considered as “No Failure”. The rows of the matrix are the classification based on the predictions from the BSM with a probability threshold of 10%. There are 29 true positive ($Num\ TP$) instances, 101 false positive instances, 74 false negative instances and 5239 true negative ($Num\ TN$) instances. Out of the 5443 water mains in the dataset, 103 pipes (P) are found to have failed in 2013, while 5340 (N) are found to be operating without any interruptions. Substituting the relevant values from the confusion matrix into Equation (3-12) and (3-13), the sensitivity and specificity are calculated as 0.2816 (29/103) and 0.9811 (5239/5340), respectively (Figure 3-11). Note that the expected failure probabilities from the BSM and the HBP are compared with the probability threshold for classification, while the probability of observing one or more failures in a pipe is compared with the probability threshold for the NHPP.

The area under the ROC curve can be used to compare the performance of different models. The area under the ROC curve represents the probability that a randomly selected pipe with a failure event will be given a higher rank than a random pipe that operates without any interruptions (Fawcett, 2006). Calculating the area under the ROC curve using the entire range of the ROC curve suggests that all the water mains in the dataset will be considered for renewal. However, as stated earlier, water utilities do not have the resources to replace their entire WDN in a year, only a small percentage of their network can be replaced. Therefore, it is more reasonable to calculate the area under part of the ROC curve, which is the partial area under the ROC curve.

If the water utility can replace 15% of the total pipe length in their network each year, the partial area under the ROC curves (standard error in brackets) are found to be 0.008(0.0011), 0.0141(0.0018) and 0.0147(0.0018) for the NHPP, HBP and BSM, respectively. The results suggest that the HBP and the BSM are preferred over the NHPP. The HBP and BSM are more likely to rank a randomly selected water main with a failure higher than a random pipe that operates without any interruptions.

The ranking performance of the three models has been compared using the ROC curve and the prediction curve. The HBP and the BSM were preferred over the NHPP. Although the prediction curve and the ROC curves assess the ranking performance of the models, they do differ in some ways. Both curves plot the percentage of failed pipes predicted correctly (percentage of failures predicted in prediction curve and sensitivity in ROC curve) by the models on the y-axis. However, the x-axis of the ROC curve is based on the number of pipes (the units in the nominator and denominator of specificity are both per pipe), while the x-axis of the prediction curve is calculated using pipe length. In practice, the use of pipe length and the prediction curve would be favoured for the following reasons:

1. The length of each pipe can vary significantly and displaying the results with a "per pipe" basis can induce bias interpretations.
2. The renewal cost of a water main is generally given in cost per meter. This can be directly used to estimate the investment required for replacement if the renewal length is known.

For example, if the water utility wants to reduce the failures by 20% next year using the HBP, the results from the prediction curve in Figure 3-9 shows that they need to replace 5% of the total pipe length in their WDN. This would allow the utility to estimate the cost of renewal. If they want to improve the service level further, they can also estimate the amount of extra investment required. However, these types of assessments are not as straightforward with the ROC curve (Figure 3-11), the renewal length would need to be calculated based on the sensitivity (0.2) and specificity values (1-0.018).

Table 3-6: Confusion matrix for BSM estimation with 10% threshold.

Threshold Probability=10%		Observation: Failure	Observation: No Failure	Observation: Total
Model Estimation	Failure	29	101	130
	No Failure	74	5239	5313
	Total	103	5340	5443

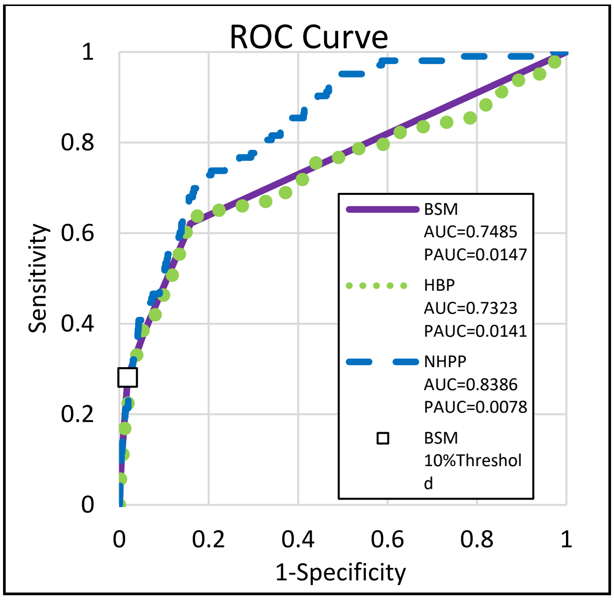

Figure 3-11: ROC Curves for the NHPP, HBP and BSM.

3.5.3 Expected Number of Failures

In addition to understanding the ranking performance of the models, it is also important to compare the number of failures predicted for water main rehabilitation planning and level of service predictions. The predicted number of failures for 2013 is shown in Table 3-7. The pipes have been categorised into groups based on their failure history because the NOKPF is the only common variable in the three models. The Pearson Chi-square test statistics have also been calculated by summing the normalised squared error from each failure group (Equation (3-14)).

$$\chi^2 = \sum_{i=1}^{g} \frac{(Z_i - N_i)^2}{N_i} \qquad (3\text{-}14)$$

where χ^2 is the Chi-square statistic; g is the number of failure groups; Z_i is the observed failures in failure group i; and N_i is the expected number of failures predicted by the model for group i.

The NHPP over-predicts the number of failures in most of the failure groups, except for those with 3 failures. The HBP tends to be more accurate for groups that have experienced more failures, the χ^2 value is extremely high for the group of pipes that have never failed in the past. The BSM under-predicts the number of failures in most of the failure groups. However, the χ^2 values suggest the prediction from the BSM is close to the observed failure data in most cases. Summing the number of failures predicted in each failure group will give the total expected number of failures in the dataset. The prediction from the HBP is the most accurate at the network level, followed by the BSM and then the NHPP.

Table 3-7: Expected number of failures predicted by the models in 2013.

Total number of failures in a pipe up to 2012	Total number of pipes in the group	Total number of failures in 2013	NHPP	NHPP χ^2	HBP	HBP χ^2	BSM	BSM χ^2
0	4498	38	57	6.5	14	44	31	1.4
1	591	23	27	0.56	37	5.0	22	0.060
2	209	13	17	0.99	25	5.9	15	0.30
3	93	18	14	1.1	17	0.10	10	5.7
4	31	5	8.5	1.4	7.4	0.77	4.8	0.0075
5	9	3	3.4		2.7		2.6	
6	8	3	6.1	4.1[2]	2.9	0.20[1]	2.7	0.017[1]
7	4	0	3.9		1.7		1.0	
Total	5443	103	137	15	107	56	90	7.5

[2] Pipes with 5, 6 and 7 failures are grouped together when calculating the test statistics to ensure a frequency greater than 5 for the observed value.

The Chi-square goodness of fit test is performed to determine if the predicted results from the models in the failure groups are consistent with the distribution of the failure data. The null hypothesis states that the distribution for the number of failures predicted by the model in the failure groups is consistent with the underlying distribution of the observed failure data for the failure groups in 2013. Based on the test statistic calculated for the NHPP (15), HBP (56) and BSM (7.5), the null hypothesis is rejected for the NHPP and HBP at 5% significant level. The distribution of the failures predicted in the failures groups by the BSM is likely to be similar to the underlying distribution of the observed failure data in each failure group.

3.5.4 Effect of Covariates

One of the limitations of the BSM and HBP is that covariates, such as pipe length, cannot be included in the model directly. Therefore, to account for the effect of these covariates, the water mains must be manually categorised into cohorts based on the covariate before model calibration. The static water pressure in the NHPP is used to divide the pipes into 3 pressure groups, Low, Medium and High, to investigate the effect of including covariate in the BSM and HBP. Low pressure ranges from 0 to 600 kPa (with 801 pipes), Medium pressure is between 600 kPa and 900 kPa (with 3512 pipes), and High pressure is greater than 900 kPa (with 1130 pipes). Other factors, such as transient pressure (Rathnayaka et al., 2016a and Rathnayaka et al., 2016b), could also be considered if the relevant information is available.

The models are calibrated to the data in each pressure group, and the results for the expected number of failures are presented in Table A - 1, Table A - 2 and Table A - 3 for the High-pressure group, Medium-pressure group and Low-pressure group, respectively. The expected number of failures in each failure group from the different pressure levels are then summed together to produce Table 3-8 and used to calculate the Chi-square statistic. This allows the effect of the additional covariate to be analysed by comparing Table 3-8 with Table 3-7.

The expected number of failures predicted by the NHPP and HBP using pressure groupings show little improvement to the results from Table 3-7. A small reduction in the Chi-square statistic for the NHPP can be observed, but it is not sufficient to change the conclusion of the hypothesis from the Chi-square goodness of fit test. It is likely that the influence of static water pressure has already been captured as a covariate in the NHPP, manually grouping the pipes into different pressure groups will not have a significant impact on the prediction. The HBP is a purely data-driven model, the predicted probability of failure is heavily dependent on the failure history of the pipe. Therefore, the influence of other factors on pipe failure is of little importance to the model.

Table 3-8: Expected number of failures predicted by models in 2013 after pressure grouping.

Total number of failures in a pipe up to 2012	Total number of pipes in the group	Total number of failures in 2013	NHPP	NHPP χ^2	HBP	HBP χ^2	BSM	BSM χ^2
0	4498	38	57	6.2	14	44	32	1.0
1	591	23	27	0.57	37	5.0	23	0.0045
2	209	13	17	1.1	25	5.9	16	0.55
3	93	18	15	0.80	17	0.10	11	4.6
4	31	5	8.3	1.3	7.4	0.77	5.6	0.055
5	9	3	3.2		2.7		2.7	
6	8	3	6.2	4.0[3]	2.9	0.19[2]	2.9	0.11[2]
7	4	0	3.9		1.7		1.3	
Total	5443	103	137	14	107	56	94	6.3

On the other hand, improvements can be found for the BSM by grouping the pipes into pressure cohorts before model calibration. The expected number of failures predicted by the model is closer to the observed failure data compare to the results from Table 3-7, leading to a reduction in the Chi-square statistic. The comparison suggests that splitting the water mains into groups before model calibration can improve the result of the BSM. However, it cannot be concluded whether the improvement is specific to this dataset or due to pressure grouping.

3.5.5 Other Datasets

The NHPP, HBP and BSM are also calibrated to four additional datasets from water utilities in Melbourne to examine the consistency of the models' performance (Table 3-9). Dataset A has been analysed in detail in the previous sections. The diameters of the pipes in the four datasets are all 100mm. Dataset B and D are water mains made of AC, while dataset C and E are cement lined cast iron (CICL) pipes. The models are trained using all available data up to 2012 and validated using the failure data in 2013. Table 3-9 summaries the results from the models for all the datasets, the table shows the expected number of failures predicted by the models, and the percentage of failures predicted from the prediction curve at three different percentage of pipe length considered for renewal.

[3] Pipes with 5, 6 and 7 failures are grouped together when calculating the test statistics to ensure a frequency greater than 5 for the observed value.

Table 3-9: Comparison of NHPP, HBP and BSM using five different datasets.

Scenario Comparison	Model	Dataset (A)	Dataset (B)	Dataset (C)	Dataset (D)	Dataset (E)
Expected Total Number of Failures in Network	Number of Pipes	5443	2242	2033	11518	1386
	Observed Failures in 2013	103	144	133	229	48
	NHPP	134	139	143	282	58
	HBP	107	116	108	205	45
	BSM	90	88	81	171	54
% Failures Predicted by Considering 5% of Total Pipe Length for Renewal	NHPP	16%	9%	10%	9%	14%
	HBP	17%	10%	11%	16%	19%
	BSM	21%	12%	9%	14%	13%
% Failures Predicted by Considering 10% of Total Pipe Length for Renewal	NHPP	26%	18%	17%	20%	27%
	HBP	31%	26%	21%	24%	29%
	BSM	32%	23%	16%	22%	20%
% Failures Predicted by Considering 15% of Total Pipe Length for Renewal	NHPP	35%	30%	25%	25%	39%
	HBP	38%	33%	28%	33%	44%
	BSM	38%	33%	27%	29%	28%

For the expected number of failures predicted, the NHPP over-predicts datasets A, C, D and E; the HBP under-predicts datasets B, C, D and E; and the BSM under-predicts datasets A, B, C and D. The BSM is the least reliable model for predicting the number of failures, it has the largest prediction error for 4 of the datasets (except dataset A). For the HBP and NHPP, their performances are dependent on the dataset under analysis. The HBP has a smaller prediction error for dataset A, D and E, while the NHPP performs better for dataset B and C. Therefore, the comparison suggests that the BSM is unlikely to be suitable for predicting the total number of failures in the network because the model tends to underpredict the number of failures. The NHPP or HBP would be preferred, but the current analysis cannot determine which of the two is more accurate in predicting the number of failures in the network.

The ranking performance of the datasets is examined by comparing the percentage of failures predicted at 5%, 10% and 15% of the total pipe length in the network from the prediction curve. The percentage of failures predicted by the models are similar for most of the datasets. The best model for pipe ranking is found in either the HBP or the BSM. This matches with the observation from dataset A in Section 3.5.1, where the HBP and BSM are preferred over the NHPP in ranking pipes.

The comparison of the ranking performance and the expected number of failures using 5 different datasets suggests that the application of the models depends on the purpose of the analysis. Both the HBP and BSM are favoured over the NHPP for pipe ranking. The advantage of the BSM over the HBP is its simplicity, the model can be programmed in spreadsheet software such as Excel©, making it an ideal preliminary assessment tool for identifying groups of pipes that are likely to fail. On the other hand, the NHPP and HBP are more desirable than the BSM in predicting the total number of failures in a network. There is no particular preference between the NHPP and HBP based on the observation from the 5 datasets. However, the NHPP would be selected for long-term failure predictions because of the limitations that are in the HBP, as well as the BSM. They will be discussed in the next section.

3.5.6 Model Limitation

The failure probability estimated from the BSM and HBP are based on the failure history of the water main. The time and order that the events occurred are not important to the models. Therefore, they cannot capture the deterioration process of the pipe over time. The failure probabilities predicted for the water mains will not change unless additional failure data are added to the calibration process. Using the result of the BSM from Table 3-2 as an example, the probability of failures for the two pipes with 7 failures are always 16.7%, regardless of the number of years the model predicts into the future. This suggests that the HBP and the BSM are only suitable for short-term failure analysis because the condition of the water mains will not change significantly. However, for long-term failures predictions, the NHPP will be preferred because it can capture the deterioration of the water mains over time.

It is also difficult to incorporate the influence of other factors (e.g. pipe length) into the BSM and HBP. Although Section 3.5.4 suggested a possible solution to the problem, there are several of limitation with it. Firstly, splitting a continuous variable (e.g. pipe length and pressure) into categorical groups can be difficult, the number of categories and the range have to be decided by the user, this could introduce bias into the model. The complexity of the grouping grows rapidly as the number of factors to be considered in the model increases. It could also lead to groups with insufficient failure data for calibration. Finally, the method suggested in Section 3.5.4 cannot be applied to time dependent factors that are discussed in Rajani and Kleiner (2008) and Kleiner and Rajani (2012). The HBP and BSM cannot take into consideration the change in the time dependent variable overtime because the models do not differentiate the order of the failure events.

The performance of the NHPP has been limited in the current study. A small number of covariates was used to model the failures in the network. Introducing additional covariates, such as time dependent factors, can enhance the accuracy of the model predictions. In addition, to maintain the consistence of the failure data used for the three models, the failure data only show whether a water main experienced a failure or not in a year, it does not provide information on the number of failures in a year. The NHPP should be used for count data, and therefore the strength of the NHPP was not fully utilised.

3.6. Conclusion

The chapter has compared the performance of the predictions from BSM, NHPP and HBP. The prediction curve and ROC curve have shown that the BSM and HBP are favoured for pipe ranking, while the NHPP and the HBP are preferred for predicting the total number of failures in the network. The major findings and the implications of the analysis are summarised below based on the datasets used in the analysis:

- The variable, NOKPF, is a crucial factor for pipe ranking. The ranking performance of the NHPP can improve up to 15% by including the NOKPF in the model. The purely data-driven model, the HBP and BSM, performs slightly better than the NHPP by only considering the failure history (NOKPF) of the water mains during model calibration.
- The BSM was developed in the research undertaken in this chapter. The simplistic nature of the BSM makes it an ideal preliminary desktop assessment tool for identifying groups of pipes that are more likely to fail. The model can be easily built into common spreadsheet programs like Excel©.
- The HBP and NHPP can both be used for predicting the number of failures in the network in the short-term. However, only the NHPP should be used for long-term failure predictions. The NHPP can account for the deterioration of the water mains and capture the change in failure rates over time. Therefore, the NHPP is more suitable to be used in rehabilitation planning.
- The HBP and BSM cannot incorporate any time dependent factors in the model. They cannot capture the deterioration of the water mains or any factors that are time dependent (e.g. climate factors). Therefore, the methods are unreliable for long-term predictions. The chapter proposed a method to incorporate pipe dependent covariates into the two models by dividing the assets into groups. However, there are several limitations with the proposed method, such as the optimal number of groups and the complexity of the grouping as the number of factors to be considered increases.

Although the prediction curve of the HBP and BSM are better than the NHPP, they are still far from the ground truth. This suggests that there are areas that can be improved upon for better pipe failure predictions. The HBP, BSM or the NHPP could be used as a baseline for models developed in the future. One of the many possible solutions that were considered in this project is to combine statistical failure data with physical deterioration mechanics. The combined approach will be discussed in Chapter 5. The next chapter will investigate the predictions of failures in the network with time dependent factors. Time dependent factors, such as temperature (Rajani et al., 2012), have shown to improve the accuracy of the NHPP in estimating failures in the network, but they were not included in the NHPP in this chapter. Prediction using these variables are difficult because their values are unknown in the future. Therefore, a method will be proposed to overcome the problem.

CHAPTER 4: PREDICTING FAILURES USING TIME DEPENDENT FACTORS IN THE NON-HOMOGENEOUS POISSON PROCESS

4.1. Introduction

The factors that influence the failure of water mains can be broadly classified into pipe dependent factors, time dependent factors and the pipe and time dependent factors (Kleiner and Rajani, 2008). Pipe dependent factors are fixed properties of the water main, such as pipe length and pipe diameter, and they have been studied extensively by researchers. Time dependent factors are variables that changes over time and are applicable to all pipes, such as seasonality. Pipe and time dependent factors are variables that vary over time and depend on the characterise of the pipe. The number of known past failures (NOKPF) is a pipe and time dependent factor that has been used as a stratification criterion (Andreou et al., 1987; Andreou et al., 1987; and Park, 2011) and a covariate in models (Røstum, 2000 and Kleiner and Rajani, 2008).

The investigation of other time dependent and pipe and time dependent factors for pipe failure predictions has increased in recent times. These factors have been able to improve the performance of statistical models (Rajani et al., 2012 and Claudio et al., 2014)). Studies (Kleiner and Rajani, 2002 and Babykina and Couallier, 2012) have found that omitting time dependent variables could lead to biased estimation of the coefficients if the failures are influenced by time dependent factors. Although, the inclusion of time dependent and pipe and time dependent factors have demonstrated to be beneficial to some statistical models (e.g. NHPP). Using these two types of variables to predict pipe failure events are challenging because their values are unknown in the future.

The first part of the chapter will investigate a network that is covered with reactive soils. The network experiences many failures in summer with little rainfall. Therefore, it is crucial for the water utility to have an estimate on the number of failures beforehand so that additional resources can be allocated in time without impacting on the level of service. The minimum monthly antecedent precipitation index (MMAPI) (calculated using rainfall data) is used to model failures in the area. It has been identified as a significant variable in modelling pipe failures in the region (Gould et al., 2009 and Gould et al., 2011). Time-lags (e.g. Jan MMAPI value to estimate Feb failures) will also be introduced to the MMAPI because of the correlation identified between the number of failures in the network and the rainfall from the last two or three months. The MMAPI is constructed using the rainfall data obtained from the Melbourne Regional Office weather station in Melbourne by the Bureau of Meteorology (2016).

The aim is to compare the performance of the time dependent factor, the MMAPI with different time-lag, in predicting the total number of failures and identifying the influence of significant covariates that contributes to water main failures using the NHPP. By introducing time-lag into the MMAPI, the NHPP can be used to predict failures using the MMAPI values that have been observed. This would allow the water utility to adjust their immediate operational planning strategies to accommodate for the possible increase in failure events, especially for networks with failures that are significantly influenced by climate factors (or other time dependent factor).

The second part of the chapter will investigate the prediction of pipe failures using the pipe and time dependent factor, the NOKPF, in the NHPP. During the prediction period, the model will first simulate the number of failures in the network, then the simulated number of failures are added to the failure history of the pipe to make predictions for the next year. The performance of the NHPP with failure simulation will be compared with the NHPP without the NOKPF, and the NHPP with a constant NOKPF in the prediction period.

4.2. Time Dependent Non-homogeneous Poisson Process (NHPP)

Time dependent and pipe and time dependent covariates can be incorporated into the NHPP by modifying the intensity function in Equation (3-1) (Kleiner and Rajani,2012). Let $N(T)$ represents the total number of failures for the pipe up to month T ($T = 1,2, \dots T_s$); $\underline{\boldsymbol{z}}$ be the vector of pipe dependent covariates; $\underline{\boldsymbol{A}}$ be the vector of coefficients corresponding to the pipe dependent covariates in $\underline{\boldsymbol{z}}$; $\underline{\boldsymbol{\phi}(\boldsymbol{T})}$ be the vector of time dependent and pipe and time dependent covariates in month T; $\underline{\boldsymbol{a}}$ be the vector of coefficients corresponding to covariates in $\underline{\boldsymbol{\phi}(\boldsymbol{T})}$; t represents the time to failure for the pipe in month T; and δ be the shape parameter of the failure intensity function (the scale parameter is incorporated as a constant term into $\underline{\boldsymbol{z}}$ as $z_0 = 1$ as in the normal NHPP). The failure intensity of the NHPP that is described by the power law model is given in Equation (4-1), and the expected number of failures in a month (between month T_a and $T_a - 1$) for pipe i can be estimated using Equation (4-2).

$$\mu(t) = \delta \mathrm{t}^{\delta-1} e^{\underline{\boldsymbol{z}_i'\boldsymbol{A}}+\underline{\boldsymbol{\phi}_i(\boldsymbol{T})'\boldsymbol{a}}} \tag{4-1}$$

$$E\big(N_i(T_a) - N_i(T_a - 1)\big) = \int_{T-1}^{T} \mu(t)dt = \big(T_a^{\delta} - (T_a - 1)^{\delta}\big) e^{\underline{\boldsymbol{z}_i'\boldsymbol{A}}+\underline{\boldsymbol{\phi}_i(\boldsymbol{T})'\boldsymbol{a}}} \tag{4-2}$$

The coefficients ($\underline{\boldsymbol{A}}$ and $\underline{\boldsymbol{a}}$) and the shape factor (δ) are estimated using the method of Maximum Likelihood (Yang and De Angelis, 2013). The likelihood function for a WDN with m pipes can be expressed as:

$$L = \prod_{T=1}^{T_s} \left\{ \prod_{i=1}^{n} \left[\prod_{j=1}^{m_{Ti}} \mu\left(t_{Tij}\right) \right] e^{-\left((T+1)^{\delta} - T^{\delta}\right) e^{\underline{z_i'A} + \underline{\phi_i(T)'\alpha}}} \right\}$$

(4-3)

where T_s is the number of months that the failure data have been collected; n is the number of pipes; m_{Ti} is the number of failures in pipe i observed in month T; and t_{Tij} is the *j*-th failure of the *i*-th pipe in month T.

A monthly time-step is selected because of the high correlation (discuss in Section 4.4.2) between the MMAPI and the total number of monthly failures. In addition, breaking down the model into smaller time-steps (e.g. weekly) may not be practical as the aggregated number of failures in the time-interval might be insufficient to train the model.

4.3. Performance Indexes

The performance of the NHPP is examined using the log-likelihood ratio (LR) test (Fox, 2008), the mean absolute error (MAE) (Chatfield, 2000) and the root mean square error (RMSE) (Chatfield, 2000).

The LR test is a statistical test that compares the goodness of fit of two models, a full model and a reduced model. The covariates in the reduced model are a proper subset of those included in the full model (there must be at least one additional covariate in the full model that is not in the reduced model). The LR test determines whether the extra covariate or group of covariates in the full model is significant with respect to the reduced model. The null hypothesis states that the additional covariate or group of covariates in the full model are not significant (the coefficients of the additional factors are equal to 0) and the reduced model is preferred. The alternative hypothesis states that the extra covariate or group of covariates in the full model are significant and the full model is preferred. The level of significance is the probability that the null hypothesis is rejected given that it is true and a significance level of 5% is chosen for the study.

Let LRT be the log-likelihood ratio test statistic; $L_{G,k}$ represents the maximum value of the log likelihood function for the full model with k covariates; and $L_{R,k-p}$ represents the maximum value of the log-likelihood function for the reduced model with p fewer covariates than the full model. The log-likelihood ratio test statistic (LRT) can be calculated using the following equation:

$$LRT = 2\left(\ln L_{G,k} - \ln L_{R,k-p}\right)$$

(4-4)

The LRT is approximately a Chi-square distribution with a degree of freedom equal to p.

Both the RMSE and MAE measure the difference between the model predictions and the observed failure data. However, outliers are penalised heavily with the RMSE because the errors are squared during the calculation. Let $Z_i(T)$ be the observed number of failures in month T; T_s represents the number of months that the failure data have been collected; $N_i(T)$ represents the total number of failures estimated by the model for pipe i up to month T; and m represents the total number of water mains, the equation to calculate the MAE and RMSE are shown in Equation (4-5) and (4-6), respectively.

$$MAE = \frac{1}{T_s}\sum_{T=1}^{T_s}\left|\sum_{i=1}^{m} E[N_i(T) - N_i(T-1)] - \sum_{i=1}^{m} Z_i(T)\right| \tag{4-5}$$

$$RMSE = \sqrt{\frac{1}{T_s}\sum_{T=1}^{T_s}\left(\sum_{i=1}^{m} E[N_i(T) - N_i(T-1)] - \sum_{i=1}^{m} Z_i(T)\right)^2} \tag{4-6}$$

4.4. Predicting Failures in Water Mains by Applying Time-lag on Time Dependent Climate Factor

The following section will introduce the data and covariates used to model the failures in the WDN for the time dependent NHPP. The covariates are first analysed systematically to determine its influence on pipe failure. Then the NHPP with different length of time-lag applied to the MMAPI is compared using the performance indexes and graphical plots. Finally, the potential usage and limitation of predicting future failures in the WDN by applying time lag to the time dependent covariates are discussed.

4.4.1 Pipe Asset and Failure Data

The time dependent NHPP is analysed using failure data provided by a water utility in Melbourne. The service area of the water utility is known to be covered with reactive soil that has high shrink/swell potential. Many failures have been observed in the area during dry summer periods. The performance of the time dependent NHPP will be compared using 100mm CICL pipes and AC pipes. A summary of failure data from the two pipe materials is shown in Table 4-1. Note that the recorded data show the total number of failures in a month, but they are plotted as lines in the figures in the chapter instead of discrete points for better visualisation.

The NHPP will consider pipe dependent, time dependent and pipe and time dependent covariates in the model. The pipe dependent factors examined include pipe length (in log form) and soil reactivity. The pipe length is a factor commonly used to account for the difference in the number of failures between pipes with different length. The water mains that are longer in the two datasets are found to have a higher failure rate (Figure 4-1). The reactivity of the soil is a categorical variable that provides an indication on the level of stress increase from the swelling/shrinkage of the reactive soil when the soil moisture content changes. There are four classes of reactivity: ST represents negligible shrink/swell potential; SE represents low shrink/swell potential; EX represents moderate shrink/swell potential; and VE represents very high shrink/swell potential (Gould, 2011). More than 90% of the pipes in the two datasets are found in EX and VE soils, therefore it is likely that a change in moisture content will have a significant impact on the failure rate of the datasets. This is also demonstrated in Figure 4-2, where the two expansive soil classes (EX and VE) have a much higher failure rate (in both failure per pipe and failure per km) than the two less expansive soil classes (ST and SE).

Table 4-1: Pipe asset information.

Cohort Properties	CICL	AC
Construction year	1950-1996	1922-1982
Observation period	1998-2013	1998-2013
Pipe length (km)	585	170
Number of failures	8521	2193
Average failure rates (failures/year/100km)	91	81

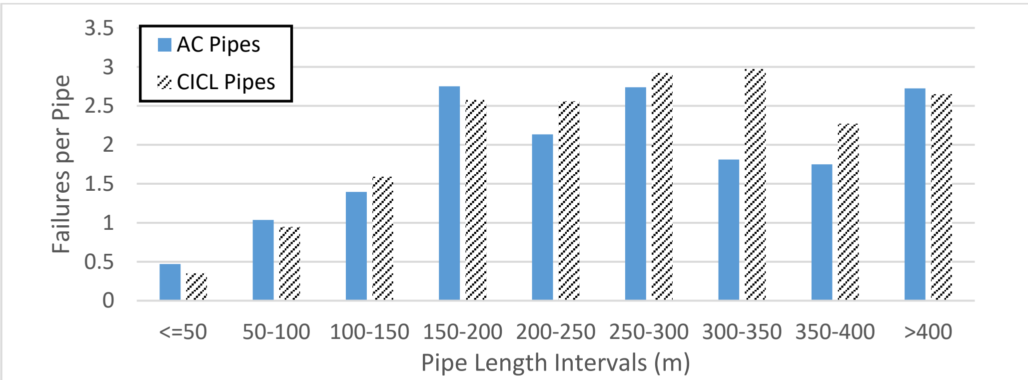

Figure 4-1: Failures in different pipe length intervals.

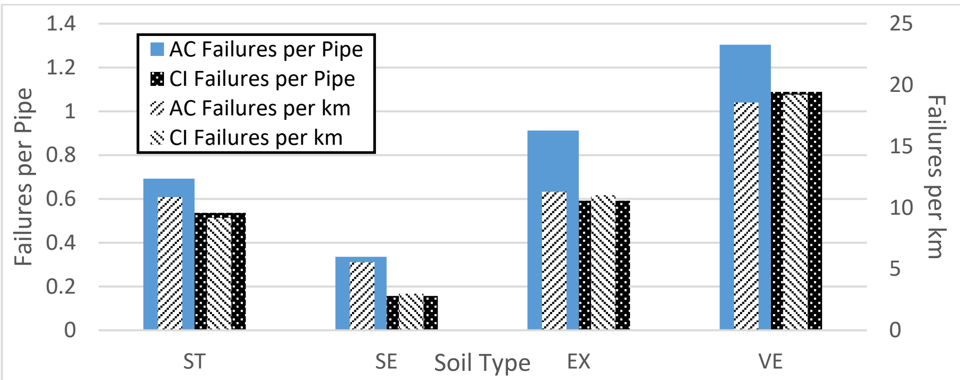

Figure 4-2: Failures in different soil types.

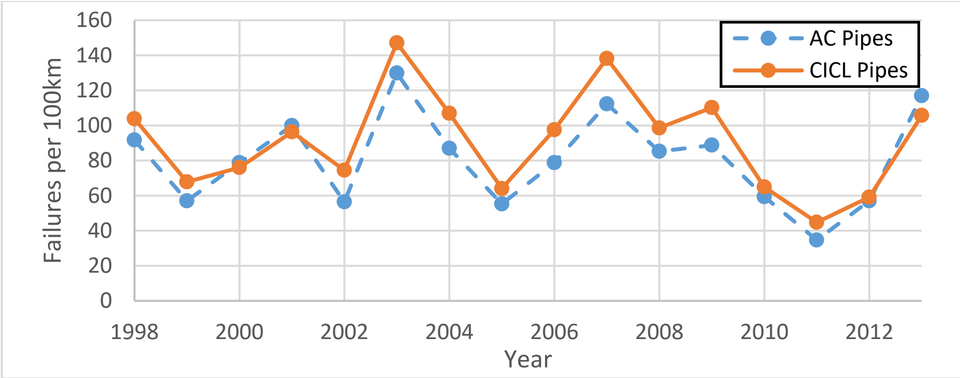

Figure 4-3: Failure per 100km for AC and CICL pipes.

Two time dependent covariates have been considered in the model. The MMAPI is a time dependent factor incorporated in the NHPP because a strong negative correlation with the failure rate has been observed by Gould et al. (2009) and Gould et al. (2011). In addition, the variable can be regarded as a surrogate measure for the soil moisture content, and in regions covered with reactive soil (such as the current study), the change in the soil moisture content can lead to significant increase in the bending stress. The calculation of the MMAPI will be discussed in detail in Section 4.4.2. The other time dependent covariate to be included in the NHPP is the categorical variable, the four seasons (spring, September to November; summer, December to February; autumn, March to May; and winter, June to August). This variable accounts for the seasonal failure patterns that might be present in the failure data but could not be captured by the other covariates in the model.

There are two pipe and time dependent factors in the NHPP. The first one is the age of the water main that represents the average deterioration of the pipes in the network. Figure 4-3 shows the failure rate over the observation period for both datasets. Large year-to-year variations can be observed from the plot, but there is no clear upward trend in the failure rate for both pipe materials. The second pipe and time dependent covariate included in the NHPP is the NOKPF, it has been used in a number of studies involving the NHPP (Røstum, 2000; Kleiner and Rajani, 2012; and Chik et al., 2017) In general, the average time to failure tends to decrease as the water main experience more failures, which are also observed for both materials in this study (Figure 4-4 and Figure 4-5). The root cause of this can be due to a combination of several factors from the external (e.g. pipe laid in areas covered with corrosive soil) and internal environments (e.g. high static pressure) of the pipe. The NOKPF can represent some of these unknown or unmeasurable effects in the operating environment of the water main and account for the higher failure rates (or shorter time to next failure) in pipes that have experienced more failures. It must be noted that the NOKPF used to estimate the failures in time T is the total number of failures the water main has experienced up to time $T-1$. The covariate is held constant during the validation period because future failures are unknown. The failure history of the water mains at the end of the training period will be used for predictions in the validation period. A possible alternative is to simulate the failures for the next year using the failure prediction model and update the NOKPF before making further predictions. The NOKPF also needs to be transformed into a categorical variable (e.g. Pipes with 1 breaks, 2 breaks and more than 2 breaks) to avoid over-predicting the number of breaks. This will be demonstrated in the second part of this chapter in Section 4.5.

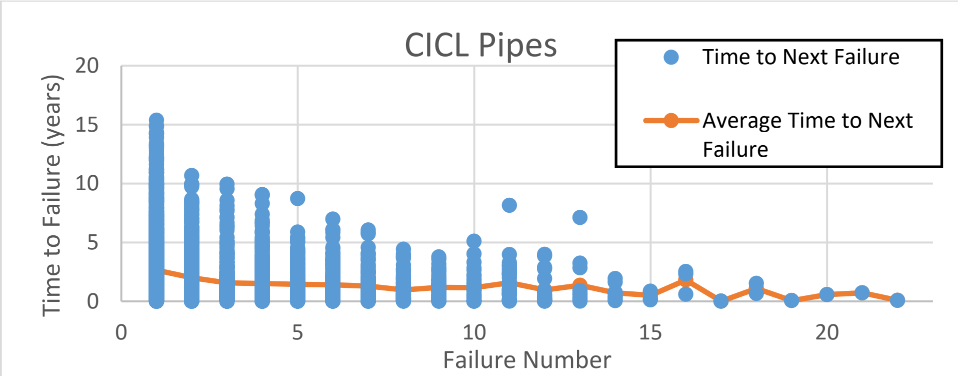

Figure 4-4: CICL pipe time to next failure based on the number of failures recorded.

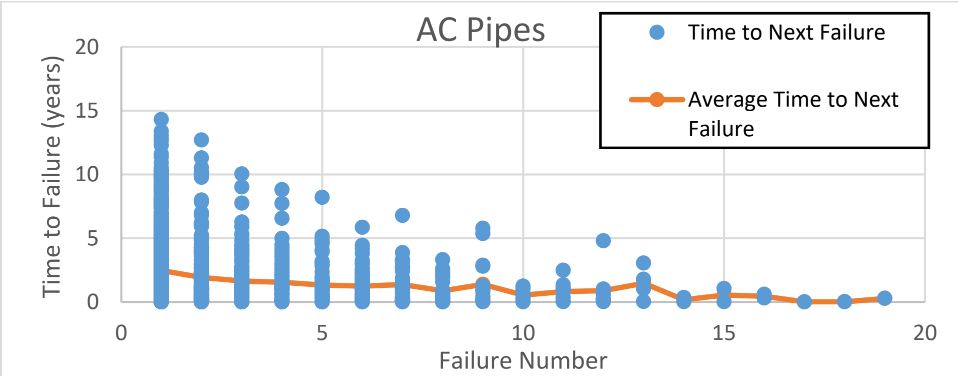

Figure 4-5: AC pipe time to next failure based on the number of failures recorded.

Six interaction terms, MMAPI-Summer, MMAPI-Autumn, MMAPI-Winter, MMAPI-ST, MMAPI-EX and MMAPI-VE, are also considered in the model. The MMAPI and season interaction terms will reflect the influence of the MMAPI during different seasons, while the MMAPI and soil interactions will try to capture the effect of the MMAPI in different soil types. The interaction terms using other covariate combinations were not considered as they are assumed to be independent of each other.

A list of the covariates, the training period and the length of time-lag applied to the MMAPI are shown in Table 4-2 and Table 4-3 for the CICL dataset and AC dataset, respectively. The NHPP will be calibrated using 5 years (1998-2002), 10 years (1998-2007) and 15 years (1998-2012) of failure data, the remaining failure data after the training period will be used for model validation. The time-lag applied to the MMAPI is from 0 (T0) to 3 (T3) months and is shown in brackets after the training period. In the table, 1998-2002(T2), means that the NHPP is calibrated using the failure data from 1998 to 2002, and a 2-month lag is applied to the MMAPI.

With the number of covariates that are considered in the model, conducting an exhaustive search to find the best combination of covariates would require many trials (2^{15}, 9 covariates + 6 interaction term). To reduce the number of models estimated, the following steps are undertaken to determine the most suitable combination of covariates to predict the failures in the two datasets:

1 Find the significant covariates
   - 1.1 Estimate the coefficients for all the covariates. Apply the LR test to each individual variable.
   - 1.2 Remove the insignificant covariates based on the results of the LR test. The remaining significant covariates in the model are referred to as M1.

2 Considering M1 from 1.2
   - 2.1 For each of the season and soil factors that are found to be significant in M1, apply the LR test to check if their interaction with the MMAPI is significant with respect to M1.
   - 2.2 Estimate the coefficients for M1 with the addition of all the interaction terms that are found to be significant from 2.1. The final model is referred to as M2.

For example, in the initial M1 model, only the two-soil type, EX and VE, are found to be significant. In step 2.1, the significance of the interaction between the two-soil type and the MMAPI is examined, one at a time. A LR test is first applied to determine if API-EX is significant with respect to the covariates in M1 (EX and VE). Then the LR test is applied again to determine the significance of API-VE with respect to the covariates in M1 (EX and VE). If API-EX is only interaction term that is found to be significant, the coefficients for the covariates, EX, VE and API-EX, will be estimated in step 2.2 for the M2 model.

It must be kept in mind that during the model selection process, the significance of two or more covariates (or interaction terms) was not tested. Therefore, the M1 and M2 model obtained by following the steps described above cannot be guaranteed to produce a model with the best covariate combination.

Table 4-2: List of training periods and significant covariates for CICL pipes.

Mat	Training Period	API k	Ageing factor	Constant (z_0)	ln(Pipe Length)	NOKPF	Min Monthly API	Season			Soil Reactivity			MMAPI-Summer	MMAPI-Autumn	MMAPI-Winter	MMAPI-ST	MMAPI-EX	MMAPI-VE
								Summer	Autumn	Winter	ST	EX	VE						
CICL (M1)	1998-2002(T0)	0.96	1.46	-7.14	0.21	0.52	-0.03	0.75	0.70	0.27	1.43	1.55	1.98						
	1998-2002(T1)	0.97	1.49	-7.84	0.21	0.53	-0.02	0.86	0.79	0.39	1.43	1.56	1.97						
	1998-2002(T2)	0.85	1.50	-8.11	0.21	0.53	-0.02	0.96	0.84	0.46	1.43	1.56	1.97						
	1998-2002(T3)	0.85	1.50	-8.18	0.21	0.53	-0.12	0.99	0.82	0.33	1.43	1.56	1.97						
	1998-2007(T0)	0.98	1.36	-6.97	0.33	0.33	-0.02	0.95	0.80	0.29	1.13	1.26	1.69						
	1998-2007(T1)	0.98	1.39	-7.41	0.33	0.33	-0.01	1.00	0.84	0.34	1.13	1.27	1.69						
	1998-2007(T2)	0.85	1.41	-7.65	0.33	0.34	-0.01	1.04	0.85	0.33	1.13	1.27	1.69						
	1998-2007(T3)	0.87	1.44	-8.00	0.33	0.34	-0.09	1.01	0.79	0.22	1.13	1.27	1.69						
	1998-2012(T0)	0.98	1.20	-6.55	0.43	0.24	-0.02	0.99	0.85	0.33	1.06	1.22	1.66						
	1998-2012(T1)	0.98	1.18	-6.72	0.43	0.24	-0.02	1.01	0.86	0.37	1.07	1.22	1.66						
	1998-2012(T2)	0.85	1.16	-6.79	0.43	0.24	-0.01	1.01	0.89	0.38	1.07	1.22	1.66						
	1998-2012(T3)	0.98	1.15	-6.78	0.43	0.24	-0.01	0.94	0.94	0.36	1.07	1.22	1.66						
CICL (M2)	1998-2002(T0)	0.96	1.48	-7.59	0.21	0.53	-0.02	1.41	1.67	-0.87	1.43	1.55	1.97	-0.02	-0.03	0.03			
	1998-2002(T1)	0.97	1.50	-8.11	0.21	0.53	-0.01	1.49	0.81	0.03	1.43	1.56	1.97	-0.03	0.00	0.01			
	1998-2002(T2)	0.85	1.51	-8.41	0.21	0.53	0.00	1.78	0.78	0.40	1.43	1.56	1.97	-0.04	0.00				
	1998-2002(T3)	0.85	1.51	-8.23	0.21	0.53	-0.09	0.96	0.97	0.34	1.43	1.56	1.97		-0.07				
	1998-2007(T0)	0.98	1.40	-8.15	0.33	0.34	0.00	2.29	1.99	-0.22	1.13	1.27	1.69	-0.02	-0.02	0.01			
	1998-2007(T1)	0.98	1.41	-8.14	0.33	0.33	0.00	1.97	1.39	0.23	1.13	1.27	1.69	-0.02	-0.01	0.00			
	1998-2007(T2)	0.85	1.41	-8.05	0.33	0.33	0.00	1.78	1.09	0.28	1.13	1.27	1.69	-0.01	0.00	0.00			
	1998-2007(T3)	0.87	1.43	-8.28	0.33	0.34	0.00	1.44	1.18	0.33	1.13	1.27	1.69	-0.12	-0.12				
	1998-2012(T0)	0.98	1.22	-7.78	0.43	0.24	0.00	2.28	1.95	0.55	1.06	1.26	1.90	-0.02	-0.02	0.00		0.00	0.00
	1998-2012(T1)	0.98	1.18	-6.89	0.43	0.24	-0.01	1.30	0.86	0.07	1.07	1.22	1.79	-0.01		0.01			0.00
	1998-2012(T2)	0.85	1.15	-7.00	0.43	0.24	-0.01	1.44	1.04	0.42	1.07	1.22	1.66	-0.01	0.00	0.00			
	1998-2012(T3)	0.98	1.14	-6.79	0.43	0.24	-0.01	1.07	0.94	0.36	1.07	1.22	1.66	0.00					

Table 4-3: List of training periods and significant covariates for AC pipes.

Mat	Training Period	API k	Ageing factor	Constant z_0	ln(Pipe Length)	NOKPF	Min Monthly API	Season			Soil Reactivity			MMAPI-Summer	MMAPI-Autumn	MMAPI-Winter	MMAPI-ST	MMAPI-EX	MMAPI-VE
								Summer	Autumn	Winter	ST	EX	VE						
AC (M1)	1998-2002(T0)	0.97	0.76	-3.64	0.10	0.59	-0.03	0.65	0.59		1.56	1.70	2.06						
	1998-2002(T1)	0.96	0.78	-4.10	0.10	0.60	-0.01	0.72	0.63	0.31	1.56	1.71	2.06						
	1998-2002(T2)	0.95	0.79	-4.40	0.10	0.60	-0.14	1.00	0.77		1.56	1.71	2.06						
	1998-2002(T3)	0.85	0.80	-4.31	0.10	0.60	-0.13	0.88	0.67		1.56	1.71	2.06						
	1998-2007(T0)	0.98	0.36	-0.79	0.20	0.34	-0.02	1.00	0.72		0.75	0.93	1.35						
	1998-2007(T1)	0.98	0.40	-1.32	0.20	0.34	-0.01	1.04	0.73		0.75	0.94	1.36						
	1998-2007(T2)	0.98	0.42	-1.77	0.20	0.34	-0.18	1.04	0.62		0.75	0.95	1.36						
	1998-2007(T3)	0.87	0.44	-2.05	0.20	0.35	-0.10	1.12	0.74		0.76	0.96	1.36						
	1998-2012(T0)	0.98	0.26	-0.05	0.28	0.26	-0.02	1.01	0.71		0.59	0.69	1.08						
	1998-2012(T1)	0.98	0.23	-0.13	0.28	0.25	-0.01	1.01	0.71		0.58	0.69	1.08						
	1998-2012(T2)	0.98	0.22	-0.42	0.28	0.25	-0.16	1.03	0.59		0.58	0.69	1.08						
	1998-2012(T3)	0.98	0.20	0.04	0.28	0.25	-0.01	0.95	0.79		0.58	0.68	1.08						
AC (M2)	1998-2002(T0)	0.97	0.77	-4.71	0.10	0.60	0.01	2.07	2.21		1.56	1.55	2.30	-0.06	-0.07			0.01	-0.01
	1998-2002(T1)	0.96	0.79	-4.58	0.10	0.60	0.00	1.64	0.67		1.56	1.71	2.06	-0.02					
	1998-2002(T2)	0.95	0.80	-4.57	0.10	0.61	-0.07	1.40	0.77	0.28	1.56	1.54	2.39	-0.17				0.07	-0.15
	1998-2002(T3)	0.85	0.80	-4.23	0.10	0.60	-0.17	0.88	0.67		1.56	1.52	2.15					0.08	-0.04
	1998-2007(T0)	0.98	0.39	-2.04	0.20	0.34	0.00	2.10	0.76		0.75	1.17	2.16	-0.02				0.00	-0.02
	1998-2007(T1)	0.98	0.41	-2.22	0.20	0.34	0.00	1.91	0.77		0.75	1.12	1.94	-0.02				0.00	-0.01
	1998-2007(T2)	0.98	0.40	-2.07	0.20	0.34	0.01	1.53	0.70		0.75	0.99	1.77	-0.23				-0.02	-0.21
	1998-2007(T3)	0.87	0.44	-2.20	0.20	0.35	-0.05	1.30	0.75		0.76	0.94	1.60	-0.06				0.01	-0.08
	1998-2012(T0)	0.98	0.28	-2.07	0.28	0.26	0.01	2.62	2.18		-0.63	1.17	2.08	-0.03	-0.03		0.02	-0.01	-0.02
	1998-2012(T1)	0.98	0.23	-0.89	0.28	0.25	0.00	1.57	0.72		-0.10	1.12	1.88	-0.01			0.01	-0.01	-0.01
	1998-2012(T2)	0.98	0.21	-0.94	0.28	0.25	0.07	1.41	0.98		0.58	0.85	1.51	-0.15	-0.18			-0.07	-0.19
	1998-2012(T3)	0.98	0.20	0.04	0.28	0.25	-0.01	0.95	0.79		0.58	0.68	1.08	0.20					

4.4.2 Antecedent Precipitation Index

A number of different indicators have been considered to represent the soil moisture content. They are the minimum daily antecedent precipitation index (API) in each month, the average daily API in each month, the maximum daily API in each month, the maximum daily rainfall in each month, the average daily rainfall in each month and the minimum daily rainfall in each month. The minimum daily API in each month had the highest correlation with the monthly failures in the dataset. In addition, the wetting and drying of soils can cause ground movement (soil shrinkage and swelling) in reactive soils, generating addition bending stress on the pipe and increase its chance of failure. The API values follow a similar wetting and drying process to the soil moisture content, which increases during a rainfall event (soil wetting, increase in soil moisture), and decreases if no rainfall is received (soil drying, decrease in soil moisture). The change in API would be able to capture some of the change in bending stress as a result of the change in soil moisture content. Therefore, the MMAPI is selected to model the failures in the datasets.

Before the MMAPI can be determined, the daily API ($API(d)$) must be calculated. The daily API is a time series that depends upon its value from yesterday and the amount of rainfall today. $API(1)$ is taken as the first day of 1990 with $API(0)$ equal to 0. The daily API can be calculated using Equation (4-7) shown below:

$$API(d) = k * API(d-1) + Rainfall(d) \tag{4-7}$$

where $Rainfall(d)$ is the recorded rainfall in day d and k $(0 < k < 1)$ is a decay factor subjected to the condition of the region under study. It can be considered as the percentage of rainfall that is retained in the soil at the end of the day and generally ranges from 0.85 to 0.98 (Linsley et al, 1982). The MMAPI value for each month can be constructed by extracting the minimum daily API in each month.

The determinate factor for the values of MMAPI is the decay factor used in Equation (4-7). Other studies (Boulaire et al., 2009; Gould et al., 2009; and Gould et al., 2011) in the same region have used a constant k of 0.85 for all analysis. In this project, The MMAPI is calculated using k values between 0.85 and 0.98 at a step size of 0.01. The k value that results in the highest correlation between the MMAPI and the total number of monthly failures in the datasets will be selected. The k values used for the NHPP with different training periods and length of time lag is shown in column 3 of Table 4-2 and Table 4-3 for CICL and AC pipes, respectively.

Figure 4-6 and Figure 4-7 plot the monthly failure (y-axis) against the MMAPI (x-axis) between 1998 and 2013 with k=0.98 for the CICL and AC dataset, respectively. The figures show that the MMAPI and the monthly failures have a negative correlation (-0.51 for CICL and -0.4 for AC pipe). The number of failure events in a month tends to decrease as the MMAPI increases. This type of relationship has also been observed for the k values shown in Table 4-2 and Table 4-3.

Figure 4-8 and Figure 4-9 plots the MMAPI with k=0.98 (left y-axis) and the recorded number of monthly failures (right y-axis) for CICL and AC pipes, respectively. The average MMAPI over the observation period is 63.83mm. There is no cyclic seasonal pattern that can be observed from the figures. However, some relationship can be found between the monthly failures and the MMAPI. An extreme peak in the monthly failures is always accompanied by a low MMAPI. Considering Figure 4-8 and Figure 4-9, a large number of failures has been recorded at the start of 2001, 2003, 2004, 2007, 2008, 2009 and 2013 for both materials. The MMAPI corresponding to these peak failure events are less than 40mm and are lower than the average MMAPI (63.83mm) in the period. It must be noted that even though a peak in the monthly failures is always associated with a low MMAPI, a low MMAPI does not always produce a peak in the monthly failures. This could be attributed to the so-called purging effect. The purging effect can cause consecutive extreme climate events (e.g. low temperature) to have different failure rates, possibly due to the removal of pipes close to failure by one extreme event, thereby reducing the pipes available to fail in a similar successive event.

Habibian (1994) has observed the purging effect as a result of water temperature drop. The study found that the water temperature dropped to a similar value in two periods within a month, but the average number of failures during the first temperature drop was much higher than the second temperature drop (the magnitude of the drop was similar). The author believed that the first cold front had failed the weakest water mains in the system, the remaining water pipes will be able to withstand a similar event. However, if the temperature drops to a new low or sufficient time have been given for some pipes to deteriorate severely, then a surge in the number of failures might be observed again.

The purging effect is only present for part of the two datasets. In Figure 4-8 and Figure 4-9, the lowest MMAPI during 2003 to 2005 is very similar, but the peak monthly failures are not. There is a reduction in the number of failures for the peak events over the three years, with 2003 being the highest. On the other hand, the purging effect was not observed between 2007 and 2009. The lowest MMAPI in the three years is similar, and only a small decrease in the peak failures can be found in 2008 for CICL pipes and in 2008 and 2009 for AC pipes.

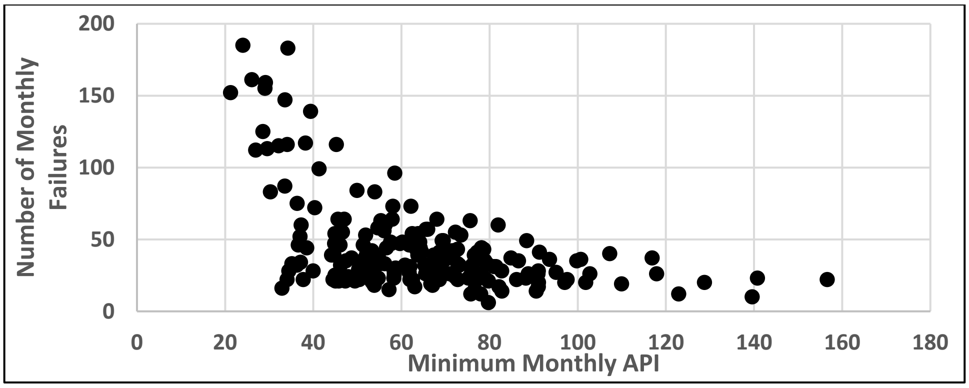

Figure 4-6: Scatter plot of monthly failures vs MMAPI for CICL pipes.

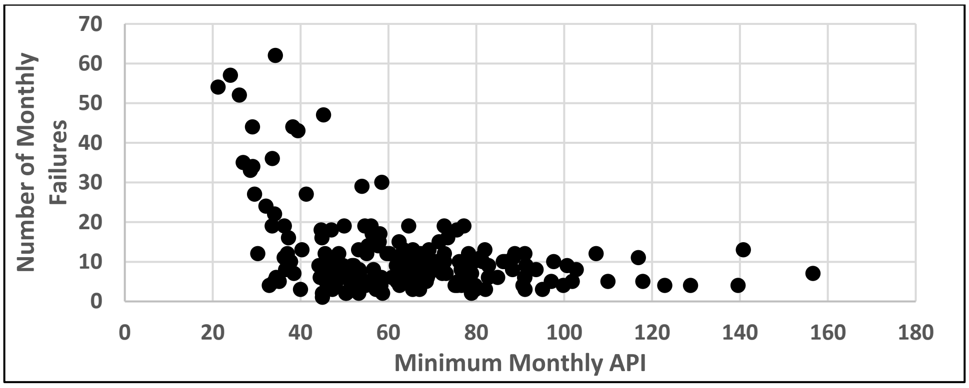

Figure 4-7: Scatter plot of monthly failures vs MMAPI for AC pipes.

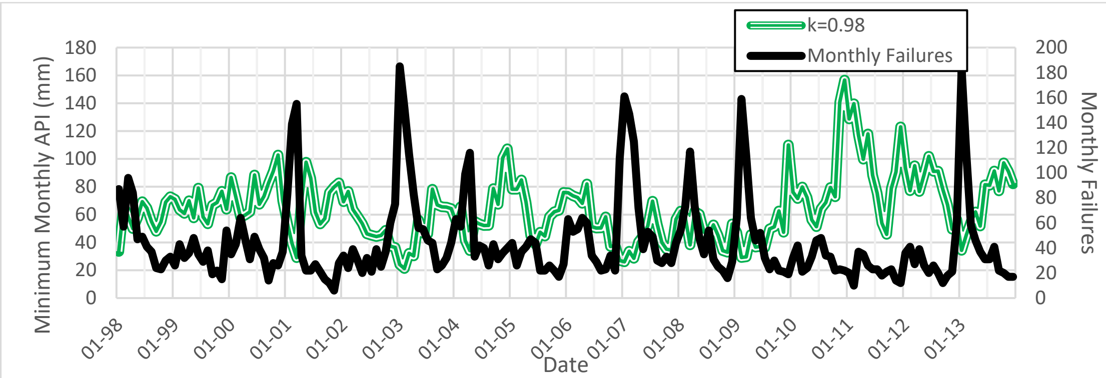

Figure 4-8: MMAPI for k=0.98 and the total number of monthly failures for CICL pipes.

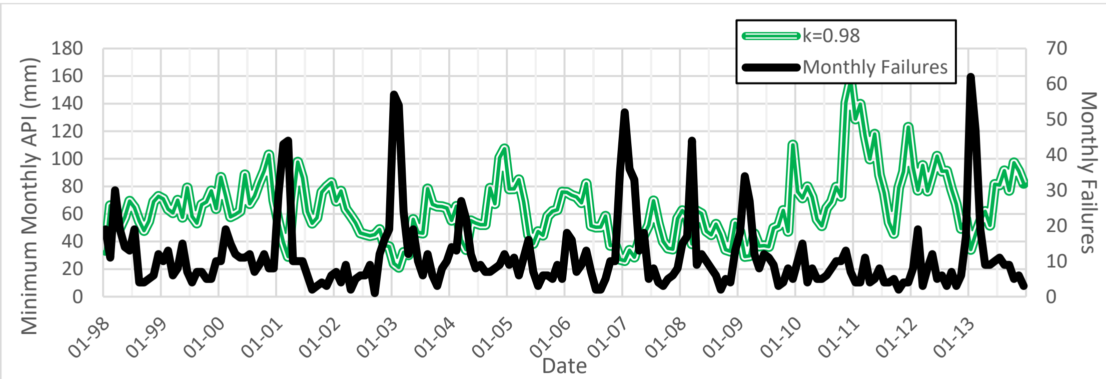

Figure 4-9: MMAPI for k=0.98 and the total number of monthly failures for AC pipes.

4.4.3 Results and Discussions

4.4.3.1. Covariates Influence

The influence of each covariate on the failures predicted by the NHPP is systematically analysed using the CICL dataset. Five NHPPs with different combinations of the covariates (excluding interaction terms) have been calibrated using failure data between 1998 and 2012. The decay factor (k) used to calculate the MMAPI has been set to 0.85 for all the models. The number of monthly failures estimated and predicted by the five models is plotted with the observed failure data in Figure 4-10.

Subplot (a) in Figure 4-10 shows the number of monthly failures estimated by the NHPP using pipe age and pipe length (in log form) as covariates. An increasing trend in the number of monthly failures can be observed from the plot, suggesting that the average condition of the water mains is deteriorating over time. The results from subplot (a) will be considered as a baseline and used to identify the effect of the other covariates in the remaining four NHPP.

The NOKPF is included in the NHPP in subplot (b) of Figure 4-10. The inclusion of the NOKPF has increased the failures estimated by the NHPP near the end of the period but decreased the failures estimated at the start of the period. The NOKPF represents the failure history of the water mains at the time of estimation (or prediction). At the start of the period, its contribution to the number of failures is small because failures have not yet been recorded. As the failure history of the water mains becomes available over time, the variables start to increase the number of failures estimated by the model.

Subplot (c) in Figure 4-10 incorporates the MMAPI into the baseline model. Since the MMAPI is a time dependent factor that is used as a measure for the change in soil moisture content over time, some of the monthly variations in the failures have been captured by the covariate. However, the model cannot capture the extreme monthly failure events over the observation periods. The monthly failures are underestimated significantly for some months in 2001, 2003, 2004, 2007, 2008, 2009 and 2013.

The NOKPF and the MMAPI are built into the baseline model in Figure 4-10 (d). The monthly variations from the MMAPI can be clearly observed from the plot. The influence of the NOKPF identified from subplot (b) can also be seen by comparing Figure 4-10 (d) with Figure 4-10 (c). The model still lacks the ability to capture the peak failure events in the observation period.

The final NHPP is comprised of pipe length (log form), pipe age, NOKPF, MMAPI, soil, and season. The number of failures estimated by the NHPP is shown in subplot (e) of Figure 4-10. A comparison of subplot (e) with subplot (d) shows that the inclusion of the soil and seasonal covariates have enhanced the performance of the NHPP in capturing the peak monthly failure events. More failures are found in summer and autumn compared to spring and winter.

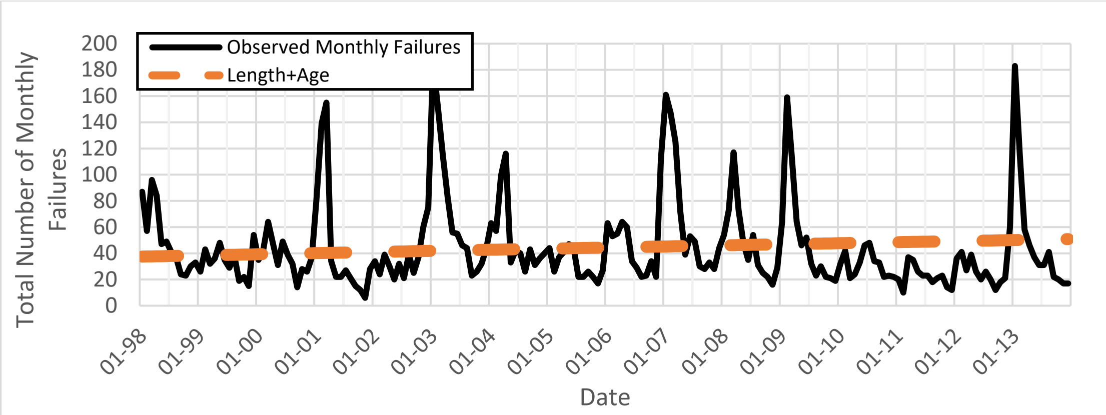

(a)

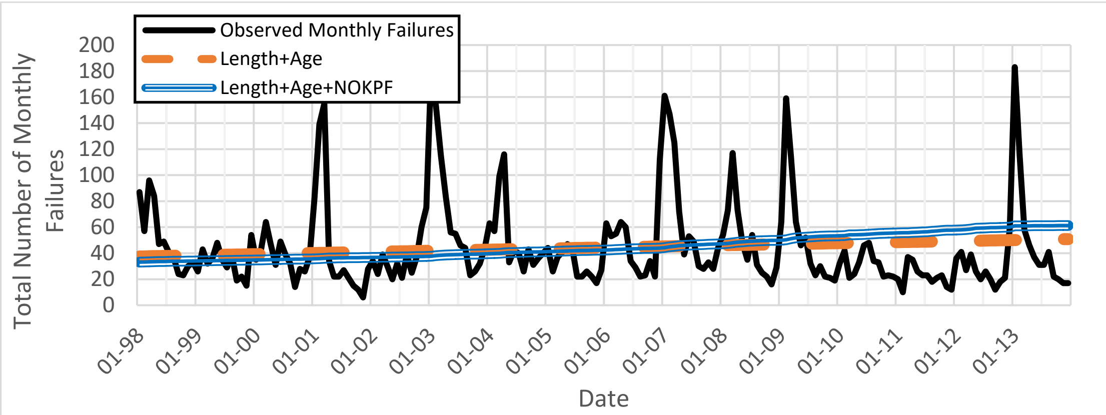

(b)

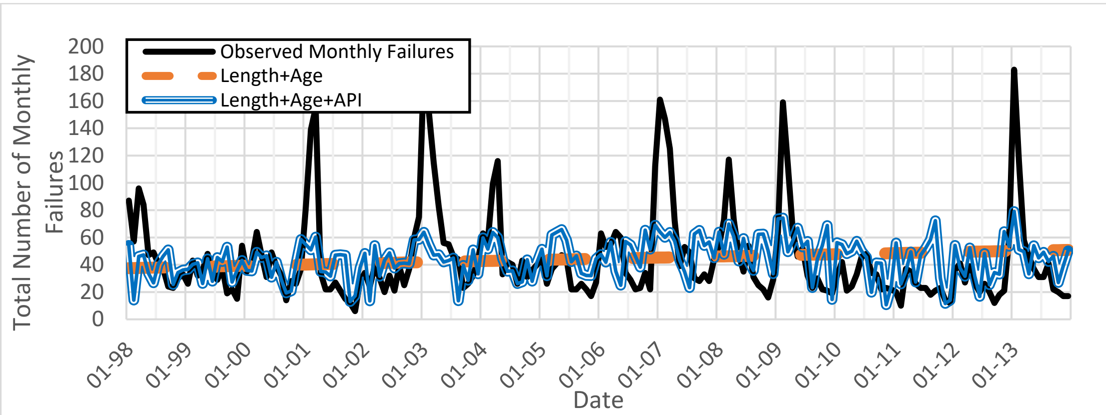

(c)

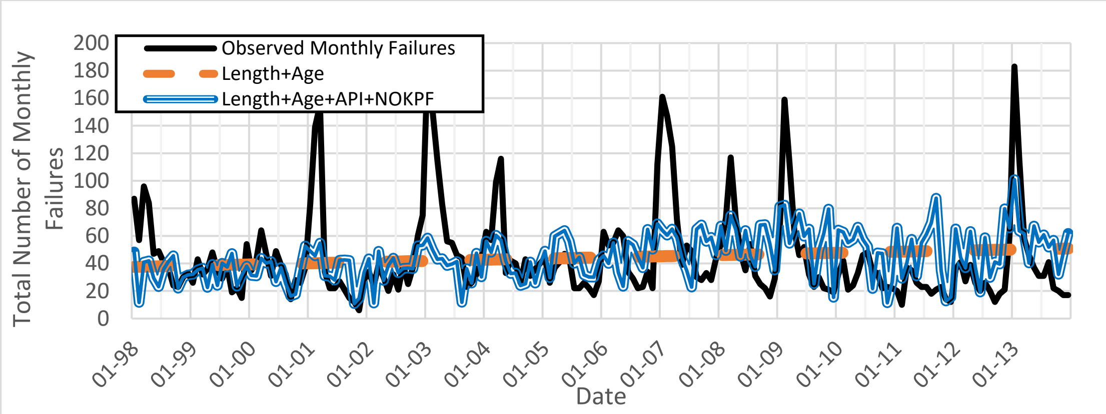

(d)

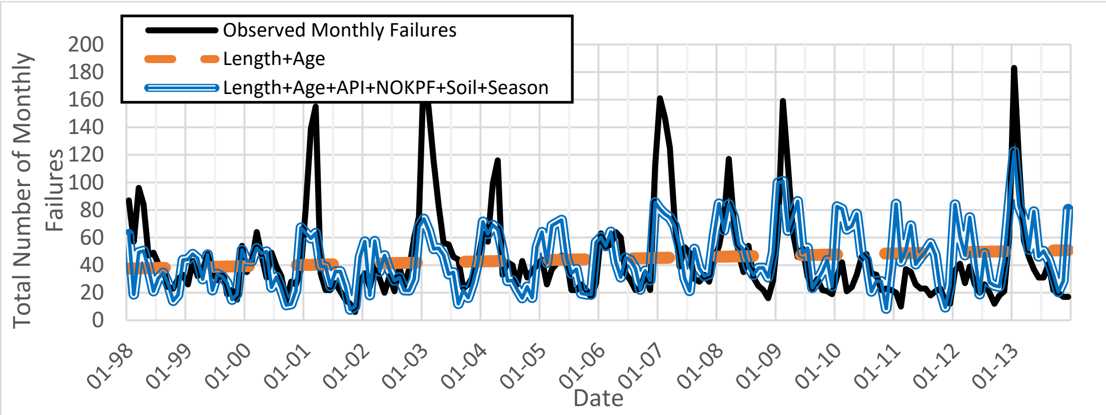

(e)

Figure 4-10: Estimated and observed monthly failures for (a): Length and Age; (b): Length, Age and NOKPF; (c): Length, Age and API; (d): Length, Age, API and NOKPF; (e): Length, Age, API, NOKPF, Soil and Season.

4.4.3.2. Model Comparison

Table 4-2 and Table 4-3 show the coefficients estimated for the NHPPs with different training periods and time-lags in the MMAPI for CICL and AC pipes, respectively. During each time step, the water main can only belong to one level in the categorical variable. For example, a water main cannot be laid in EX and SE soil at the same time. For the seasonal covariates, the water main will switch from season to season, but it will not occupy two seasons in a single time step. Note that the two tables only show 3 out of the 4 levels in the two categorical covariates. The remaining level (spring and SE soil) have been accounted by the coefficient estimated for the constant term. The covariate is not significant in the NHPP if its corresponding cell in the table is empty.

The covariates in the NHPP for the CICL datasets are all significant regardless of the training periods and length of time-lag applied to the MMAPI. On the other hand, the season, winter, is found to be not significant in most of the NHPPs for the AC dataset, except for one instance. This is suggesting that the average number of failures in AC water mains are similar during spring and winter, given that all other covariates are held constant. The influence of time-lag in the MMAPI is reflected in the coefficients estimated for the time dependent covariates, the effect on the coefficients estimated for the pipe dependent covariates is limited.

The outcomes of the significant covariates inspected in the models are as anticipated beforehand, except for the ageing factor for AC pipes. The interpretation of the coefficients for the following paragraphs has assumed that all other covariates are held constant.

The models suggest that longer pipes are expected to have a higher number of failures. Water mains that have experienced more breaks (higher NOKPF) in the past are also more likely to fail in the future. The coefficients estimated for the MMAPI indicate that failure rates are higher during periods with low MMAPI. Gould et al. (2009), Boulaire et al. (2009) and Gould et al. (2011) also identified the same type of relationship in their studies between the MMAPI and the monthly failures. The results for the two categorical covariates, season and soil, agrees with the observations from Gould et al. (2009) and Gould et al. (2011). The water mains laid in expansive soils (EX and VE) are more likely to fail, and the monthly failures tend to peak during summer.

The ageing factors estimated for the NHPPs are dependent on the training period selected for calibration. The length of time-lag applied to the MMAPI has a negligible effect on the ageing factor. For both material types, the ageing factors are smaller for models with a longer training period. It is suggesting that the water mains are degrading at a slower rate over time, which is different from the general expectation. After the initial burn-in phase, the water main is expected to degrade at a constant or increasing rate over time as shown in the bathtub curve (Figure 1-1). A plausible explanation for this is due to the climate effect. Melbourne had experienced an extended drought period starting from the beginning of the observation period, generating a high level of bending stress on pipes laid in reactive soils, leading to a high number of failures. As the drought wears off around the year 2010 and 2011, the rise in rainfall increased the moisture content in the soils and released some of the bending stress acting on the pipe, which reduced the number of failures in the datasets.

In addition to the unexpected observations for the ageing factors with different training periods, the ageing factors for the AC dataset suggest that the average condition of the water mains is improving over time (ageing factor less than 1). This is also counter-intuitive as the failure rate of the pipe would only decrease during the burn-in phase. The AC pipes under investigation have already passed the burn-in phase and are more likely to be in the in-usage phase of the bathtub curve (Figure 1-1). The NHPP for the AC water mains might have omitted some significant covariates, such as the omission of drought effect discussed in the last paragraph. Furthermore, it is difficult to capture the climate effect with the inclusion of a single time dependent factor. This might have introduced bias into the AC pipe models as other significant time dependent climate factors have been left out of the model (Kleiner and Rajani 2002 and Babykina and Couallier, 2012).

Most of the interaction terms between the season and the MMAPI are significant for the CICL datasets. The interaction between MMAPI and summer and the interaction between MMAPI and expansive soils (EX and VE) is significant for AC pipes. The common significant interaction term in the two datasets, MMAPI and summer, suggests that the change in failure rate due to a unit change in the MMAPI during summer is different to a unit change in the MMAPI in other seasons.

4.4.3.3. Performance Indexes and Graphical Plots

The MAE and RMSE have been calculated for the NHPPs for the entire observation period (Table 4-4). The model with a smaller MAE and RMSE is preferred because it implies that the estimations from the model are more accurate.

The T0 models (no time-lag applied to MMAPI) are the most accurate model in both materials. They have the lowest MAE and RMSE. The error tends to increase as the length of time-lag applied to the MMAPI increases. Therefore, the performance indexes suggest that the NHPP with no time-lag applied to the MMAPI provides the most accurate estimation of the total number of failures. In regard to the performances of the M1 and M2 models, the inclusion of interaction terms in the M2 models have led to a lower MAE and RMSE with respect to the M1 models for some cases, but the improvements are minor. In other cases, the inclusions of interaction terms are found to be redundant, and the MAE and RMSE have increased in the M2 models compared to the corresponding M1 models. Since the additional interaction terms only provide minor enhancement to the M1 models and are redundant in some cases, it would be more efficient to only consider the simpler M1 models for pipe failure modelling.

Figure 4-11 to Figure 4-14 show the number of monthly failures estimated by the NHPP (both M1 and M2 models plotted). The dataset, length of the training period and the length of time-lag are displayed on the title of the figures. For example, CICL (1998-2008 T0) plots the results for the number of monthly failures in the CICL datasets calibrated using the failure data between 1998 and 2007, and no lag is applied to the MMAPI. The results for the T2 and T3 models for the same training period are shown in APPENDIX B.

The plots show that the results of the models are similar, except for the peak failure events. During the peak failure events (such as January 2003 and 2013), the T1, T2, and T3 models are further away from the observed monthly failures compared to the T0 models. The discrepancy also tends to be higher for models with a longer lag in the MMAPI, and therefore, the T3 models perform poorly. This is consistent with the results from the performance indexes, where errors are generally larger for models with a longer time lag in the MMAPI.

Comparing the monthly failures estimated by the M1 and M2 models in the same figure, the results are very similar. The monthly failures estimated by the M2 models during peak failure events tend to be higher than the M1 models, leading to a higher RMSE for some of the M2 models. The number of failures for the other NHPPs shown in Table 4-2 and Table 4-3 has not been plotted because similar observations to those discussed have been found.

Table 4-4. Performance indexes for CICL and AC Pipes.

Mat	Training Period	MAE (M1)	MAE (M2)	$RMSE$ (M1)	$RMSE$ (M2)
CICL	1998-2002(T0)	17.1	16.7	21.7	22.5
	1998-2002(T1)	20.0	19.6	27.2	26.6
	1998-2002(T2)	21.5	21.4	28.9	29.4
	1998-2002(T3)	22.9	22.7	31.3	31.2
	1998-2007(T0)	17.6	17.4	23.8	23.9
	1998-2007(T1)	21.0	21.1	29.3	29.7
	1998-2007(T2)	22.8	22.8	32.0	32.3
	1998-2007(T3)	25.4	25.3	35.3	36.2
	1998-2012(T0)	14.9	13.8	20.4	18.8
	1998-2012(T1)	17.8	17.7	26.0	25.8
	1998-2012(T2)	19.1	18.9	28.2	27.8
	1998-2012(T3)	19.2	19.1	29.5	29.4
AC	1998-2002(T0)	5.7	5.1	7.8	6.9
	1998-2002(T1)	6.1	5.9	8.8	8.4
	1998-2002(T2)	6.3	6.1	8.7	8.5
	1998-2002(T3)	6.7	6.7	9.5	9.6
	1998-2007(T0)	5.1	4.9	7.0	6.7
	1998-2007(T1)	5.7	5.6	8.4	8.4
	1998-2007(T2)	6.0	6.0	8.6	8.6
	1998-2007(T3)	6.7	6.7	9.8	9.9
	1998-2012(T0)	4.7	4.1	6.7	5.9
	1998-2012(T1)	5.3	5.2	8.1	7.9
	1998-2012(T2)	5.5	5.3	8.3	8.1
	1998-2012(T3)	5.6	5.6	9.0	9.0

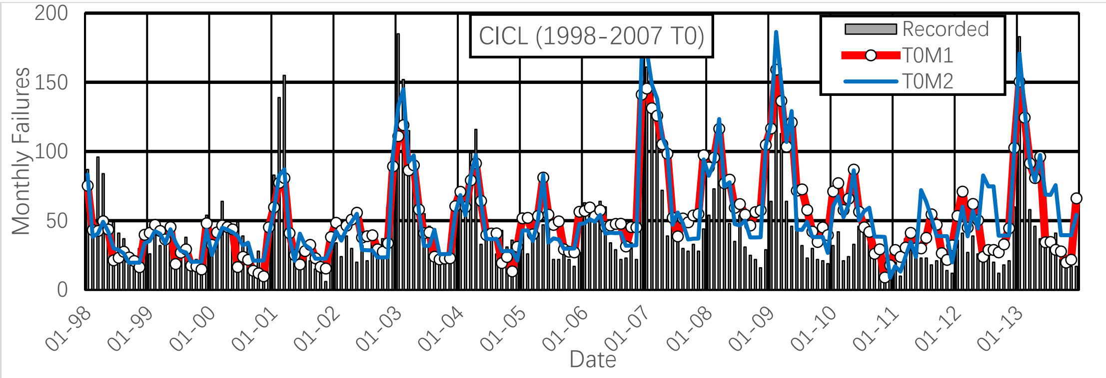

Figure 4-11: CICL dataset T0 monthly failures.

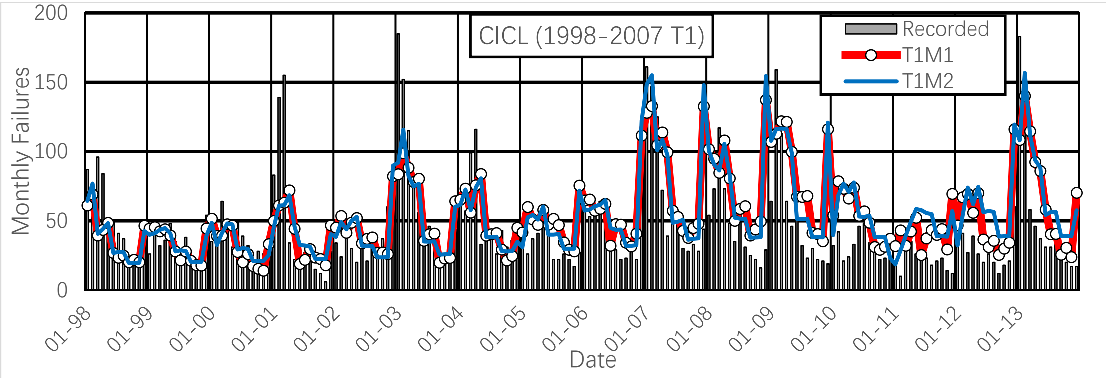

Figure 4-12: CICL dataset T1 monthly failures.

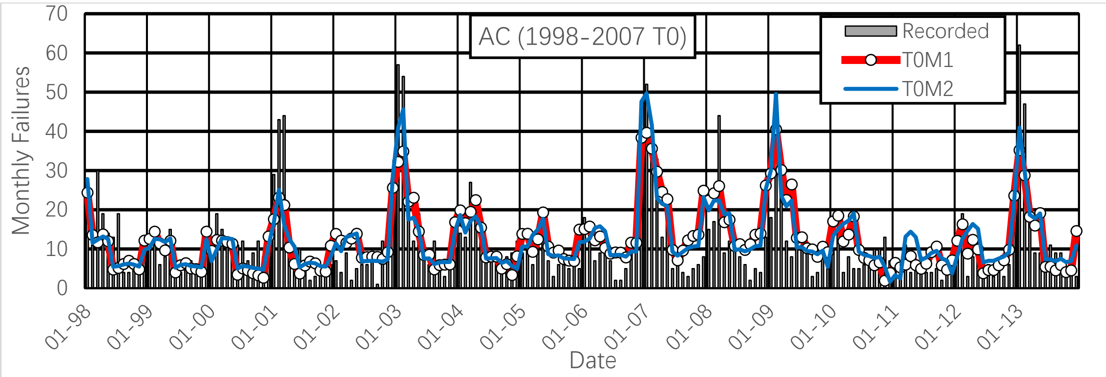

Figure 4-13: AC dataset T0 monthly failures.

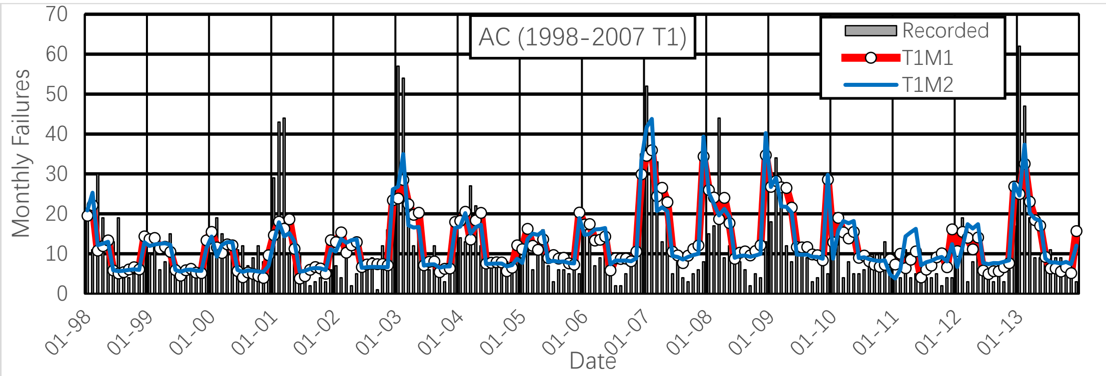

Figure 4-14: AC dataset T1 monthly failures.

The performance of the models in making predictions for individual water mains are also examined by investigating the ranking of the pipes. The number of breaks predicted for the individual pipe is not compared directly because the failures were grouped together in the calibration process, making the predictions only reliable at group/network level.

The ranking performance of the models is examined following a similar approach to Kleiner and Rajani (2012), but other methods can also be used (Claudio et al., 2014; Li et al., 2014; and Chik et al., 2017). Consider a group of pipes with 0 to n failures during the validation period:

1 Let $N = n$

2 Loop from 1 to n

  2.1 Collect the pipes with a total of N or more failures in the validation period into a list. The list is referred to as L_f and has m_N pipes.

  2.2 Rank the pipes in descending order based on the total number of failures predicted for the pipe in the validation period. The first m_N pipes that have been predicted with the highest probability of failure are put into list L_M.

  2.3 Record the number of water mains that are in both list L_f and L_M, they are referred to as a hit (H).

  2.4 $N = N - 1$

The models that are better at ranking would give a higher probability of failure to water mains that will fail. Therefore, the model that has more hits will be preferred and could be used in the prioritization of water main rehabilitation.

The number of hits for models with a training period from 1998 to 2002 and 1998 to 2007 is shown in Table 4-5 for both materials. The number of hits for the models with the same training period is very similar. The influence of time-lag in the MMAPI is nearly negligible when considering pipe ranking. The primary factor that influences the ranking performance of the model for the water mains is likely to be the NOKPF. An improvement of up to 15% has been found by Chik et al. (2017) when the NOKPF is included in the NHPP. The NOKPF can partly capture the shorter time to next failure as the water main experienced more failures, leading to a higher probability of failure estimated by the model.

Table 4-5: Comparison of ranking performance.

Training Period	n	Pipes with failures $\geq n$	NHPPT0	NHPPT1	NHPPT2	NHPPT3
1998-2002 CICL	16	2	0	0	0	0
	15	3	0	0	0	0
	14	5	1	1	1	1
	13	7	1	1	1	1
	12	10	1	1	1	1
	11	12	1	1	1	1
	10	27	1	1	1	1
	9	43	7	7	7	7
	8	71	17	17	17	17
	7	114	34	35	34	34
	6	187	55	54	54	54
	5	299	98	98	98	98
	4	467	170	171	170	170
	3	802	325	326	325	326
	2	1392	697	693	690	688
	1	2630	1545	1543	1543	1546
1998-2007 CICL	9	1	1	1	1	1
	8	6	2	2	2	2
	7	15	3	3	3	3
	6	27	4	4	4	4
	5	58	12	12	12	12
	4	133	39	39	39	39
	3	294	96	96	94	94
	2	655	265	268	269	269
	1	1640	877	876	878	878
1998-2002 AC	15	2	0	0	0	0
	14	3	0	0	0	0
	12	4	1	1	1	1
	11	6	1	1	1	1
	10	10	1	1	1	1
	9	17	3	3	3	3
	8	22	4	4	4	4
	7	37	7	7	7	7
	6	50	10	10	10	11
	5	83	26	26	26	26
	4	119	39	39	39	39
	3	211	79	79	79	79
	2	348	176	176	176	177
	1	625	354	355	355	355
1998-2007 AC	11	1	0	0	0	0
	9	2	0	0	0	0
	8	5	1	1	1	1
	7	9	1	1	1	1
	6	12	1	1	1	1
	5	29	7	7	7	7
	4	47	11	10	10	10
	3	89	30	30	30	30
	2	171	61	60	60	60
	1	386	199	199	200	199

4.4.4 Model Potentials and Limitations

In the previous section, the length of time-lag applied to the MMAPI has shown to impact on the accuracy of the model predictions. The number of monthly failures estimated by the T0 models provides the best match to the training and validation failure data. However, the T0 model cannot predict failures in the future without knowing the future rainfall. This difficulty presented has limited the application of the T0 models.

On the other hand, the models with time-lag applied to the MMAPI can predict the number of failures in the future. The prediction of future rainfall scenario is not required because recorded rainfall from the past is used to calculate the MMAPI. The length of prediction depends on the length of time-lag applied to the MMAPI. The T1, T2 and T3 model can predict the number of failures for the next 1, 2 and 3 months, respectively.

Although making predictions using the models with time-lag is not as accurate as the T0 models, the T1 and T2 models can still predict failures in the network ahead of time with reasonable accuracy using the MMAPI. Most statistical models are applied to small diameter pipes (≤300mm), which are generally renewed in a reactive manner. These pipes will remain in service until a specific failure threshold has been exceeded. Therefore, the predictions at a network level from the models with time-lag in the MMAPI can be considered as the number of repair jobs that have to be done for the next one or two months. For network similar to the one under study, where failures are strongly influenced by the MMAPI (or other time dependent factors), the prediction using MMAPI with time-lag will allow the water utility to arrange the required resource (e.g. addition crews and materials) to satisfy the demand of future repairs in a timely manner.

4.5. Predicting Failures in Water Mains by Simulation

The remainder of the chapter will investigate the usage of the NOKPF for long-term failure predictions. The NOKPF has been used as a covariate in some models (Røstum, 2000; Kleiner and Rajani, 2012; and Chik et al., 2017) and as a stratification criterion in others (Andreou et al., 1987; Andreou et al., 1987; Mailhot et al., 2000; and Park, 2011). Since the NOKPF is pipe and time dependent, the value that it takes for the water mains is unknown in the future. The failure prediction model can be used to simulate future failures. This can be feedbacked to update the NOKPF for predictions. The time dependent NHPP has already been described in Section 4.2.

The NOKPF is converted into a categorical variable for the simulation study, where each level represents the number of failures the water main has experienced in the past. This format is used because the impact on the number of failures from a unit change in the NOKPF might not be linear. For example, the first failure event might increase the failure probability of the water main by 10%, but the second failure event could increase the failure probability by 50%. In addition, if the NOKPF can take all positive integer values as well as 0, the prediction from the NHPP will eventually approach infinity when the simulated failures are used to update the NOKPF.

Let T_0 and T_c be the start and end of the training period, respectively; $NOKPF_i(T_c)$ represents the NOKPF for pipe i at time T_c (may not be a whole number); $NOKPF\_P_i(T_c)$ represents the NOKPF group pipe i belongs to at time T_c; $E[N_i(T_c+1)-N_i(T_c)]$ represents the expected number of failures for pipe i at time T_c+1; $N_{s,i}(T_c+1)$ be the number of failures simulated for pipe i at time T_c+1. The process used to predict failures by simulating the NOKPF is described below:

1 Calibrate the NHPP using failure data between T_0 and T_c.
2 Calculate $NOKPF_i(T_c)$ from the failure data by summing the failures that have been recorded during the training period.
3 For iter=1 to number of simulations
  3.1 For j=1 to number of prediction years
    3.1.1 Predict the expected number of failures for each water main ($E[N_i(T_c+j)-N_i(T_c+j-1)]$) for time T_c+j using $NOKPF_i(T_c+j-1)$.
    3.1.2 Randomly draw $N_{s,i}(T_c+j)$ based on the Poisson process with parameter $\mu=E[N_i(T_c+j)-N_i(T_c+j-1)]$.
    3.1.3 $NOKPF_i(T_c+j)= NOKPF_i(T_c+j-1)+N_{s,i}(T_c+j)$.
    3.1.4 $NOKPF\_P_i\,(T_c+j)= \text{round down}\big(NOKPF_i(T_c+j)\big)$.
    3.1.5 Move to the next year ($j+1$)
  3.2 Move to next iteration (iter+1)
4 Calculate the average of the expected number of failures predicted from the simulation

$$\frac{\sum_{iter} E[N_i(T_c+j)-N_i(T_c+j-1)]}{iter}$$

Table 4-6 shows a list of models that will be investigated. The limits have been set for the number of levels that are in the NOKPF. They are represented with Max(number). For example, the NOKPF has 3 levels in the NHPP-Max2 model, where the first-level represents water mains with 0 failure, the second-level represents water mains with 1 failure, and the third-level represents water mains with 2 or more failures. Two other NHPPs are also included for comparison, the NHPP-CNOKPF is the model where the NOKPF is held constant for the validation/prediction period, based on the NOKPF calculated from the last year of the training period. This is the case used for the NHPP in Chapter 3 and Chapter 4. The NHPP-Basic is the model without the NOKPF.

Table 4-6: List of models under investigation.

Model	Description
NHPP-Basic	No NOKPF
NHPP-CNOKPF	NOKPF is constant after training year
NHPP-Max1	NOKPF is categorised into NOKPF=0 and NOKPF≥1
NHPP-Max2	NOKPF is categorised into NOKPF=0, NOKPF=1 and NOKPF≥2
NHPP-Max3	NOKPF is categorised into NOKPF=0, NOKPF=1, NOKPF=2 and NOKPF≥3
NHPP-Max4	NOKPF is categorised into NOKPF=0, NOKPF=1, NOKPF=2, NOKPF=3 and NOKPF≥4

The remaining sections will present the data used for the analysis. The coefficients estimated by the NHPPs are interpreted, followed by a comparison of the performance of the NHPPs using performance indexes and graphical plots for the number of failures estimated/predicted by the NHPP. The potential applications of the simulation study are also discussed.

4.5.1 Pipe Asset and Failure Data

All CI pipes laid before 1929 (mostly pit CI pipes) are used to compare the performance of the NHPP. A brief description of the failure data is shown in Table 4-7. The failure data have been collected between 1994 and 2015, and the failure rate of the network is plotted in Figure 4-15. Note that the recorded data show the total number of failures in a month, but they are plotted as lines in the figures in the chapter instead of discrete points for better visualisation.

There is a general upward trend in the failure rate over the observation period, with some year-to-year variations. Therefore, the average condition of CI pipe is likely to be deteriorating. The models will be calibrated using data from 1994 to 2010, the remaining data will be used for validation purposes. The model will also compare the failure predictions for the models in the long-term (more than 10 years).

The number of iterations required in the simulation is determined by checking the convergence of the predicted number of failures. The number of simulation is increased until the difference between the expected number of failures from consecutive iteration becomes less than 0.01. This requirement is satisfied by running 500 iterations.

The covariates incorporated in the NHPP are pipe age, pipe length (log form) (Figure 4-16), static water pressure (in kPa) (Figure 4-17), pipe diameter (Figure 4-18), soil reactivity (Figure 4-19) and NOKPF (Figure 4-20). The failure rate for longer pipes tends to be higher (Figure 4-16) and water mains operating at a higher pressure are more likely to fail (Figure 4-17). The pipe diameter (<100mm, 100mm to less than 200mm, 100mm to less than 200mm and >=300mm) and soil reactivity (High, Moderate, Low and Negligible) are both categorical variables. Smaller diameter pipes have a higher failure rate (Figure 4-18). The plot (Figure 4-19) for soil reactivity shows a slight increase in failure rate for pipes laid in soils with a higher reactivity. Finally, the water mains that have experienced more breaks (higher NOKPF) in the past tend to have a shorter time to next failure (Figure 4-20). The other time dependent factors, such as the MMAPI, are not considered in this model. This is because the NHPP will predict failures in the long-term (more than 10 years) and the MMAPI is unknown in the future.

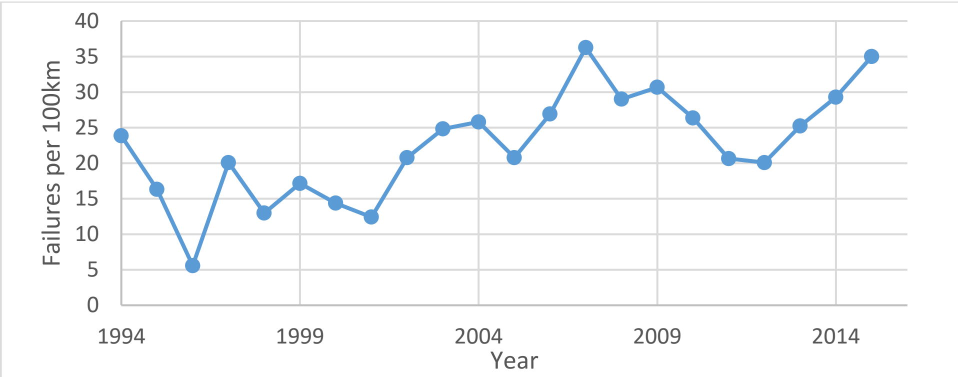

Figure 4-15: Failure rate over time.

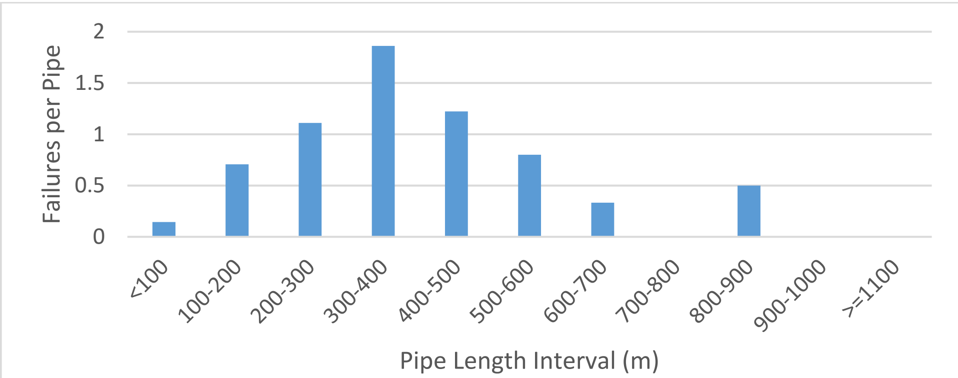

Figure 4-16: Failures in different pipe length intervals.

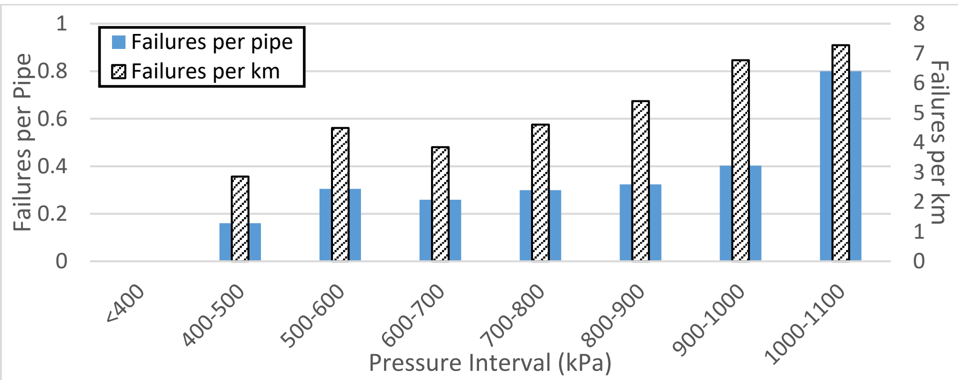

Figure 4-17: Failures in different pressure intervals.

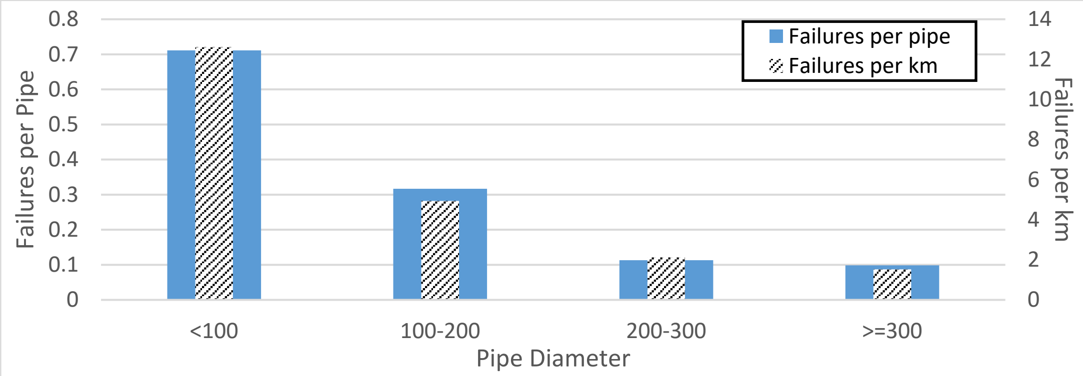

Figure 4-18: Failures in different pipe diameter interval.

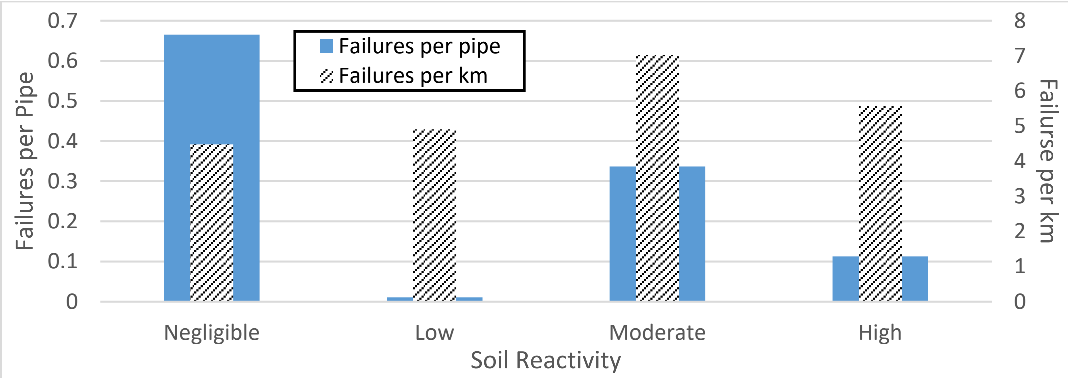

Figure 4-19: Failures in different soil types.

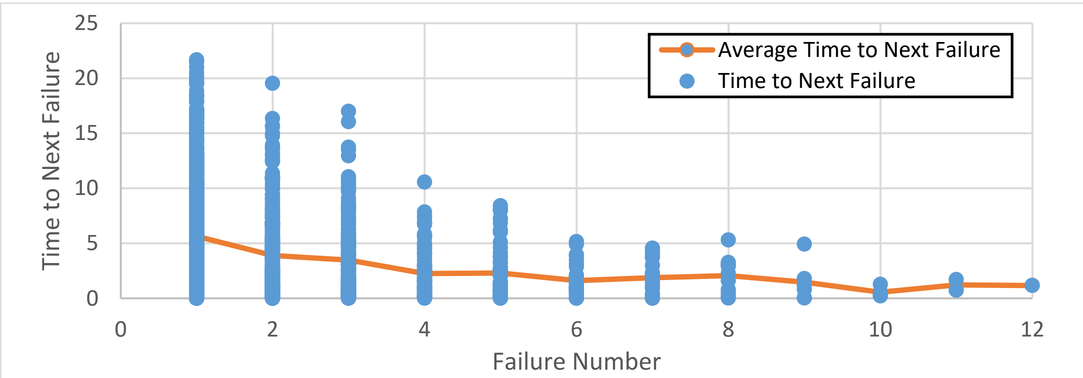

Figure 4-20: Time to next failure based on the number of failures recorded.

Table 4-7: Pipe asset information.

Data Properties	Range of data
Number of assets	11337
Number of failures	3545
Construction period	1860-1939
Observation period	1994-2015
Total pipe length	717
Average failure rates (failures/year/100km)	22.46

4.5.2 Results and Discussions

The coefficients for the significant covariates in the NHPP-Basic and NHPP-CNOKPF are shown in Table 4-8, while the estimated coefficients for the significant covariates in the NHPP-Max1, NHPP-Max2, NHPP-Max3 and NHPP-Max4 are shown in Table 4-9. The maximum number of levels in the NOKPF (5 in NHPP-Max4) is determined by applying the LR test to a modified version of the NHPP (NHPP-Max4-Modified). Using the NHPP-Max4 model as an example, the constant term (z_0 in Equation (4-1)) in the model captures the failure rate of the water mains with no past failure history (NOKPF=0), the estimated coefficients for the other levels in the NOKPF will shift the failure rate up or down. In NHPP-Max4-Modified, the constant term represents the failure rate of water mains with 3 past failures (NOKPF=3). The influence on the failure rates with no failures (NOKPF=0) in the past is estimated in Table 4-10. The LR test can be applied (Section 4.3) to determine whether the failure rate of water mains with NOKPF>=4 is different (or significant) with respect to NOKPF=3. The maximum likelihood value (MLV) for the full model (with NOKPF>=4) and the reduced model (without NOKPF>=4) are 11856 (“Constant” row in Table 4-10) and 11861 (“NOKPF>=4” row in Table 4-10), respectively. The LR test found that the NOKPF>=4 is significant at 5% significant level, it suggests that the failure rate for water mains with 3 past failures are likely to be different to those with 4 or more past failures. The process was applied to all NHPP shown in Table 4-9, until NHPP-Max5. The LR test result for NHPP-Max5-Modified shown in Table 4-11 found that the NOKPF>=5 is not significant, implying that there is little difference in the failure rates for water mains with NOKPF=4 and those with NOKPF>=5. Therefore, the maximum number of levels in the NOKPF is set at 5 with the NHPP-Max4 model.

The interpretation of the coefficients in the following paragraphs has assumed that all other covariates are held constant. The NHPP-Basic model has the greatest ageing factor. Therefore the failures predicted by the NHPP-Basic model will grow at the fastest rate. The ageing factors for the remaining 5 models as well as the coefficients estimated for the pipe dependent factors are very similar. The inclusion of the NOKPF in the models have reduced the ageing factor. This suggests that part of the increase in failure due to the deterioration of the water main in the NHPP-Basic model might be caused by the reduction in time to failure for water mains that have experienced more failures in the past.

Table 4-8: Estimated coefficients for NHPP-Basic and NHPP-CNOKPF.

NHPP-Basic	Coefficient	NHPP-CNOKPF	Coefficient
Ageing Factor	2.59	Ageing Factor	2.22
Constant	-17.11	Constant	-14.83
ln(Pipe Length) (m)	0.97	ln(Pipe Length) (m)	0.88
Pressure (kPa)	1.12	Pressure (kPa)	0.93
Reactivity-Negligible	-0.21	Reactivity-Negligible	-0.22
		NOKPF	0.43

Table 4-9: Estimated coefficients for NHPP-Max1, NHPP-Max2, NHPP-Max3 and NHPP-Max4.

NHPP-Max1	Coefficients	NHPP-Max2	Coefficients	NHPP-Max3	Coefficients	NHPP-Max4	Coefficients
Ageing Factor	2.22	Ageing Factor	2.16	Ageing Factor	2.15	Ageing Factor	2.15
Constant	-14.91	Constant	-14.57	Constant	-14.51	Constant	-14.46
ln(Pipe Length) (m)	0.87	ln(Pipe Length) (m)	0.86	ln(Pipe Length) (m)	0.86	ln(Pipe Length) (m)	0.85
Pressure (kPa)	0.94	Pressure (kPa)	0.93	Pressure (kPa)	0.92	Pressure (kPa)	0.91
Reactivity-Negligible	-0.17	Reactivity-Negligible	-0.17	Reactivity-Negligible	-0.18	Reactivity-Negligible	-0.18
NOKPF>=1	0.99	NOKPF=1	0.81	NOKPF=1	0.81	NOKPF=1	0.81
		NOKPF>=2	1.38	NOKPF=2	1.29	NOKPF=2	1.29
				NOKPF>=3	1.52	NOKPF=3	1.31
						NOKPF>=4	1.86

Table 4-10: Estimated coefficients and significance of covariates in the modified NHPP-Max4 model.

NHPP-Max4-Modified	Coefficients	Maximum Log Likelihood Value (MLV)[4]	Significant
Ageing Factor	2.15		
Constant	-13.15	11856	
ln(Pipe Length)	0.85	12925	TRUE
Pressure	0.91	11872	TRUE
Reactivity-Moderate	-0.18	11864	TRUE
NHPP=0	-1.31	11902	TRUE
NOKPF=1	-0.50	11864	TRUE
NOKPF=2	-0.02	11856	TRUE
NOKPF>=4	0.55	11861	TRUE

Table 4-11: Estimated coefficients and significance of covariates in the modified NHPP-Max5 model.

NHPP-Max5-Modified	Coefficients	Maximum Log Likelihood Value (MLV)[5]	Significant
Ageing Factor	2.15		
Constant	-12.61	11856	
ln(Pipe Length)	0.85	12925	TRUE
Pressure	0.91	11872	TRUE
Reactivity-Moderate	-0.18	11864	TRUE
NHPP=0	-1.85	11894	TRUE
NOKPF=1	-1.04	11871	TRUE
NOKPF=2	-0.56	11861	TRUE
NOKPF=3	-0.54	11860	TRUE
NOKPF>=5	0.02	11856	FALSE

The categorical variable, pipe diameter, is not significant. The models could not pick up any difference in failure rate between water mains in different pipe diameter groups. On the other hand, the failure rates of the water mains are impacted by the soil types. The baseline scenario captured by the constant term are the water mains

[4] Constant represents the MLV for the full model, the MLV for the covariates represents the MLV for the restricted model with a d.o.f=1.
[5] Constant represents the MLV for the full model, the MLV for the covariates represents the MLV for the restricted model with a d.o.f=1.

laid in highly reactive soils. The pipes that have been constructed in soil with negligible reactivity have a lower failure rate than other pipes. However, the failure rate for the water mains in moderate and low reactive soils is similar to those laid in soils with high reactivity. This result was not as expected, the failure rate of the water mains should increase as the reactivity of the soil increases. Therefore, it is likely that the impact from the shrinkage/swelling of the soil on the breakage of the water main is not as significant in the area under study as the dataset in Section 4.4.1.

The estimated coefficients for the other covariates in the NHPPs are as expected. The water mains that are longer and have a higher static water pressure are more prone to failures. The coefficients estimated for the NOKPF implies that the more failures the pipe has experienced, the more likely the pipe will fail again in the future.

4.5.2.1. Performance Indexes and Graphical Plots

The MAE and RMSE for the training period, validation period and the entire observation period are shown in Table 4-12. The NHPP-Max1 to NHPP-Max4 models have a lower MAE and RMSE compare to the NHPP-Basic and NHPP-CNOKPF models in the training period. However, the NHPP-Basic model has the lowest errors during the validation period. In terms of the entire observation period, the NHPP-Max1 is the best out of the 6 models. Comparing the NHPP-Max1 to NHPP-Max4 models, the error in the training period reduces as the number of levels in the NOKPF increases. However, the opposite is observed for the validation period and the entire observation period.

The performances of the models are further examined by comparing the number of failures estimated and predicted by the models. The expected number of failures are plotted for the 6 NHPPs up till 2030, along with the recorded failure data in Figure 4-21. All 6 models can capture the general upward trend in the recorded failure data during the training period, but the year-to-year variations could not be modelled because time dependent covariates (such as MMAPI) are not included in the model.

Table 4-12: MAE and RMSE for all models.

Model	MAE-Training	MAE-Validation	MAE-Overall	RMSE-Training	RMSE-Validation	RMSE-Overall
NHPP-Basic	36.6	31.0	35.3	45.3	36.3	43.4
NHPP-CNOKPF	31.4	50.1	35.6	39.1	57.4	43.9
NHPP-Max1	30.8	41.4	33.2	38.9	46.9	40.9
NHPP-Max2	30.2	47.3	34.1	38.1	55.3	42.6
NHPP-Max3	30.1	49.9	34.6	38.0	57.2	43.1
NHPP-Max4	30.2	55.1	35.8	38.0	61.1	44.3

The figure shows that the NHPP-Basic model predicts fewer failures compared to the other 5 NHPPs in the validation period. Holding the NOKPF constant after the training period has caused the NHPP-CNOKPF model to behave differently before and after the training period. The rate of increase in the number of failures is driven by both the NOKPF and the ageing of the pipe during the training period. After 2011, without updating the NOKPF in the water mains, the upward trend in the validation and the prediction period are only driven by the ageing of the water mains. On the other hand, the NHPP-Max1 to NHPP-Max4 models account for the combined effect of the NOKPF and pipe deterioration for the validation period and prediction period (as in the training period) by simulating the failures events in the water mains.

The difference in the number of failures estimated by the NHPP-Max1, NHPP-Max2, NHPP-Max3 and NHPP-Max4 models are small during the training period. The number of failures estimated by the NHPP-Max1 model starts to depart from the other 3 models in the validation period. The rate of increase in the predicted failures for the NHPP-Max4 model becomes much higher than the NHPP-Max3 and NHPP-Max2 models in the prediction period. The number of failures estimated by the 4 models is similar during the training period because only a small portion of water mains has experienced a failure, and an even smaller number of water mains would have failed multiple times. Therefore, the pipe dependent covariates and pipe age would be the main contributors to the number of failures estimated by the model at the start of the training period. The effect of the NOKPF becomes more significant as the water mains experience more failures.

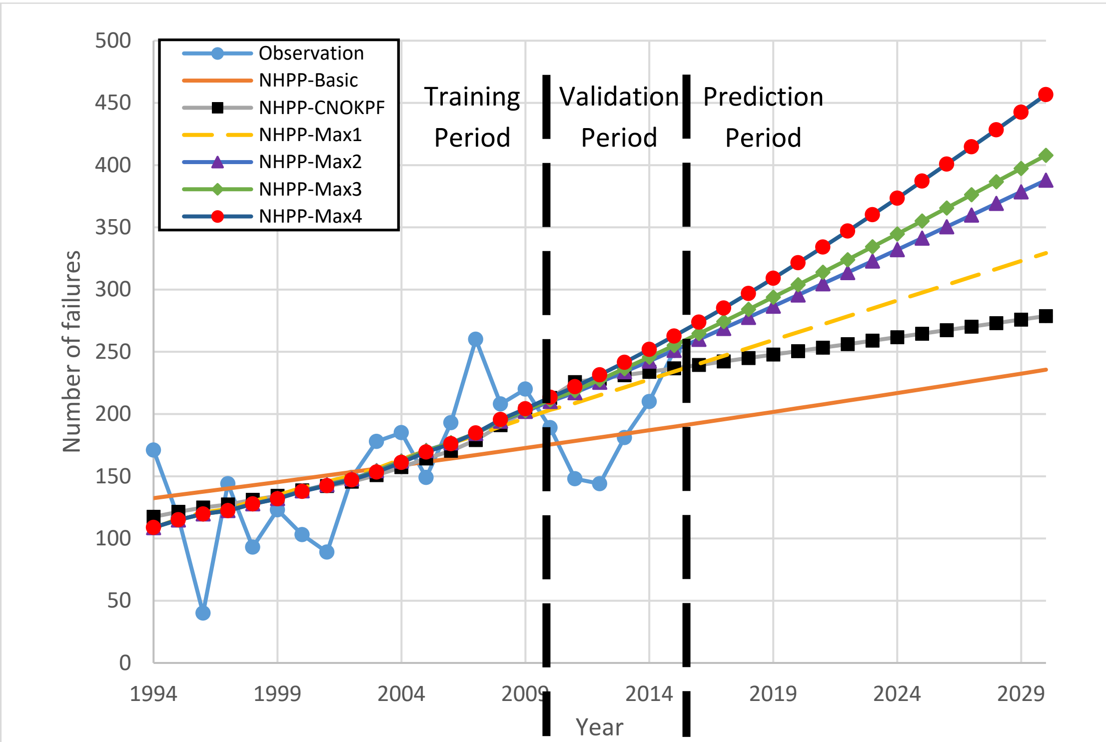

Figure 4-21: Expected number of failures estimated/predicted for all models.

4.5.3 Model Applications

The analysis of results in the last section showed the influence of the NOKPF on the number of failures predicted by the NHPP. By simulating the failures using the NHPP each year, the number of failures predicted by the NHPP is much higher than those from the NHPP-Basic and NHPP-CNOKPF models.

The performance indexes have suggested that the NHPP-Basic model is preferred in the validation period. However, the model does not capture the shorter failure time that has been observed (Figure 4-20) for the water mains in the dataset. Therefore, it is likely that the NHPP-Basic model will underestimate the failures in the future.

Underpredicting the number of future failures in the network can have a significant impact on the day-to-day operation of the water utility. The amount of investment would have to increase by a significant amount to "catch up" on the renewals that should have been replaced in the past. The increase in investment might also lead to an increase in the pricing of water to raise sufficient funds for the program. Therefore, the NHPP that simulates future failures more accurately would be preferred. In addition, simulating future failures to update the NOKPF could also represent a worst-case scenario for the network, which is always better to be used in planning than investing more money in the future to replace water mains that should have been renewed in the past. The NHPP-Max3 model has been used as the pipe failure prediction model for the water plan in one of the water utilities from Melbourne. Some of the results will be discussed in Chapter 6.

4.6. Conclusion

This chapter has developed an approach to predict failures in the WDN using time dependent (MMAPI) and pipe and time dependent (NOKPF) covariates. The first part of the chapter introduced time-lag into the time dependent covariate, the MMAPI, in the NHPP, allowing the number of failures in the future to be predicted using the MMAPI values from the past. The influence of each covariate was systematically analysed, and the performance of the NHPP with different length of time-lag introduced into the MMAPI was compared using error statistics and graphical plots. The main findings from the application of time-lag to the MMAPI in the NHPP are summarised below on the basis of the datasets used in the analysis:

- A negative correlation between MMAPI and the number of monthly failures in the network can be observed. In addition, a peak in the monthly failures is always related to a low in the MMAPI, but a small MMAPI does not always produce a peak in the monthly failure.
- The MMAPI can capture the monthly variations in the number of failures, but additional covariates, season and soil, have to be included in the NHPP to improve the model's ability in capturing the peak monthly failures.

- A shift from a drought to a wetter climate near the end of the observation period might have led to smaller ageing factors for models that were trained using a longer training period.
- The models for AC pipes might have omitted significant covariates that influence its failure rate, causing the estimated ageing factor to be less than 1, which is different to the general expectation for pipes already laid in the ground.
- For models using the same training period and lag in the MMAPI, the inclusion of interaction terms does not always reduce the error in the model. This implies that the interaction terms considered may be redundant in some cases.
- There is a trade-off between the prediction accuracy and the number of months the model can predict into the future:
    - The NHPP with no time lag provides the most accurate prediction, but cannot make predictions unless the MMAPI (or rainfall) values are predicted for the future using rainfall models
    - The T1, T2 and T3 models can predict failures by using past MMAPI values up to 1, 2 and 3 months, respectively. However, the accuracy of the predictions reduces as a longer time-lag is applied.

Although the results show that models with time-lag in the MMAPI are not as accurate as the T0 model in predicting the total number of failures, the T1 and T2 model can still capture part of the monthly variation and make reasonable failure predictions for the network. This could be used as an estimate for the number of repairs that might occur and allow additional crews (or other resources) to be allocated in time, and possibly reducing the intervention time during periods with many failures.

The second part of the chapter predicted the number of failures in the long-term using the pipe and time dependent covariates, the NOKPF. In each prediction year, the NOKPF is updated by simulating the failures that will occur in the year using the Poisson distribution. Then the updated NOKPF is used to predict the number of failures in the next year. The performance of the NHPP with simulations (NHPP-Max1 to NHPP-Max4 models) was compared with the NHPP-Basic and NHPP-CNOKPF models using the performance indexes and graphical plots. The main findings of the study are summarised below on the basis of the dataset used in the analysis:

- Water mains that have experienced more failures are estimated with a higher chance of failure in the future.
- The NHPP with the NOKPF (NHPP with simulations and NHPP-CNOKPF models) are better at estimating the number of failures during the training period. However, they tend to over-predict the failures in the validation period. The NHPP-Max1 model has the lowest MAE and RMSE for the entire observation period.

- The increasing trend in the NHPP-CNOKPF model is different before and after the training period because the NOKPF is held constant after the training period. The model only captures the effect of pipe deterioration, but not the effect of the NOKPF after the training period.
- On the other hand, the NHPP with simulation (NHPP-Max1 to NHPP-Max4 models) can capture the combined effect of the NOKPF and pipe deterioration over time by simulating the failures events in the water mains.
- Long-term failure prediction models are used for water main rehabilitation planning. Therefore, the worst-case scenario should be considered. Using the NHPP-Basic for water renewal planning can under-predict the level of investments and impact on the level of service. This could increase the future investment required to return the network to a satisfying condition.

The previous chapter has developed the BSM as a preliminary desktop assessment tool for identifying groups of pipes with a high chance of failure. The current chapter tried to predict failures in the WDN using variables that are dependent on time. The time dependent NHPP with time-lag can be used to predict the occurrence of a large number of failure events in the short-term. The NHPP that simulated future failure events can predict the failure rates of the WDN in the long-term. Without simulating the future failure events to update the NOKPF, the NHPP (e.g. NHPP-Basic model) can under-predict the number of failures, impacting on the level of service and increasing the level of investment in the future. The next chapter will discuss the Monash Pipe Failure Prediction model that integrated the physical approach with statistical failure data for water main failure predictions.

CHAPTER 5: INTEGRATION OF THE PHYSICAL APPROACH WITH STATISTICAL FAILURE DATA FOR PIPE FAILURE PREDICTION

5.1. Introduction

Failure prediction models for water main breakages can be broadly classified into the statistical approach and physical approach. Based on the literature review conducted in Chapter 2, the two approaches have different applications and limitations. They are summarised in Table 5-1 below:

Table 5-1: Summary of statistical and physical approach.

	Applications	Limitations
Statistical approach	• Can be applied to all water mains regardless of material and size. • Failure predictions are reasonably accurate at a network/group level (e.g. all pipes made of the same material). • The predictions can be used for water main rehabilitation planning.	• Predictions are unreliable for individual pipes for most statistical models. • Assume trends from the past will continue into the future. Therefore, patterns that have never appeared in the failure data cannot be predicted.
Physical approach	• Captures the physical failure mechanism of the water main. • Predicts failure for individual pipes because the models considered the deterioration process of each water main. • Captures the change in stress over time (e.g. bending stress from the change in soil moisture content), if the relevant input data are available.	• Not all input data are known (e.g. corrosion rate), and collecting this information can be costly if applied to the entire WDN (e.g. condition assessments). • A single physical model is not applicable to all materials because of different material properties.

An innovative approach to overcome some of the limitations in the two approaches is to combine the two modelling techniques. Statistical models are poor in making predictions for individual pipe, but physical models can be used to predict the condition of the water main. Some of the inputs in the physical model, such as corrosion rates, are unknown, but statistical failure data are available. This can be used to back-calculate the corrosion rate that is required for the water main to fail at the specific time recorded in the data. The failure data can also be used to update the input parameters (e.g. corrosion rate) as the model is under calibration.

The following chapter will discuss the original development of the Monash Pipe Failure Prediction (MPP) model. A framework has been developed to integrate the physical modelling approach with statistical failure data for pipe failure prediction. Currently, the MPP model has only been designed for CI pipes subjected to longitudinal split and broken back failures. CI pipes are assumed to deteriorate because of corrosion, resulting in a reduction of pipe wall thickness and creating a concentration of stress around the corrosion pit. The MPP model first estimates the condition of the pipe with a physical model. The results from the physical model are then compared with the observed failure history to update the corrosion parameters. At the end of the updating process in each time step, further adjustments are made to the corrosion parameters by applying a failure influence factor. Pipes that are located close by geographically are likely to be operating in a similar environment (e.g. similar pressure and corrosion rate). Therefore, the failure influence factor will adjust the corrosion parameters of the pipe as a function of distance from the failed pipes (closer pipes have a larger influence on each other).

Section 5.2 provides a detail description of the processes in the MPP model. Section 0 and Section 5.4 compare the results of the MPP model with the BSM and the NHPP for longitudinal and broken back failures, respectively. Then the results of the MPP models are discussed in Section 5.5, followed by the conclusion of the chapter.

5.2. Monash Pipe Failure Prediction (MPP) Model

Two modelling processes based on different assumptions have been considered in the MPP model and are listed in Table 5-2. Some of the parameters in the models are shown in Table 5-3. The model has assumed that a pipe can be split into many small segments. A segment of a pipe refers to the portion of the pipe that is replaced when a failure occurs. In real life settings, there would be a limit on the number of segments that a pipe can have. However, in this chapter, the upper threshold on the number of segments has not been set. This is because setting a threshold would further increase the level of complexity of the model and would also shift the model towards an optimisation problem for renewal planning. Renewal planning of water mains will be considered in Chapter 6.

The general process for the two approaches shown in Table 5-2 is similar. They are:

i. Initialisation of input variables

ii. Estimating the condition of the pipe based on the physical model

iii. Updating the corrosion parameters using statistical failure data and recalculating the condition of the water main with the physical model

iv. Applying the failure influence factor to pipes that operate normally in the time step under consideration

v. Predicting the future condition of the pipes

Each component listed above will be discussed. The difference in the components, if any, for the two approaches will be pointed out as well.

Table 5-2: Two modelling processes for the MPP model.

	MPP-P1	MPP-P2
Description	Pipe coating can protect the water main from corrosion. The failure of the coating will initialise the corrosion of the pipe wall. Given two pipes with the same pipe characteristics and operating environments, the pipe with a better coating (e.g. good manufacturing and construction practice) will have a longer service life because the initialisation of corrosion (a honeymoon period) is delayed.	The time to failure of a pipe segment is mainly governed by the long-term corrosion rate. Given two pipes with the same pipe characteristics and operating environments, the pipe with a higher longer-term corrosion rate will fail first because it has experienced more corrosion. Although the long-term corrosion rate can be small, the MPP model is studied using CI pipes, which belong to one of the oldest pipe materials in the WDN. The magnitude of corrosion can be a significant factor in old pipes (Ji et al., 2015).
Common assumptions	• A pipe can be divided into multiple small segments. • Only 1 pipe segment can fail in a year • The water main fails in the second phase of the bi-linear corrosion model (discussed in more detail in Section 5.2.2) • Water mains that are close by are assumed to be operating in a similar environment	
Assumptions	• Given that the other conditions are the same, the difference in failure time for the pipe segments is due to the quality of coating. Better coating can delay the start of corrosion which increases the time to failure.	• Pipes are not coated, they will corrode immediately after it is laid in the ground. • Pipe segment with a higher corrosion rate will fail first, given that the other conditions are the same.

Table 5-3: Parameters in the MPP model.

Parameter	Definition	Initial Value/Description
$\boldsymbol{i}$	Pipe $\boldsymbol{i}$ up to $\boldsymbol{n}$ pipes	-
$\boldsymbol{t}$	Year $\boldsymbol{t}$	-
$\boldsymbol{rs_i(t)}$	Corrosion rate of the segment with the highest corrosion rate	Drawn randomly from a Weibull distribution.
$\boldsymbol{cs_i(t)}$	Intercept for long-term corrosion rate	Initial value is drawn based on the degree of saturation.
$\boldsymbol{D_i}$	Pipe diameter	Drawn from data.
$\boldsymbol{t_i'}$	Pipe thickness	$\boldsymbol{t_i' = 0.0252D_i + 6.8889}$
$\boldsymbol{c_i}(t)$	Corrosion pit depth	$\boldsymbol{c_i(t) = cs_i(t) + rs_i(t)Age_i(t)}$
$\boldsymbol{Pa}$	Patch radius to patch depth ratio	corrosion patch radius= $\boldsymbol{Pa * c_i(t)}$
$\boldsymbol{Age_i(t)}$	Pipe age	-
$\boldsymbol{f_i(t)}$	Failure influence factor	Use to distribute the information from a failure to surrounding pipes.
$\boldsymbol{\Delta T_i(t)}$	Time to next failure	Drawn randomly from a Weibull distribution.
$\boldsymbol{F_i(t)}$	$\boldsymbol{F_i(t) = 1}$ if pipe failed at time $\boldsymbol{t}$	$\boldsymbol{F(0) = 0}$
$\boldsymbol{SCF_i\big(c_i(t) = cs_i(t) + rs_i(t)Age_i(t)\big)}$	Stress concentration factor. Inverse of the strength reduction factor from Antaki (2003) for broken back failures	-
$\boldsymbol{\sigma_{m,i}(t)}$	Maximum pipe stress	Longitudinal failures: $\boldsymbol{\sigma_{m,i}(t) = \sigma_{n,i}(t)SCF_i(t)}$ Broken back failures: $\boldsymbol{\sigma_{m,i}(t) = \sigma_{b,i}(t)SCF_i(t)}$
$\boldsymbol{\sigma_{n,i}(t)}$	Nominal stress for longitudinal failure	
$\boldsymbol{\sigma_{b,i}(t)}$	Bending stress due to ground movement	
$\boldsymbol{E}$	Elastic modulus	83.4
$\boldsymbol{M}$	Soil-pipe stiffness factor	
$\boldsymbol{I}$	Second moment of area	
$\Delta\boldsymbol{\theta_{w,i}(t)}$	Change in soil moisture from average value	
$\boldsymbol{\Delta G}$	Soil moisture variation depth	2300mm
$\boldsymbol{S_{i,max}}$	Maximum movement of soil relative to lowest movement at pipe level	
$\boldsymbol{j}$	Characteristic length of bending curve	
$\boldsymbol{\sigma_t(t)}$	Pipe tensile strength	100 MPa
$\boldsymbol{L_{i,j}}$	Distance between the midpoint of pipe $\boldsymbol{i}$ and pipe $\boldsymbol{j}$	-
$\boldsymbol{a}$	failure influence factor	Controls the strength on how much a failure affects the surrounding pipes based on the distance between the two pipes.

5.2.1 Corrosion Model for Cast Iron Pipes

The wall of the CI pipe is assumed to deteriorate following a bi-linear model (Peterson and Melchers, 2012 and Peterson and Melchers, 2014) as part of the development in the 'Advanced Condition Assessment & Pipeline Failure Prediction Project'. It can also be replaced by other corrosion models, such as the exponential corrosion model from Rajani et al. (2000). Jiang et al. (2017) noted that both the bi-linear corrosion model and exponential corrosion model display similar corrosion characteristics for new pipe and pipes that have been exposed for a long time. The authors were able to restate the exponential corrosion model with the parameters in the bi-linear corrosion model, almost making them identical despite the exponential model representing a smooth progression of pit depth.

The bi-linear corrosion model shown in Equation (5-1) (Figure 5-1) is defined using the initial corrosion rate ($r_{0,i}$); long-term corrosion rate ($rs_i(t)$); intercept of the long-term corrosion rate ($cs_i(t)$); transition time (τ_i); and a holiday period ($T_{0,i}(t)$), where the pipe is assumed to be free from failures as a result of the protection from pipe coating.

An example of the bi-linear corrosion model is shown in Figure 5-1. The first corrosion model (in black) assumed that there is no holiday period, and the pipe starts corroding as soon as it is laid in the ground (modelling process-P2). In the initial phase, the water main will corrode at a rate of $r_{0,i}$ until time τ_i. Then, the second corrosion phase begins, and the pipe corrodes at a slower rate of rs_i. The second corrosion model (in green) has a holiday period of 20 years, which can be attributed to the protection from the pipe coating (modelling process-P1). Note that the corrosion rates are constant because the updating process of the corrosion parameters are not implemented in the figure.

$$c_i(t) = \begin{cases} r_{0,i} Age_i(t), & Age_i(t) < \tau_i \\ cs_i(t) + rs_i(t) Age_i(t), & Age_i(t) \geq \tau_i \end{cases} \tag{5-1}$$

where i is the index for the *i-th* pipe; t represents time; and $Age_i(t)$ is the age of the pipe at time t.

Although a model has been selected to represent the corrosion in the pipe, no corrosion information has been collected using non-destructive techniques for any of the pipes in the network. Therefore, the corrosion parameters in the bi-linear model must be estimated through other means. They will be discussed in the following section.

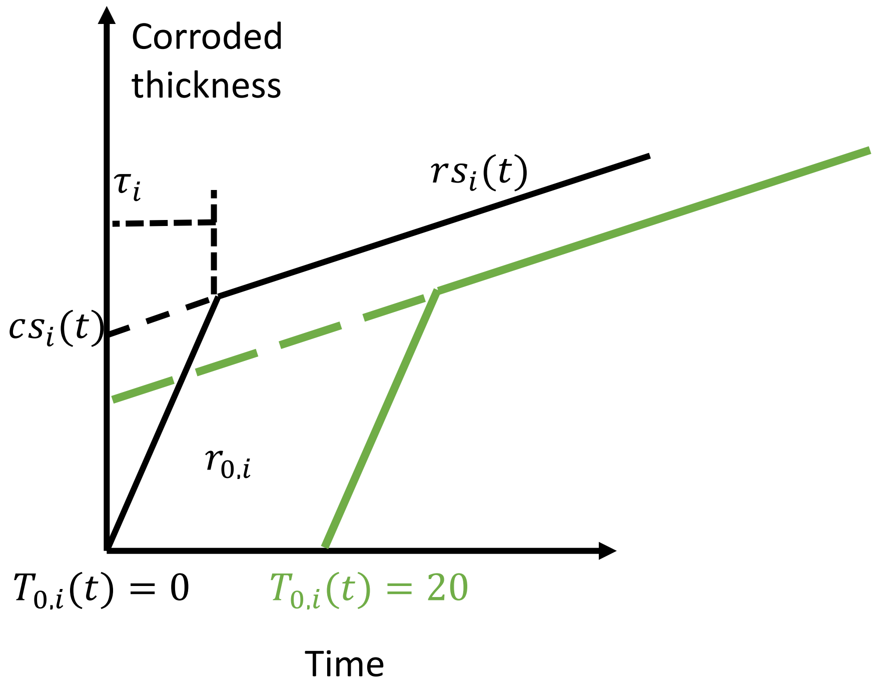

Figure 5-1: Bi-linear corrosion model.

5.2.2 Initialisation of Input Variables

Most of the parameters from Table 5-3 can be drawn directly from the data. However, the initial corrosion rate ($r_{0,i}$), long-term corrosion rate ($rs_i(t)$), intercept of the long-term corrosion rate ($cs_i(t)$), transition time (τ_i) and the time to next failure ($\Delta T_i(t)$) still need to be determined.

The degree of saturation is one of the influential parameters in the corrosion of CI pipes (Peterson and Melchers, 2012 and Peterson and Melchers, 2013). Therefore, it is used here to estimate the corrosion parameters. The failure data are used to estimate the time to next failure and is also as an alternative method to estimate the corrosion parameters.

5.2.2.1. Initialising Corrosion Rate using Degree of Saturation

The degree of saturation (S_r) for pipe i can be calculated using the average monthly volumetric soil moisture content ($\theta_{w,i,avg}$) and the soil porosity (ϕ_i) shown in Equation (5-2).

$$S_{r_i} = \theta_{w,i,avg}/\phi_i$$

(5-2)

The soil moisture data are collected from the Bureau of Meteorology (BOM) for the entire Victoria region as an 8km by 8km grid. They represent the percentage of available water in the soil that can be extracted by plants and vegetations. The dataset is in daily time-step and values from 2005 to 2016 have been collected. The data were converted into volumetric soil moisture content based on soil reactivity (ST- negligible shrink/swell potential, SE-low shrink/swell potential, EX- moderate shrink/swell potential; and VE-very high shrink/swell potential) and the Wealth from Water Fact Sheet developed for Tasmania (Cotching, 2011) (assuming similar soil characteristic in Tasmania and Melbourne) using Equation (5-3). The permanent wilting point (pwp) and field capacity (FC) for each soil type are shown in Table 5-4.

$$\theta_{w,i}(d) = pwp + \%AW_i(d) * (FC - pwp) \tag{5-3}$$

where $\theta_{w,i}(d)$ is the soil moisture content at day d for pipe i ; pwp is the permanent wilting point; $\%AW_i(d)$ is the percentage of available water from BOM for pipe i; and FC is the field capacity.

The monthly soil moisture content in month m is calculated as:

$$\theta'_{w,i}(m) = \frac{\sum_{d=1}^{d_m} \theta_{w,i}(d)}{d_m} \tag{5-4}$$

where d_m is the number of days in month m and $\theta'_{w,i}(m)$ is the average daily soil moisture for pipe i in month m.

The maximum and minimum yearly soil moisture content are needed to calculate the stress for broken back failures, they are shown in Equation (5-5) and (5-6) below:

$$\theta^{y}_{w,i,max}(t) = \max_{m_t \in t} \theta'_{w,i}(m_t) \tag{5-5}$$

$$\theta^{y}_{w,i,min}(t) = \min_{m_t \in t} \theta'_{w,i}(m_t) \tag{5-6}$$

where $\theta^{y}_{w,i,max}(t)$ is the maximum soil moisture content in year t; $\theta^{y}_{w,i,min}(t)$ is the minimum soil moisture content in year t; m_t is the months that is in year t; and $\theta'_{w,i}(m_t)$ is the monthly soil moisture content in month m_t.

The average monthly soil moisture (Equation (5-7)) between 2005 and 2016 will be used to calculate the degree of saturation.

$$\theta_{w,i,avg} = \frac{\sum_{m=1}^{12*(2016-2005+1)} \theta'_{w,i}(m)}{12 * (2016 - 2005 + 1)} \tag{5-7}$$

Table 5-4: Permanent wilting point and field capacity for different soil types.

Soil Reactivity	Soil Type in Fact Sheet	Permanent Wilting Point (mm water/m soil depth)	Field Capacity (mm water/m soil depth)
ST	Sand	70	130
SE	Light clay	240	390
EX	Light clay	240	390
VE	Medium-heavy clay	250	390

The porosity of the soil is also required to estimate the S_{r_i} in Equation (5-2). Soil texture information for the Melbourne metropolitan region was developed as part of the Smart Water Fund based on Mckenzie and Hook (1992) and Mckenzie et al. (2000). The size of the soil texture grids is 1km by 1km. Each water main can be found in at least one grid and the soil texture information is converted into soil porosity based on the equations developed by Saxton et al. (2006). If a pipe is found in multiple grids, the average porosity value is used instead.

With the S_r estimated for each water main, they can be used to estimate the corrosion parameters. The 'Advanced Condition Assessment & Pipeline Failure Prediction' project examined corrosion data from CI pipes samples, NBS database and other databases. Relationship between the parameters in the corrosion model with the degree of saturation was investigated. A summary of the values for the corrosion parameters based on the data analysed are shown in Table 5-5. The corrosion parameters are filled in for S_r values from 0.7 to 0.8 and 0.9 to 1.0 (underlined) because no data were available for S_r in these ranges.

The corrosion parameters for the water mains will be drawn from Table 5-5 at the start of the MPP model depending on the value of S_r. Although, the errors for some of the results in Table 5-5 are quite large, the mean value in each S_r bin class can still serve as a good starting point for the corrosion parameters in the MPP model.

Table 5-5: Corrosion parameters for different Sr ranges.

Sr	rs ($\times 10^{-2}$ mm yr^{-1})	cs (mm)	τ (yrs)	r_o ($\times 10^{-2}$ mm yr^{-1})
$0.0 < S_r < 0.1$	1.62 ± 1.13	0.64 ± 0.34	3.2 ± 2.2	21.62 ± 25.5
$0.1 \leq S_r < 0.2$	3.53 ± 0.46	0.34 ± 0.09	2.1 ± 0.2	19.51 ± 6.1
$0.2 \leq S_r < 0.3$	2.0 ± 1.4	1.1 ± 0.43	4.0 ± 0.92	29.5 ± 18.3
$0.5 \leq S_r < 0.6$	4.49 ± 1.54	4.2 ± 1.3	9.5 ± 4.3	48.7 ± 35.2
$0.6 \leq S_r < 0.7$	3.58 ± 3.5	5.1 ± 2.6	17 ± 9	33.6 ± 34.8
$\underline{0.7 \leq S_r < 0.8}$	<u>3.58 ± 3.5</u>	<u>5.1 ± 2.6</u>	<u>17 ± 9</u>	<u>33.6 ± 34.8</u>
$0.8 \leq S_r < 0.9$	8.92 ± 2.44	1.6 ± 0.38	2.5 ± 1.7	72.9 ± 61.1
$\underline{0.9 \leq S_r < 1.0}$	<u>8.92 ± 2.44</u>	<u>1.6 ± 0.38</u>	<u>2.5 ± 1.7</u>	<u>72.9 ± 61.1</u>

5.2.2.2. Initialising Corrosion Rate using Failure Data

An alternative method to initialise the corrosion parameters is to use the available failure data and part of the results from Table 5-5. The failure data provide the time of failure for water mains that have failed in the past. In addition, the failure data can also be used to determine an upper bound for the corrosion rate. If the corrosion rate of the water main is higher than the upper bound, at least one failure should have been recorded for the pipe.

Given that τ_i, $r_{0,i}$ and $cs_i(t)$ are drawn from Table 5-5 with the known degree of saturation, the long-term corrosion rate required for the water main to fail at the specific time can be estimated using the physical model (discuss in detail in Section 5.2.3).

For water mains that have failed, only the first recorded failure event is used to estimate the long-term corrosion rate. The $rs_i(t)$ and $cs_i(t)$ are assumed to be constant until the first failure event ($t_{f,i,1}$) ($rs_i(1) = rs_i(2) = \cdots rs_i(t_{f,i,1})$ and $cs_i(1) = cs_i(2) = \cdots cs_i(t_{f,i,1})$). The $rs_i(t_{f,i,1})$ that is required for the pipe to fail at the recorded year can be calculated given that the time to failure is known. For example, if a pipe is laid in 1920 and the first failure is recorded in 2005. The initial $rs_i(t_{f,i,1})$ that will create a sufficient stress concentration factor ($SCF_i(c_i(85))$ for the pipe to fail at 85 years old can be estimated.

For pipes without any failures during the observation period, an "artificial" failure event is created for the pipe one year after the training period. Then an upper bound for the corrosion rate is back calculated following the same process for water mains with failures. This is because if the corrosion rate of the water main is higher than the upper bound, a failure would have been recorded for the pipe in the failure data. The corrosion rates for these pipes are considered as left censored data because only the upper bound is known.

The processes described above can be repeated for every pipe. Then a left-censored Weibull distribution is fitted to the back-calculated corrosion rates. When the MPP model starts, $rs_i(1)$ values are randomly drawn from the distribution for each pipe in the dataset.

The steps described above are summarised below:

1. Calculate the age of the pipe at its first recorded failure ($t_{f,i,1}$) (or the "artificial" failure), and the stress concentration factor (SCF) that will cause the nominal stress ($\sigma_{n,i}$) or the maximum bending stress[6] ($\sigma_{b,i}(t)$) to exceed the tensile strength of the pipe (σ_t) with Equation (5-8) or Equation (5-9), respectively.

   Given that $cs_i(t_{f,i,1})$ is drawn from Table 5-5:

[6] The maximum bending stress over the training period for the water main is used because using the average or minimum bending stress will largely over-estimate the failures in the dataset.

$$SCF_i\left(c\big(t_{f,i,1}\big) = cs_i\big(t_{f,i,1}\big) + rs_i\big(t_{f,i,1}\big)Age_i\big(t_{f,i,1}\big)\right) = \frac{\sigma_t}{\sigma_{n,i}}$$

(5-8)

$$SCF_i\left(c\big(t_{f,i,1}\big) = cs_i\big(t_{f,i,1}\big) + rs_i\big(t_{f,i,1}\big)Age_i\big(t_{f,i,1}\big)\right) = \frac{\sigma_t}{\sigma_{b,i}(t)}$$

(5-9)

2. Estimate the $rs_i\big(t_{f,i,1}\big)$ required for the SCF to reach the value determined from Equation (5-8) or (5-9). As the equations for the SCF (discuss in more detail in Equation (5-15) and (5-21), Section 5.2.3, for longitudinal and broken back failures, respectively) are very complex, a graphical method was employed to estimate $rs_i(t_{f,i,1})$. The SCF is plotted against corrosion depth at a small step size (Figure 5-2). Given the SCF calculated from Equation (5-8) or (5-9), the corroded depth ($c(t_{f,i,1})$) can be found from the graph, and then $rs_i(t_{f,i,1})$ can be estimated with the known $cs_i\big(t_{f,i,1}\big)$ and pipe age.
3. Repeat Step 1. to 2. for every pipe.
4. Fit a left-censored Weibull distribution to the $rs_i(t_{f,i,1})$ values estimated using the method of Maximum Likelihood. The likelihood function is shown in Equation (5-10) below:

$$L\big(rs_i\big(t_{f,i,1}\big), \gamma, \kappa\big) = \prod_{i \in NC}\left[\frac{\gamma}{\kappa}\left(\frac{rs_i\big(t_{f,i,1}\big)}{\kappa}\right)^{\gamma-1} e^{-\left(\frac{rs_i(t_{f,i,1})}{\kappa}\right)^{\gamma}}\right]\prod_{i \in LC}\left[1 - e^{-\left(\frac{rs_i(t_{f,i,1})}{\kappa}\right)^{\gamma}}\right]$$

(5-10)

where γ is the shape parameter of the Weibull distribution; κ is the scale parameter of the Weibull distribution; NC represents data points that are not censored; and LC represents data points that are left-censored.

5. Draw from the left-censored Weibull distribution for the water mains at the start of the MPP model.

Initialising the corrosion parameters in this way assumes that there were no failure events in the network before the failures were recorded by the water utility. This is unlikely to be true, but it is a limitation due to data collection. The missing failure record could affect the performance of the MPP model as the fitted distribution only captures the corrosion rate for a portion of the failures that have occurred in the past.

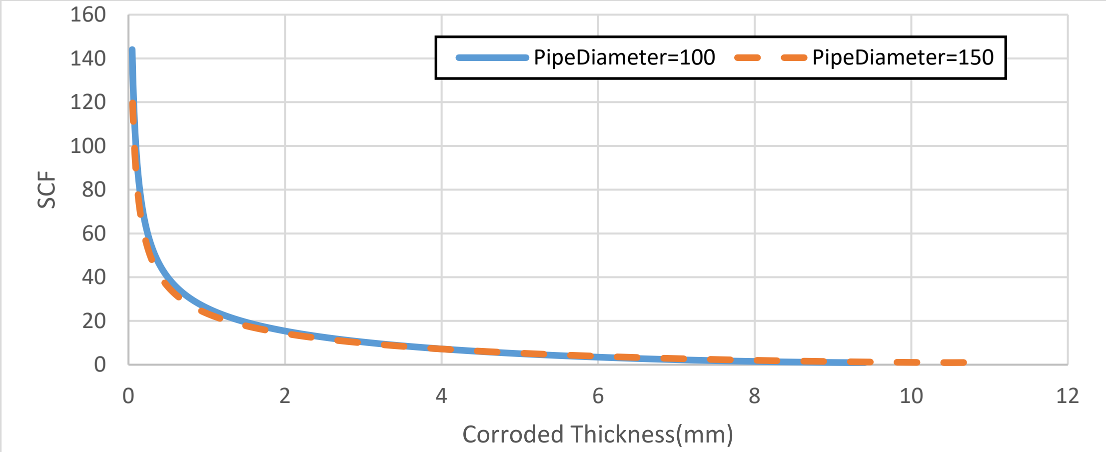

Figure 5-2: SCF (longitudinal failure) for 100mm and 150mm diameter pipes at different corrosion depths.

5.2.2.3. Initialising Time to Next Failure

The method used to initialise the time to next failure ($\Delta T_i(t)$) is also based on failure data. The first step is to calculate the time between consecutive failure events for the water mains that have multiple failures recorded. The exact time to next failure can be calculated except for the first and last failure event (Figure 5-3 in green). The first and last failure event can be used to obtain an upper and lower bound for $\Delta T_i(t)$. This is demonstrated using Figure 5-3. The first failure event can provide an upper bound for $\Delta T_i(t)$ regardless of the number of unknown failure event that have occurred before the observation period (Figure 5-3 in green), the time to failure for pipe i will not exceed $t_{f,i,1}$. The last recorded failure ($m-th$ failure) ($t_{f,i,m}$) can be used to calculate a lower bound for the $\Delta T_i(t)$ because failure $m+1$ must occur after the observation period.

For upper bound (left-censored data):

$$\Delta t_{i_{LC}} = t_{f,i_{LC},1}$$

For data with the exact time to failure known:

$$\Delta t_{i_{NC},j} = t_{f,i_{NC},j+1} - t_{f,i_{NC},j} \qquad j = 1,2 \dots m-1$$

For the lower bound (right-censored data):

$$\Delta t_{i_{RC}} = t_{ce} - t_{f,i_{RC},m}$$

where NC is the uncensored data point; LC is the left-censored data point;RC is the right-censored data point; $\Delta t_{i_{NC},j}$ is the time to next failure after the *j-th* event for the *i-th* pipes that is uncensored; $\Delta t_{i_{LC}}$ is the upper bound data point for pipe i that is left-censored; $\Delta t_{i_{RC}}$ is the lower bound data point for pipe i that is right-censored; $t_{f,i,j}$ is the time to the *j-th* failure for pipe i; and t_{ce} the end of data collection

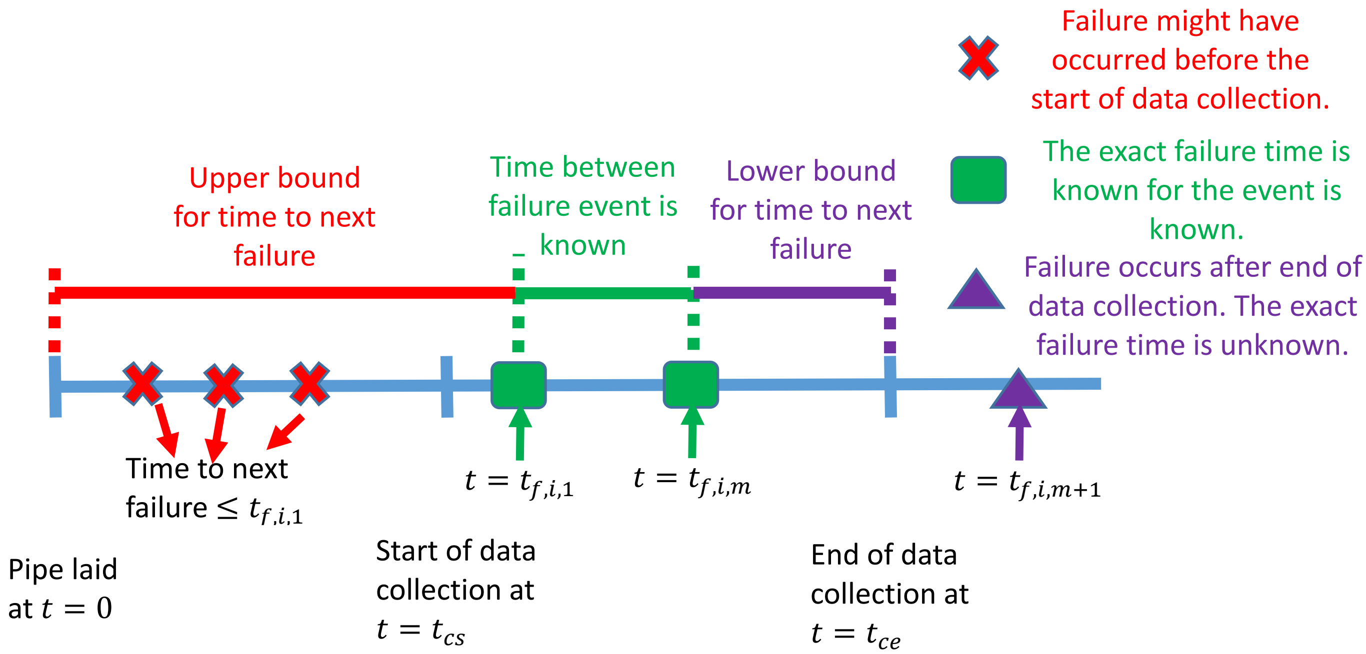

Figure 5-3: Time to next failure for censored and uncensored data.

For example, given that the failure data have been collected between 1999 and 2004, a pipe that was constructed in 1980 has two failures recorded, one in 2000 and one in 2002. An upper bound can be found for the pipe using the first failure, the time to next failure must not exceed 20 years (1999-1980). Otherwise, the first failure should have been recorded after 2000. For the first failure event, the time to next failure will be 2 years (2002-2000). For the second failure event, a lower bound can be calculated because it is the last recorded failure in the observation period. The time to next failure must be at least 3 years or more. Otherwise, another failure would have been recorded for the pipe.

After calculating the time between the failure events for all the failed pipes, the values are fitted to a left- and right-censored Weibull distribution. When a pipe failure occurs, a value will be randomly drawn from the distribution for $\Delta T_i(t)$ to adjust the corrosion parameters in the model. The steps in estimating the time to next failure is listed below:

1. Calculate the time to next failure for all the pipes with failures recorded.
2. Fit the time between failure events to the left- and right-censored Weibull distribution using the method of Maximum Likelihood. The likelihood function can be expressed as:

$$L(\gamma,\kappa) = \prod_{i=1}^{n_{NC}} \prod_{j=1}^{m_i-1} \left[\frac{\gamma}{\kappa} \left(\frac{\Delta t_{i,j}}{\kappa} \right)^{\gamma-1} e^{-\left(\frac{\Delta t}{\kappa}\right)^{\gamma}} \right] \prod_{i=1}^{n_{LC}} \left[1 - e^{-\left(\frac{\Delta t_i}{\kappa}\right)^{\gamma}} \right] \prod_{i=1}^{n_{RC}} \left[e^{-\left(\frac{\Delta t_i}{\kappa}\right)^{\gamma}} \right] \tag{5-11}$$

where γ is the shape parameter of the Weibull distribution; κ is the scale parameter of the Weibull distribution; m_i is the maximum number of observed failures in pipe i; n_{NC} is the number of pipes that are not censored; n_{LC} is the number of pipes that are left-censored; and n_{RC} is the number of pipes that are right censored.

3. When $\Delta T_i(t)$ is required, draw a value randomly from the distribution.

Since the time to next failure is based on the failure data, it will suffer from the same drawback as those discussed with initialising corrosion parameters using failure data (Section 5.2.2.2).

5.2.3 Physical Models

Two different physical models are used in the MPP model, one to account for longitudinal split failures, and one to account for broken back failures in CI pipes.

5.2.3.1. Longitudinal Split Failures

Longitudinal split failures are modelled using the work from the 'Advanced Condition Assessment & Pipeline Failure Prediction Project'. The project developed a physical model for large diameter (>=300mm) CI pipes with elliptical corrosion patches on the external surface (Ji et al., 2015). The model will be applied to both small and large diameter pipes in this study, and the configuration of the corrosion patch is shown in Figure 5-4, where the patch is simplified to a circular shape. The maximum stress of the pipe at time *t* can be defined as shown in Equation (5-12). The nominal stress is calculated using the equation for thin-walled pressure vessel (Equation (5-13)) but can be replaced by the equation developed by Robert et al. (2016) as part of the 'Advanced Condition Assessment & Pipeline Failure Prediction Project'. The SCF can be estimated using Equation (5-15).

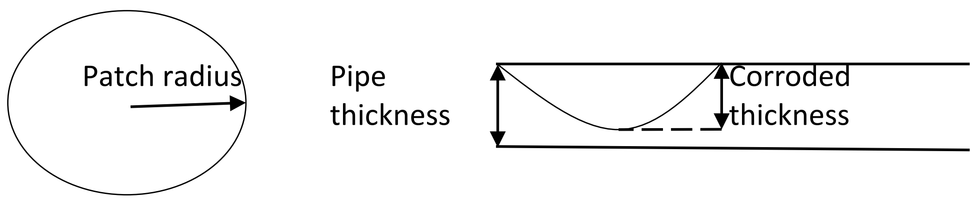

Figure 5-4: Configuration of corrosion patch.

$$\sigma_{m,i} = \sigma_{n,i} SCF_i(c_i(t))$$

(5-12)

$$\sigma_{n,i} = \frac{P_i D_i}{2t'_i}$$

(5-13)

$$c_i(t) = cs_i(t) + rs_i(t)Age_i(t)$$

(5-14)

$$SCF_i(c_i(t)) = \frac{\frac{\sqrt[4]{3(1-\nu^2)}}{2} + \alpha_1\left(\frac{Pa * c_i(t)}{\sqrt{\frac{D_i}{2}t'_i}}\right)^{\beta_1} + \alpha_2\left(\frac{Pa * c_i(t)}{\sqrt{\frac{D_i}{2}t'_i}}\right)^{\beta_2} + \alpha_3\left(\frac{c_i(t)}{\sqrt{\frac{D_i}{2}t'_i}}\right)^{\beta_3}}{\frac{\sqrt[4]{3(1-\nu^2)}}{2} + \alpha_4\left(\frac{Pa * c_i(t)}{\sqrt{\frac{D_i}{2}t'_i}}\right)^{\beta_4} + \alpha_5\left(\frac{Pa * c_i(t)}{\sqrt{\frac{D_i}{2}t'_i}}\right)^{\beta_5} + \alpha_6\left(\frac{c_i(t)}{\sqrt{\frac{D_i}{2}t'_i}}\right)^{\beta_6}}\left(\frac{t'_i}{t'_i - c_i(t)}\right)^{\beta_7}$$

(5-15)

where ν is the Poisson ratio and is taken as 0.3 for all pipes; P is the static water pressure of the pipe; and α_1 to α_6 and β_1 to β_7 (Table 5-6) are coefficients that have been estimated from a large number of Finite Element Analysis using nonlinear least square regression methods (Ji et al., 2015). Other parameters have already been defined in Table 5-3 . The corrosion process is modelled as described in Section 5.2.1. Since the CI pipes under consideration have been laid for a long time, they are assumed to have past the first corrosion stage of the bi-linear model and only the second stage of the corrosion model is considered in the study (Equation (5-1)). Note that a minimum nominal stress of 1MPa was imposed on the pipes as some of the steady-state pressure estimated (based on a hydraulic model used by the utility) was lower than expected.

As stated earlier, the physical model used to estimate longitudinal failure was developed for the large diameter pipe. The model is still applicable to the small diameter pipe because the failure mechanism is the same. The possible limitation of the model would likely come from the nominal stress equation (Equation (5-13)). Equation (5-13) is developed on the basis of a thin-walled pressure vessel. This requires the thickness of the pipe wall to be much less than the radius of the pipe (general rule is that the ratio of radius to wall thickness is greater than 10) (Gere, 2003). Based on the equation for pipe thickness in Table 5-3, the thickness of a 300mm large diameter pipe is estimated to be 14.45mm and satisfies this general rule. Therefore, it is considered that the thin-walled pressure vessel equation is applicable for large diameter pipes.

On the other hand, the wall thickness is approximately 9.41mm for a 100mm diameter pipe, which just satisfies this general rule. As the pipe diameter reduces, the ratio of pipe radius to pipe wall thickness can no longer be considered as a thin-walled pressure vessel. Therefore, using Equation (5-13) to estimate the nominal stress for small diameter pipes may impact on the overall performance of the MPP model.

Table 5-6: Estimated coefficients for the parameters in Equation (5-15).

Parameters	Coefficients
α_1	33.91
α_2	34.89
α_3	0.00
α_4	17.74
α_5	20.01
α_6	94.57
β_1	1.90
β_2	3.67
β_3	5.00
β_4	2.42
β_5	1.69
β_6	3.38
β_7	0.51

5.2.3.2. Broken Back Failures

The bending stress equation has been developed for water mains subjected to ground movements in reactive soil regions. The common hotspots for broken back failures are under the driveway and around locations where the pipe cross covered areas (e.g. road). These areas can restraint the movement of soils and can control the change of soil moisture content. During dry summer periods, a differential in soil moisture content is created around driveways as the driveway reduces the rate of soil moisture loss, causing the pipe to bend in the manner shown in Figure 5-5 and generates high bending stress close to the centre of the driveway. In wet winter periods, the driveway restraints the swelling of the soils, causing the pipe to bend as shown in Figure 5-6 and the maximum bending stress can be found near the edge of the driveway. In the case of corroded CI pipes, the bending stress on the pipe is further intensified as a result of external corrosion (the SCF is taken as the inverse of the stress intensity factor developed by Antaki (2003)).

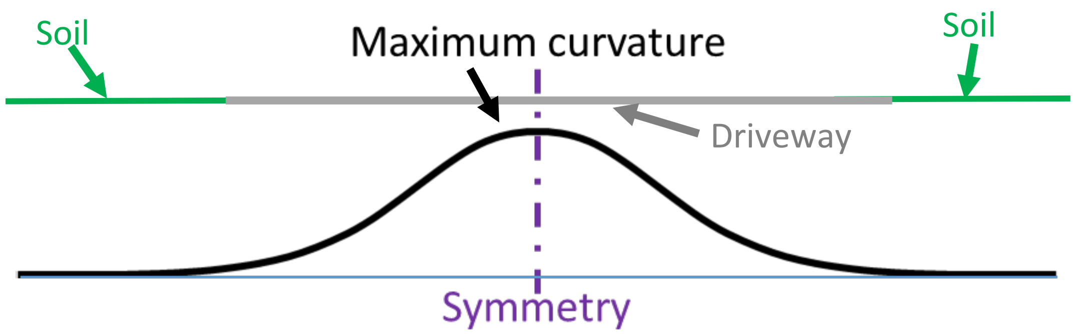

Figure 5-5: Bending of pipe subjected to soil drying.

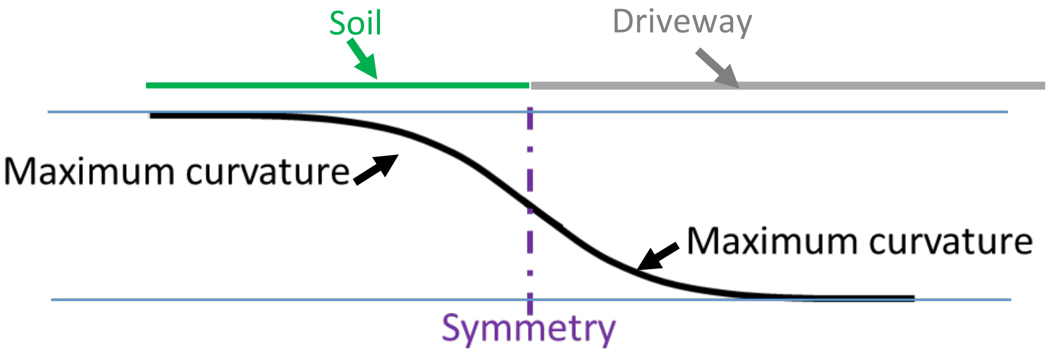

Figure 5-6: Bending of pipe subjected to soil wetting.

The equations to estimate the wetting and drying bending stress (more detail on the development of the bending stress equations can be found in Weerasinghe (in preparation)) of the pipe in year t are shown in Table 5-7. The coefficients used in the bending stress equation are subjected to the soil moisture conditions and the size of the driveway above the pipe. In this study, all pipes analysed are assumed to cross a single driveway because the location and the size of the driveway are not currently linked to the pipe asset database. There will be cases where this assumption will not hold and might impact on the performance of the model.

The maximum change in the soil moisture content in year t for the drying and wetting scenario are calculated using Equation (5-16) and (5-17), respectively; the second moment of area, I, can be calculated using Equation (5-18); the maximum bending stress in year t is the maximum bending stress out of all months in year t (Equation (5-19)); the equation for the maximum stress is shown in Equation (5-20); and the calculation of the SCF is shown in Equation(5-21).

Table 5-7: Bending stress equations for broken back failures under different conditions.

Change in Soil Moisture	Single Driveway	Dual Driveway
Soil Drying $\Delta\theta_{w,i,dry}(t)$ is negative	$\sigma'_{b,i,dry}(t) = \frac{EMS_{i,max}}{j_i^2}\frac{(D_i + 2t'_i)}{2}$ $S_{i,max} = 0.5\frac{0.52\Delta G\Delta\theta_{w,i,dry}(t)}{2}$ $M = \frac{1}{1 + 765.314\left(\frac{I}{j^4}\right)^{0.5647}}$ $j = 943$	$\sigma'_{b,i,dry}(t) = \frac{EMS_{i,max}}{j_i^2}\frac{(D_i + 2t'_i)}{2}$ $S_{i,max} = 0.75\frac{0.52\Delta G\Delta\theta_{w,i,dry}(t)}{2}$ $M = \frac{1}{1 + 765.314\left(\frac{I}{j^4}\right)^{0.5647}}$ $j = 1932$
Soil Wetting $\Delta\theta_{w,i,wet}(t)$ is positive	$\sigma'_{b,i,wet}(t) = \frac{EMS_{i,max}}{j_i^2}\frac{(D_i + 2t'_i)e^{-0.5}}{\sqrt{8\pi}}$ $S_{i,max} = 0.5\frac{0.52\Delta G\Delta\theta_{w,i,wet}(t)}{2}$ $M = \frac{1}{1 + 186.182\left(\frac{I}{j^4}\right)^{0.3217}}$ $j = 390$	$\sigma'_{b,i,wet}(t) = \frac{EMS_{i,max}}{j_i^2}\frac{(D_i + 2t'_i)e^{-0.5}}{\sqrt{8\pi}}$ $S_{i,max} = 0.75\frac{0.52\Delta G\Delta\theta_{w,i,wet}(t)}{2}$ $M = \frac{1}{1 + 186.182\left(\frac{I}{j^4}\right)^{0.3217}}$ $j = 321$

$$\Delta\theta_{w,i,wet}(t) = \theta_{w,i,avg} - \theta^{y}_{w,i,max}(t)$$

(5-16)

$$\Delta\theta_{w,i,dry}(t) = \theta_{w,i,avg} - \theta^{y}_{w,i,min}(t)$$

(5-17)

$$I_i = \frac{\pi}{64}[(D_i + 2t'_i)^4 - D_i^4]$$

(5-18)

$$\sigma_{b,i}(t) = \max\left(\sigma'_{b,i,dry}(t)m, \sigma'_{b,i,wet}(t)\right)$$

(5-19)

$$\sigma_{m,i}(t) = \sigma_{b,i}(t)SCF_i(c_i(t))$$

(5-20)

$$SCF_i(c_i(t)) = \frac{1}{1 - d_{eff}t'_i}$$

(5-21)

$$d_{eff} = \frac{c_i(t)(1 - 1/f)}{1 - c_i(t)/t'_i f}$$

(5-22)

$$f = \sqrt{1 + \frac{(Pa * c_i(t)/t'_i)^2}{2}}$$

(5-23)

$$c_i(t) = cs_i(t) + rs_i(t)Age_i(t)$$

(5-24)

where $\Delta\theta_{w,i,wet}(t)$ is the maximum change in average soil moisture content for the wetting scenario in year t for pipe i; $\Delta\theta_{w,i,dry}(t)$ is the maximum change in average soil moisture content for the drying scenario in year t for pipe i; $\theta_{w,i,avg}$ is the average monthly soil moisture for the observation period (Equation (5-7));$\theta^{y}_{w,i,max}(t)$ is the maximum average soil moisture content estimated from Equation (5-5); $\theta^{y}_{w,i,min}(t)$ is the minimum average soil moisture content estimated from Equation (5-6); $\sigma'_{b,i,dry}(t)$ is the drying bending stress; $\sigma'_{b,i,wet}(t)$ is the wetting bending stress; $\sigma_{b,i}(t)$ is the maximum bending stress in year t for pipe i; and the rest of the other parameters have been defined in Table 5-3.

The condition of the pipe is represented using the damage factor ($DF_i(t)$) for both failure modes. It is expressed as (inverse of the factor of safety):

$$DF_i(t) = \frac{\sigma_{m,i}(t)}{\sigma_t}$$

(5-25)

When $DF_i(t) \geq 1$, the MPP model estimates a failure in year t (Equation (5-26)), if $DF_i(t) < 1$, the water main operates normally in year *t* (Equation (5-26)).

$$F_i(t) = \begin{cases} 1, DF_i(t) \geq 1 \\ 0, DF_i(t) < 1 \end{cases}$$

(5-26)

In the first training year of the model (before the corrosion parameters are updated), it is possible for the estimated $DF_i(t)$ to be much larger than 1. This is because the high corrosion rate estimated from S_r or drawn from the corrosion rate distribution is combined with a high nominal or bending stress, leading to a large $DF_i(t)$ value. However, as the model progress through the years, the updating of the corrosion parameters (discussed in the next section) will be able to solve this issue for the remaining periods

5.2.4 Update of Corrosion Parameters

The main variables that control the $DF_i(t)$ are the two corrosion parameters ($rs_i(t)$ and $cs_i(t)$) in the physical model. If the corrosion parameters are not reflecting the corrosion environment of the pipe correctly, the $DF_i(t)$ estimated for the pipe will not be accurate. For example, a failure could be found in a pipe where the physical model estimates $DF_i(t) < 1$ in year t because the corrosion parameters were underestimated. Therefore, to improve the accuracy of the estimated $DF_i(t)$, the corrosion parameters are updated when there is a mismatch between the damage factor and the failure data. This only applies to the training period of the model because failure records are not available in the future.

Two updating approaches have been considered, one for MPP-P1 (Table 5-8) and one for MPP-P2 (Table 5-9). The method used to initialise the long-term corrosion rate does not affect the updating process. A (*) is used to represent the updated corrosion parameters. Each time the parameters are updated, the model will recalculate the $DF_i(t)$ and compare it with the observed failure data to check whether further adjustments are required. However, the failure of a pipe ($F_i(t)$) is calculated only before the corrosion parameters are updated (equals to 1 if model estimates a failure in time t). Note that an upper bound is set for the $rs_i(t)$, it must not exceed the initial corrosion rate ($r_{0,i}$) estimated using the S_r from Table 5-5.

Table 5-8: Updating method for MPP-P1 model.

Observed Failure Data	Estimated $DF_i(t) \geq 1$	Explanation	Action
Yes	Yes	The water main is corroding at the correct rate. A failure has occurred, $cs_i(t)$ is reduced for the remaining segments using $\Delta T_i(t)$ as they have better coating quality, giving a longer holiday period. A failure is estimated for the pipe.	• Corrosion parameters for next period: $rs_i(t+1) = rs_i(t)$ $cs_i(t+1) = cs_i(t) - \Delta T_i(t) rs_i(t)$ • Record a failure for the pipe: $F_i(t) = 1$
Yes	No	The water main is corroding too slow, the corrosion rate has to be increased. The updated corrosion rate for the year is estimated with the equation shown on the right using the graphical method discussed in Section 5.2.2.2. The failure influence factor is calculated as well because an unexpected failure has occurred (discussed in more detail in Section 5.2.5).	• Increase corrosion rate by finding the $rs_i^*(t)$ that satisfies the following equation: Longitudinal failure: $SCF_i\left(cs_i(t) + rs_i^*(t) Age_i(t)\right) = \frac{\sigma_{t,i}}{\sigma_{n,i}}$ Broken back failure: $SCF_i\left(cs_i(t) + rs_i^*(t) Age_i(t)\right) = \frac{\sigma_{t,i}}{\sigma_{b,i}(t)}$ • If $rs_i^*(t)$ is estimated to be greater than $r_{0,i}$, $cs_i(t)$ is increased by 0.1 until the model estimate a failure ($DF_i(t) \geq 1$). • The failure influence factor: $f_i(t) = \frac{rs_i^*(t)}{rs_i(t)} - 1$
No	Yes	The water main is corroding too fast. The corrosion rate is updated with the equation shown on the right using the graphical method discussed in Section 5.2.2.2. $cs_i(t)$ is reduced using $\Delta T_i(t)$ because the coating quality is better than expected. The pipe will fail again in $\Delta T_i(t)$ year. A failure is estimated for the pipe.	• Reduce corrosion rate by finding the $rs_i^*(t)$ that satisfies the following equation, this ensures that the pipe is not corroding too fast (e.g. failure before the start of the analysis period): Longitudinal failure: $SCF_i\left(cs_i(t) + rs_i^*(t) Age_i(t)\right) = \frac{\sigma_{t,i}}{\sigma_{n,i}}$ Broken back failure: $SCF_i\left(cs_i(t) + rs_i^*(t) Age_i(t)\right) = \frac{\sigma_{t,i}}{\sigma_{b,i}(t)}$ • Update the intercept of the corrosion parameter $cs_i^*(t) = cs_i(t) - \Delta T_i(t) rs_i^*(t)$ • Record a failure for the pipe $F_i(t) = 1$
No	No	No action required to adjust the corrosion parameters.	

Table 5-9: Updating method for MPP-P2 model.

Observed Failure Data	Estimated $DF_i(t) \geq 1$	Explanation	Action
Yes	Yes	The water main is corroding at the correct rate. A failure has occurred, $rs_i(t)$ is reduced for the remaining segments of the pipe using $\Delta T_i(t)$. A failure is estimated for the pipe.	• Corrosion parameters for next period: $$rs_i(t+1) = \frac{rs_i(t)Age_i(t)}{Age_i(t) + \Delta T_i(t)}$$ • Record a failure for the pipe: $$F_i(t) = 1$$
Yes	No	The water main is corroding too slow, the corrosion rate has to be increased. The updated corrosion rate for the year is estimated with the equation shown on the right using the graphical method discussed in Section 5.2.2.2. The failure influence factor is calculated because an unexpected failure has occurred (discussed in more detail in Section 5.2.5).	• Increase corrosion rate by finding the $rs_i^*(t)$ that satisfies the following equation: Longitudinal failure: $$SCF_i\big(cs_i(t) + rs_i^*(t)Age_i(t)\big) = \frac{\sigma_{t,i}}{\sigma_{n,i}}$$ Broken back failure: $$SCF_i\big(cs_i(t) + rs_i^*(t)Age_i(t)\big) = \frac{\sigma_{t,i}}{\sigma_{b,i}(t)}$$ • If $rs_i^*(t)$ is estimated to be greater than $r_{0,i}$, $cs_i(t)$ is increased by 0.1 until the model estimate a failure ($DF_i(t) \geq 1$). • The failure influence factor: $$f_i(t) = \frac{rs_i^*(t)}{rs_i(t)} - 1$$
No	Yes	The water main is corroding too fast. The corrosion rate is reduced by assuming that it will fail again in $\Delta T_i(t)$ years. The updated corrosion rate for the year is estimated with the equation shown on the right using the graphical method discussed in Section 5.2.2.2. A failure is estimated for the pipe.	• Reduce corrosion rate by finding the $rs_i^*(t)$ that satisfies the following equation: Longitudinal failure: $$SCF_i\big(cs_i(t) + rs_i^*(t)(Age_i(t) + \Delta T_i(t))\big) = \frac{\sigma_{t,i}}{\sigma_{n,i}}$$ Broken back failure: $$SCF_i\big(cs_i(t) + rs_i^*(t)(Age_i(t) + \Delta T_i(t))\big) = \frac{\sigma_{t,i}}{\sigma_{b,i}(t)}$$ • Record a failure for the pipe $$F_i(t) = 1$$
No	No	No action required to adjust the corrosion parameters.	

A graphical illustration of the adjustment to the corrosion parameters in Table 5-8 and Table 5-9 are shown in APPENDIX C (Figure C - 1 to Figure C - 3 for Table 5-8 and Figure C - 4 to Figure C - 6 for Table 5-9). Note that the change in the long-term corrosion parameters will affect the τ and $r_{0,i}$ (as shown in Figure C - 1 to Figure C - 6). However, as the failure of the pipe is assumed to be in the second linear phase of the corrosion model, the changes in τ and $r_{0,i}$ are not considered.

5.2.5 Failure Influence Factor

An unexpected failure event is defined as a failure that has been recorded for the pipe at time t, but $DF_i(t) < 1$ is estimated from the physical model. In this case, the long-term corrosion rate is increased as shown in Table 5-8 or depending on the updating method used.

Assuming pipes within a certain radius are operating in a similar environment, it is possible that the long-term corrosion rates for pipes surrounding the unexpected failure have also been underestimated. Therefore, the long-term corrosion rates of these pipes are also increased as a function of the failure influence factor and the distance between the pipes. The failure influence factors are only applied in the training period because failure records are not available when making predictions into the future.

The failure influence factor for the pipe with the unexpected failure event can be calculated as:

$$\boldsymbol{f_i(t) = \frac{rs_i^*(t)}{rs_i(t)} - 1}$$

(5-27)

where $f_i(t)$ is the failure influence factor for pipe i at time t and $rs_i^*(t)$ is the updated corrosion rate (should be greater than $rs_i(t)$).

Let t_1 be the time under examination; k is the *k-th* pipe without failure; R is the radius of influence; i is the *i-th* ($i = 1,2 \dots I$) pipe with the unexpected failure event and are within R meters of the *k-th* pipe; $L_{k,i}$ is the distance between the centre of pipe k and i; and a is a decay factor that controls the portion of failure influence factor that is passed onto the surrounding pipes. The corrosion rate for the *k-th* pipe without failure in the next time period ($rs_k(t_1 + 1)$) is calculated as shown in Equation (5-28). Note, a maximum bound of $r_{0,k}$ is set for the long-term corrosion rate.

$$rs_k(t_1 + 1) = \max_{\mathrm{i \in I}}(1 + f_i(t_1)e^{-aL_{k,i}})\, rs_k(t_1)$$

(5-28)

The study will consider a range of values for the radius of influence and a to determine the optimal values for the two parameters.

5.2.6 Failure Prediction

The final part of the MPP model is to predict the condition of water mains in the future. The corrosion depth of the pipe is allowed to grow until failure, in which the segment of the pipe is replaced. The corrosion parameters for the remaining segments are adjusted based on $\Delta T_i(t)$ similar to Table 5-8 and Table 5-9, depending on the updating method used (Table 5-10).

Table 5-10: Adjustment for the corrosion parameters during prediction.

Estimated $DF_i(t) \geq 1$	MPP-P1	MPP-P2
Yes	A failure has occurred, and $cs_i(t)$ is reduced for the remaining segments using $\Delta T_i(t)$ as they have better coating quality, giving a longer holiday period. • Corrosion parameters for next time period: $rs_i(t+1) = rs_i(t)$ $cs_i(t+1) = cs_i(t) - \Delta T_i(t) rs_i(t)$ • Record a failure for the pipe $F_i(t) = F_i(t) + 1$	A failure has occurred, and $rs_i(t)$ is reduced for the remaining segments of the pipe using $\Delta T_i(t)$. • Corrosion parameters for next time period: $rs_i(t+1) = \frac{rs_i(t) Age_i(t)}{Age_i(t) + \Delta T_i(t)}$ • Record a failure for the pipe $F_i(t) = F_i(t) + 1$
No	No action is required to adjust the corrosion parameters.	

5.2.7 Process Summary

Figure 5-7 provides a flowchart that summaries the process of the MPP model. The model is started by initialising the corrosion parameters (use one of the two methods proposed) and time to next failure using the steps described in Section 5.2.2. Other input variables can be drawn from the data or estimated from equations that have been developed (Table 5-3). Then the damage factor of the pipe is estimated using the physical model for longitudinal failure or broken back failures (Section 5.2.3). If the model is in the training period, the damage factor is compared with the failure data to update the corrosion parameters (Section 5.2.4). After the updating processes have been repeated for all the water mains, the failure influence factor is applied before moving onto the next year (Section 5.2.4). After the training period, the model can be used to predict failure events in the future. The corrosion parameters during predictions are adjusted using Table 5-10 from Section 5.2.5.

For the MPP model with corrosion parameters initialised using failure data, the long-term corrosion rate is represented using a stochastic distribution. Therefore, simulation is used to estimate the damage factor and the probability of observing a failure according to the following steps:

1. Estimate the distribution for the long-term corrosion rate based on Section 5.2.2.2.
2. For iteration=1 to number of simulations
   2.1 Draw a value from the long-term corrosion rate distribution for each water main.
   2.2 Follow the flowchart in Figure 5-7 and estimate the damage factor (Equation (5-25)) and the probability of observing a failure (Equation (5-26)).
   2.3 Move to the next simulation.
3. Calculate the expected damage factor and probability of failure:

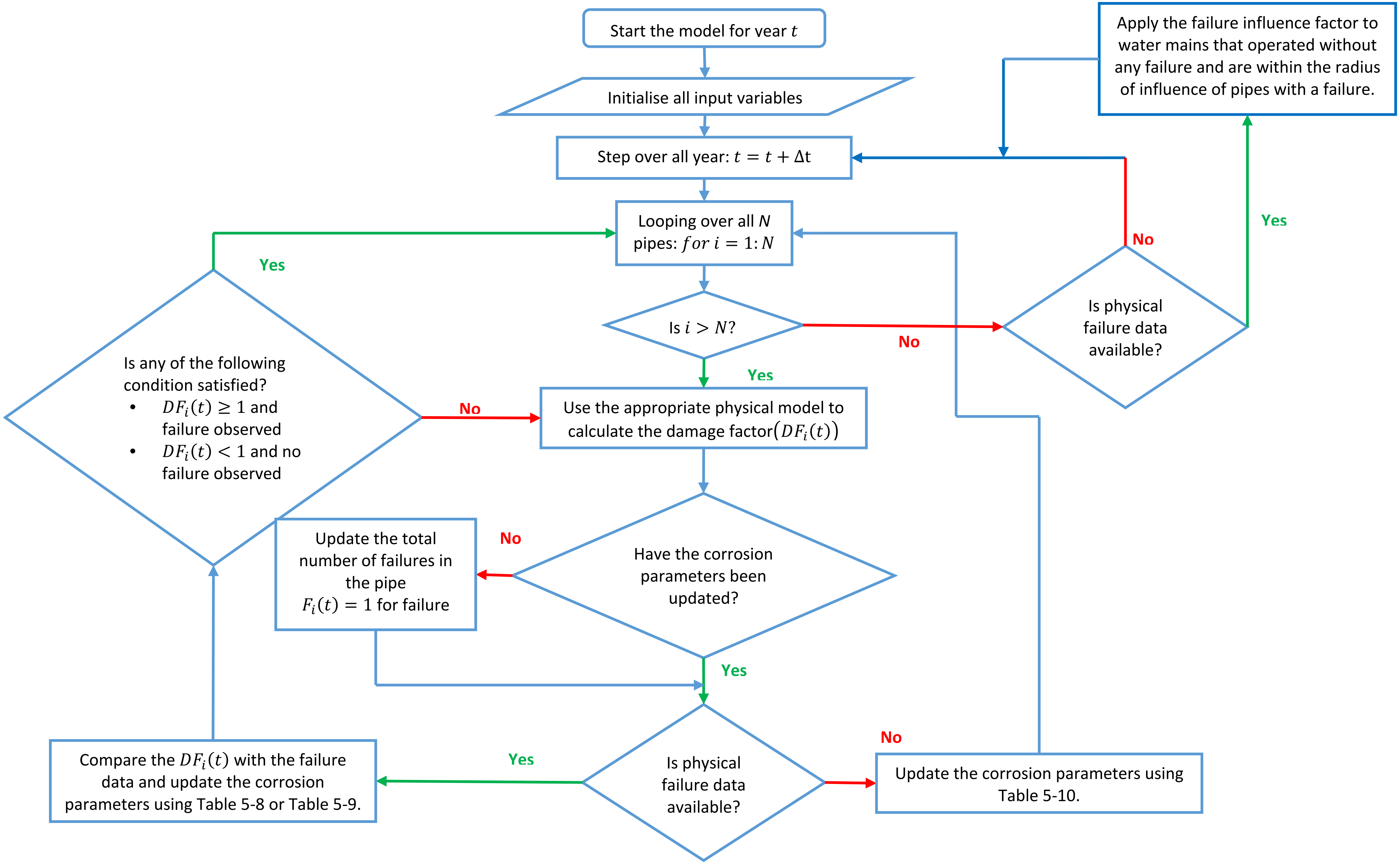

Figure 5-7: MPP model flowchart.

$$DF_{m,i}(t) = \frac{\sum_{n=1}^{iter} DF_{n,i}(t)}{iter}$$

(5-29)

$$F_{m,i}(t) = \frac{\sum_{n=1}^{iter} F_{n,i}(t)}{iter}$$

(5-30)

where m represents the average value; $DF_{m,i}(t)$ is the expected value for the damage factor for pipe i at time t; $DF_{n,i}(t)$ is the damage factor for pipe i at time t for iteration n; $F_{m,i}(t)$ is the expected probability of failure for pipe i at time t; $F_{n,i}(t)$ represents whether pipe i failed or not at time t for iteration n; and $iter$ is the total number of iterations.

The number of iterations required in the simulation is determined by checking the convergence of the damage factor. The number of simulation is increased until the difference between the damage factor from consecutive iteration becomes less than 0.01. This requirement is satisfied by running 500 iterations.

5.3. Modelling Longitudinal Failures Using the Monash Pipe Failure Prediction Model

This section of the chapter will use the MPP model to analyse longitudinal split (LS) failures. To differentiate the two modelling processes (P1 and P2 in Table 5-2), the method used to initialise the long-term corrosion rate, and the years of failure data used to calibrate the model, the following naming conventions are used:

- MPP-LS-P1-Sr-TrainYr: Modelling process P1 and the S_r are used to initialise the long-term corrosion rate. The failure data from the start of the observation period to the Training Year (TrainYr) are used to calibrate the model.
- MPP-LS-P1-Basic-TrainYr: Modelling process P1 and the failure data are used to initialise the long-term corrosion rate (Basic). The failure data from the start of the observation period to the Training Year (TrainYr) are used to calibrate the model.
- MPP-LS-P2-Sr-TrainYr: Modelling process P2 and S_r are used to initialise the long-term corrosion rate. The failure data from the start of the observation period to the Training Year (TrainYr) are used to calibrate the model.
- MPP-LS-P2-Basic-TrainYr: Modelling process P2 and the failure data are used to initialise the long-term corrosion rate (Basic). The failure data from the start of the observation period to the Training Year (TrainYr) are used to calibrate the model.

The models will be compared with the BSM (Section 3.3.3) and NHPP (Section 4.5). Their accuracy in estimating the number of pipes with at least 1 failure in the network each year and their ability in identifying the water mains that are more likely to fail (ranking performance) are assessed. Note that only the failure probability can be calculated for the MPP and BSM. Therefore, the failure data are converted into binary format when calibrating the two models, where 1 represents that one or more failure has occurred for the pipe and 0 means that the pipe is operating without any interruptions. The same data format will also be used for the NHPP to keep the dataset consistent between the models. A range of failure influence factor (α=0.1 to 2 at a step size of 0.1) and radius of influence (R=50m, 100m, 200m and 500m) will also be taken into consideration during the process.

5.3.1 Pipe Asset, Failure Data and Input data

5.3.1.1. Pipe Asset and Failure Data

The MPP models are analysed using failure data (only longitudinal failures) provided by a water utility in Melbourne. The dataset (Table 5-11) consists of CI water mains with all pipe diameters. The failures have been recorded between 1994 and 2015. The model will be calibrated using data from 1994-2005 and 1994-2010, the remaining failure data outside the calibration period will be used for model validation purposes.

Table 5-11: Asset data description.

Cohort Properties	Cast Iron Water Mains
Construction year	1860-1993
Observation period	1994-2015
Number of pipes	36460
Pipe length (km)	2070
Number of failures	1761

Although a large number of assets have been included in the analysis, few longitudinal failures have been recorded. Large diameter water mains subjected to high water pressure are more susceptible to longitudinal failures. However, only a small portion of the network are large diameter pipes (usually 300mm or more, Figure 5-8) and the normal operating pressure of the network cannot be considered as high (Figure 5-9). Therefore, it is expected that only a small number of longitudinal failures are recorded in the dataset.

The failure rate (failures per 100km) of the dataset is plotted in Figure 5-10 for the observation period. An increasing trend can be observed from the data. The year-to-year variations in the longitudinal failure data are generally less than the dataset that has been analysed in the previous sections (Figure 3-1, Figure 4-3 and Figure 4-15). This is because longitudinal failures are mainly caused by high water pressure, and therefore, other time dependent factors, such as climate effects, have less influence on this failure mode. Note that the recorded data show the total number of failures in a year, but they are plotted as lines in the figures in the chapter instead of discrete points for better visualisation.

Most input parameters, such as the pipe tensile strength and pipe thickness, can be either drawn from the pipe asset data or found in Table 5-3. The calibration process for the MPP model can be started after the initial corrosion parameters and time to next failure have been initialised.

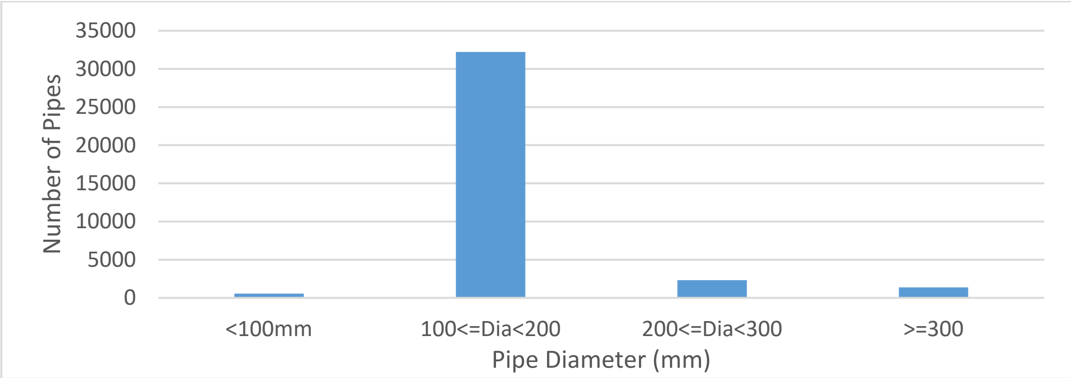

Figure 5-8: Pipe diameter of water mains.

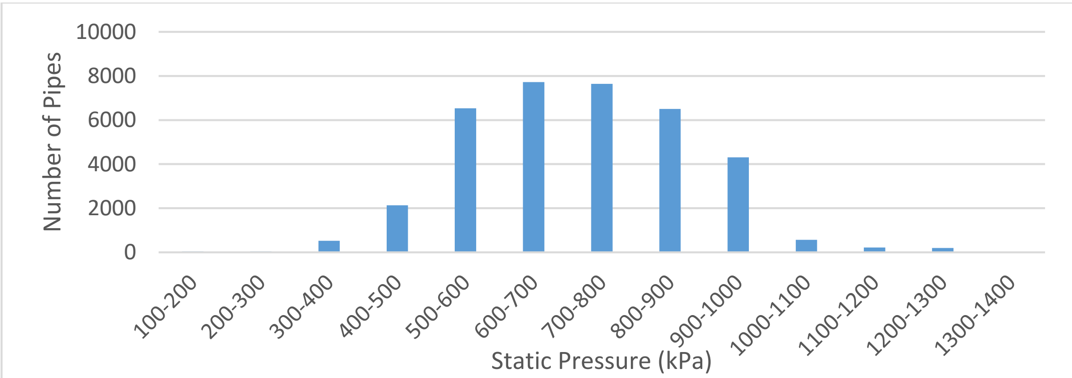

Figure 5-9: Static water pressure of water mains.

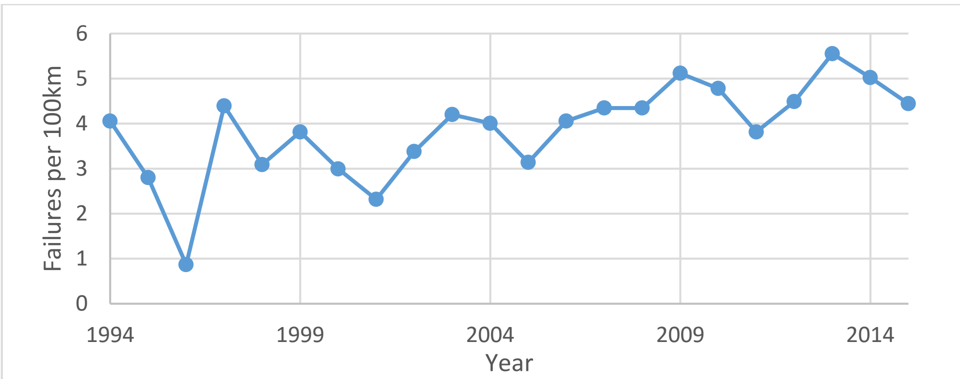

Figure 5-10: Failure rate of the dataset over time.

5.3.1.2. Initial Corrosion Parameters and Time to Next Failure Distribution

The corrosion parameters are initialised using the two approaches described in Section 5.2.2. The CI assets are mapped in Figure 5-11, along with the reactivity of the soil in Figure 5-12. Majority of the water mains are in SE and EX soils. The permanent wilting point and the field capacity can be found in Table 5-4 (Section 5.2.2.1) for the soil types shown in the maps.

A histogram of the soil porosity and soil moisture content for the water mains are shown in Figure 5-13 and Figure 5-14, respectively. The variation of the soil porosity between the water mains are minimal, most of the values are between 0.46 and 0.47.

The soil moisture content ($\theta_{w,i,avg}$) estimated with Equation (5-7) using data from the BOM are found to be clustered into two groups. Most of the water mains are found in soil with a moisture content of about 0.32, while some are found in soil with a moisture content of around 0.1. The water mains with a lower soil moisture content are laid in ST soils, it has a much lower permanent wilting point and field capacity than the other three soil types (SE, EX and VE). Therefore, a smaller soil moisture content is estimated. S_r relevant to the water mains are also split into two groups (Figure 5-15). Most of the water mains have a S_r around 0.7, but for pipes laid in ST soils, the S_r are around 0.2.

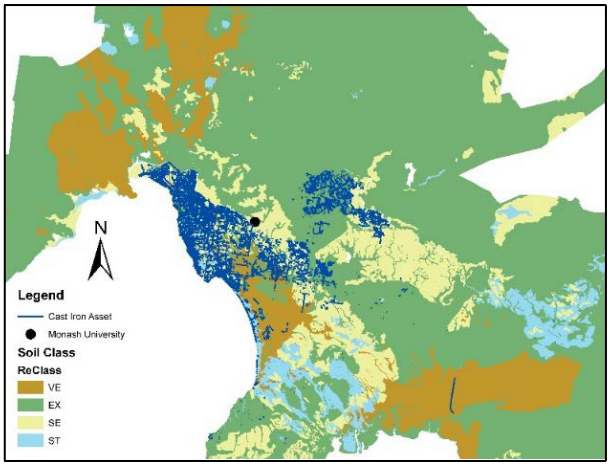

Figure 5-11: Location of cast iron assets with soil reactivity map.

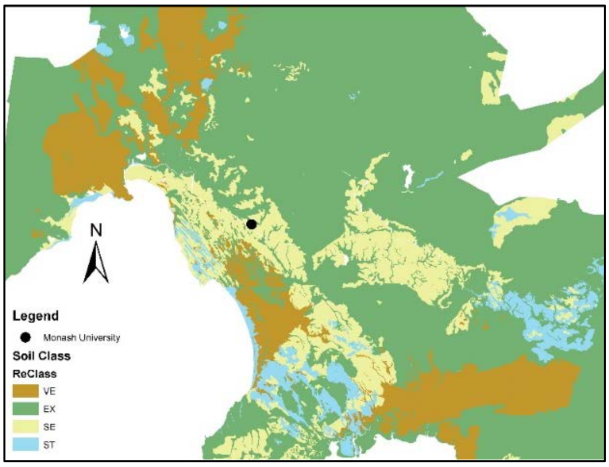

Figure 5-12: Soil reactivity map.

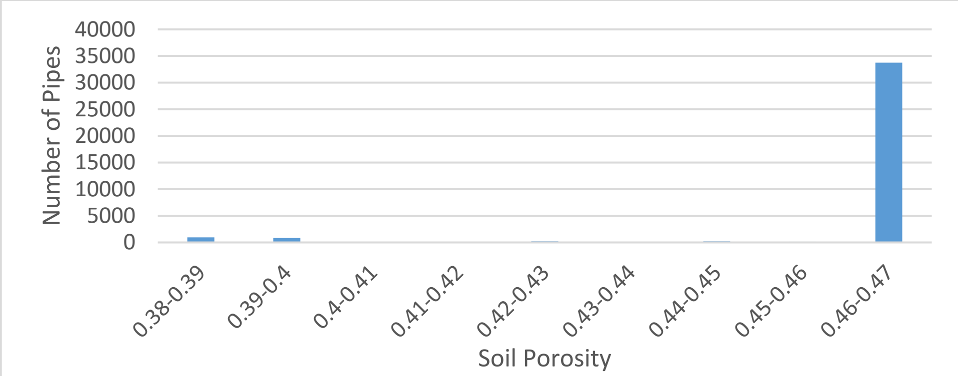

Figure 5-13: Estimated soil porosity for the water mains.

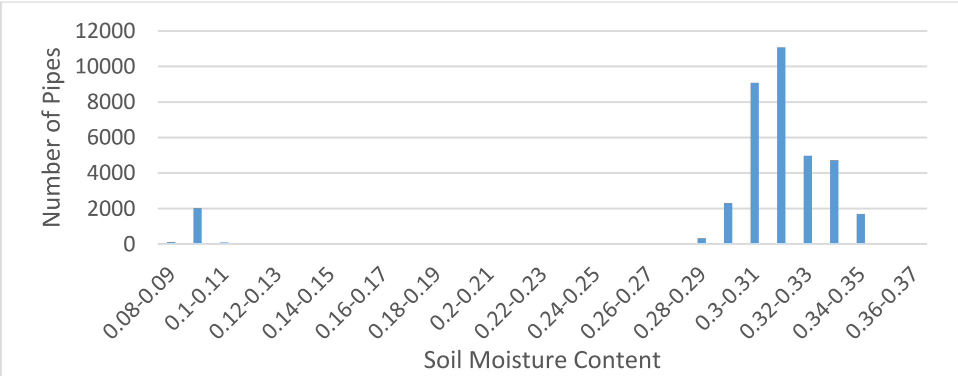

Figure 5-14: Estimated soil moisture content for the water mains.

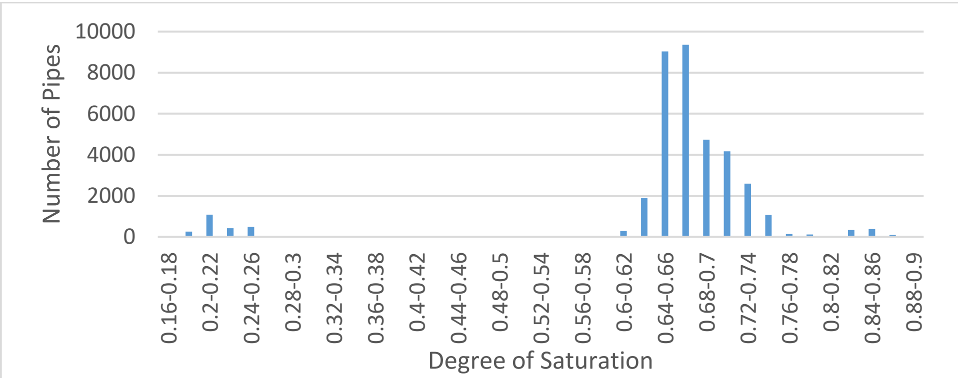

Figure 5-15: Estimated degree of saturation for the water mains.

S_r is converted into corrosion parameters using Table 5-5 for the MPP-LS-P1-Sr-TrainYr and the MPP-LS-P2-Sr-TrainYr models. The distribution of the long-term corrosion rate ($rs_i(t)$) for the MPP-LS-P1-Basic-TrainYr and MPP-LS-P2-Basic-TrainYr models are estimated using the method described in 5.2.2.2. The distributions for $r_{0,i}$ (upper bound), $cs_i(t)$ and $rs_i(t)$ using the two initialisation methods under different training periods are shown in Figure 5-16, Figure 5-17 and Figure 5-18, respectively. The shape and scale parameter of the fitted Weibull distribution for the long-term corrosion rates are shown in Table 5-12. Note, the average soil moisture content ($\theta_{w,i,avg}$) between 2005 and 2016 are used to estimate the S_r to initialise the corrosion parameters. Therefore, the values selected for the parameters are the same regardless of the training period when the S_r is used.

The long-term corrosion rates based on S_r are generally higher than those back-calculated using failure data. Therefore, it is likely that the number of failures estimated for the MPP-LS-P1-Sr-TrainYr and MPP-LS-P2-Sr-TrainYr will be higher than the MPP-LS-P1-Basic-TrainYr and MPP-LS-P2-Basic-TrainYr models.

The time to next failure ($\Delta T_i(t)$) is estimated using the method described in Section 5.2.2.3. Its distributions are plotted in Figure 5-19 for the two training periods (1994-2005 in yellow and 1994-2010 in grey using the left y-axis). The distribution for $\Delta T_i(t)$ using only uncensored data (in blue using right y-axis) is also included to demonstrate the importance of censored data. The shape and scale parameters for the distributions are shown in Table 5-13.

The distributions of the time to next failure for the two training periods are similar. The peak of the distribution for the training period between 1994 and 2005 is about 15 years, while for the training period between 1994 and 2010, the peak of the distribution is about 20 years. The probability distributions approach 0 for both training periods at around 85 years, suggesting that the time to next failure of a pipe after a break is most likely to be less than 85 years.

For the time to next failure without using any censored data, the distribution is spread over a much lower range of values (from about 0 to 30 years) compared to the ones using censored data. This is because it is considered in the model that the entire population has been collected in the uncensored data. In addition, the distribution is biased because the failure data have only been recorded for a short period of time, the maximum time to next failure in the dataset cannot be more than 17 years. Therefore, including censored data in the fitting of $\Delta T_i(t)$ can produce a distribution that is more representative of the actual situation compared to the distribution fitted without censored data. Using the distribution without censored data will likely result in an over-estimation of failures from the MPP model because the time to next failure has been underestimated.

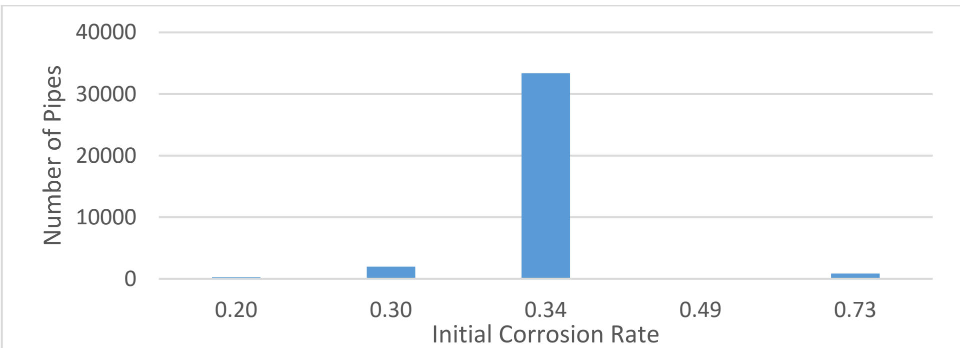

Figure 5-16: Estimated Initial corrosion rate for the water mains.

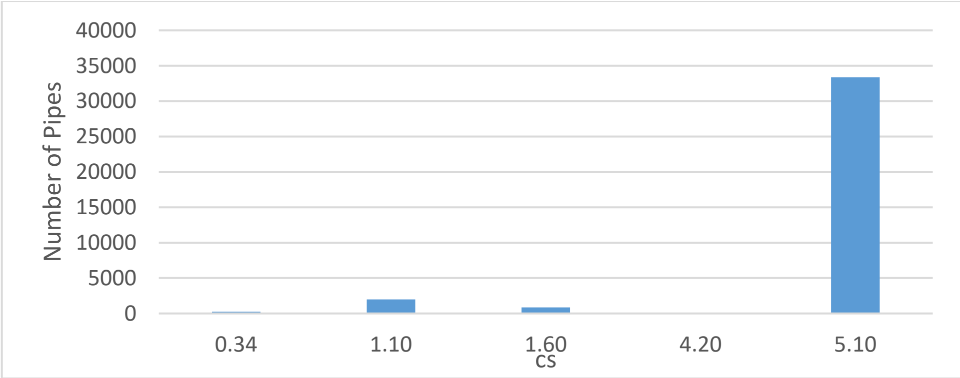

Figure 5-17: Estimated intercept of long-term corrosion rate for the water mains.

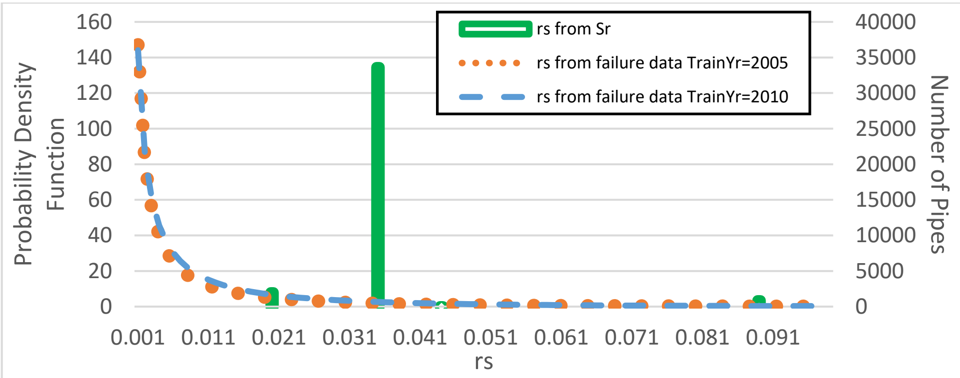

Figure 5-18: Estimated long-term corrosion rate for the water mains.

Table 5-12: Estimated parameters for the Weibull distribution of long-term corrosion rate.

TrainYr	2005	2010
Scale	0.0028	0.0048
Shape	0.44	0.50

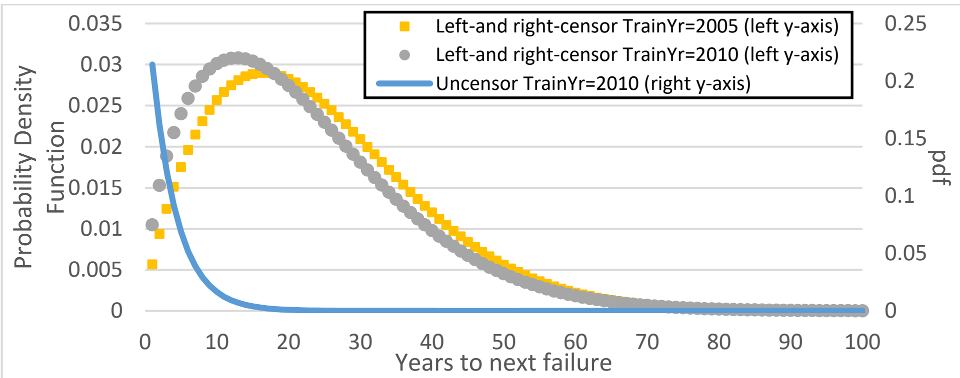

Figure 5-19: Estimated distribution for the time to next failure.

Table 5-13: Estimated parameters for the Weibull distribution of time to next failure.

Parameters	Uncensored	Left-and Right-Censor TrainYr=2005	Left-and Right-Censor TrainYr=2010
scale	3.5	27.2	24.5
shape	1.0	1.7	1.6

5.3.2 Results and Discussions

The section will first compare the accuracy of the MPP model with the BSM and NHPP in estimating the number of pipes that have failed using error statistics (MAE and RMSE in Section 4.3) and graphical plots. Then the ranking performance of the models will also be compared using the prediction curve (Section 3.4).

5.3.2.1. Expected Number of Failures Estimated by the MPP Models

The performance of the different MPP models is first examined before comparing with the BSM and NHPP. The expected total number of failure (Equation (5-30)) for the MPP models (MPP-LS-P1-Sr-2010, MPP-LS-P2-Sr-2010, MPP-LS-P1-Basic-2010, MPP-LS-P2-Basic-2010, MPP-LS-P1-Sr-2005, MPP-LS-P2-Sr-2005, MPP-LS-P1-Basic-2005and MPP-LS-P2-Basic-2005) with no failure influence factor and a training period from 1994-2005 and 1994-2010 are plotted in Figure 5-20 and Figure 5-21, respectively. Note that the results for the first year (1994) of the training period are not shown because it consistently overestimates the expected number of failures, regardless of the models used (Figure C - 7 and Figure C - 8 in APPENDIX C for training period 1994-2010 and 1994-2005, respectively). It is likely that the initial corrosion parameters estimated from the methods proposed in Section 5.2.2.1 and 5.2.2.2 have overestimated the long-term corrosion rate for a large number of pipes, and therefore, those pipes are failing much earlier than they are recorded in the failure data. The updating process will be able to rectify the problem after the first training year. The corresponding MAE and RMSE (without including the first training year, 1994) are also shown in Table 5-14.

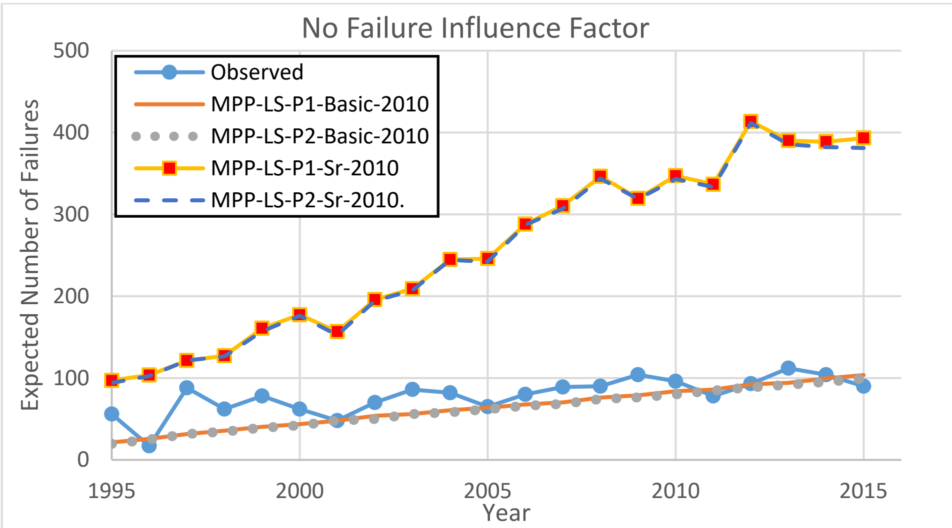

Figure 5-20: Expected number of failures estimated by the MPP model using failure data up to 2010.

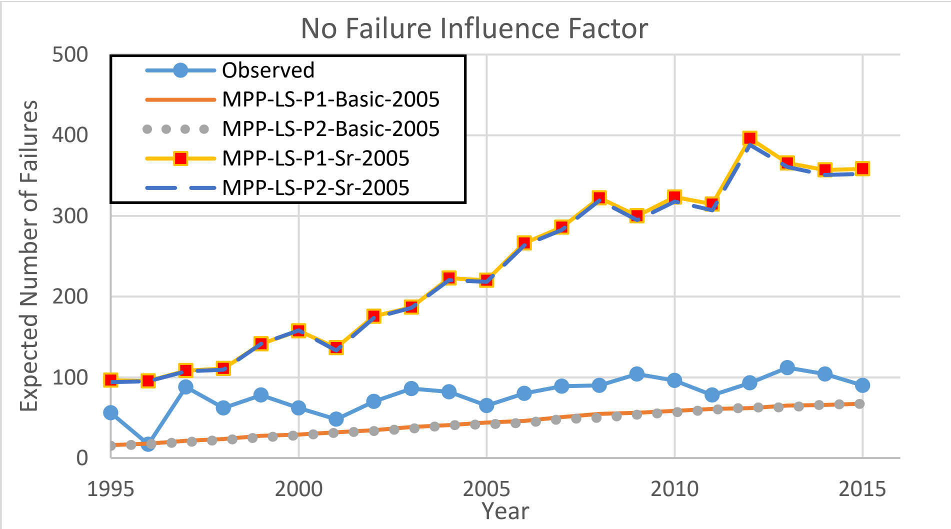

Figure 5-21: : Expected number of failures estimated by the MPP model using failure data up to 2005.

Table 5-14: Error statistics of MPP models with no failure influence factor.

Model	RMSE Training	RMSE Validation	RMSE Overall	MAE Training	MAE Validation	MAE Overall
MPP-LS-P1-Basic-2010	25	11	22	21	9	18
MPP-LS-P2-Basic-2010	26	12	24	22	11	19
MPP-LS-P1-Sr-2010	159	284	198	142	283	177
MPP-LS-P2-Sr-2010.	110	252	195	100	249	174
MPP-LS-P1-Basic-2005	39	35	38	35	34	35
MPP-LS-P2-Basic-2005	41	37	39	37	35	37
MPP-LS-P1-Sr-2005	94	232	178	85	228	157
MPP-LS-P2-Sr-2005	93	226	174	84	223	154

The expected number of failures estimated by the models increase over time. The results of the two updating processes (P1 and P2) are very similar, given the same initialisation method for the corrosion parameters and training period. Models trained using data from 1994 to 2010 tend to estimate more pipes with failures compared to the models trained using failure data between 1994 and 2005.

A comparison between the two initialisation methods for the corrosion parameters showed that initialising parameters using the degree of saturation (MPP-LS-P1-Sr-TrainYr and MPP-LS-P2-Sr-TrainYr) overestimates the expected number of failures significantly. This is likely due to the high initial long-term corrosion rates estimated by the degree of saturation (Figure 5-18). The results of the error statistics in Table 5-14 matches with the observations from the two graphs, the MPP-LS-P1-Sr-TrainYr and MPP-LS-P2-Sr-TrainYr models have a much higher error compare to the MPP-LS-P1-Basic-TrainYr and MPP-LS-P2-Basic-TrainYr models.

A closer examination of the MPP-LS-P1-Basic-2010, MPP-LS-P2-Basic-2010, MPP-LS-P1-Basic-2005 and MPP-LS-P2-Basic-2005 models are shown in Figure 5-22. The MPP-LS-P1-Basic-2010 and MPP-LS-P2-Basic-2010 models perform better than the MPP-LS-

P1-Basic-2005 and MPP-LS-P2-Basic-2005 models, which underestimates the expected number of failures for most of the time. The models trained using failure data up to 2010 have a slightly higher long-term corrosion rate distribution (Figure 5-18) and a shorter time to next failure distribution (Figure 5-19). Therefore, the pipes will corrode faster and fail more frequently for the TrainYr=2010 models. The results suggest that using more failure data to calibrate the MPP model can provide better performance in estimating the expected number of failures in the network.

The MPP models using a range of failure influence factors (α=0.1 to 2 at a step size of 0.1) and radius of influences (R=50m, 100m, 200m and 500m) have also been calibrated. The expected number of failures estimated by the MPP-LS-P1-Basic-2010, MPP-LS-P2-Basic-2010, MPP-LS-P1-Basic-2005 and MPP-LS-P2-Basic-2005 models with the lowest error (MAE and RMSE) in the entire observation period (1994-2015) are plotted in Figure 5-23, Figure 5-24, Figure 5-25 and Figure 5-26, respectively. Each of the plots includes the recorded failure data (Observed), the result of the MPP model without the failure influence factor (e.g. MPP-LS-P1-Basic-2010 in Figure 5-23) and the results of the MPP models with the failure influence factor (e.g. MPP-LS-P1-Basic-2010-a0.1-R500 in Figure 5-23 has a radius of influence of 500m and a decay factor a=0.1).

The MAE and RMSE for the models plotted in the figures are shown in Table 5-15 and Table 5-16 for MPP-LS-P1-Basic-TrainYr and MPP-LS-P2-Basic-TrainYr, respectively. The error statistics for the other MPP models can be found in Table C - 1 and Table C - 2 in APPENDIX C. The results for the MPP models initialised using the degree of saturation have also been estimated. They are not plotted because they overestimate the expected number of failures significantly.

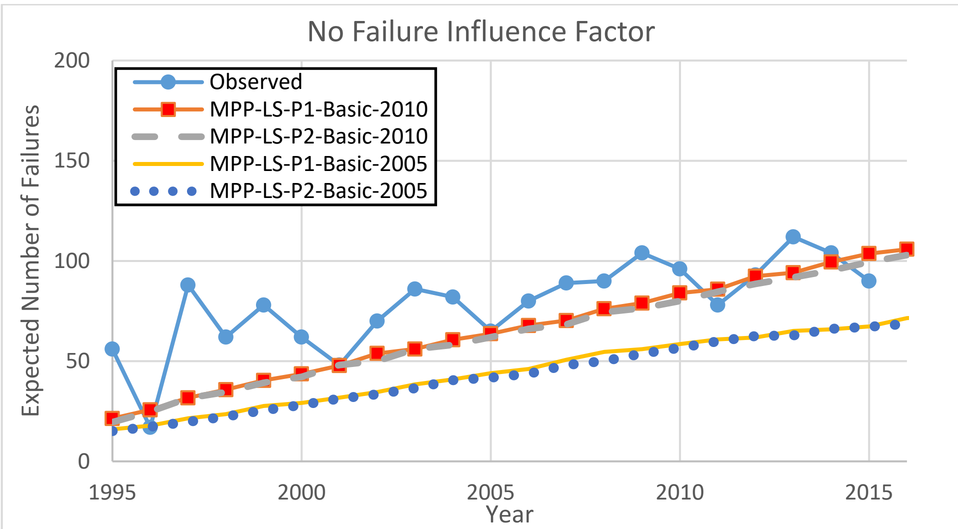

Figure 5-22: : Expected number of failures estimated by the MPP-LS-P1-Basic and MPP-LS-P2-Basic models.

The MPP models that incorporated the failure influence factor are more accurate compared to the MPP models without the failure influence factor. They provide a better fit to the observed failure data and have a lower MAE and RMSE. The application of the failure influence factor is able to increase the long-term corrosion rate of water mains that are close to an unexpected failure event, accelerating the deterioration of the pipe, leading to a shorter time to failure. A common observation in the models with the failure influence factor is the reduction in the expected number of failures predicted right after the end of the training period (very obvious in Figure 5-25 after 2005). This is because the failure influence factor is not applied in the failure prediction process after the training period as no failure data are available.

Although the performance of the MPP models trained using failure data up to 2005 have improved, especially during the training period, the MPP models trained using failure data up to 2010 are still preferred as they are more accurate in estimating the expected number of failures in the network.

Comparing the models in Figure 5-23 and Figure 5-24 show that a smaller decay factor (a) produce more failures. The estimations from the MPP models trained using failure data up to 2005 (Figure 5-25 and Figure 5-26) can be used to compare the effect of the radius of influence because the same decay factor has been used. The expected number of failures estimated with $R = 500$m, $R = 200$m and $R = 100$m are very similar and are greater than the results estimated with $R = 50$m. The similar results estimated using $R = 500$m, $R = 200$m and $R = 100$m are due to the power function used in calculating the long-term corrosion rate in Equation (5-27). The failure influence factor has little effect when the distance between the water mains are greater than 100m even with the smallest decay factor, $a = 0.1$ (e.g. $e^{-0.1*100} = 4.5 * 10^{-5}$).

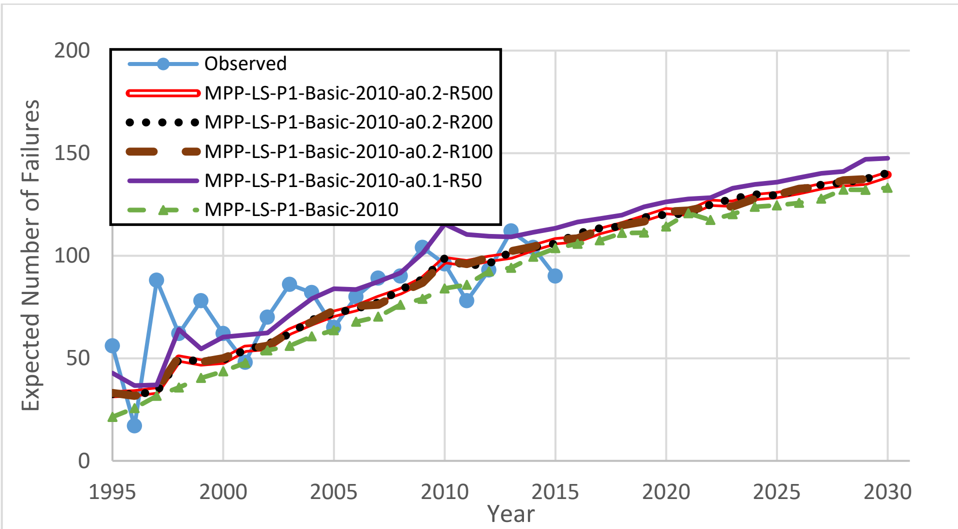

Figure 5-23: : Expected number of failures estimated by MPP-LS-P1-Basic-2010 models with failure influence factor.

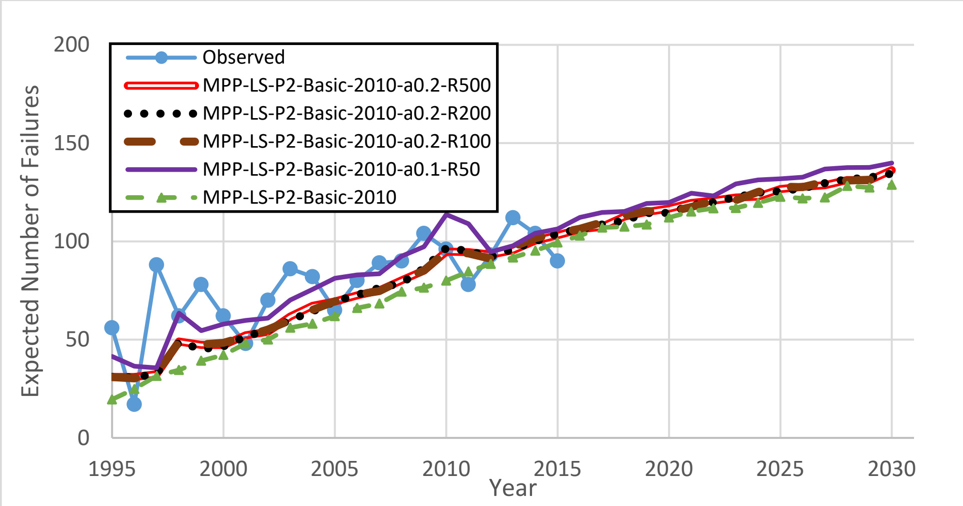

Figure 5-24: : Expected number of failures estimated by MPP-LS-P2-Basic-2010 models with failure influence factor.

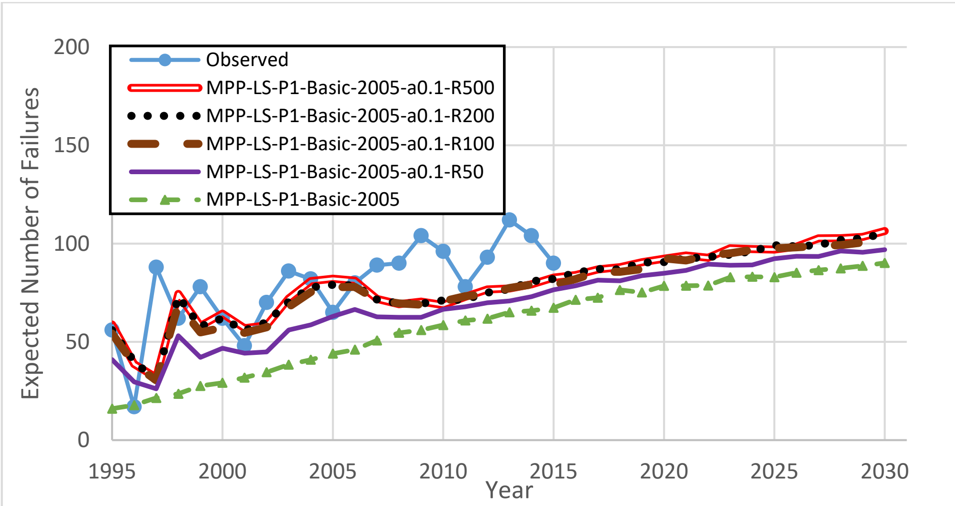

Figure 5-25: : Expected number of failures estimated by MPP-LS-P1-Basic-2005 models with failure influence factor.

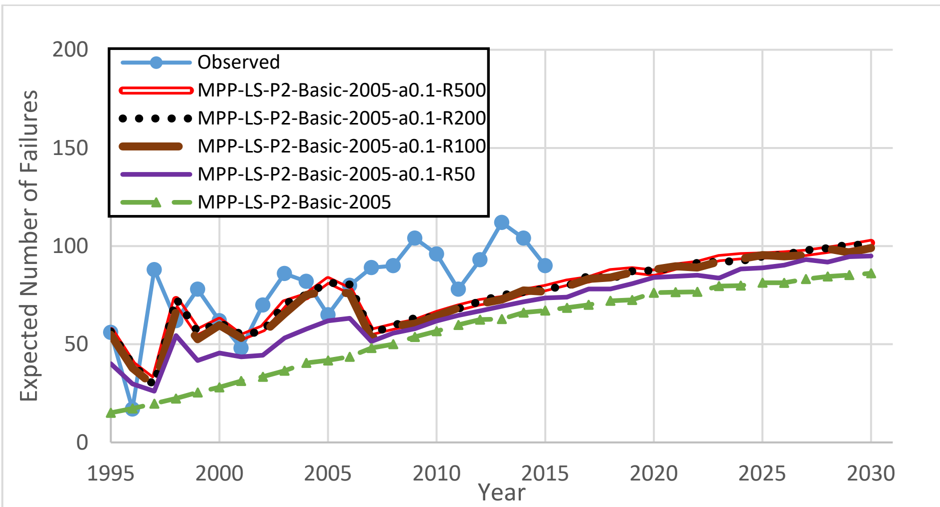

Figure 5-26: : Expected number of failures estimated by MPP-LS-P2-Basic-2005 models with failure influence factor.

Table 5-15: Error statistics for the MPP-LS-P1-Basic-TrainYr models.

Model Parameters	MPP-LS-P1-Basic							
	TrainYr=2010				TrainYr=2005			
	a0.2-R500	a0.2-R200	a0.2-R100	a0.1-R50	a0.1-R500	a0.1-R200	a0.1-R100	a0.1-R50
RMSE Overall	18.7	18.5	18.6	18.3	21.7	21.8	22.4	27.0
MAE Overall	14.6	14.6	14.6	13.5	17.2	17.2	18.0	23.2

Table 5-16: Error statistics for the MPP-LS-P2-Basic-TrainYr models.

Model Parameters	MPP-LS-P2-Basic							
	TrainYr=2010				TrainYr=2005			
	a0.2-R500	a0.2-R200	a0.2-R100	a0.1-R50	a0.1-R500	a0.1-R200	a0.1-R100	a0.1-R50
RMSE Overall	19.5	19.2	19.5	17.5	24.6	24.6	25.3	29.7
MAE Overall	15.5	15.2	15.6	12.7	20.0	19.9	20.8	26.0

5.3.2.2. Comparing MPP Models with the BSM and NHPP

Table 5-17: Failure probability from the BSM.

Num Past Failures	BSM2010			BSM2005		
	Num Pipe	Num Failures (2010)	Prob Failure	Num Pipe	Num Failures (2005)	Prob Failure
0	35429	72	0.002	35778	52	0.001
1	920	17	0.019	633	10	0.017
2	95	4	0.047	48	3	0.071
3	14	3	0.233	1	0	0.250
4	2	0	0.167			

Table 5-18: Coefficients estimated for the NHPP.

NHPP2005		NHPP2010	
Covariate	**Coefficient**	**Covariate**	**Coefficient**
Ageing Factor	1.11	Ageing Factor	1.22
Constant	-10.41	Constant	-11.81
ln(PipeLength)	0.88	ln(PipeLength)	0.93
Pressure	0.01	Pressure	0.01
100mm<PipeDia<=200	-0.67	100mm<PipeDia<=200	-0.41
200mm<PipeDia<=300	-1.65	200mm<PipeDia<=300	-1.16
PipeDia>=300	-1.82	PipeDia>=300	-1.83
Soil-EX	0.36	Soil-SE	0.44
Soil-VE	0.41	Soil-EX	0.80
NOKPF>=1	1.31	Soil-VE	0.79
		NOKPF=1	1.26
		NOKPF>=2	1.71

The results of the BSM model and the coefficients estimated for the NHPP are shown in Table 5-17 and Table 5-18 respectively. The MPP model with the smallest error from each training period (MPP-LS-P2-Basic-2010-a0.1-R50 and MPP-LS-P1-Basic-2005-a0.1-R500) will be compared with the BSM and NHPP. The expected number of failures predicted by the MPP models (MPP-LS-P2-Basic-2010-a0.1-R50 and MPP-LS-P1-Basic-2005-a0.1-R500) are plotted with the BSM and NHPP in Figure 5-27 and Figure 5-28 for the calibration period 1994-2010 and 1994-2005, respectively. The error statistics for the models in Figure 5-27 and Figure 5-28 is also shown in Table 5-19 and Table 5-20, respectively.

Both the MPP and NHPP are able to capture the upward trend in the expected number of failures over the observation period. The expected number of failures estimated by the NHPP is higher than the MPP model at the start of the observation period, but the rate of increase is higher for the MPP model. Therefore the MPP model eventually estimates more failures than the NHPP. The BSM predicts the same expected number of failures for the future because it cannot account for the ageing of the pipes over time.

The BSM underestimates the number of failed pipe in the validation period with the training data from 1994-2005. It has the highest error out of the 3 models. Although the performance of the BSM improves with additional failure data (1994-2010), the model is only suitable for short-term failure prediction because it does not account for the ageing of the water main. For long-term failure predictions, the model must account for the deterioration of the water main as it is one of the main contributors to pipe failure (Ji et al., 2015).

Comparing the accuracy of the MPP models with the NHPP, the error statistics showed that the NHPP is preferred in estimating the number of failures in the network. The errors in the training, validation and entire observation period are all smaller for the NHPP.

There are signs that the NHPP will underestimate the expected number of failures in the future. In both Figure 5-27 and Figure 5-28, the expected number of failures estimated by the NHPP in the validation period is often lower than the recorded values (3 times out of 5 for Figure 5-27 and 9 times out of 10 for Figure 5-28). In addition, the upward trend in the failure data for the entire observation period also seems to be stronger than the one calibrated in the NHPP. This suggests that the ageing factor for the NHPP is likely to be underestimated, leading to an underestimation for the expected number of failures in the future. On the other hand, the MPP model has a higher rate of increase for the expected number of failures over time. The MPP model is likely to be more accurate in modelling the failures in the long-term.

The expected number of failures estimated by the NHPP is calibrated using the failure data. It assumes that the patterns from the past will continue into the future (Kleiner and Rajani, 2001), but it cannot capture any trend that is outside the recorded data. If the ageing factor during the training period is lower than the ones in the validation/prediction period, the expected number of failures in the future will be underestimated. However, the MPP model integrates the physical deterioration process of the pipe with its failure history. The corrosion parameters are calibrated using the failure data, but the prediction of failure is determined by a physical model. Therefore, the breakage of the water main is governed by the physical failure mechanism and not purely dependent on the failure data. The increasing trend for the number of failed pipe over time in the MPP model can be greater than those that are learned from the failure data.

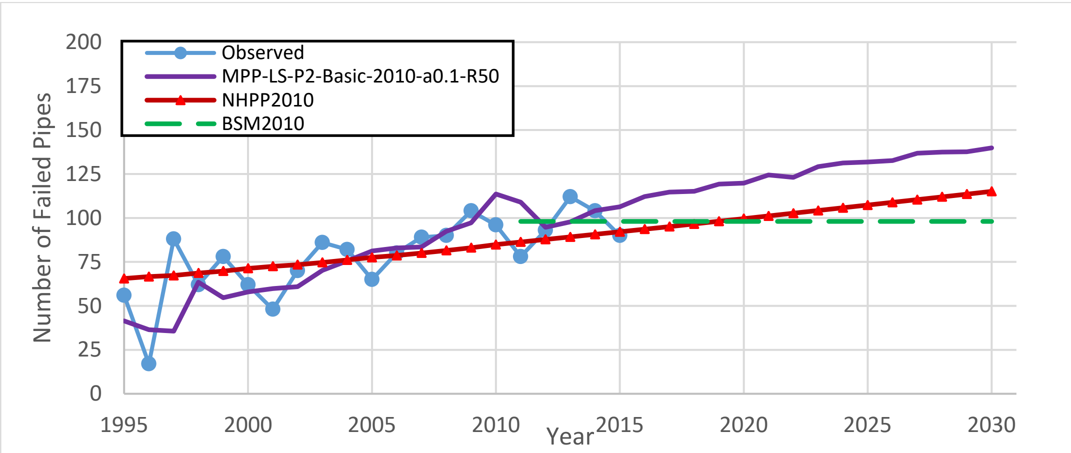

Figure 5-27: Expected number of failures estimated by the models trained using data between 1994 and 2010.

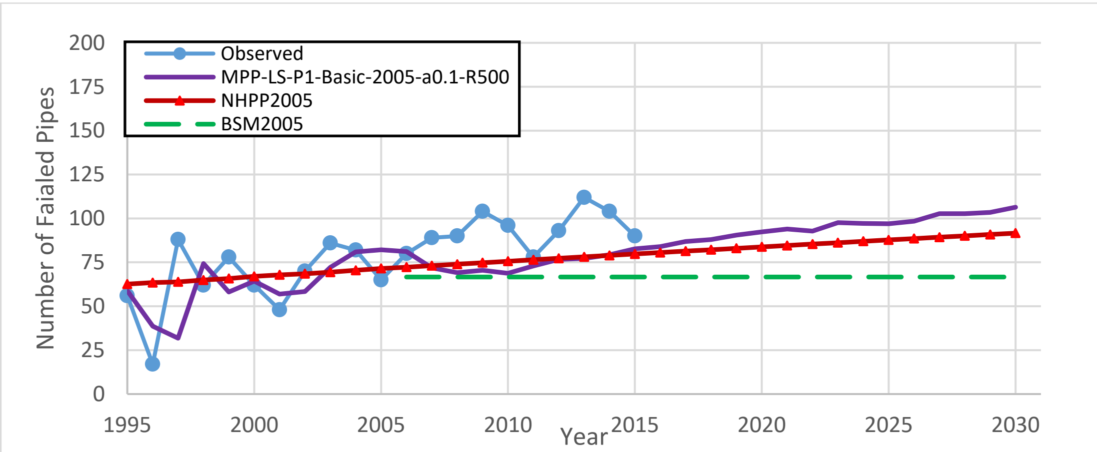

Figure 5-28: Expected number of failures estimated by the models trained using data between 1994 and 2005.

Table 5-19: Error statistics for models trained using data between 1994 and 2010.

Model	RMSE Training	RMSE Validation	RMSE Overall	MAE Training	MAE Validation	MAE Overall
MPP-LS-P2-Basic-2010-a0.1-R50	17.8	17.0	17.6	13.1	13.5	13.0
NHPP2010	17.4	12.4	16.4	13.3	10.5	12.6
BSM2010	N/A	11.0	N/A	N/A	9.2	N/A

Table 5-20: Error statistics for models trained using data between 1994 and 2005.

Model	RMSE Training	RMSE Validation	RMSE Overall	MAE Training	MAE Validation	MAE Overall
MPP-LS-P1-Basic-2005-a0.1-R500	21.1	21.4	21.4	15.3	18.7	16.9
NHPP2005	18.6	18.6	19.0	13.9	16.0	15.4
BSM2005	N/A	27.5	N/A	N/A	24.6	N/A

5.3.2.3. Prediction Curve Comparison

The prediction curve for the MPP models, BSM and NHPP with training period from 1994-2010 and 1994-2005 are plotted in Figure 5-29 and Figure 5-30, respectively. The ranking of the water mains for the MPP models, BSM and the NHPP are ordered using the damage factor, expected failure probability and the expected number of failures, respectively. The prediction curve plotted is slightly different to the ones shown in Section 3.4 as the percentage of failure predicted on the y-axis is calculated for the whole validation period instead of the next year (failure data in 2013 for step 2 in Section 3.4 is replaced with failure data from the entire validation period). The naming of the models in the legend is the same as the last section.

The area under the prediction curve for the first 20% length considered for renewal for the MPP models with $R = 50$m can be found in Table C - 3 to Table C - 6 in APPENDIX C. The results are not shown for $R = 100$m, $R = 200$m and $R = 500$m because they are similar to the MPP models with $R = 50$m. The comparisons are not made for the MPP models initialised using the degree of saturation because of their poor performance in estimating the expected number of failures from the previous section.

The prediction curves for the MPP models are similar given the same training period and updating method. The failure influence factor does not have a significant effect on the ranking performance of the pipe. The updating methods (P1 and P2) do impact on the ranking performance of the MPP model slightly. In both figures, the MPP model that is updated using the P2 process Table 5-9 can predict more failures in the validation period at the start of the prediction curve.

The ranking performance of the MPP models is at least as good as the NHPP in the prediction curve. The BSM is also preferred over the NHPP for pipe ranking because the BSM can predict more failures at the start of the prediction curve. For the first 5% of pipe length considered for renewal, the ranking performances of the MPP models and the BSM are similar.

Using the MPP models to rank the water mains have shown a slight improvement in the ranking performance compare to the BSM and NHPP. However, there is still a significant difference between the performance of the MPP model and the actual ground truth. Therefore, potentials for further improvements in the failure prediction models are still possible. The components in the MPP model (Section 5.2.1 to 5.2.6) also has the capacity to be improved to achieve better performance in terms of both pipe ranking and pipe failure predictions.

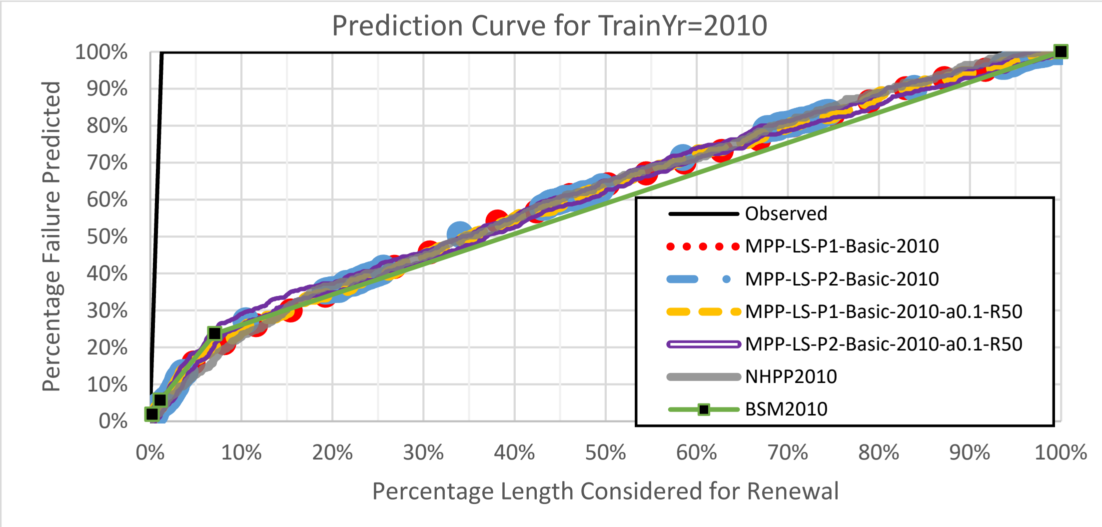

Figure 5-29: Model prediction curves for training period between 1994 and 2010.

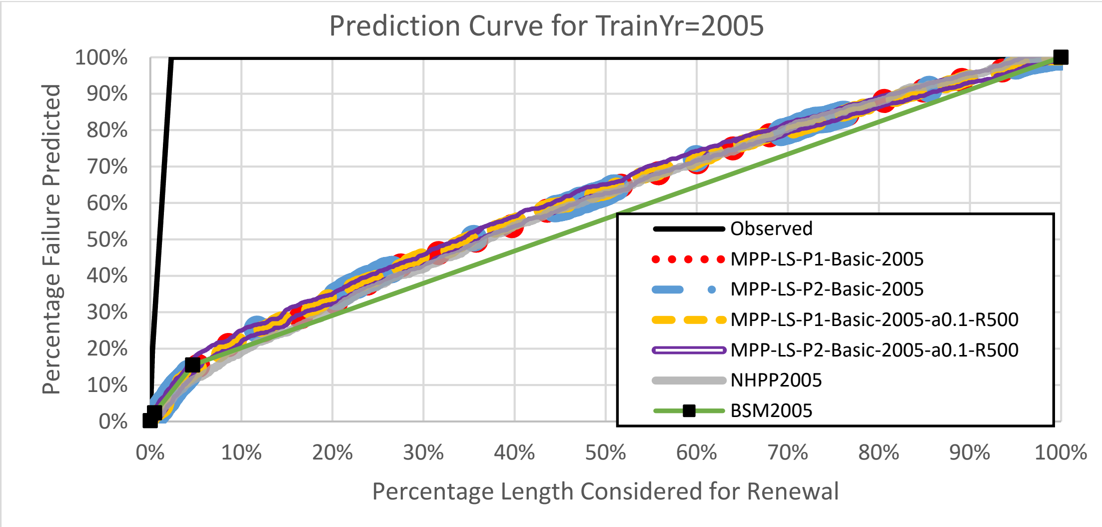

Figure 5-30: Model prediction curves for training period between 1994 and 2005.

5.4. Modelling Broken Back Failures Using the Monash Pipe Failure Prediction Model

This section of the chapter will model broken back (BB) failures in water mains using the MPP model. The following naming convention is used to identify the different modelling assumptions (P1 or P2), initialisation methods for the corrosion parameters and the failure data used to calibrate the model:

- MPP-BB-P1-Sr-TrainYr: Modelling process P1 and the S_r are used to initialise the long-term corrosion rate. The failure data from the start of the observation period to the Training Year (TrainYr) are used to calibrate the model.
- MPP-BB-P1-Basic-TrainYr: Modelling process P1 and the failure data are used to initialise the long-term corrosion rate (Basic). The failure data from the start of the observation period to the Training Year (TrainYr) are used to calibrate the model.
- MPP-BB-P2-Sr-TrainYr: Modelling process P2 and S_r are used to initialise the long-term corrosion rate. The failure data from the start of the observation period to the Training Year (TrainYr) are used to calibrate the model.
- MPP-BB-P2-Basic-TrainYr: Modelling process P2 and the failure data are used to initialise the long-term corrosion rate (Basic). The failure data from the start of the observation period to the Training Year (TrainYr) are used to calibrate the model.

The BSM (Section 3.3.3) and the NHPP (Section 4.5) will again be used to compare the performance of the MPP model for broken back failures in estimating the expected number of failures in the network, as well as the ranking performance of the model. The failure data are transformed into binary format as for longitudinal failures before model calibration. The failure influence factor and the radius of influence that have been considered are the same as the MPP model for longitudinal failures (α=0.1 to 2 at a step size of 0.1 and R=50m, 100m, 200m and 500m)

5.4.1 Pipe Asset, Failure Data and Input data

5.4.1.1. Pipe Asset and Failure Data

The dataset used to train the MPP model consists of CI water mains from all pipe diameters. Some properties of the dataset are shown in Table 5-21. The failure data have been recorded between 1998 and 2013. The MPP model for broken back failures requires soil moisture content data from BOM, which are only available after 2005. Therefore, only broken back failures from 2005 to 2013 have been included in the analysis. The model will be calibrated using 5 (2005-2009) and 7 (2005-2011) years of failure data. The failure data after the calibration period will be used for model validation purposes. Predictions after the validation period will not be considered because the soil moisture data are unknown in the future.

Table 5-21: Asset data description.

Cohort Properties	Cast Iron Water Mains
Construction year	1860-1996
Observation period	1998-2013
Number of pipes	30821
Pipe length (km)	1730
Number of failures	7095 (from 2005 to 2013)

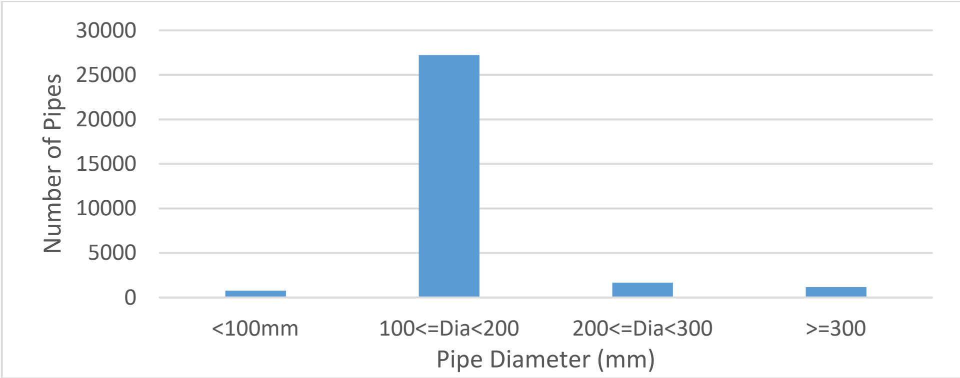

Figure 5-31: Pipe diameter of the water mains.

Most of the water mains in this dataset are small diameter pipes (<300mm) (Figure 5-31) that were laid in reactive soils. The small diameter pipes are weak in bending. The shrinkage/swelling of reactive soils as a result of the change in soil moisture content can generate bending stress that is sufficient to fail these small pipes. Therefore, it is expected that a higher number of broken back failures are recorded in the dataset relative to the longitudinal failure data.

The failure rate of the dataset is shown in Figure 5-32, along with the average soil moisture content estimated using Equation (5-31). Note that the recorded data show the total number of failures in a year, but they are plotted as lines in the figures in the chapter instead of discrete points for better visualisation.

$$\theta_w^y(t) = \frac{\sum_{i=1}^{n} \sum_{m_t=1}^{12} \theta'_{w,i}(m_t)}{12n}$$

(5-31)

where $\theta_w^y(t)$ is the average soil moisture content in year t; $\theta'_{w,i}(m_t)$ is the soil moisture content of pipe i in month m of year t (Equation (5-4)); and n is the total number of pipes in the dataset.

There is an inverse relationship between the failure rate of the dataset and the average soil moisture content. An increase in soil moisture content will decrease the failure rate, while a decrease in soil moisture content will increase the failure rate. It is difficult to determine whether there is an upward trend in the failure rate because of the large year-to-year variations.

As with the MPP model for longitudinal failures, most of the input parameters can be either drawn from the pipe asset data or found in Table 5-3. The initial corrosion parameters and time to next failure estimated based on the methods discussed in Section 5.2.2 are presented in the next section.

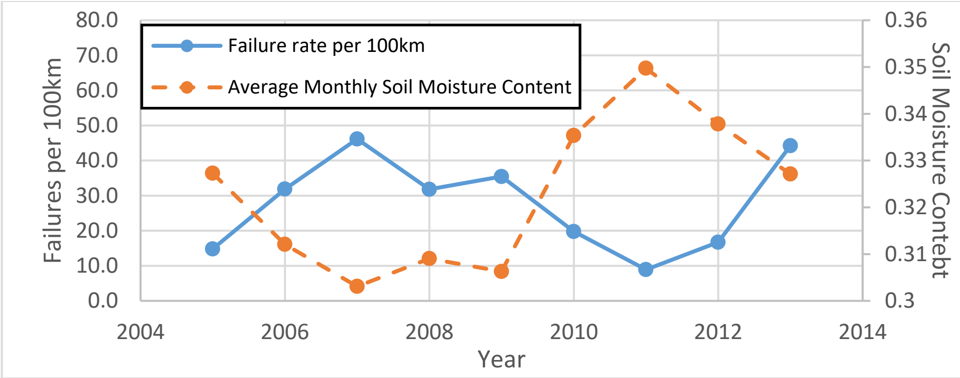

Figure 5-32: Failure rate and average monthly soil moisture content of the dataset over time.

5.4.1.2. Initial Corrosion Parameters

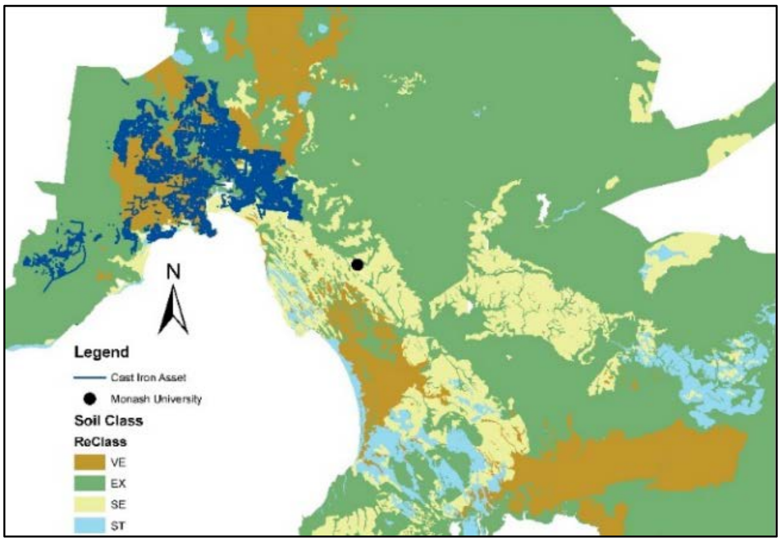

Figure 5-33: Location of cast iron assets with soil reactivity map.

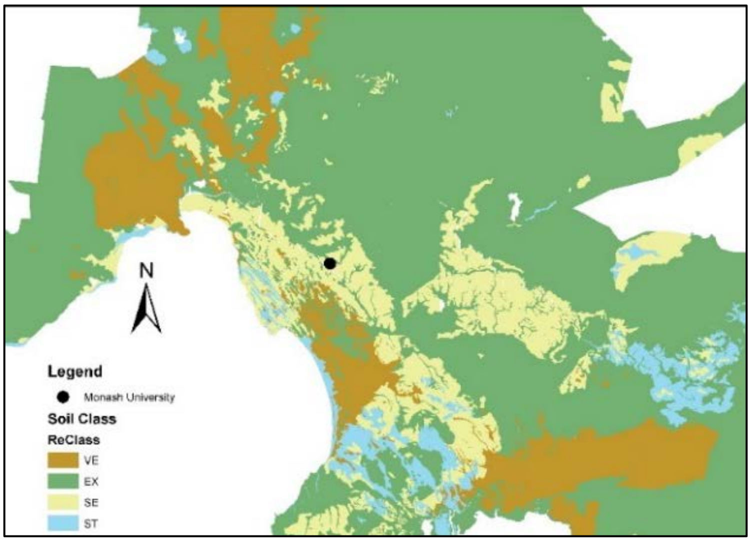

Figure 5-34: Soil reactivity map.

The CI water pipes are mapped in Figure 5-33, with the soil reactivity in the background and mapped in Figure 5-34. For this dataset, most of the water mains are laid in EX and VE soils. Therefore, it is expected that S_r for the water mains are going to be higher in this dataset compare to the longitudinal failure dataset.

The soil porosity and soil moisture content for the pipes are shown in Figure 5-35 and Figure 5-36, respectively. The general pattern is very similar to the longitudinal failure dataset. Most of the water mains are laid in soil with a porosity value that falls between 0.46 to 0.47, and only a small portion of pipes are laid in soil that has a porosity value between 0.38 to 0.46. The soil moisture content estimated for the majority of the pipes are between 0.26 and 0.38. The soil moisture content for water mains in ST soil is between 0.08 and 0.14 due to its low permanent wilting point and field capacity.

S_r of the soil in which the pipes are laid in are shown in Figure 5-37. Due to the two-distinct groups of soil moisture content estimated for pipes laid in ST soil and the other soil types, S_r for the water mains are also clustered into two groups. The pipes in ST soil have a much lower S_r (0.2-0.22) compared to those laid in the other soil types (0.52-0.94).

The corrosion parameters can be initialised with S_r using Table 5-5 for the MPP-BB-P1-Sr-TrainYr and MPP-BB-P2-Sr-TrainYr models (Section 5.2.2.1). Using $cs_i(t)$ from Table 5-5, the initial long-term corrosion rate can also be back-calculated for the MPP-BB-P1-Basic-TrainYr and MPP-BB-P2-Basic-TrainYr models with the method described in 5.2.2.2. The distributions for $r_{0,i}$ (upper bound), $cs_i(t)$ and $rs_i(t)$ using the two initialisation methods under different training periods are shown in Figure 5-38, Figure 5-39 and Figure 5-40, respectively. The shape and scale parameters of the fitted Weibull distribution for the long-term corrosion rates are shown in Table 5-22. Note that the average soil moisture content ($\theta_{w,i,avg}$) between 2005 and 2016 is used to estimate the S_r to initialise the corrosion parameters, therefore, the values selected for the parameters are the same regardless of the training period when S_r is used.

The long-term corrosion rates estimated based on S_r are higher than the ones calculated using the failure data. This is very similar to the comparison of the long-term corrosion rates for the longitudinal failure dataset. The number of failures estimated by the MPP-BB-P1-Sr-TrainYr and MPP-BB-P2-Sr-TrianYr are likely to be higher than those from the MPP-BB-P1-Basic-TrainYr and MPP-BB-P2-Basic-TrainYr models.

The distribution for the time to next failure ($\Delta T_i(t)$) is estimated as described in Section 5.2.2.3. The distributions for the training period 2005-2009 and 2005-2011 are shown in Figure 5-41. The parameters for the distribution are shown in Table 5-23. The two distributions are very similar because only two years of additional failure data have been included in the training period 2005-2011.

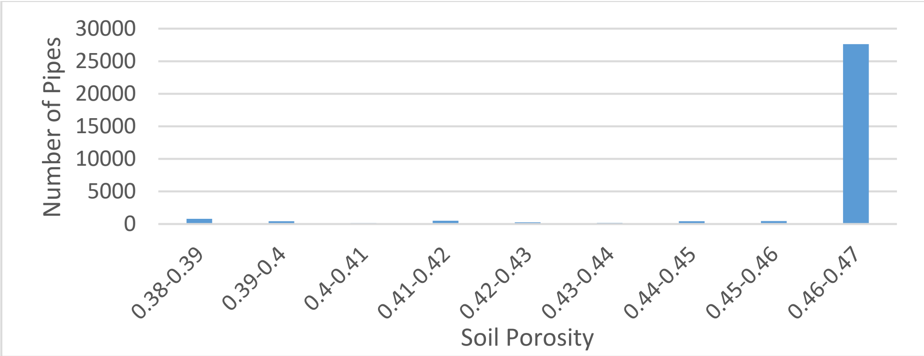

Figure 5-35: Estimated soil porosity for the water mains.

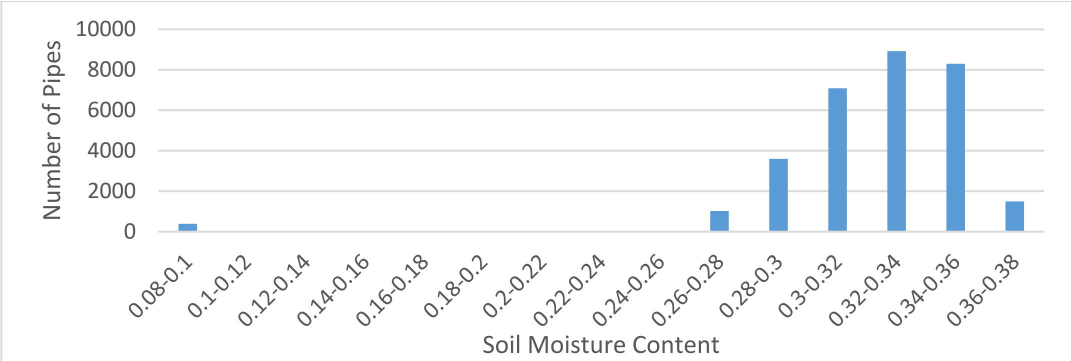

Figure 5-36: Estimated soil moisture content for the water mains.

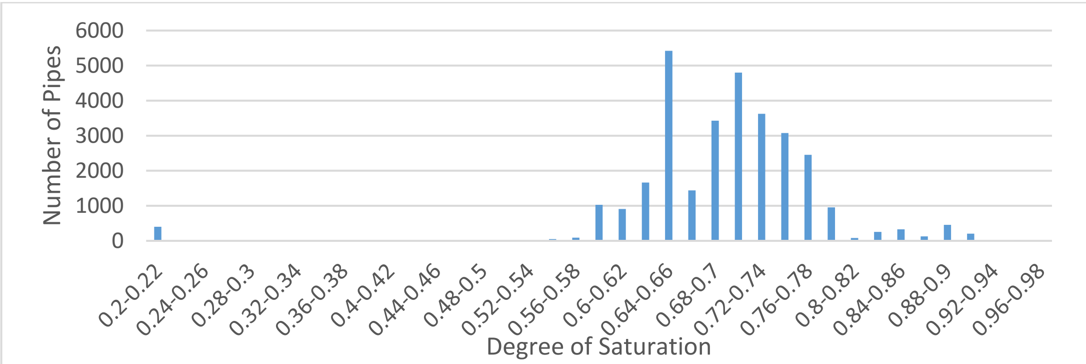

Figure 5-37: Estimated degree of saturation for the water mains.

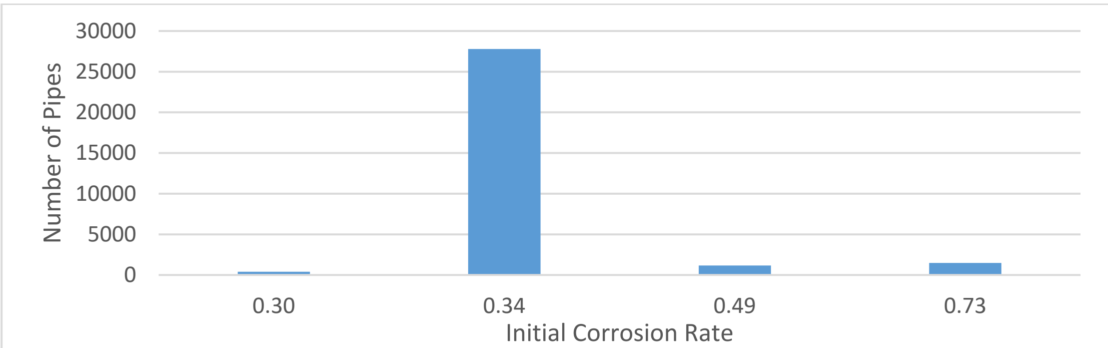

Figure 5-38: Estimated Initial corrosion rate for the water mains.

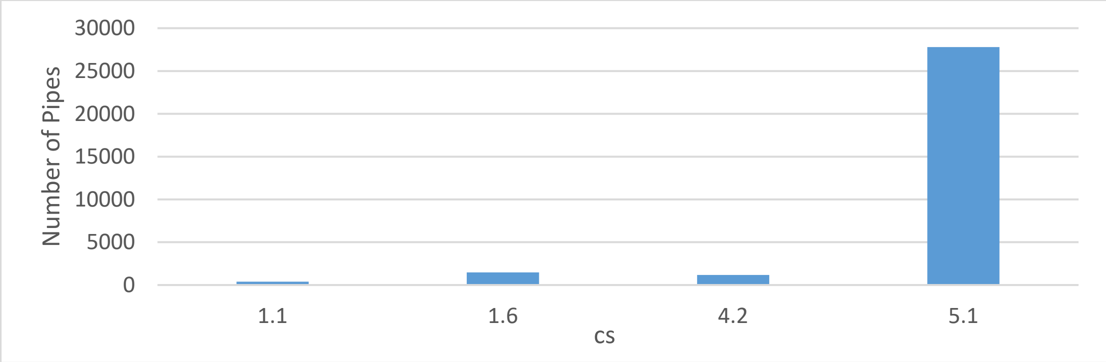

Figure 5-39: Estimated intercept of long-term corrosion rate for the water mains.

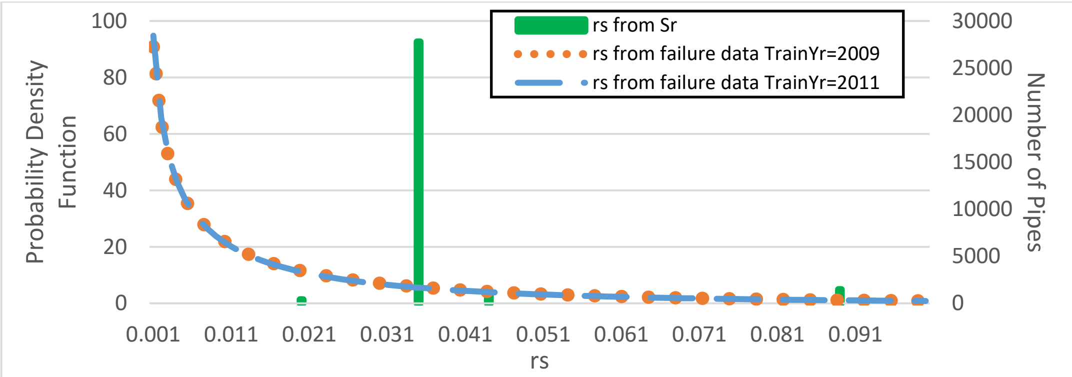

Figure 5-40: Estimated long-term corrosion rate for the water mains.

Table 5-22: Estimated parameters for the Weibull distribution of long-term corrosion rate.

TrainYr	2009	2011
Scale	0.0165	0.0155
Shape	0.63	0.61

Table 5-23: Estimated parameters for the Weibull distribution of time to next failure.

Parameters	Left-and Right-Censor TrainYr=2009	Left-and Right-Censor TrainYr=2011
scale	13.8	12.6
shape	0.85	0.88

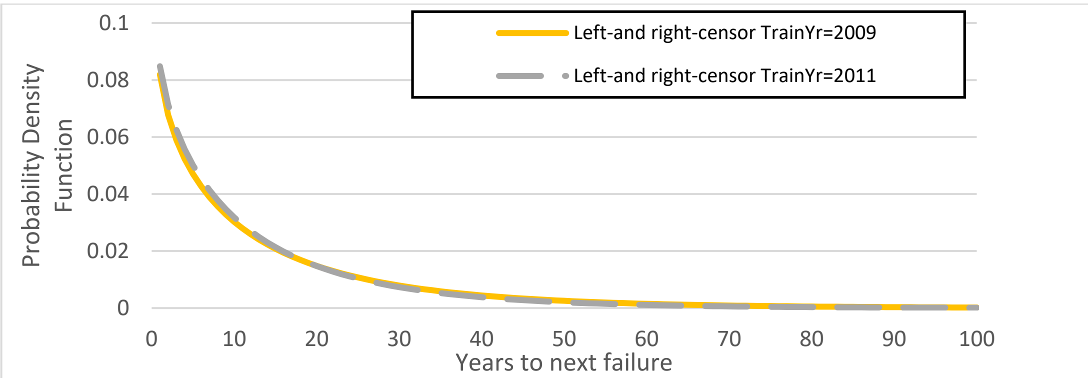

Figure 5-41: Estimated distribution for the time to next failure.

5.4.2 Results and Discussions

The performance of the MPP models in estimating the total number of failures in the dataset are compared with the NHPP and BSM using error statistics and graphical plots. The prediction curves are then used to compare the ranking performance of the models. Note that the results for the MPP model with $R = 500$m and $R = 200$m have not been shown because their results are similar to the MPP model with $R = 100m$. The failure influence factors were found to have little effect at large distance even with the smallest decay factor (e.g. $R = 100\ and\ a = 0.1, e^{-0.1*100} = 4.5 * 10^{-5}$).

5.4.2.1. Expected Number of Failures Estimated by the MPP Models

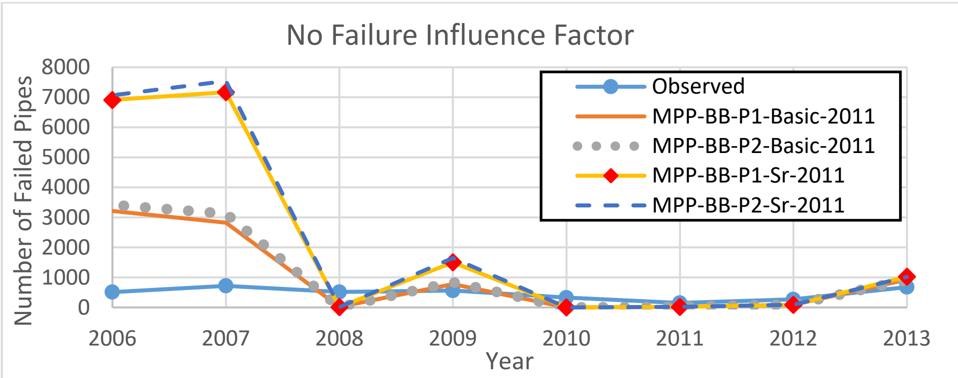

Figure 5-42: Expected number of failures estimated by the MPP model using failure data up to 2011.

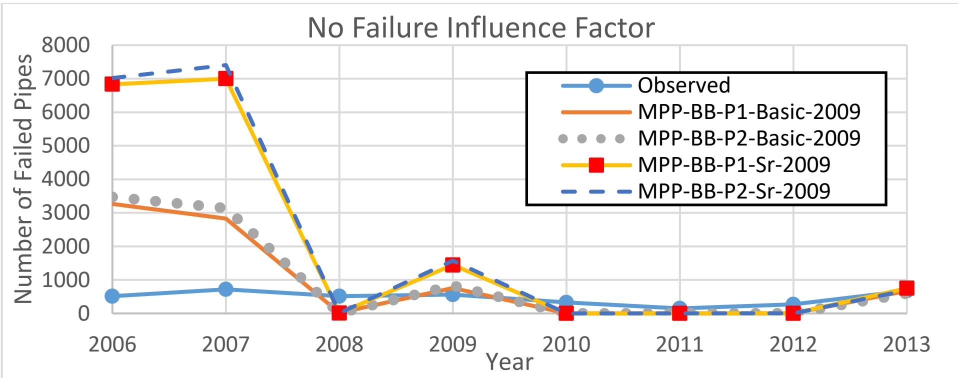

Figure 5-43: Expected number of failures estimated by the MPP model using failure data up to 2019.

The expected number of failures (Equation (5-30)) estimated by the MPP models without the failure influence factor are first compared. The results are plotted in Figure 5-42 and Figure 5-43 for the training period 2005-2011 and 2005-2009, respectively. The error statistics are shown in Table 5-24. The results for 2005 are not shown because the models consistently overestimate the number of failures.

Large year-to-year variations in the number of failures estimated by the MPP models can be observed from both figures. They are caused by the change in soil moisture content each year, which generates different level of bending stress. The average bending stress of the pipe over the observation period can be found in Figure 5-44.

The direction of the change in bending stress is generally the same as the change in the expected number of failures. An increase in the average bending stress also leads to an increase in the expected number of failures estimated for the year.

Similar to the MPP models for longitudinal failures, the errors statistics shows that the MPP-BB-P1-Sr-TrainYr and MPP-BB-P2-Sr-TrainYr models have a higher error compare to the MPP-BB-P1-Basic-TrainYr and MPP-BB-P2-Basic-TrainYr models. However, the performance of all the MPP models for broken back failures is poor because the variations from the model are much higher than the variations in the failure data. The expected number of failures is often over or underestimated by a large degree. The inclusion of additional failure data (training using 2005-2011 rather than 2005-2009) does not show a significant improvement in estimating the expected number of failures.

Table 5-24: Error statistics for the MPP models without failure influence factor.

Models	RMSE Training	RMSE Validation	RMSE Overall	MAE Training	MAE Validation	MAE Overall
MPP-LS-P1-Basic-2011	1422	194	1237	996	188	801
MPP-LS-P2-Basic-2011	1562	186	1357	1091	181	870
MPP-LS-P1-Sr-2011	3738	239	3240	2458	221	1910
MPP-LS-P2-Sr-2011	3896	235	3377	2571	217	1993
MPP-LS-P1-Basic-2009	1755	218	1251	1389	188	787
MPP-LS-P2-Basic-2009	1933	236	1376	1538	218	872
MPP-LS-P1-Sr-2009	4485	444	3176	3497	339	1850
MPP-LS-P2-Sr-2009	4700	496	3327	3679	354	1934

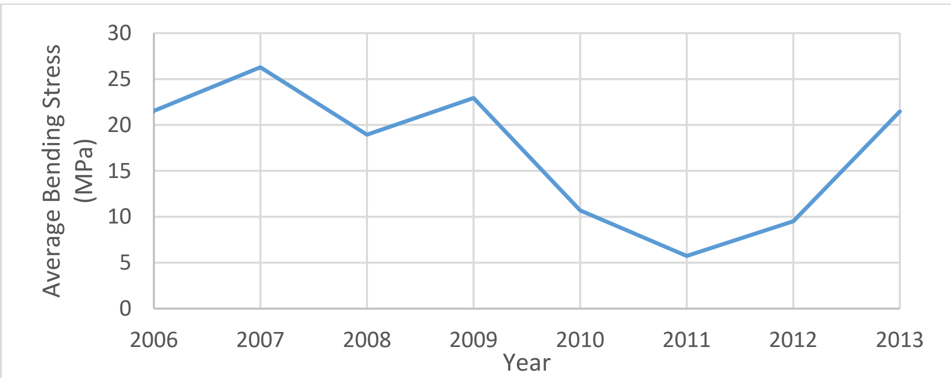

Figure 5-44: Average bending stress in the water main.

5.4.2.2. Comparing MPP Models with the BSM and NHPP

The results of the BSM model and the coefficients estimated for the NHPP are shown in Table 5-25 and Table 5-26, respectively. The expected number of failures estimated by the MPP models with and without the failure influence factor is compared with the BSM and NHPP in Figure 5-45 and Figure 5-46. The MPP model with the failure influence factor has only been plotted for the decay factor with the smallest RMSE and R=100m (e.g. MPP-BB-P1-Basic-2011-a1.5-R100 has a decay factor of 1.5 and R=100m in Figure 5-45). The error statistics for the results plotted in Figure 5-45 and Figure 5-46 is shown in Table 5-27 and Table 5-28, respectively. The RMSE and MAE for the MPP models with a range of decay factors (a) for $R = 50$m and $R = 100$m are shown in Table C - 7 and Table C - 8 in APPENDIX C, respectively.

Table 5-25: Failure probability estimated from the BSM.

	BSM2011			BSM2009		
Num Past Failures	Num Pipe	Num Failures (2011)	Prob Failure	Num Pipe	Num Failures (2009)	Prob Failure
0	28601	84	0.003	29141	337	0.012
1	1685	40	0.024	1399	161	0.115
2	428	17	0.041	251	54	0.216
3	88	5	0.062	27	8	0.304
4	17	3	0.194	3	1	0.375
5	2	0	0.167	2	0	0.167

Table 5-26: Coefficients estimated for the NHPP.

NHPP2009		NHPP2011	
Covariates	**Coefficient**	**Covariates**	**Coefficient**
Ageing Factor	0.37	Ageing Factor	0.31
Constant	-3.74	Constant	-3.58
ln(PipeLength)	0.74	ln(PipeLength)	0.76
200mm<PipeDia<=300	-1.30	200mm<PipeDia<=300	-1.34
PipeDia>=300	-2.39	PipeDia>=300	-2.49
Soil-SE	-0.90	Soil-SE	-0.95
Soil-VE	0.51	Soil-VE	0.48
NOKPF=1	1.31	NOKPF>=1	1.12
NOKPF>=2	1.52	NOKPF>=2	1.00

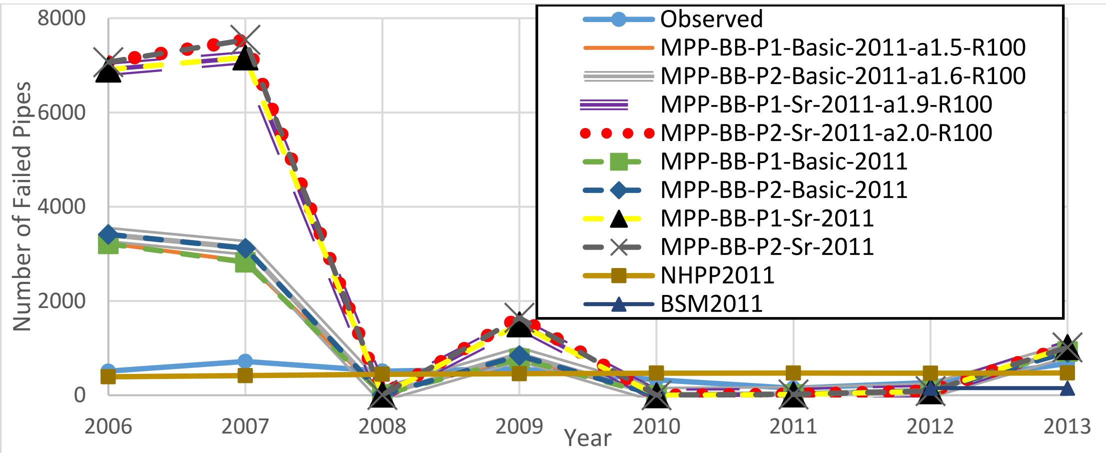

Figure 5-45: Expected number of failures estimated by the models trained using data between 2005 and 2011.

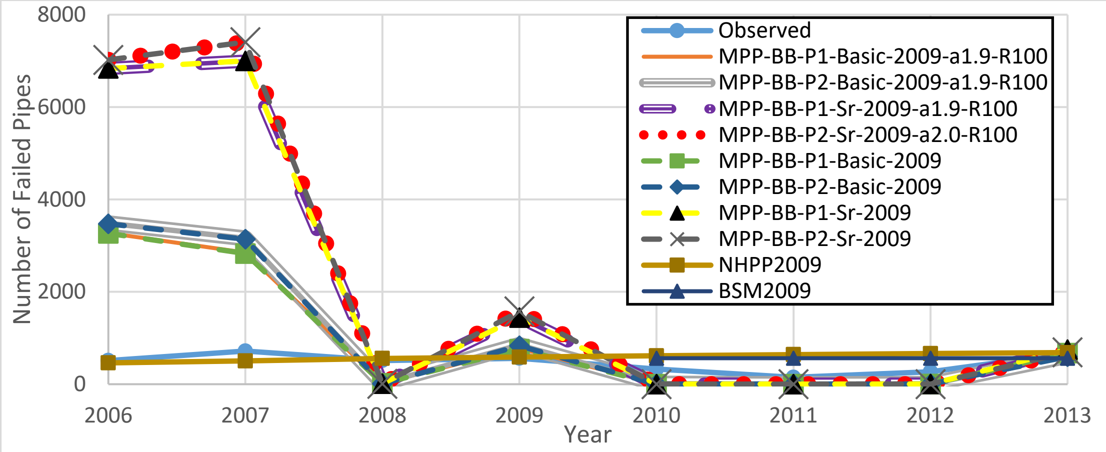

Figure 5-46: Expected number of failures estimated by the models trained using data between 2005 and 2011.

Table 5-27: Error statistics for models trained using data between 2005 and 2011.

Model Parameters	RMSE Overall	MAE Overall
MPP-BB-P1-Basic-2011-a1.5-R100	1242	804
MPP-BB-P2-Basic-2011-a1.6-R100	1357	871
MPP-BB-P1-Basic-2011	1237	801
MPP-LS-P2-Basic-2011	1357	870
MPP-BB-P1-Sr-2011-a1.9-R100	3240	1912
MPP-BB-P2-Sr-2011-a2.0-R100	3378	1995
MPP-BB-P1-Sr-2011	3240	1910
MPP-BB-P2-Sr-2011	3377	1993
NHPP2011	201	182
BSM2011	285	263

Table 5-28: Error statistics for models trained using data between 2005 and 2009.

Model Parameters	RMSE Overall	MAE Overall
MPP-BB-P1-Basic-2009-a1.9-R100	1256	790
MPP-BB-P2-Basic-2009-a1.9-R100	1382	872
MPP-BB-P1-Basic-2009	1251	787
MPP-LS-P2-Basic-2009	1376	872
MPP-BB-P1-Sr-2009-a1.9-R100	3176	1851
MPP-BB-P2-Sr-2009-a2.0-R100	3326	1935
MPP-BB-P1-Sr-2009	3176	1850
MPP-BB-P2-Sr-2009	3327	1934
NHPP2009	257	189
BSM2009	380	321

The expected number of failures estimated by the MPP models with and without the failure influence factor is very similar, given the same updating process, training period and method used to initialise the corrosion parameters (e.g. MPP-BB-P1-Basic-2011-a1.5-R100 and MPP-BB-P1-Basic-2011 in Figure 5-45). This is because the decay factor with the smallest RMSE is relatively high. The increase of the long-term corrosion rate for water mains surrounding the pipe with an unexpected failure is small. Therefore, the failure influence factor does not have a substantial impact on expected number of failures estimated by the MPP model.

Unlike the MPP model for longitudinal failure, the errors of the MPP models for broken back failures are much higher than the BSM and NHPP because the expected number of failures are often overestimated or underestimate. In addition, the inclusion of the failure influence factor does not seem to make any improvement to the model. One of the reasons for the poor performance of the MPP model in broken back failure is that there is an additional level of complexity compared to the longitudinal failure. The bending stress in the MPP model for broken back failures is time dependent, but the stress in the MPP model for longitudinal failure is constant since no variation in water pressure was assumed. As the training process for the two failure modes is the same, the current model cannot account for the time dependent stresses in broken back failures. Therefore, the performance of the model for broken back failures is poor. Further improvements in the MPP model is needed to handle time dependent stress variations for broken back failures in water mains.

5.4.2.3. Prediction Curve Comparison

The prediction curves for the MPP models without the failure influence factor, BSM and NHPP with a training period from 2005-2011 and 2005-2009 are plotted in Figure 5-47 and Figure 5-48, respectively. The ranking of the water mains for the MPP models, BSM and the NHPP are ordered using the damage factor, expected failure probability and the expected number of failures, respectively. The prediction curves plotted are the same as Section 5.3.2.3, which show the percentage of failure predicted on the y-axis for the validation period. The results from MPP models with the failure influence factor from the previous section have not been plotted because they did not show any improvements in estimating the expected number of failures, and their prediction curves are found to be similar to the models without the failure influence factor.

For the MPP models that have been plotted, the ranking performance of the models is worse if the corrosion parameters are initialised using the degree of saturation. The updating process, P2, is also preferred over P1. The MPP-BB-P2-Basic-TrainYr model is the best out of the 4 MPP models shown in the prediction curve, regardless of the training period that has been used to calibrate the model.

The ranking performance of the MPP models is worse than the NHPP for broken back failures. However, the BSM is preferred over the two as it can predict more failures for the first 20% length of pipe considered for renewal, which is the most critical part of the curve due to the limitation in the length of renewal each year.

For broken back failures, the MPP model is unable to show any improvement in ranking the water mains compared to the BSM and NHPP. It is likely that the MPP model could not adapt to the time dependent bending stress. Therefore, the damage factor cannot be estimated accurately for the water mains, leading to pipes that are not in a critical condition to be ranked higher than the ones that are close to failure.

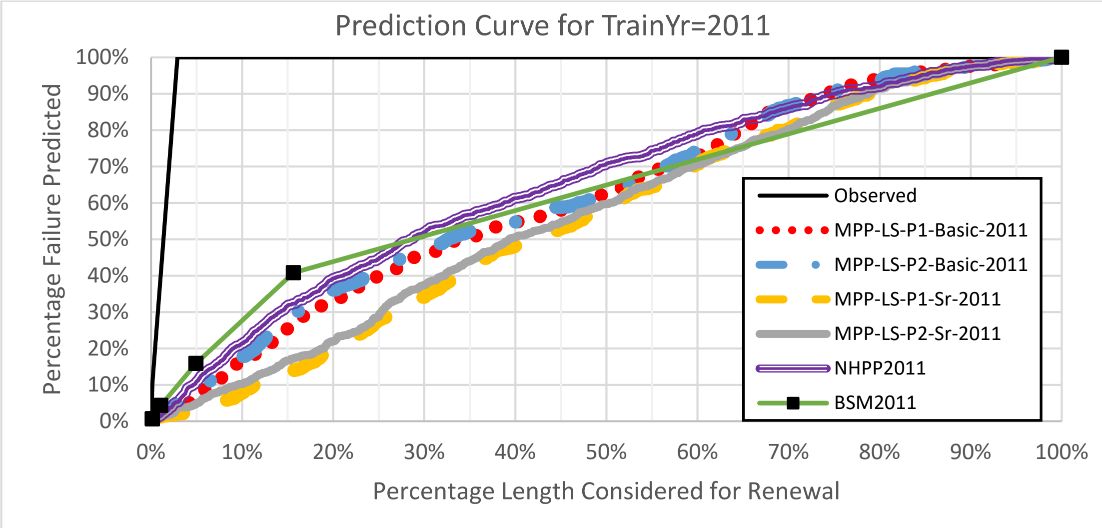

Figure 5-47: Model prediction curves for training period between 2005 and 2011.

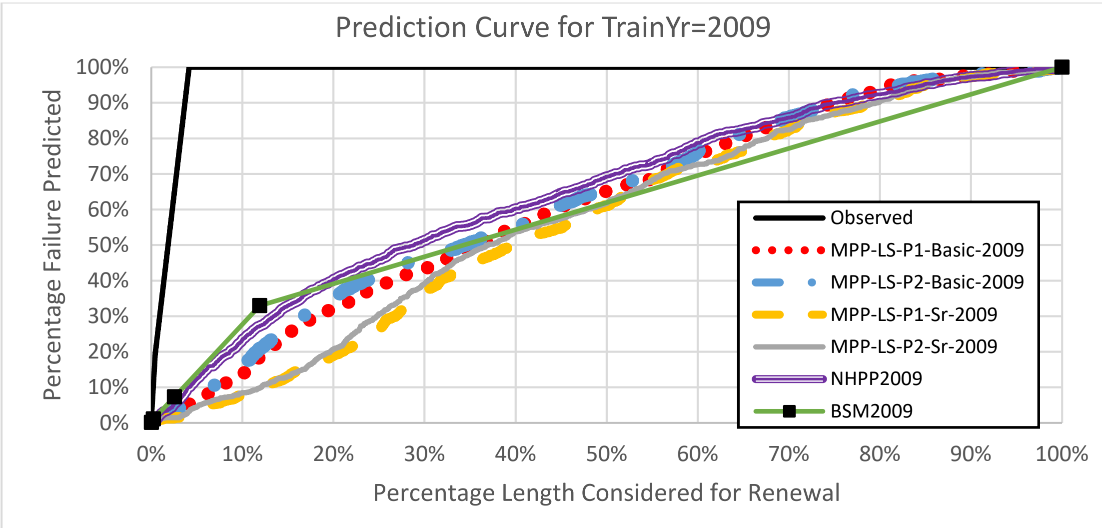

Figure 5-48: Model prediction curves for training period between 2005 and 2009.

5.5. Discussion on the MPP Model

In the MPP model, the parameters in the corrosion model are estimated using failure data or from the soil's degree of saturation. They are also continuously updated by comparing the failure data with the result from the physical model. This allows the corrosion parameters to be continuously improved and use more data that become available over time. This is different in comparison to the study conducted by Rajani and Tesfamariam (2007). The authors collected pit depth using non-destructive techniques and calculated the initiation time of corrosion based on known or assumed soil corrosivity. The parameters in the corrosion model are estimated initially but are not updated as more data are received.

The performance of the MPP models for longitudinal failures and broken back failures using the two updating processes (Section 5.2.4) and initialisation methods for the corrosion parameters (Section 5.2.2) have been compared with the BSM and NHPP. The length of water mains in the longitudinal failure and broken back failure dataset are similar (about 2000km and 1800km). The longitudinal failure dataset has been observed over a more extended period of time even though the number of failures recorded is less than the broken back failures.

Using the BSM and NHPP as a baseline of comparison, the current MPP model is more adapted to longitudinal failures rather than broken back failures. The number of longitudinal failure estimated by the MPP models matches well with the recorded failure data. However, the MPP model cannot capture the year-to-year variations for the broken back failures accurately and tends to underestimate or underestimate the number of fail pipes by a large degree.

The ranking performance of the MPP model for longitudinal failures is comparable to or better than the BSM and NHPP for the training periods considered. However, the ranking performance of the MPP model for broken back failures is worse than the NHPP and BSM. Therefore, the MPP model is better at ranking water mains that are subjected to longitudinal failures at the present stage of development.

In terms of the updating method (P1 and P2) and the method used to initialise the corrosion parameters (Basic and S_r) in the MPP model. The influence of the updating methods is not significant for estimating the expected number of failures given the same failure modes, initialisation method for the corrosion parameters and training periods. However, the P2 models tends to be slightly better at ranking pipes based on the results from the prediction curve. On the other hand, the method used to initialise the corrosion parameters has a greater impact on the result of the MPP models. Using the degree of saturation to initialise the corrosion parameters tends to be less accurate in estimating the number of failures in both failure modes. The ranking performances are also found to be the worse than those initialised using the failure data in the prediction curves for broken back failures (Figure 5-47 and Figure 5-48).

There are several possible reasons that the MPP model performs poorly when the corrosion parameters are initialised based on the soil's degree of saturation. Together, they may have led to the long-term corrosion rates in Table 5-5 to be higher than the long-term corrosion rate distribution calculated from the failure data.

The collected available water content data from an 8km by 8km grid is very coarse. Water mains are constructed as a network that requires much finer resolutions to capture the variations in the soil water content between water mains.

The conversion from the available water content to soil moisture content was based on a document from Tasmania (Cotching, 2011). The permanent wilting point and the field capacity selected for each soil reactivity (e.g. ST) dictates the range of soil moisture content estimated for the pipe. If the permanent wilting point and field capacity selected for the soil type do not approximate the actual condition of the soil in the area, the estimated soil moisture content, the degree of saturation and the corrosion parameters will not be accurate.

Finally, the conversion from the degree of saturation to the corrosion parameters was based on Table 5-5. The corrosion parameters were based on data collected from a number of projects with a limited number of samples. In addition, the operating environments of the samples are also different to the ones in Melbourne. Therefore, the corrosion parameters estimated from Table 5-5 may not be accurate for the study.

The MPP model for broken back failures performed poorly compared to the MPP model for longitudinal failures. Firstly, the assumption of all the pipes crossing a single driveway is not entirely satisfied. Also, the bending stress is calculated based on soil moisture data in an 8km by 8km grid from the BOM. The coarse resolution of the moisture data means that the variations in the soil moisture content between the water mains in the same grid cannot be captured. A large number of pipes will have the same soil moisture content values.

The MPP model was initially developed for longitudinal failures. The calibration process of the model might not be suitable for broken back failures. In addition, the bending stress for broken back failure is time dependent, whereas the stress for longitudinal failures is assumed to be constant. The variation in stress over time can make it very difficult for the model to estimate the expected number of failures accurately under the current updating processes. For example, let the estimated bending stress of a pipe to be 10MPa and 20MPa for 2006 and 2007, respectively. The corresponding SCF that needs to fail the water mains are 10 (for 2006) and 5 (for 2007). Given that a failure has been estimated from the model in 2006, the long-term corrosion rate and SCF (less than 10) will be reduced. However, the model can estimate a failure again in 2007 if the reduced SCF is greater than 5. This can lead to an over-estimation in the expected number of failures for the year.

Although the performance of the MPP model has been shown to be comparable to the BSM and NHPP for longitudinal failures, the model still has a large potential for further improvements and developments. To improve the estimation of broken back failures, the updating process (P1 and P2 in Section 5.2.4) needs to be modified to account for the time dependent bending stress. The two updating processes (Section 5.2.4) used in the MPP models are simple, and the uncertainty in the updating of the corrosion parameters in the model is not properly modelled. More advanced updating techniques (e.g. Bayesian updating) could be built into the updating process to improve the performance of the model.

The failure influence factor in the MPP model was applied to all water mains to increase its long-term corrosion rate when an unexpected failure occurs. However, the failure influence factor should be applied to the specific region of the network that is found to have clustering of failures. In addition, the minimum bound for the failure influence factor is set to 1, but it might also be useful to reduce this bound to 0 so that the long-term corrosion rates of surrounding pipes are reduced if the model anticipated a failure that did not occur.

The current application of the MPP model is limited because other pipe materials (e.g. AC pipes) and failure modes (e.g. joint failure) have not been considered. However, the components in the MPP model can be replaced easily. The physical model in the MPP model controls the type of failure modes and type of materials that will be analysed. Therefore, replacing the physical model component with other physical models that are designed for a different pipe material or failure mode can extend the application of the MPP model.

5.6. Conclusion

This chapter has discussed the development of the Monash Pipe Failure Prediction (MPP) model for pipe failure prediction. The MPP model integrates the physical model with statistical failure data. The physical model is used to estimate the condition of the pipe, while the failure data are used to update the corrosion parameters. Two updating processes and two initialisation methods for some of the initial parameters in the model have been considered to estimate failures in CI pipes subjected to longitudinal and broken back failures. The accuracy in estimating the number of failures and the ranking performance of the MPP models were compared with the BSM and NHPP.

The main findings of the chapter are summarised below based on the datasets used in the analysis:

- The performance of the MPP model initialised using the degree of saturation is not as good as the MPP model initialised using failure data. The updating process used in the MPP model does not have a significant impact on the number of failures estimated but do influence the ranking performance.
- The MPP model is better at modelling longitudinal failures than broken back failures. The number of failures estimated by the model with the failure influence factor matches well with the recorded longitudinal failure data. Its ranking

performance based on the prediction curve is also comparable to or better than the BSM and NHPP.

- The MPP model for broken back failures cannot capture the year-to-year variations in the failure data, and the number of failures is often overestimated or underestimated. The ranking performance of the model is only comparable to the NHPP but not as good as the BSM. The application of the failure influence factor in the model for broken back failures does not improve the performance of the model.

The chapter has developed the basic framework for the MPP model. It still has a large potential for future improvements and developments. The updating process needs to be modified to account for the time dependent bending stress in broken back failures. In addition, the uncertainty in the updating of the corrosion parameters have not been captured, more advanced algorithms could be incorporated into the updating process of the model. The application of the failure influence factor has not been fully explored, other functional forms for the decay function could be considered, and regions with clustering of failures should also be identified to apply the failure influence factor. Currently, the application of the MPP model is limited to CI pipes subjected to longitudinal and broken back failures, the model needs to be extended to other pipe materials and failure modes.

CHAPTER 6: APPLICATION OF FAILURE PREDICTION MODELS IN WATER MAIN REHABILITATION PLANNING

6.1. Introduction

The rehabilitation (including replacement) planning of the WDN is one of the most important operations for water utilities. It enables the water utility to forecast the future investment required to achieve the level of service that has been set for the network.

The water main rehabilitation planning consists of two components. The first is the prediction of failures for pipes in the network. Previous chapters provided detailed discussions on a number of failure prediction models. Some of these models will be used to demonstrate their applications in water main rehabilitation planning.

The second component is the consequence of failure, it includes the cost associated with the pipe itself, such as repair cost and renewal cost, as well as other cost generated as a result of the failure event, such as flooding damage and delay travel cost. In most cases, it is very difficult to obtain a reasonable estimate for some of these cost variables because they are either not available or are hard to quantify.

Several optimisation methods have been developed in the literature to identify the water mains to be replaced. Some methods (Shamir and Howard, 1978; Walski and Pelliccia, 1982; and Mailhot et al., 2003) are simple, and the optimal solution can be obtained easily, but they are only capable of modelling a single-objective. Other more advanced methods, such as genetic algorithms (Dandy and Engelhardt, 2006; Berardi et al., 2009a; Berardi et al., 2009b; Dridi et al., 2009; and Giustolisi and Berardi, 2009), are more complex and require an in-depth understanding of the problem and optimisation techniques to correctly setup the model. They are also computationally expensive, which can become an issue if there are a large number of water mains in the network. These models are generally able to consider multiple objectives (e.g. minimisation of total cost and pressure deficit).

In this chapter, a simple, single-objective optimisation method will be used to demonstrate the application of the failure prediction models discussed in previous chapters for water main rehabilitation planning. Advanced optimisation methods such as genetic algorithm could also be used in place of the simpler methods. The application of the MPP model in water main rehabilitation will be demonstrated with the NHPP. Then a number of different water main rehabilitation scenarios will be used to assess the future condition of the entire network using the NHPP (MPP model is only applicable to CI pipes). Part of this work has been utilised in developing the water plan for a water utility in Melbourne. Therefore, it is vital to ensure that the assumptions and objectives used in the process reflect upon the action that the utility will undertake in the future. This is implemented on the basis of expert opinions from the operating managers and has been used to determine the types of scenarios to analyse.

6.2. Failure Prediction Models

The first part of water main rehabilitation planning is to predict the number of failures in the future. The Non-homogeneous Poisson Process (NHPP) with simulation of the covariate, the NOKPF (Section 4.5), and the Monash Pipe Failure Prediction (MPP) model (Section 5.2) will be used. The Bayesian Simple Model (BSM) discussed in Section 3.3.3 could not be applied as the model is not time dependent (no ageing factor). The two models will first be used to model a CI dataset that only contains longitudinal failures to demonstrate the application of the MPP model in rehabilitation planning. Then the NHPP will be used to analyse the future performance of the entire network as the MPP model is only applicable to CI pipes.

6.3. Consequence of Failure and Cost of Renewal

The second component of water main rehabilitation planning is estimating the failure consequence of the break events and the cost of replacing the water mains. The estimation processes are discussed below using data provided by one of the water utility in Melbourne.

6.3.1 Consequence of Failure

The failure consequence of pipe i (Equation (6-1)) consists of cost that is associated with the failure of the asset (C_i^{rep}); the loss of service to customers (C_i^{LS}); direct damage (C_i^{dir}) (e.g. flooding of basement and damage to surrounding assets); indirect cost (C_i^{indir}); and social cost (C_i^{soc}) (e.g. traffic delays and loss of business for customers) (Nafi and Kleiner, 2009). It is difficult to estimate most of the cost mentioned above because data are rarely available or are hard to quantify (e.g. traffic delay).

$$FC_i = C_i^{rep} + C_i^{dir} + C_i^{LS} + C_i^{dir} + C_i^{indir} + C_i^{soc}$$

(6-1)

The repair cost is the only available cost data and has been collected between 2007 and 2014. Other cost that has been mentioned in Equation (6-1) can also be included if they are available. The repair cost data are first filtered by removing any values that are less than $1,000 (value selection was discussed with asset manager) because they are likely to be errors from the data entry process.

The first attempt to model the repair cost is to fit a simple regression model to the data. Many variables related to the properties of the water main have been considered, including pipe characteristics (e.g. water pressure and pipe diameter), traffic information (e.g. road type and average annual daily traffic), failure information (e.g. failure mode and location of failure) and time of failure (e.g. work duration and time of day). However, after a large number of trials using different combinations of variables, none of the simple regression models could capture the variability in the repair cost. Therefore, the average repair cost in each material type is used instead (Table 6-1, Conc-concrete, DI-ductile iron, MS-mild steel, PE- polyethylene, PVC-polyvinyl chloride, WI-wrought iron). For CI and AC pipes, the average repair cost in each local council area (Table 6-2) is used because sufficient repair cost data are available for CI and AC pipes in most locations.

Table 6-1: Average repair cost for different pipe materials.

Material Group	Repair Cost
CONC	$ 3,914
DI	$ 2,730
MS	$ 5,005
PE	$ 2,780
PVC	$ 2,478
WI	$ 2,762
Other	$ 2,585

Table 6-2: Average repair cost for CI and AC pipes in different local council areas.

LGA	CI	AC
BAW BAW	$ 3,697[7]	$ 3,032[6]
BAYSIDE	$ 4,106	$ 3,160
CARDINIA	$ 3,697[6]	$ 2,701
CASEY	$ 2,265	$ 2,717
FRANKSTON	$ 4,113	$ 2,507
GLEN EIRA	$ 4,047	$ 3,563
GREATER DANDENONG	$ 3,108	$ 3,417
KINGSTON	$ 4,126	$ 3,782
KNOX	$ 3,209	$ 2,486
MAROONDAH	$ 3,697[2]	$ 3,032[2]
MELBOURNE	$ 3,697	$ 3,532
MONASH	$ 3,005	$ 2,920
MORNINGTON PENINSULA	$ 3,516	$ 2,669
PORT PHILLIP	$ 4,435	$ 4,876
STONNINGTON	$ 3,956	$ 1,827
WHITEHORSE	$ 3,697[6]	$ 3,032[6]
YARRA	$ 3,697[6]	$ 3,032[6]
YARRA RANGES	$ 2,267	$ 2,298

[7] Average repair cost is used since repair cost data were not available for the council area.

6.3.2 Cost of Renewal

Renewal cost data for small diameter pipes (<300mm diameter) in the 2013/14 financial year has been provided by the water utility to estimate the renewal cost. A summary of the renewal conducted is shown in Table 6-3.

Table 6-3: Renewal cost data.

Cohort Properties	Cast Iron Water Mains
Total Length (km)	60
Number of Pipes	112
Old Materials	CI, AC and PVC
New Materials	PE, PVC and CU
Total Spending ($m)	19

A total of 112 pipes made from CI, AC and PVC has been renewed according to the data. Most of them were replaced with PE pipes, 9 of them were replaced with PVC pipes, and only 1 was replaced with a copper (CU) pipe.

A simple linear regression model was used to estimate the renewal cost using pipe length. Different functional form of the renewal cost and pipe length was investigated, including log transformation and squaring of pipe length. The model with the highest R^2 out of those tested is shown in Equation (6-2) (all units in thousands of dollars) and the estimated renewal cost from the model is plotted against the recorded renewal cost in Figure 6-1

$$\begin{aligned} CR_i &= M + Cr * l_i \\ &= 12.24 + 0.27 l_i \end{aligned} \tag{6-2}$$

where i is the *i-th* pipe; CR_i is the replacement cost (in thousands); M is the constant term and can be interpreted as the fixed cost involved with each replacement job (e.g. equipment hiring and mobilisation cost); l_i is the pipe length; and Cr can be considered as the cost per meter of pipe replaced (variable cost).

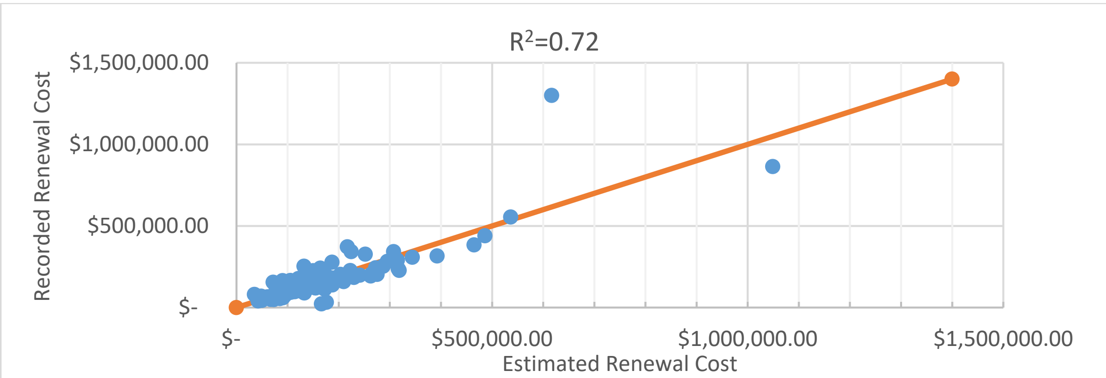

Figure 6-1: Recorded renewal cost vs estimated renewal cost.

The model has an R^2 value of 0.72, suggesting that the model's estimation fits the data reasonably well. The results of the model were discussed with the asset manager and it is believed that the variable cost (Cr) is lower than those observed in the field. There are several possible reasons for this as follows:

- The number of data points is limited as it only has 1 year of reliable data.
- The linear model is very simple and does not account for other factors, such as the surrounding environment of the work.
- The asset manager believes that the renewal cost can vary significantly between council areas, which is not accounted for in the linear model due to limited data.

The variable cost was increased to \$450 per meter based on the advice of the asset manager. The model for the renewal cost of the water main becomes:

$$CR_i = 12.24 + 0.45l_i \tag{6-3}$$

6.4. Level of Service Indicators

The following lists some of the objectives and constraints that have been used in water main rehabilitation planning studies from the literature:

Table 6-4: Objectives and constraints commonly considered.

Objectives and Constraints	Studies
Minimisation of the total cost (renewal cost + failure consequence)	Shamir and Howard (1978); Walski and Pelliccia (1982); Mailhot et al. (2003); Nafi and Kleiner (2009) and many others
Satisfy hydraulic demands	Dridi et al. (2009); Kim and Mays (1994); and Luong and Nagarur (2005)
Budget constraint	Dridi et al. (2009); Nafi and Kleiner (2009); Li et al. (2015)
Pipe selection preference	Berardi et al. (2009b) and Giustolisi and Berardi (2009)
Maximise system reliability	Dandy and Engelhardt, (2006); Berardi et al. (2009b); and Giustolisi and Berardi (2009);
Satisfy water flow demand	Kim and Mays (1994) and Dridi et al., 2008
Maximise system availability	Luong and Nagarur (2005)

The minimisation of the total cost (or cost related objectives) has been used in nearly all studies that have been reviewed. Therefore, it was the first approach considered in the study for water main rehabilitation planning. The approach was discussed with the asset managers from the water utility. It is believed that although the minimisation of total cost seems to be the most attractive solution in theory because it provides the cheapest and most effective option in the selection of water main for renewal, it might not be the most practical objective for water renewal planning. This is because the selection of pipes for renewal is hardly based on the minimisation of total cost due to other service level and regulatory requirements that need to be satisfied. The objectives used in rehabilitation planning need to be tailored to the operation of the water utility for it to be practically applicable to the network.

For the network under analysis, a renewal is proposed for the small diameter pipe if it has experienced 3 or more failures in a 12-month period. In addition, the utility is required to provide rebates to customers that experience 5 or more unplanned interruptions in a 12-month period. Considering the two points above, the following service level indicators are used to represent the service level of the network and will be minimised in the planning process:

- The failure rate (failure per 100km) of the network.
- The number of customers that experience with 3 or more unplanned interruptions (CI3), assuming that all customers in a shutoff block will experience an unplanned interruption if any of the pipes in the shutoff block experience a failure.

In addition, the water plan is undertaken to predict the future investment that is required to maintain the service level of the network at a specific level. Therefore, the current approach sets a target for the future service level of the network to predict the required investment (budget) in the future. The process used to determine the order of renewal each year by minimising the two service level indicators is described in the next section.

6.4.1 Minimising Failure Rate of the Network

The failure rate of the network can be estimated easily using the predictions from the failure prediction model divided by the total pipe length of the network.

$$FR(t) = \frac{\sum_{i=1}^{n} k_i(t)}{\sum_{i=1}^{n} l_i}$$

(6-4)

where $FR(t)$ is the failure rate of the network at time t; $k_i(t)$ is the expected probability of failure for the MPP model or the expected number of failures for the NHPP for pipe i at time t; l_i is the length of pipe i; and n is the number of pipes in the dataset.

The following is a list of steps that are used to order the water mains for renewal:

Let the maximum allowable failure rate be equal to FR_t up till the end of the planning period (T_p); $L_c(t)$ be the list of pipes candidate for renewal in time t; $L_R(t)$ be the list of pipes renewed at time t; and L_p be the list of pipes that have been renewed.

1. Predict the failures of all water mains in the dataset ($k_i(t)$).
2. Put all the pipes into $L_c(1)$.

3. Loop: For t=1 to year T_p
   3.1. For the pipes in list $L_c(t)$, rank them in descending order based on the prediction $k_i(t)$.
   3.2. Calculate the $FR(t)$ of the network using all pipes (all pipes in $L_c(t)$ and L_p) with Equation (6-4).
   3.3. Loop: while $FR(t) > FR_t$
      3.3.1. Move the first pipe in $L_c(t)$ into list $L_R(t)$.
      3.3.2. Recalculate $FR(t)$ with the pipes in $L_c(t)$ and L_p.
   3.4. Pipes that are moved to $L_R(t)$ will be replaced in year t. Recalculate the prediction for the pipes in $L_R(t)$ for the remaining planning period using the NHPP for PE pipes. Put them into list L_p.
   3.5. Calculate the renewal cost for those pipes that are replaced using Equation (6-3).
   3.6. Calculate the repair cost for those pipes that are allowed to fail using Equation (6-1).

In step 3.1, the water mains are ranked in descending order using $k_i(t)$, therefore, pipes higher in the list will be renewed first in step 3.3 because they cause the most breaks in the network.

By following the process described above, the failure rate of the network can be minimised to satisfy the level of service set by the utility. The repair and renewal cost for each planning year can also be estimated during the process.

6.4.2 Minimising Number of Customer Interruptions

The estimation for the number of customers with 3 or more unplanned interruptions (CI3) combines the predictions from NHPP with the number of customers in each shutoff block (a pipe failure is assumed to cause an interruption to all customers in the shutoff block). The MPP model is not used because it cannot estimate the probability of observing a specific number of failures for the water main.

If the break events of water mains in the same shutoff block are independent, the expected number of customers with 3 or more unplanned interruptions from shutoff block s can be estimated using Equation (6-5), with the principal of superposition for the Poisson process.

$$CI3(t) = \sum_{s=1}^{S} CI3_s\,(t) = \sum_{s=1}^{S} \left[1 - \sum_{x=0}^{2} Pr(X_s(t) = x)\right] Cus_s(t) \tag{6-5}$$

$$Pr(X_s(t) = x) = \frac{\left(\sum_{i=1}^{n_s} k_i(t)\right)^x e^{-\sum_{i=1}^{n_s} k_i(t)}}{x!}$$

(6-6)

where $CI3(t)$ is the expected total number of customers with 3 or more unplanned interruptions in the network at time t; $CI3_s(t)$ is the expected number of customers with 3 or more unplanned interruptions in shutoff block s at time t; $Pr(X_s(t) = x)$ is the probability of observing x failures in shutoff block s at time t; $Cus_s(t)$ is the number of customers in shutoff block s at time t; n_s is the number of pipes in shutoff block s; and $k_i(t)$ is the expected number of failures for pipe i at time t.

The following is a list of steps that are used to order the water mains for renewal by minimising the expected CI3:

Let the maximum allowable number of customers with 3 or more unplanned interruptions be equal to $CI3_t$ till the end of the planning period (T_p); $L_c(t)$ be the list of pipes candidate for renewal at time t; L_s be the list of pipes in shutoff block s; $L_{CIR}(t)$ shows the reduction of CI3 by the removal of each pipe at time t; $L_R(t)$ be the list of pipes renewed at time t; and L_p be the list of pipes that have been renewed.

1. Predict the failures for all water mains in the dataset ($k_i(t)$).
2. Put all the pipes into $L_c(1)$.
3. Loop: For t=1 to year T_p
   - 3.1. Group the pipe into shutoff blocks. Put all the pipes in shutoff block s into L_s.
   - 3.2. Calculate $CI3_s(t)$ and $CI3(t)$ using Equation (6-5) with pipes in $L_c(t)$ and L_p.
   - 3.3. Loop: for s=1 to S (total number of shutoff block in the network)
     - 3.3.1. For the pipes in L_s, rank the pipes in descending based on $k_i(t)$.
     - 3.3.2. Loop: for i=1 to n_s (total number of pipes in shutoff block s)
       - 3.3.2.1. Remove pipe i in L_s and calculate the reduction in $CI3$ after pipe i is removed from shutoff block s ($CI3_{R,s,i}(t)$):

$$CI3_{R,s,i}(t) = CI3_s(t) - \sum_{j=1}^{i-1} CI3_{R,s,j}(t) - \left[1 - \sum_{x=0}^{2} \frac{\left(\sum_{i'=i+1}^{n_s} k_{i'}(t)\right)^x e^{-\sum_{i'=i+1}^{n_s} k_{i'}(t)}}{x!}\right] Cus_s(t)$$

(6-7)

where $CI3_{R,s,i}(t)$ is the reduction of CI3 if pipe i is removed at time t; i' is the pipes remaining in shutoff block s; and $\sum_{j=1}^{i-1} CI3_{R,s,j}(t)$ is the reduction of CI3 from pipes that have already been removed in time t (rank higher than pipe i in L_s) and only applies after $i > 1$ (i.e. $\sum_{j=1}^{i-1} CI3_{R,s,j}(t) = 0$, given $i = 1$).

3.3.2.2. Record $CI3_{R,S,i}(t)$ in $L_{CIR}(t)$.

3.4. Reorder the pipes in $L_{CIR}(t)$ in descending order.

3.5. Loop: while $CI3(t) > CI3_t$

3.5.1. Move the first pipe in $L_{CIR}(t)$ that is also present in list $L_c(t)$ into list $L_R(t)$.

3.5.2. Recalculate $CI3(t)$ with the remaining pipes in $L_c(t)$ and L_p.

3.6. Pipes that are moved to $L_R(t)$ will be replaced in year t. Recalculate the prediction for the pipes in $L_R(t)$ for the remaining planning period using the NHPP for PE pipes. Put them into list L_p (number of pipes in $L_c(t) + L_p = m$).

3.7. Calculate the renewal cost for those pipes that are replaced using Equation (6-3).

3.8. Calculate the repair cost for those pipes that are allowed to fail using Equation (6-1).

The loop of step 3.3.2 determines the reduction in the number of customers with 3 or more unplanned interruptions ($CI3_{R,s,i}$) when a pipe is selected to be replaced. Then, in step 3.4, the pipes are ranked in descending order based on $CI3_{R,s,i}(t)$ so that the water main that is expected to cause the most number of customers with 3 or more unplanned interruptions is renewed first in step 3.5.

The steps listed above can be used to estimate the repair and renewal cost in the future to achieve the level of service target that has been set out by the water utility.

6.5. Application of the Monash Pipe Failure Prediction (MPP) Model for Water Main Rehabilitation Planning

The application of the MPP model and NHPP in water main rehabilitation planning is demonstrated using the CI dataset with longitudinal failures in Section 5.3.1.1 (Table 5-11). The MPP-LS-P1-Basic-a0.1-R50 and NHPP2010 models from Section 0 are used as the failure prediction model for rehabilitation planning. It has been assumed that the replaced water mains are removed from the analysis because the period of comparison is relatively short (2011-2015). Therefore, the NHPP for PE pipes is not used to replace the predictions in step 3.4 of Section 6.4.1.

The failure rate estimated from the failure prediction models are plotted in Figure 6-2, along with the failure rate observed during the period. The two models were trained using failure data between 1994 and 2010. They can capture the increasing trend in the recorded failure data. However, the year-to-year variations in the failure data could not be captured as time dependent factors, such as rainfall, were not incorporated in the two models. Note that the recorded data show the total number of failures in a year, but they are plotted as lines in the figures in the chapter instead of discrete points for better visualisation.

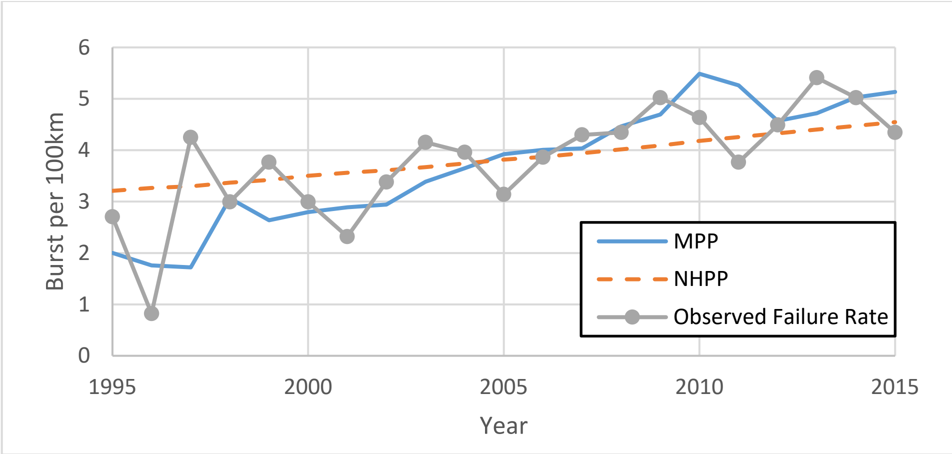

Figure 6-2: Failure rate of the network estimated by the models.

The aim is to estimate the level of investment to maintain the failure rate from the models at 4 bursts per 100km in the validation period. It would be more logical to try and maintain the level of service estimated in 2010, but as the estimated failure rates for the two models are not the same, a specific target has to be set. The procedure described in Section 6.4.1 is used to determine the pipes to be renewed each year. The performance of the MPP model in reducing the failure rate can be compared with the NHPP by using the failure data in the validation period (2011-2015).

6.5.1 Level of Investments and Network Conditions

The renewal length and replacement cost required to maintain the estimated failure rate of the models at 4 bursts per 100km are shown in Figure 6-3 and Figure 6-4 respectively. The renewal length and renewal cost for both models decrease over time because pipes that have been replaced are removed from the analysis, they will not contribute to the failure rate of the network.

Although the length of water main renewed in 2011 is very similar for the two failure prediction models, the cost of renewal is higher for the MPP model. The renewal cost model is comprised of a fixed cost component associated with the renewal of each pipe, as well as a variable cost component for the length of pipe renewed. Since the length of renewal for the two models is approximately the same, the total variable costs are similar. The MPP model has a higher total fixed cost because more pipes are renewed in the model. As a result of this, the renewal cost for the MPP model becomes higher than the NHPP in 2011.

The renewal cost of the NHPP decreases from about $13m to $5m from 2011 to 2012, then fluctuates around $5m after 2012. The rapid reduction in renewal cost is due to the model renewing a large number of water mains in the first year to reach the target level of service. Once the condition of the network reaches the burst rate that has been set out, it can be maintained by spending around $5m each year.

On the other hand, the renewal cost of the MPP model reduces gradually over time and is higher than the NHPP. This is because the MPP model predicts more failures than the NHPP. In addition, the rate of increase in the expected number of failures from water mains remaining in the network is higher for the MPP model compared to the NHPP. Therefore, the length of pipe renewal is longer for the MPP model.

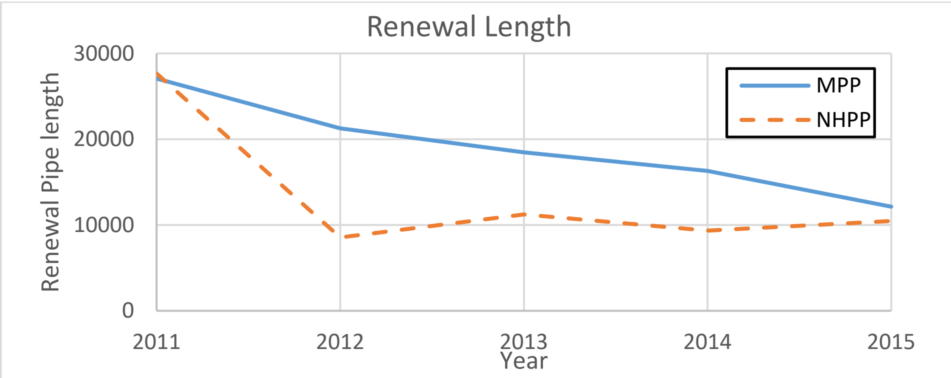

Figure 6-3: Renewal length each year.

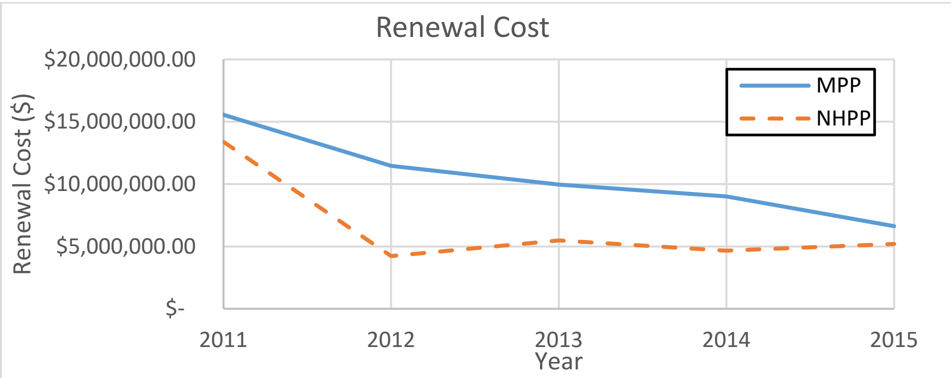

Figure 6-4: Renewal cost each year.

To compare the effectiveness of the two failure prediction models in reducing the failure rate. The remaining failure rate after the water mains are renewed are calculated using Equation (6-8) below, with the failure data in the validation period:

$$FR_r(t) = \frac{\sum_{i=1}^{n_r(t)} Z_i(t)}{\sum_{i=1}^{n_r(t)} l_i}$$

(6-8)

where $FR_r(t)$ is the remaining failure rate in the network at time t; $Z_i(t) = 1$ if pipe i failed at time t, otherwise $Z_i(t) = 0$; n_r is the number of pipes that remains in the network after the renewal program up to time t;and l_i is the length of pipe i.

The $FR_r(t)$ for the two failure predictions models in the validation period (2011-2015) are plotted in Figure 6-5. The shape of the remaining failure rates is the same as the recorded failure rate shown in Figure 6-2 between 2011 and 2013. The failure rates increase from 2011 to 2013 and then decreases till the end of the observation period

(2015). The plot shows that both models can reduce the burst per 100km by at least 0.25 each year (compare with Figure 6-2). The remaining failure rate in the network from the MPP model is generally lower than the NHPP for the observation period. However, it could be caused by the higher level of investments that is needed for the MPP model to reach the target level of service.

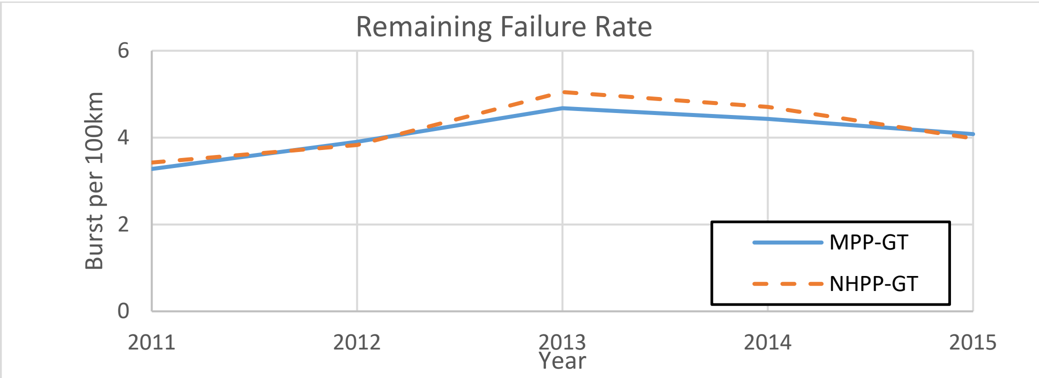

Figure 6-5: Remaining failure rates in the network.

The main limitation of the MPP model in rehabilitation planning is that the model cannot be applied to other failure modes and pipe materials yet. Therefore, it cannot be used to determine the future investment for the entire water distribution network. On the other hand, the NHPP can be applied to the entire network, regardless of pipe materials and failure modes. The next section will show some of the work undertaken for a real water utility in developing their water plan using the NHPP.

6.6. Rehabilitation Planning for the Water Distribution Network using the NHPP

This section will present part of the work used in the water plan for a water utility in Melbourne. The water plan is used to estimate the budget for the next 5 years, but predictions have been made between 2017 and 2031 (15 years) to understand the future condition of the network. The NHPP-Max3 model from Section 4.5 is used as the failure prediction model in the water plan. The model can capture the deterioration of the pipe over time, as well as simulate future failures to account for shorter failure times in water mains that have experienced more failures. The NHPP-Max3 models are calibrated using failure data between 1994 and 2015 with a range of covariates, including the pipe properties (e.g. pipe length and pipe diameter), the soil properties (e.g. soil type, shrinkage swelling potential), the water properties (e.g. water hardness and water pH) and the NOKPF (up to a maximum of 3). The process assumed that the water main will only be replaced once in the entire planning period. The replaced pipe will be made of PE, and the failure prediction model will be replaced by the NHPP for PE pipes after replacement. The coefficients estimated for the PE pipes are listed in Table 6-5. Note that the failure data from 2016 were excluded in the failure prediction model because the failure data were not fully available at the time of analysis.

The pipe assets are broken up into material groups (pit cast iron (PCI), spun cast iron (SCI), asbestos cement (AC), concrete (CONC), ductile iron (DI), mild steel (MS), PE, PVC, wrought iron (WI) and OTHER) for calibration because of the different physical properties with each material type.

Table 6-5: Coefficients for PE pipes.

Covariates	Coefficient
Constant	-6.54
ln(Pipe Length) (m)	0.78
Pressure (kPa)	1.51
100mm<PipeDia<=200mm	-0.74
Soil Type=Sand	-0.36
Aggressive index[8]	-1.33
Average water hardness	0.04
Water pH	1.28
NOKPF=1	1.04
NOKPF=2	1.85
NOKPF>=3	2.24
Ageing factor	0.96

The estimated ageing factors for the different material groups are shown in Table 6-6. The failure rate for most of the pipes is expected to increase over time, except for OTHER and PE pipes. PE is one of the newest pipe material that is introduced in the network (around 1980), and therefore, their failure rate is not expected to increase for the period of analysis. Materials (e.g. PCI, AC, MS and WI) estimated with a high ageing factor suggest that the number of failures will increase at a high rate because they are approaching the end of their design life. These materials will likely be the ones that are selected to be replaced in the network.

Table 6-6: Ageing factor for each pipe material.

Material	Ageing Factor
PCI	2.11
SCI	1.49
AC	1.92
CONC	1.75
DI	1.10
MS	1.86
OTHER	0.89
PE	0.96
PVC	1.58
WI	2.05

The estimated burst per 100km for the WDN is plotted in Figure 6-6, along with the observed failure rate. The observed burst rate varies over the years, but a general

[8] Aggressive index=pH+log(alkalinity*Hardness)

upward trend can be found, indicating a reduction in the average condition of the pipes. The burst rate predicted by the NHPP can capture the general upward trend in the data, but not the year to year variations. Other time dependent factors, such as temperature and rainfall, will need to be included in the NHPP to capture the year to year variations. However, as the value for these time dependent factors (e.g. rainfall) are generally unknown in the future and cannot be predicted with sufficient accuracy, they have been excluded from the model.

The total number of customers in the network and the estimated/predicted CI3 for the WDN (Equation (6-5)) are plotted in Figure 6-7, along with the observed CI3. The data on the number of customers in the network between 1994 and 2014 were not collected, and therefore the number of customers in 2015 is used instead. Customer growth was projected by the water utility for the planning period, which shows a rapid increase in the number of customers for the next 15 years. This is a result of the growth in population, leading to a rise in demand for high-rise buildings. Comparing the estimated and observed CI3, there is an upward trend in both the observed and estimated results. The estimation from the model tend to underestimate the observed data at the beginning but does catch up to the observed value as the failure rate of the network increased. In the prediction period, the model predictions increase rapidly because of the increase in the failure rate, as well as the high customer growth projected by the water utility.

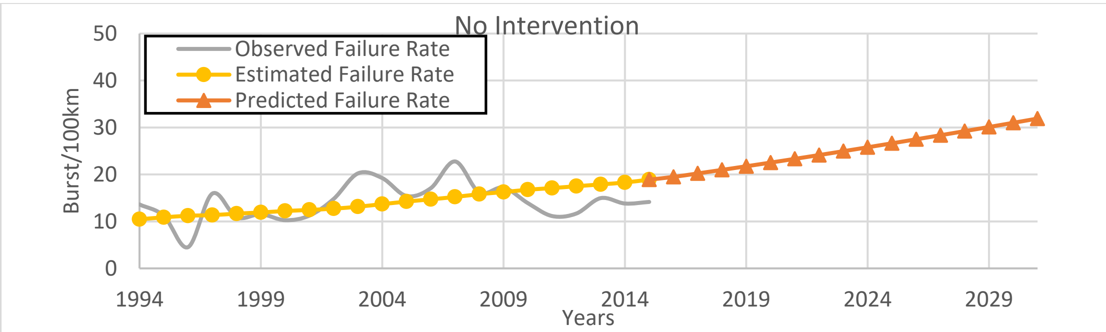

Figure 6-6: Predicted Burst rate of the network.

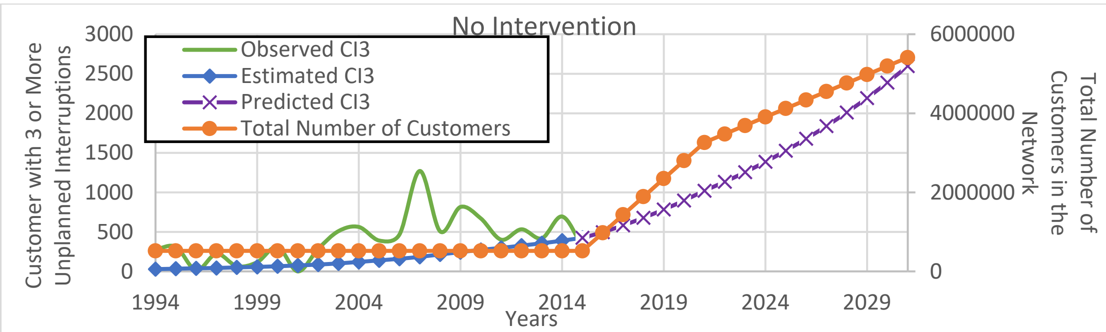

Figure 6-7: Predicted CI3 of the network.

6.6.1 Scenario Analysis for the Water Distribution Network

The future condition of the WDN cannot be predicted with a hundred percent certainty. However, by analysing the probable future scenarios based on expert knowledge from asset managers can provide a strong basis and support for the development of investment budget in the future.

The projection shown in Figure 6-6 and Figure 6-7 can be considered as a no intervention scenario. It assumes that the water mains in the network will only be repaired but not replaced during the planning period. Therefore, the failure rate will continue to increase over time, leading to an increase in customer interruptions. The models projected that the failure rate of the network will increase from 20.22 burst/100km in 2017 to 31.90 burst per 100km in 2031, while CI3 will increase from 582 in 2017 to 2596 in 2031.

The following scenarios will be investigated and compared:

- Scenario 1: Investment required to achieve 5 different level of service for customers with 3 or more unplanned interruptions by minimising CI3.
- Scenario 2: Investment required to maintain 6 different level of burst rate by minimising the failure rate of the network.
- Scenario 3: Define a constant budget for pipe renewal in the water plan period (the next 5 years, 2017-2021). The target level of service set out in scenario 1 is achieved at the end of 2021.
- Scenario 4: Define a constant budget for pipe renewal in the water plan period (the next 5 years, 2017-2021). The target level of service set out in scenario 2 is achieved at the end of 2021.

The cost values (renewal and repair costs) in the future will not be discounted back to the current value as it is more important to determine the cash flow in the future. However, they can be easily discounted if the discount rate is known.

6.6.1.1. Scenario 1

Scenario 1 investigates the amount of investment that is required to maintain CI3 at 5 levels, including the predicted level of service for customers with 3 or more unplanned interruptions in 2016 (approximately 500). The 5 level of service considered in the analysis are:

- Number of customers with 3 or more interruptions cannot exceed 300.
- Number of customers with 3 or more interruptions cannot exceed 350.
- Number of customers with 3 or more interruptions cannot exceed 400.
- Number of customers with 3 or more interruptions cannot exceed 450.
- Number of customers with 3 or more interruptions cannot exceed 500.

The process used to determine water mains selected for renewal has been discussed in Section 6.4.2. The predicted burst rate, pipe length replaced, repair cost and replacement cost are shown in Figure 6-8, Figure 6-9, Figure 6-10 and Figure 6-11, respectively. The level of service is represented using colour lines in the figures. For example, the blue line stands for the case where the maximum CI3 cannot be more than 300.

The results show that if the current level of customer interruptions based on the model's prediction (about 500 customers) is maintained in the network, the burst rate and repair cost will increase over the years. The length of pipe renewed will increase from about 5km per year to about 60km per year by the end of 2031. The replacement cost will increase from about $2.5m per year to about $30m per year by 2031.

If the level of service is to be maintained at the rate in 2015 (about 314 customers with more 3 or more interruptions), the burst rate and repair cost still increase over time. It is predicted that 60 to 80km and 30 to 40km of pipes will need to be replaced in 2017 and 2018, respectively. Then the replacement length increases slowly and approaches 70km in 2031. This leads to an investment of $30m to $50m in 2017, $15m to $20m in 2018, and up to about $35m in 2031. The investment in renewal is much lower in 2018 because a large number of pipes have to be replaced to bring the level of service to the target level in 2017.

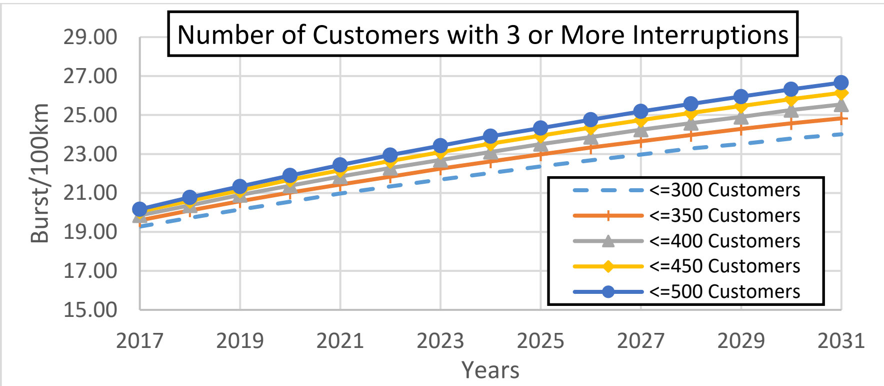

Figure 6-8: Burst rate for cases in Scenario 1.

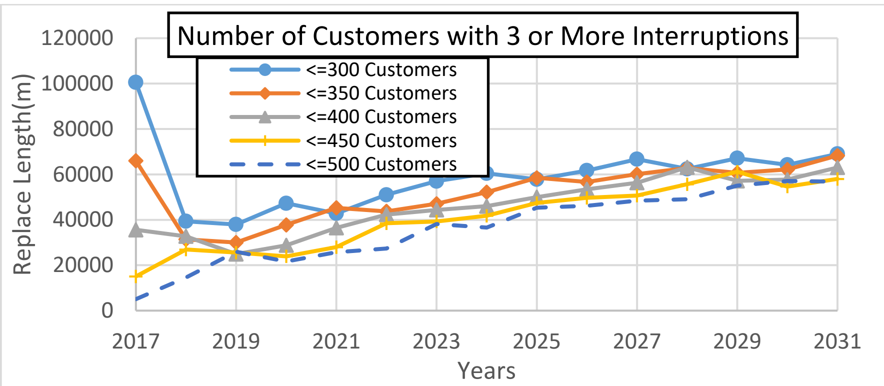

Figure 6-9: Pipe length replaced for cases in Scenario 1.

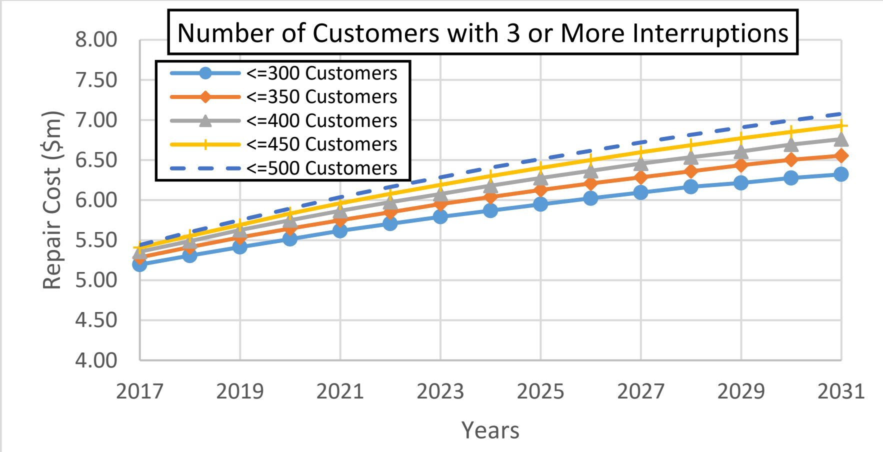

Figure 6-10: Repair cost for cases in Scenario 1.

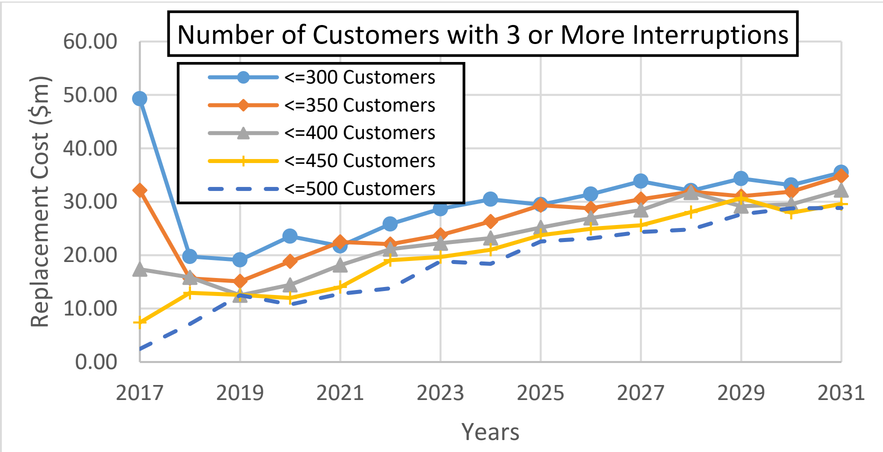

Figure 6-11: Replacement cost for cases in Scenario 1.

6.6.1.2. Scenario 2

Scenario 2 estimates the amount of investment that is required to maintain the burst rate of the network at 6 levels, including the failure rate predicted by the model in 2016 (about 19.4 failures per 100km). The 6 level of service that is considered in the scenario are:

- Maximum failure rate cannot exceed 19.2 break/100km.
- Maximum failure rate cannot exceed 19.4 break/100km.
- Maximum failure rate cannot exceed 19.6 break/100km.
- Maximum failure rate cannot exceed 19.8 break/100km.
- Maximum failure rate cannot exceed 20.0 break/100km.
- Maximum failure rate cannot exceed 20.2 break/100km.

The process used to select water mains for renewal has been detailed in Section 6.4.1. The repair cost, predicted length of pipe replaced, replacement cost and the CI3 are shown in Figure 6-12, Figure 6-13, Figure 6-14, and Figure 6-15 respectively. The figures show six level of burst rate for the network, each represented using a colour line. For example, the maximum number of failures per 100km for the case in red line will not exceed 19.2 failures per 100km.

The repair cost for all level of service reduces over time because the water mains with the highest expected number of failures are replaced with PE pipes. The new pipe will have a lower expected number of failures and repair cost in most cases (Table 6-1).

To maintain the current level of burst rate in the network, it is predicted that $44m has to be spent to replace about 93km of pipes in 2017. Then, the renewal budget is expected to increase to about $45m to replace about 93km of pipes in 2018. After 2018, the spending on pipe renewal and the renewal length gradually increases to about $55m and 110km in 2029, respectively. The CI3 rises from 455 to 550 in 2025 and then reduces back to about 450 in 2031.

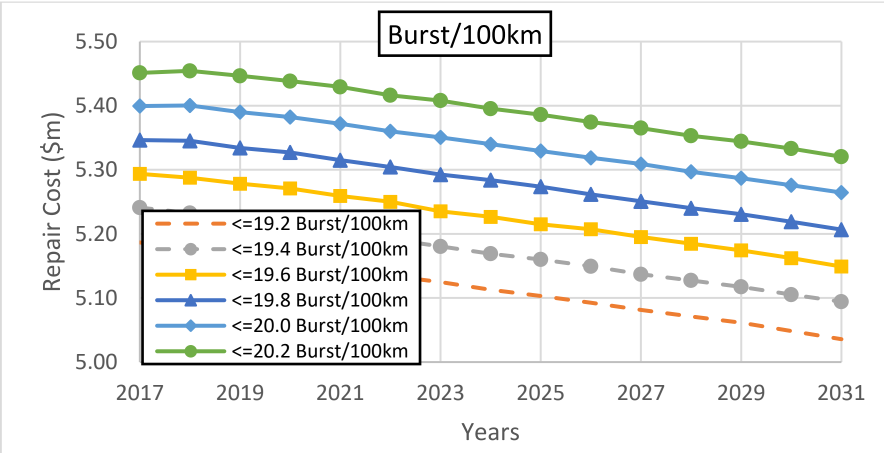

Figure 6-12: Repair cost for cases in Scenario 2.

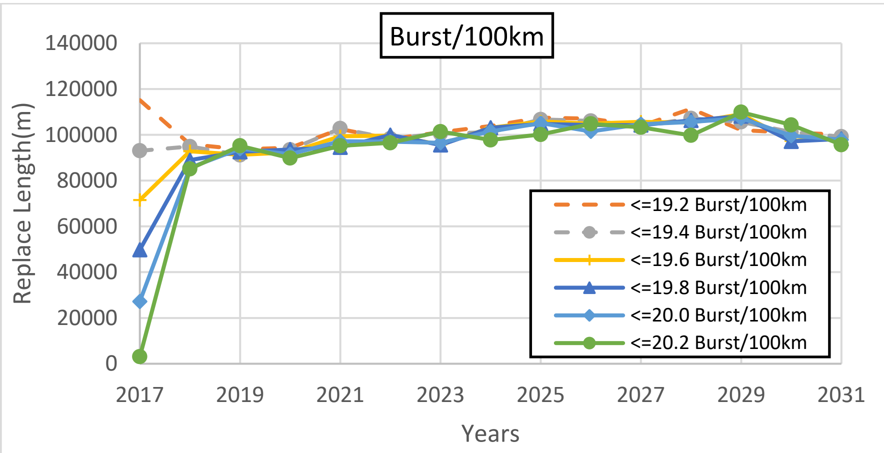

Figure 6-13: Replace length for cases in Scenario 2.

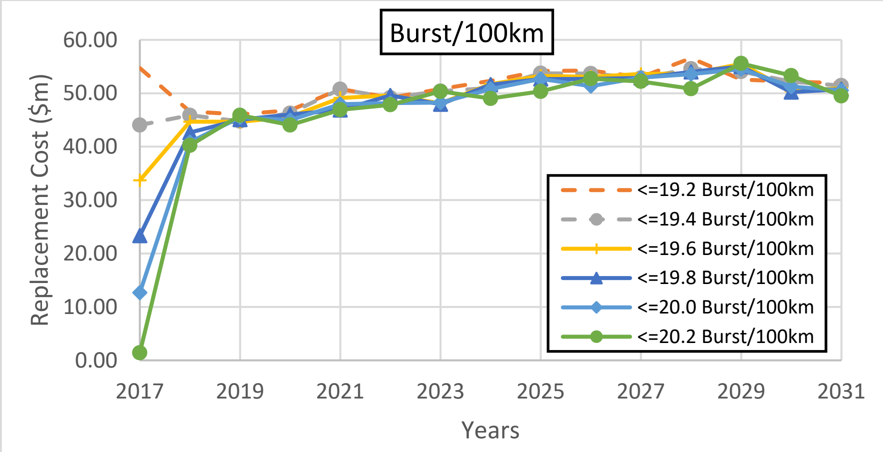

Figure 6-14: Replacement cost for cases in Scenario 2.

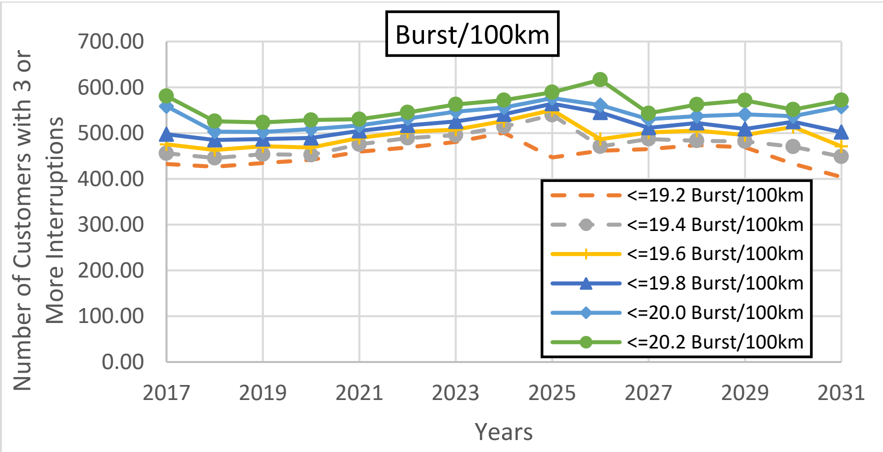

Figure 6-15: Number of customers with 3 or more interruptions for cases in Scenario 2.

An improvement in the level of service in the WDN in terms of the burst rate would only require additional investments in 2017, the level of investment for the years after 2017 are similar to the ones predicted if the current level of service is maintained. To reduce the burst rate by 0.1, the investment on pipe renewal in 2017 has to increase by approximately $10m to replace an addition 20km of pipes. Reducing the burst rate in the network also reduces the CI3, but the improvements are not substantial.

6.6.1.3. Scenario 3

Scenario 1 and 2 showed significant variations in the renewal cost between 2017 and 2018 when a substantial improvement was targeted in the level of service. These types of investment levels are generally not practical because of the limitation with resources that can be allocated in a year. To allow a more realistic and even level of investment each year for the next water plan period, scenario 3 defines a constant investment level for pipe renewal in the water plan period (2017-2021) to achieve the level of service set out in scenario 1 by the end of 2021. The predicted burst rate, replaced pipe length, replacement cost, repair cost and the CI3 are shown in Figure

6-16, Figure 6-17, Figure 6-18, Figure 6-19 and Figure 6-20, respectively. The same colour from figures in scenario 1 is used here.

The results show that the burst rates and repair cost for the 5 cases are similar in 2017 and then increases over the period of analysis. The predicted burst rate and repair cost by the end of 2031 are similar to the ones in scenario 1.

For the network to maintain 500 customers with 3 or more interruptions in 2021, an annual investment of about $10m (about 20km renewal length) is required for the next five years. Then, the investment in pipe renewal will have to increase to about $30m by 2031 to compensate for growth in failure rates and customers in the shutoff blocks. Improving the level of service in terms of customer interruptions from the current level to 400 customers would require an additional investment of about $5m per year (addition 10km renewal length). To achieve the level of service in 2015 (314 customers with 3 or more interruptions) by the end of the water plan period, the expected annual renewal investment ranges between $21m to $26m per year (42 to 54km of pipes renewal).

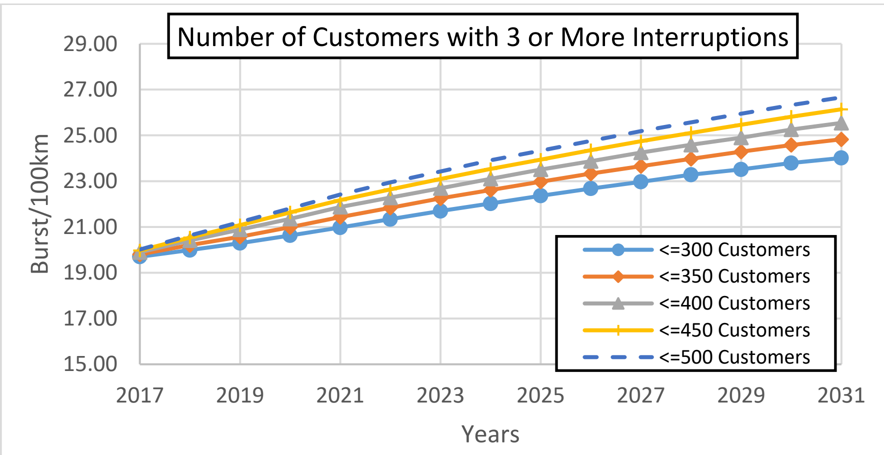

Figure 6-16: Burst rate for cases in Scenario 3.

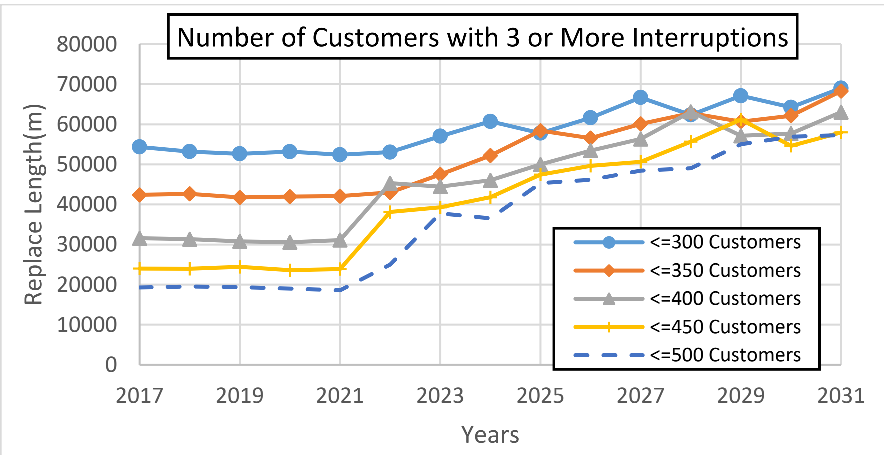

Figure 6-17: Replace length for cases in Scenario 3.

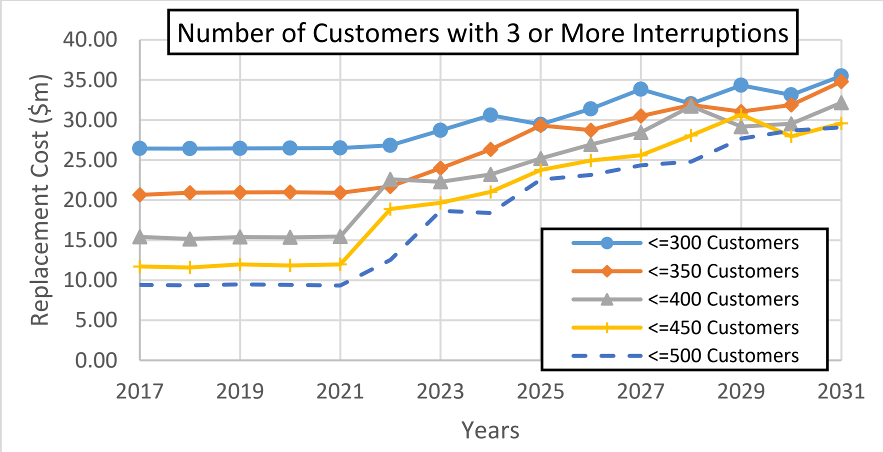

Figure 6-18: Replacement cost for cases in Scenario 3.

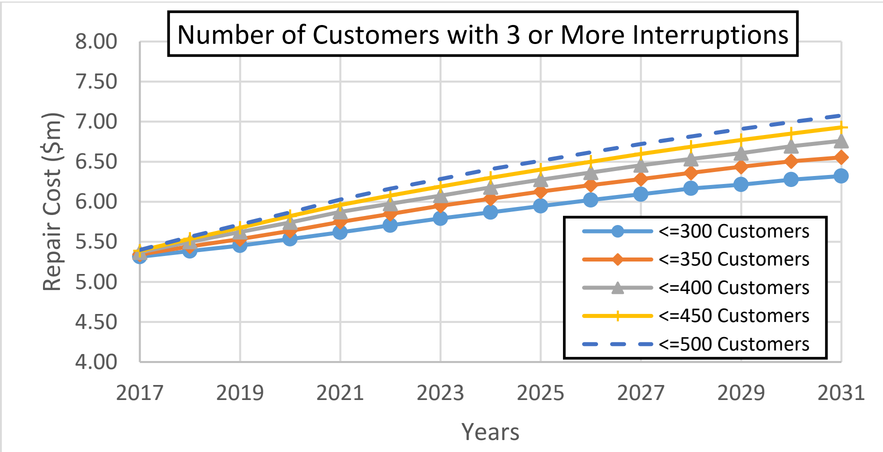

Figure 6-19: Repair cost for cases in Scenario 3.

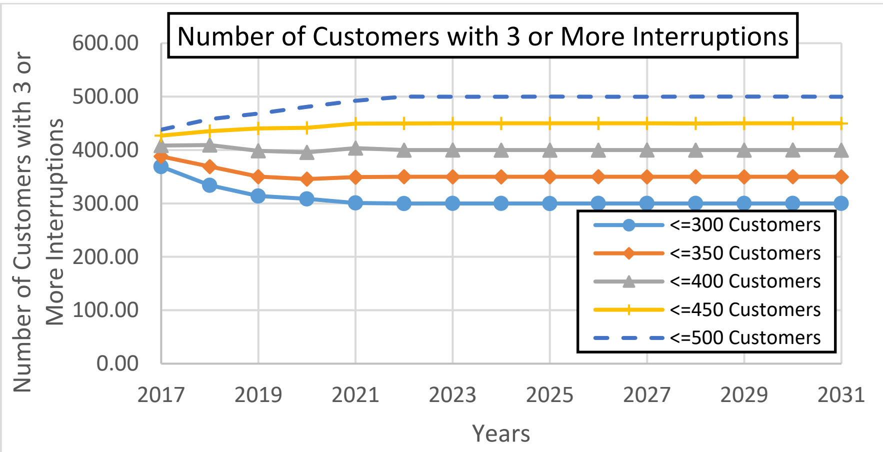

Figure 6-20: Number of customers with 3 or more interruptions for cases in Scenario 3.

6.6.1.4. Scenario 4

Scenario 4 defines a constant investment level in the renewal budget for each year for the first 5 years (2017-2021). The aim is to reach the level of burst rate set out in scenario 2 by the end of 2021. This will provide a more realistic and practical level of investment for pipe renewal during the water plan period compared to scenario 2.

The predicted repair cost, burst rate, replaced pipe length, replacement cost and the CI3 are shown in Figure 6-21, Figure 6-22, Figure 6-23, Figure 6-24 and Figure 6-25, respectively. The same colour code from the figures in scenario 2 is used here.

The predicted repair cost increases between 2017 and 2021 if the burst per 100km is maintained above 19.4 burst per 100km. The repair cost starts to decrease after 2022 for all level of failure rate that has been considered.

The current level of burst rate (about 19.4 failures per 100km) in the network can be maintained by investing $46.5m to replace about 98km of water mains per year during the water plan period. An increase or decrease in the level of service in terms of burst rate by 0.2 will change the annual investment by about $2m. After 2021, the expected investment in pipe renewal fluctuates between $50m to $55m (100km to 110km renewal length) for all cases in the scenario.

The CI3 is similar for the different cases in 2017. It is expected to be maintained at the level in 2017, if the burst rates are kept at 19.6 failures per 100km or below, otherwise, the CI3 is expected to increase by the end of 2031.

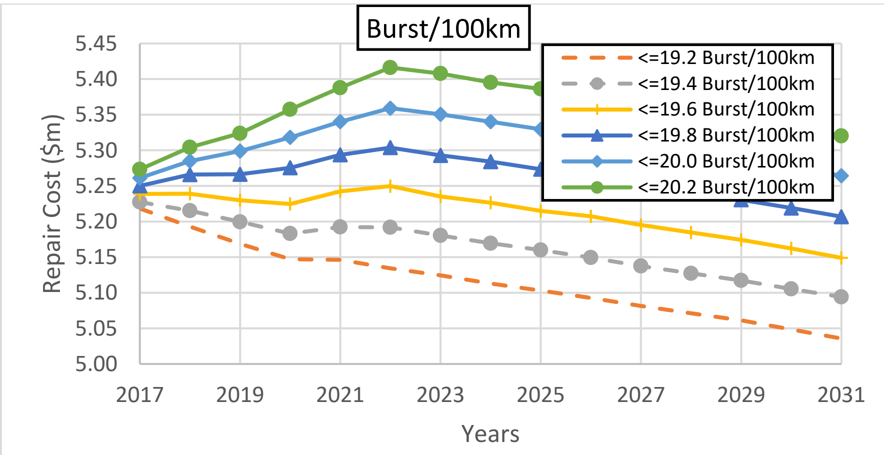

Figure 6-21: Repair cost for cases in Scenario 4.

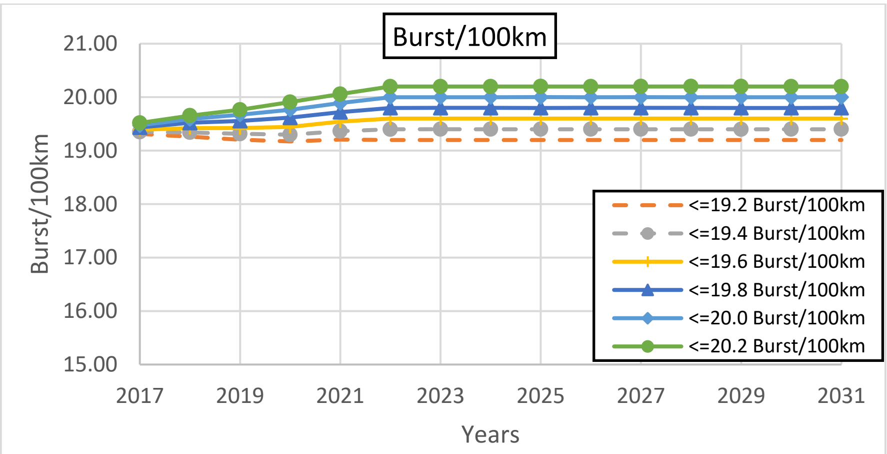

Figure 6-22: Burst rate for cases in Scenario 4.

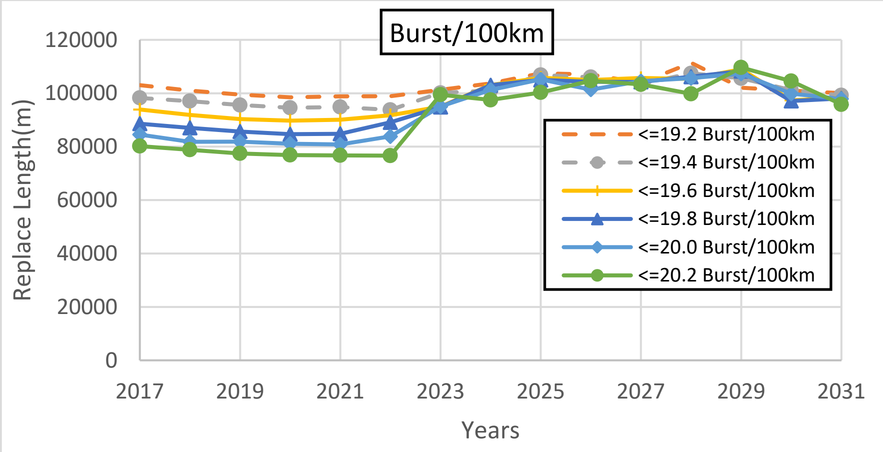

Figure 6-23: Replace length for cases in Scenario 4.

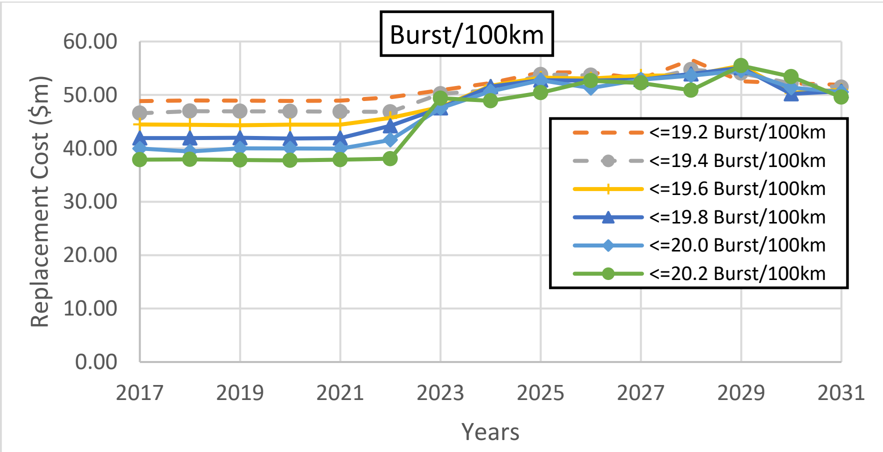

Figure 6-24: Replacement cost for cases in Scenario 4.

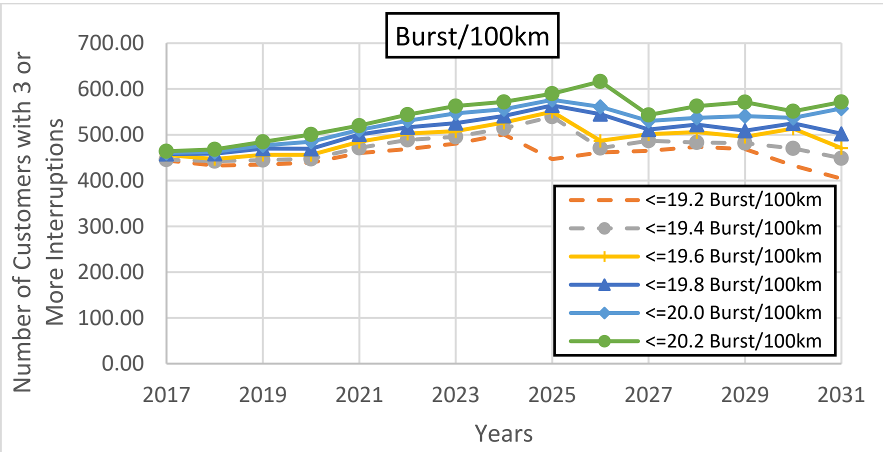

Figure 6-25: Number of customers with 3 or more interruptions for cases in Scenario 4.

6.6.1.5. Discussion

The scenarios that have been analysed above are some of the many that have been considered by the water utility. They have presented the investments that are required to maintain the level of service for the water distribution network at various levels under two renewal strategies. The complexity of the scenarios increases as the objectives (from no intervention to minimising failure rate and CI3) and constraints are included in the model to provide a more realistic representation of the aims (e.g. minimise failure rate) and limitations (e.g. constant budget in the water plan period) in the rehabilitation of water mains. The water utility can use the information gathered from the different scenarios to adjust their strategic, tactical and operational management plan.

Based on the four scenarios that have been compared in the chapter, the length of water mains that can be replaced by spending $20m (about 40km) is less than the amount shown in Table 6-3 ($19m for 60km). This is because the cost per meter of pipe renewal has been increased to 0.45 (Equation (6-3)) from 0.27 (Equation (6-2)). Comparing the level of investment between the scenarios, it is generally more expensive to maintain the burst rate of the network at a constant level than to maintain the CI3. The length of water mains that needs to be renewed each year in scenario 2 and 4 are much longer than scenario 1 and 3.

The renewal cost for various level of service in each scenario converges to a common value ($30-35m for scenario 1 and 3, $50m for scenario 2 and 4). It suggests that in the long-term, $30-35m has to be spent on pipe renewal each year for scenario 1 and 3, while $50m has to be spent each year on pipe renewal for scenario 2 and 4. The water utility can plan on the basis of these predictions to anticipate for the increase in renewal work and allocate sufficient resources to fund these renewal programs in the future. They could also consider other rehabilitation alternatives, such as reducing the size of shutoff blocks, to help reduce the investment needed for the future.

One of the drawbacks with the current approach for water main rehabilitation planning is that the scenarios have only considered a single objective. Therefore the level of service can only be maintained for one of the service level indicators (e.g. either only failure rate or only CI3). Multi-objective optimisation methods such as genetic algorithms can be used instead to come up with a set of solutions can achieve the level of service set for the two service level indicators.

In addition to predicting the level of investment and the condition of the network in the future, the scenario analysis also produces a list of water mains that are selected to be renewed each year. As the prediction model is statistically based, the prediction in the number of failures are reliable at a group/network level, but generally over-underpredicts the number of failures in individual pipes. Therefore, using the statistically based model to predict the level of investment and the condition of the water distribution network are more desirable. However, the selection of individual water mains for renewal is based on predictions at a pipe level, which can lead to pipes being replaced earlier or later than they should be. Therefore, the list of pipes for renewal produced from the scenario analysis should only be considered as renewal candidates for future rehabilitation and a more detail investigation (e.g. condition assessment) should be conducted before the pipes are selected for renewal.

6.7. Conclusion

The chapter has demonstrated the application of the MPP model and the NHPP in water main rehabilitation planning. The two models were first applied to a CI pipe dataset subjected to longitudinal failures due to the limitation of the MPP model. Then the NHPP is used in the rehabilitation planning of the entire water distribution for a water utility in Melbourne. The objectives were to predict the level of investment that is required to maintain the service level of the network at varies levels under four different renewal strategies (scenarios). Although it is not possible to conduct an analysis to cover all the scenarios that will happen in the future, the selection of several scenarios that are more likely to occur based on expert knowledge can provide valuable insights for water renewal planning.

The main outcomes of the rehabilitation planning are summarised below based on the datasets used in the analysis:

- For the CI pipe dataset with longitudinal failures, the MPP model requires a higher level of investment to maintain the burst rate at 4 breaks per 100km. However, the observed failure rate remaining in the dataset after the pipes are renewed based on the selection of the MPP model is less than the NHPP.
- For the rehabilitation planning of the entire network, it is more expensive to maintain the burst rate at a constant level compared to maintaining the number of customers with 3 or more unplanned interruptions.
- The level of investments in the long-term tends to converge to a common value for the scenarios that have been analysed. It suggests that regardless of the target that is set for the level of service in the scenarios, the investment in renewal for the long-term future is approximately the same and the water utility must have sufficient resource to satisfy this demand in the future.
- The list of pipes selected for renewal in the process should only be considered as renewal candidates. Additional investigation should be conducted before they are selected to be renewed.

For the water plan to be accurate and relevant to the water distribution network, it is critical that the selected objectives and constraints match with the renewal strategies that are undertaken by the water utility. Otherwise, the prediction from the rehabilitation model is not going to be useful. It is also important to communicate closely with the water utility asset managers. Their practical knowledge and experience in the planning and management of the water distribution can significantly improve the application and practicality of the water plan developed.

CHAPTER 7: CONCLUSION AND RECOMMENDATION FOR FUTURE WORKS

The accurate prediction of failures in the water distribution network is crucial for predicting the future condition and the level of investment required in the future. The thesis has compared several models for failure predictions in the water distribution network. Based on the literature review, the following gaps were identified in the failure prediction of the water distribution network:

- Statistical models are generally poor in making predictions for individual pipes. Pipe ranking models could be an alternative in locating pipes that are more likely to fail.
- Time dependent factors in statistical models have shown improvements in estimating the number of failures during the training period. However, the prediction of future failures with time dependent factors are limited because their values are unknown in the future.
- The integration of the physical model with statistical failure data to predict water main failures have not yet been investigated. Physical models estimate the condition of the pipe based on the physical deterioration process, while statistical models predict failures based on the collected failure data. The failure data could be used to support the physical model in estimating the condition of the pipe and produce promising result for failure prediction.

7.1. Summary of Research

Based on the gaps identified from the literature review, the BSM was developed for identifying groups of water mains that are more likely to fail in the future; time-lag was introduced into the time dependent factor (MMAPI) of the NHPP to predict failures in the short-term future; the NOKPF was used for long-term failure prediction by simulating the breakages in the water main using the NHPP; and finally, the basic framework for the MPP model was developed to integrate the physical model with statistical failure data. A summary of the models developed are listed below:

- The BSM estimated the failure probability of a group of water mains with similar failure history. The BSM is simple and performs well in identifying pipes that are likely to fail compared to the HBP and the NHPP. However, after testing the model with several datasets, the BSM was found to be unsuitable for predicting the actual number of failures in the future as the model does not account for any time dependent factors, such as pipe age.
- The introduction of time-lag into the MMAPI allowed the model to predict failures using MMAPI values from the past. Although the results show that the longer the time-lag, the prediction for the total number of failures in the network becomes

less accurate. A lag of 1 or 2 months in the MMAPI can still capture part of the monthly variations in the failure data and make reasonable failure predictions for the network. This can be valuable to networks that suffer from occasional spikes in the monthly failures because of time dependent factors, such as the MMAPI. The early prediction of these spikes allows the utility to adjust their short-term operational planning so that the interruptions to the customers can be minimised as much as possible.

- The NOKPF can be used to account for the reduction in the time to next failure as the number of past failure increases in the water main. Failure prediction models without accounting for this effect can under-predict the number of failures in the future. The main limitation in using the variable for failure predictions is that it is both pipe and time dependent, and its values are unknown in the future. However, the failure prediction model can be used to simulate the future failures that might occur, this can be feedbacked into the model to update the NOKPF for long-term failure prediction and water main rehabilitation planning.
- The MPP model integrates the physical model with statistical failure data to predict longitudinal and broken back failures in CI pipes. The physical model is used to estimate the condition of the pipe to capture the physical deterioration of the water main. The failure data are used to update the corrosion parameters in the physical model during the calibration process. The performance of the model in estimating longitudinal failures were comparable to the NHPP in terms of the total number of failures in the network, and the BSM in identifying water mains that are more likely to fail. However, the MPP model did not perform as expected for broken back failures, and there are many areas that the model can be improved upon.

The failure prediction models were applied in water main rehabilitation planning to demonstrate its main applications in the water distribution network. The water main rehabilitation planning is one of the most important operations performed by the water utility once every few years. The main objective is to predict the future condition of the pipes in the network as well as the level of investment that is required. The application of the MPP model in water main rehabilitation planning was demonstrated using a CI dataset, and the NHPP was used to predict the future level of investment and condition of the entire water distribution network under a number of renewal scenarios as part the water plan for a real water utility.

7.2. Contribution of Thesis

The contributions of the thesis in the failure prediction of the water distribution networks are summarised below:

- Statistical models generally over- or underestimates the number of failures for individual pipes. The BSM is a data-driven method developed to identify groups of pipes that are more likely to fail. The method is simple, but its performance is comparable to other complex models. It can be used as a preliminary desktop assessment tool to select candidates for further investigation (e.g. condition assessment).

- Time dependent factors can capture the monthly or yearly variations in the failure data. The application of time-lag in the time dependent factor allows the NHPP to predict failures using values that have been already recorded. Water utility operating networks with failures highly correlated to time dependent factors (e.g. MMAPI) can adjust their operational planning to minimise the customer interruptions in times when the model predicts an abnormal increase in the number of failures.
- The main contribution of the research project is the development of the framework to integrate the physical model with statistical failure data to predict water main failures. The approach utilities the physical model to estimate the condition of the pipe and the failure data to calibrate the input corrosion parameters in the physical model. There are a number of advantages in the combined approach:
    - The model is physically based, it can capture the failure trend in the deterioration process of the pipe even if it is not present in the failure data.
    - The failure data can be used to estimate the input corrosion parameters in the physical model if it is not available.
    - The corrosion parameters can be updated using failure data to improve the performance of the physical model.

7.3. Recommendation for Future Works

Based on the knowledge gained from the research project, there is no perfect model for predicting failures in the water distribution network. Some models (e.g. BSM and HBP) are more suitable for identifying pipes that are more likely to fail, while others (e.g. NHPP) are better at predicting the total number of failures in the future. The combined approach, the MPP model, has shown to be capable of modelling longitudinal failures in CI pipes. The model has the potential to be extended to other materials and further developed to enhance its results:

- The physical model and corrosion model components have been designed to be easily replaceable. New models that are developed can be used to replace the ones that are currently used.
- Extending application of the MPP model to all pipes by replacing the physical model with those designed for other pipe materials (e.g. AC pipes) and failure modes (e.g. joint failures).

- The updating process of the corrosion parameters in the model is very basic at the moment. More advanced updating algorithm could be used to capture the uncertainty into the updating process.
- The strength of the failure influence factor was not fully investigated in the MPP model. Other functional relationships between the distance and the strength of the failure influence factor were not explored. In addition, a more detailed analysis should be undertaken to determine the region that the failure influence factor is applicable in the network.

7.4. Final Remarks

With the growth of populations in cities, and the pressure to reduce expenditure without impacting on the level of service of the network, the proper management and maintenance of the water distribution network are becoming an ever-increasing challenge for water utilities.

The failure predictions models that have been developed in the thesis can be used to assist water utilities in selecting pipe renewal candidates, and predict the number of failures/repairs in the future. It can also be used in rehabilitation planning to predict the level of investment and future condition of the network.

REFERENCES

Achim, D., Ghotb, F., and McManus, K. (2007). "Prediction of Water Pipe Asset Life Using Neural Networks." *Journal of Infrastructure Systems*, 13(1), 26-30, doi:10.1061/(ASCE)1076-0342(2007)13:1(26).

Ahammed, M. (1998). "Probabilistic estimation of remaining life of a pipeline in the presence of active corrosion defects." *International Journal of Pressure Vessels and Piping*, 75(4), 321-329, http://dx.doi.org/10.1016/S0308-0161(98)00006-4.

Ahammed, M., and Melchers, R. E. (1995). "Probabilistic analysis of pipelines subjected to pitting corrosion leaks." *Engineering Structures*, 17(2), 74-80, http://dx.doi.org/10.1016/0141-0296(95)92637-N.

Ahammed, M., and Melchers, R. E. (1997). "Probabilistic analysis of underground pipelines subject to combined stresses and corrosion." *Engineering Structures*, 19(12), 988-994, http://dx.doi.org/10.1016/S0141-0296(97)00043-6.

Al-Barqawi, H., and Zayed, T. (2006). "Condition Rating Model for Underground Infrastructure Sustainable Water Mains." *Journal of Performance of Constructed Facilities*, 20(2), 126-135, doi:10.1061/(ASCE)0887-3828(2006)20:2(126).

Andreou, S. A., Marks, D. H., and Clark, R. M. (1987a). "A new methodology for modelling break failure patterns in deteriorating water distribution systems: Applications." *Advances in Water Resources*, 10(1), 11-20, 10.1016/0309-1708(87)90003-0.

Andreou, S. A., Marks, D. H., and Clark, R. M. (1987b). "A new methodology for modelling break failure patterns in deteriorating water distribution systems: Theory." *Advances in Water Resources*, 10(1), 2-10, 10.1016/0309-1708(87)90002-9.

Asnaashari, A., and Shahrour, I. (2007). "Analysis of Water Mains Failure Frequencies: Artificial Neural Networks Versus Poisson Regression, Case Study—Sanandaj-Iran." *Proc., ASME 2007 International Mechanical Engineering Congress and Exposition*, American Society of Mechanical Engineers, 195-202.

Berardi, L., Colombo, A., and Giustolisi, O. (2009a). "Optimal Pipe Replacement Accounting for Leakage Reduction and Isolation Valves." *Water Distribution Systems Analysis 2008*, American Society of Civil Engineers, 1-14.

Berardi, L., Giustolisi, O., and Savic, D. (2009b). "An Operative Approach to Water Distribution System Rehabilitation." *World Environmental and Water Resources Congress 2009*, American Society of Civil Engineers, 1-13.

Bubtiena, A. M., Elshafie, A. H., and Jafaar, O. (2011). "Application of Artificial Neural networks in modeling water networks." *Proc., Signal Processing and its Applications (CSPA), 2011 IEEE 7th International Colloquium on*, 50-57.

Chatfield, C. (2000). *Time-Series Forecasting*., Chapman and Hall/CRC, New York.

Chik, L., Albrecht, D., and Kodikara, J. (2017). "Estimation of the Short-Term Probability of Failure in Water Mains." *Journal of Water Resources Planning and Management*, 143(2), 10.1061/(ASCE)WR.1943-5452.0000730.

Chik, L., Albrecht, D., and Kodikara, J. (2018). "Modeling Failures in Water Mains Using the Minimum Monthly Antecedent Precipitation Index." *Journal of Water Resources Planning and Management,* 144(2)**,** 10.1061/(ASCE)WR.1943-5452.0000926.

Claudio, K., Couallier, V., and Le Gat, Y. (2014). "Integration of time dependent covariates in recurrent events modelling: application to failures on drinking water network." *Journal of the French Statistical Society*, 155(3), 62-77.

Cotching, B. (2011). "Wealth from Water factsheet". [Fact sheet]. Retrieved from dpipwe.tas.gov.au/Documents/Soil-water%20availabe_factsheet.pdf

Dandy, G., and Engelhardt, M. (2001). "Optimal Scheduling of Water Pipe Replacement Using Genetic Algorithms." *Journal of Water Resources Planning and Management*, 127(4), 214-223, doi:10.1061/(ASCE)0733-9496(2001)127:4(214).

Dandy, G., and Engelhardt, M. (2006). "Multi-Objective Trade-Offs between Cost and Reliability in the Replacement of Water Mains." *Journal of Water Resources Planning and Management*, 132(2), 79-88, 10.1061/(ASCE)0733-9496(2006)132:2(79).

Davis, P., Burn, S., and Gould, S. (2008). "Fracture prediction in tough polyethylene pipes using measured craze strength." *Polymer Engineering & Science*, 48(5), 843-852, 10.1002/pen.20982.

Davis, P., Burn, S., Moglia, M., and Gould, S. (2007). "A physical probabilistic model to predict failure rates in buried PVC pipelines." *Reliability Engineering & System Safety*, 92(9), 1258-1266, 10.1016/j.ress.2006.08.001.

Davis, P., De Silva, D., Marlow, D., Moglia, M., Gould, S., and Burn, S. (2008). "Failure prediction and optimal scheduling of replacements in asbestos cement water pipes." *Aqua:Journal of Water Supply*, 57(4), 239-252.

Davis, P., Moglia, M., Burn, S., and Farlie, M. "Estimating failure probability from condition assessment of critical cast iron water mains." *Proc., Proc. 6th National Australasian Society for Trenchless Technology Conf., Melbourne, Australia*.

De Silva, D., Moglia, M., Davis, P., and Burn, S. (2002). "Condition Assessment and Probabilistic Analysis to Estimate Failure Rates in Buried Pipelines." *Proc., Proceedings of ASTT 5th Conference*.

Dridi, L., Mailhot, A., Parizeau, M., and Villeneuve, J. (2005) "A strategy for optimal replacement of water pipes integrating structural and hydraulic indicators based on a statistical water pipe break model." *Proc., Proceedings of the 8th*

International Conference on Computing and Control for the Water Industry, Citeseer, 65-70.

Dridi, L., Mailhot, A., Parizeau, M., and Villeneuve, J. (2009). "Multiobjective Approach for Pipe Replacement Based on Bayesian Inference of Break Model Parameters." *Journal of Water Resources Planning and Management*, 135(5), 344-354, 10.1061/(ASCE)0733-9496(2009)135:5(344).

Dridi, L., Parizeau, M., Mailhot, A., and Villeneuve, J.-P. (2008). "Using Evolutionary Optimization Techniques for Scheduling Water Pipe Renewal Considering a Short Planning Horizon." *Computer-Aided Civil and Infrastructure Engineering*, 23(8), 625-635, 10.1111/j.1467-8667.2008.00564.x.

Duan, D.-M., and Williams, J. G. (1998). "Craze testing for tough polyethylene." *Journal of Materials Science*, 33(3), 625-638, 10.1023/a:1004369107748.

Economou, T., Kapelan, Z., and Bailey, T. (2009). "A Zero-Inflated Bayesian Model for the Prediction of Water Pipe Bursts." *Water Distribution Systems Analysis 2008*, American Society of Civil Engineers, 1-11.

Fawcett, T. (2006), "An introduction to ROC analysis", *Pattern Recognition Letters,* 27, 861-874, doi:10.1016/j.patrec.2005.10.010.

Fahimi, A., Evans, T. S., Farrow, J., Jesson, D. A., Mulheron, M. J., and Smith, P. A. (2016). "On the residual strength of ageing cast iron trunk mains: Physically-based models for asset failure." *Materials Science and Engineering: A*, 663, 204-212, http://dx.doi.org/10.1016/j.msea.2016.03.029.

Fox, J. (2008). *Applied regression analysis and generalized linear models*. Sage, Los Angeles.

Fuchs-Hanusch, D., Friedl, F., Scheucher, R., Kogseder, B. and Muschalla, D. (2013). "Effect of seasonal climatic variance on water main failure frequencies in moderate climate regions". *Water Science and Technology: Water Supply,* 13**,** 435.

Gat, Y. L. (2009). "*Une extension du Processus de Yule pour la modélisation stochastique des événements récurrents - Application aux défaillances de canalisations d'eau sous pression (Extending the Yule Process to model recurrent events: Application to the failures of pressure water mains)*". PhD thesis, Engref-AgroParisTech, Paris, France.

Geem, Z. W., Bae, C., Tseng, C.-L., and Kim, J. (2007). "Trenchless Water Pipe Condition Assessment Using Artificial Neural Network." *Pipelines 2007*, 1-9.

Gelman, A., Carlin, J., Stern, H. and Rubin, D. (2000). *Bayesian Data Analysis,* CRC Press, London.

Gen, M., Cheng, R., and Lin, L. (2010). *Network Models and Optimization: Multiobjective Genetic Algorithm Approach*, Springer London.

Gere, J. M. (2003). *Mechanics of Materials,* Thomson-Engineering, USA.

Giustolisi, O., and Berardi, L. (2009). "Prioritizing Pipe Replacement: From Multiobjective Genetic Algorithms to Operational Decision Support." *Journal* *of Water Resources Planning and Management*, 135(6), 484-492, 10.1061/(ASCE)0733-9496(2009)135:6(484).

Gould, S., Boulaire, F., Burn, S., Zhao, X. L. and Kodikara, J. K. (2011). "Seasonal factors influencing the failure of buried water reticulation pipes". *Water Science and Technology,* 63**,** 2692-2699, doi: 10.2166/wst.2011.507.

Gould, S., Boulaire, F., Marlow, D., and Kodikara, J. (2009). "Understanding how the Australian climate can affect pipe failure." *Proc., OzWater*, QUT ePrints, Australia.

Habibian, A. (1994). "Effect of Temperature Changes on Water-Main Breaks". *Journal of Transportation Engineering,*120**,** 312-321, doi: 10.1061/(ASCE)0733-947X (1994)120:2(312).

Halhal, D., Walters, G., Ouazar, D., and Savic, D. (1997). "Water Network Rehabilitation with Structured Messy Genetic Algorithm." *Journal of Water Resources Planning and Management*, 123(3), 137-146, 10.1061/(ASCE)0733-9496(1997)123:3(137).

Harvey, R., McBean, E., and Gharabaghi, B. (2014). "Predicting the Timing of Water Main Failure Using Artificial Neural Networks." *Journal of Water Resources Planning and Management*, 140(4), 425-434, doi:10.1061/(ASCE)WR.1943-5452.0000354.

Ho, C.-I., Lin, M.-D., and Lo, S.-L. (2010). "Use of a GIS-based hybrid artificial neural network to prioritize the order of pipe replacement in a water distribution network." *Environmental monitoring and assessment*, 166(1-4), 177-189.

Hoeting, J. A., Madigan, D., Raftery, A. E. and Volinsky, C. T. (1999). "Bayesian Model Averageing: A Tutorial". *Statistical Science,* 14**,** 382-401.

Jafar, R., Shahrour, I., and Juran, I. (2010). "Application of Artificial Neural Networks (ANN) to model the failure of urban water mains."*Mathematical and Computer Modelling*, 51(9–10), 1170-1180, http://dx.doi.org/10.1016/j.mcm.2009.12.033.

Ji, J., Zhang, C., Kodikara, J., and Yang, S.-Q. (2015). "Prediction of stress concentration factor of corrosion pits on buried pipes by least squares support vector machine." *Engineering Failure Analysis*, 55(9), 131-138, 10.1016/j.engfailanal.2015.05.010.

Jiang, R., Shannon, B., Deo, R. N., Rathnayaka, S., Hutchinson, C. R., Zhao, X.-L. & Kodikara, J. (2017). "Classification of major cohorts of Australian pressurised cast iron water mains for pipe renewal." Australasian Journal of Water Resources, 21(2), 77-88, doi: 10.1080/13241583.2017.1402979.

Kabir, G., Demissie, G., Sadiq, R. and Tesfamariam, S. (2015a). "Integrating failure prediction models for water mains: Bayesian belief network based data fusion." *Knowledge-Based Systems,* 85(3)**,** 159-169.

Kabir, G., Tesfamariam, S., Francisque, A. and Sadiq, R. (2015b). “Evaluating risk of water mains failure using a Bayesian belief network model.” *European Journal of Operational Research,* 240(1)**,** 220-234.

Kabir, G., Tesfamariam, S., Loeppky, J. and Sadiq, R. (2016). “Predicting water main failures: A Bayesian model updating approach.” *Knowledge-Based Systems,* 110**,** 144-156.

Kabir, G., Tesfamariam, S. and Sadiq, R. (2015c). “Bayesian model averageing for the prediction of water main failure for small to large Canadian municipalities.” *Canadian Journal of Civil Engineering,* 43(3)**,** 233-240.

Kabir, G., Tesfamariam, S. and Sadiq, R. (2015d). “Predicting water main failures using Bayesian model averageing and survival modelling approach.” *Reliability Engineering & System Safety,* 142**,** 498-514.

Kettler, A. J., and Goulter, I. C. (1985). "An analysis of pipe breakage in urban water distribution networks." *Canadian Journal of Civil Engineering*, 12(2), 286-293, 10.1139/l85-030.

Kim, J., and Mays, L. (1994). "Optimal Rehabilitation Model for Water‐Distribution Systems." *Journal of Water Resources Planning and Management*, 120(5), 674-692, 10.1061/(ASCE)0733-9496(1994)120:5(674).

Kimutai, E., Betrie, G., Brander, R., Sadiq, R., and Tesfamariam, S. (2015). "Comparison of Statistical Models for Predicting Pipe Failures: Illustrative Example with the City of Calgary Water Main Failure." *Journal of Pipeline Systems Engineering and Practice*, 6(4), 04015005, 10.1061/(ASCE)PS.1949-1204.0000196.

Kleiner, Y., Adams, B., and Rogers, J. (2001). "Water Distribution Network Renewal Planning." *Journal of Computing in Civil Engineering*, 15(1), 15-26, 10.1061/(ASCE)0887-3801(2001)15:1(15).

Kleiner, Y., Adams, B. J., and Rogers, J. S. (1998). "Selection and scheduling of rehabilitation alternatives for water distribution systems." *Water Resources Research*, 34(8), 2053-2061, 10.1029/98WR01281.

Kleiner, Y., and Rajani, B (2000). "Considering Time dependent Factors in the Statistical Prediction of Water Main Breaks." *Proc., PROC., AMERICAN WATER WORKS ASSOCIATION INFRASTRUCTURE CONFERENCE*, Citeseer.

Kleiner, Y., and Rajani, B. (2001). "Comprehensive review of structural deterioration of water mains: statistical models." *Urban Water*, 3(3), 131-150.

Kleiner, Y., and Rajani, B. (2002). "Forecasting Variations and Trends in Water-Main Breaks." *Journal of Infrastructure Systems*, 8(4), 122-131, 10.1061/(ASCE)1076-0342(2002)8:4(122).

Kleiner, Y., and Rajani, B. (2008). “Prioritising individual water mains for renewal.” *ASCE/EWRI World Environmental and Water Resources Congress*, ASCE, Reston, Va.

Kleiner, Y., and Rajani, B. (2012). "Comparison of four models to rank failure likelihood of individual pipes." *Journal of Hydro-informatics*, 14(3), 659-681, 10.2166 /hydro.2011.029.

Korb, K. B., and Nicholson, A. E. (2010). *Bayesian artificial intelligence*, CRC press, London.

Kutylowska, M. (2015). "Modelling of Failure Rate of Water-pipe Networks." *Periodica Polytechnica. Civil Engineering*, 59(1), 37-43, 10.3311/PPci.7541

Lawless, J. F. (1987). "Regression methods for Poisson process data." *Journal of the American Statistical Association*, 82(399), 808-815.

Li, C. Q., and Mahmoodian, M. (2013). "Risk based service life prediction of underground cast iron pipes subjected to corrosion." *Reliability Engineering & System Safety*, 119, 102-108, http://dx.doi.org/10.1016/j.ress.2013.05.013.

Li, D., and Haimes, Y. Y. (1992). "Optimal maintenance-related decision making for deteriorating water distribution systems: 1. Semi-Markovian Model for a water main." *Water Resources Research*, 28(4), 1053-1061, 10.1029/91WR03035.

Li, F., Ma, L., Sun, Y., and Mathew, J. (2015). "Optimized Group Replacement Scheduling for Water Pipeline Network." *Journal of Water Resources Planning and Management*, 142(1), 04015035, 10.1061/(ASCE)WR.1943-5452.00005 59.

Li, Z., Zhang, B., Wang, Y., Chen, F., Taib, R., Whiffin, V., and Wang, Y. (2014). "Water pipe condition assessment: a hierarchical beta process approach for sparse incident data." *Machine Learning*, 95(1), 11-26.

Lin, P., Zhang, B., Wang, Y., Li, Z., Li, B., Wang, Y., and Chen, F. (2015). "Data-driven Water Pipe Failure Prediction: A Bayesian Nonparametric Approach." *Proceedings of the 24th ACM International on Conference on Information and Knowledge Management*, ACM, Melbourne, Australia, 193-202.

Lindsey, R. K., Kohler, M. A., and Paulhus, J. L. H. (1975). Hydrology for engineers, McGraw-Hill, New York.

Lunn, D.J., Thomas, A., Best, N., and Spiegelhalter, D. (2000), "WinBUGS -- a Bayesian modelling framework: concepts, structure, and extensibility", *Statistics and Computing*, 10:325—337, doi:10.1023/A:1008929526011.

Luong, H., and Nagarur, N. (2005). "Optimal Maintenance Policy and Fund Allocation in Water Distribution Networks." *Journal of Water Resources Planning and Management*, 131(4), 299-306, 10.1061/(ASCE)0733-9496(2005)131:4(299).

Mailhot, A., Pelletier, G., Noël, J.-F., and Villeneuve, J.-P. (2000). "Modeling the evolution of the structural state of water pipe networks with brief recorded pipe break histories: Methodology and application." *Water Resources Research*, 36(10), 3053-3062, 10.1029/2000WR900185.

Mailhot, A., Poulin, A., and Villeneuve, J.-P. (2003). "Optimal replacement of water pipes." Water Resources Research, 39(5), n/a-n/a, 10.1029/2002WR001904.

Malm, A., Ljunggren, O., Bergstedt, O., Pettersson, T. J. R., and Morrison, G. M. (2012). "Replacement predictions for drinking water networks through historical data." *Water Research*, 46(7), 2149-2158, http://dx.doi.org/10.1016/j.watres. 2012.01.036.

Martins, A., Leitão, J., and Amado, C. (2013). "Comparative Study of Three Stochastic Models for Prediction of Pipe Failures in Water Supply Systems." *Journal of Infrastructure Systems*, 19(4), 442-450, doi:10.1061/(ASCE)IS.1943-555X.0000154.

McKenzie, N., Jacquier, D., Ashton, L., Cresswell, H. (2000). “Estimation of soil properties using the atlas of Australian soils”. Tech. rep., CSIRO land and water technical report 11/00.

McKenzie, N.J., Hook, J. (1992). “Interpretations of the atlas of australian soils”. Consulting report to the environmental resources information network (erin). Tech. rep., CSIRO division of soils technical report.

Mitchell, T. M. (1997). *Machine Learning*, McGraw-Hill, Inc. Portland, Oregon, USA,

Moglia, M., Davis, P., and Burn, S. (2008). "Strong exploration of a cast iron pipe failure model." *Reliability Engineering & System Safety*, 93(6), 885-896, 10.1016/j.ress .2007.03.033.

Mooney, C. Z. (1997). *Quantitative Applications in the Social Sciences: Monte Carlo simulation*,Thousand Oaks, CA: SAGE Publications Ltd doi: 10.4135/9781412985116

Nafi, A., and Kleiner, Y. (2009). "Scheduling Renewal of Water Pipes While Considering Adjacency of Infrastructure Works and Economies of Scale." *Journal of Water Resources Planning and Management*, 136(5), 519-530, 10.1061/(ASCE)WR.1 943-5452.0000062.

Nishiyama, M., and Filion, Y. (2014). "Forecasting breaks in cast iron water mains in the city of Kingston with an artificial neural network model." *Canadian Journal of Civil Engineering*, 41(10), 918-923, 10.1139/cjce-2014-0114.

Park, S. (2011). "Estimating the timing of the economical replacement of water mains based on the predicted pipe break times using the proportional hazards models." *Water Resources Management*, 25(10), 2509-2524.

Park, S., Jun, H., Agbenowosi, N., Kim, B. J., and Lim, K. (2011). "The proportional hazards modeling of water main failure data incorporating the time dependent effects of covariates." *Water Resources Management*, 25(1), 1-19.

Peterson, R., Melchers, R. (2012). “Long-term corrosion of cast iron cement lined pipes”, *Annual Conference of the Australasian Corrosion Association*, Melbourne, Australia, 146-157.

Petersen, R., Dafter, M. and Melchers, R., (2013). “Long-term corrosion of buried cast iron water mains: field data collection and model calibration.” Water Asset Management International, 9, 13-17.

Petersen, R., Melchers R., (2014). “Long-term corrosion of buried cast iron pipes in native soil”. *In Proc. ACA Conference,* Darwin*,* Paper 028*.*

Rajani, B., and Abdel-Akher, A. (2012). "Re-assessment of resistance of cast iron pipes subjected to vertical loads and internal pressure." *Engineering Structures*, 45, 192-212, http://dx.doi.org/10.1016/j.engstruct.2012.06.019.

Rajani, B., Kleiner, Y., and Sink, J.-E. (2012). "Exploration of the relationship between water main breaks and temperature covariates." *Urban Water Journal*, 9(2), 67-84, 10.1080/1573062X.2011.630093.

Rajani, B. and Makar, J. (2000). "A methodology to estimate remaining service life of grey cast iron water mains." *Canadian Journal of Civil Engineering*, 27(6), 1259-1272, 10.1139/l00-073.

Rajani, B. and Makar, J., McDonald, S., Zhan, C., Kuraoka, S., Jen, C.-K., Veins, M. (2000). “Investigation of grey cast iron water mains to develop a methodology for estimating service life”, *American Water Works Association Research Foundation*, Denver, CO, USA.

Rajani, B., and Tesfamariam, S. (2004). "Uncoupled axial, flexural, and circumferential pipe–soil interaction analyses of partially supported jointed water mains." *Canadian Geotechnical Journal*, 41(6), 997-1010, 10.1139/t04-048.

Rajani, B.B. and Tesfamariam, S. (2007). “Estimating time to failure of ageing cast iron water mains under uncertainties.” *ICE Water Management Journal*, 160(2), 83-88

Rathnayaka, S., Keller, R., Kodikara, J. and Chik, L. (2016a). "Numerical Simulation of Pressure Transients in Water Supply Networks as Applicable to Critical Water Pipe Asset Management". *Journal of Water Resources Planning and Management,* 142**,** 04016006, doi: 10.1061/(ASCE)WR.1943-5452.0000636.

Rathnayaka, S., Shannon, B., Rajeev, P. and Kodikara, J. (2016b). "Monitoring of Pressure Transients in Water Supply Networks". *Water Resources Management,* 30**,** 471-485, doi: 10.1007/s11269-015-1172-y.

Robert, D. J., Rajeev, P., Kodikara, J., and Rajani, B. (2016). "Equation to predict maximum pipe stress incorporating internal and external loadings on buried pipes." *Canadian Geotechnical Journal*, 53(8), 1315-1331, 10.1139/cgj-2015-0500.

Rokstad, M. M., and Ugarelli, R. M. (2015). "Minimising the total cost of renewal and risk of water infrastructure assets by grouping renewal interventions." *Reliability Engineering and System Safety*, 142, 148-160, http://dx.doi.org/10.10 16/j.ress.2015.05.014.

Roshani, E., and Filion, Y. (2013). "Event-Based Approach to Optimize the Timing of Water Main Rehabilitation with Asset Management Strategies." *Journal of Water Resources Planning and Management*, 140(6), 04014004, 10.1061/(ASCE)WR.1943-5452.0000392.

Ross, S. M. (1996). *Stochastic processes*, Wiley, USA.

Ross, S. M. (2010). *A First Course in Probability*, Pearson Prentice Hall, New Jersey.

Røstum, J. (2000). "Statistical modelling of pipe failures in water networks." doctoral thesis, Norwegian University of Science and Technology, Trondheim, Norway.

Sadiq, R., Rajani, B., and Kleiner, Y. (2004). "Probabilistic risk analysis of corrosion associated failures in cast iron water mains." *Reliability Engineering and System Safety*, 86(1), 1-10, http://dx.doi.org/10.1016/j.ress.2003.12.007.

Saxton K. E. and Rawls W. J. (2006). "Soil Water Characteristic Estimates by Texture and Organic Matter for Hydrologic Solutions." *Soil Science Society American Journal*, 70, 1569–1578. Soil & Water Management & Conservation, Soil Physics, doi:10.2136/sssaj2005.0117.

Scheidegger, A., Scholten, L., Maurer, M., and Reichert, P. (2013). "Extension of pipe failure models to consider the absence of data from replaced pipes." *Water Research*, 47(11), 3696-3705, http://dx.doi.org/10.1016/j.watres.2013.04.0 17.

Schlick, W. J. (1940). *Supporting strengths of cast-iron pipe for water and gas service*. Ames, Ia, Iowa State College of Agriculture and Mechanic Arts.

Scholten, L., Scheidegger, A., Reichert, P., Mauer, M., and Lienert, J. (2014). "Strategic rehabilitation planning of piped water networks using multi-criteria decision analysis." *Water Research*, 49, 124-143, 10.1016/j.watres.2013.11.017.

Seica, M., and Packer, J. (2006). "Simplified Numerical Method to Evaluate the Mechanical Strength of Cast Iron Water Pipes." *Journal of Infrastructure Systems*, 12(1), 60-67, 10.1061/(ASCE)1076-0342(2006)12:1(60).

Shamir, U., and Howard, C. D. (1978). "An analytic approach to scheduling pipe replacement." *Journal of the American Water Works Association*, 71(5), 248-258.

Shin, H., Joo, C., and Koo, J. (2016). "Optimal Rehabilitation Model for Water Pipeline Systems with Genetic Algorithm." *Procedia Engineering*, 154, 384-390, http://dx.doi.org/10.1016/j.proeng.2016.07.497.

Singh, A. (2011). "Bayesian analysis for causes of failure at a water utility." *Built Environment Project and Asset Management*, 1(2), 195-210, 10.1108/2044124 1111180433.

Tesfamariam, S., Rajani, B., and Sadiq, R. (2006). "Possibilistic approach for consideration of uncertainties to estimate structural capacity of ageing cast iron water mains." *Canadian Journal of Civil Engineering*, 33(8), 1050-1064, 10.1139/l06-042.

Thibaux, R., and Jordan, M. I. (2006). "Hierarchical beta processes and the Indian buffet process." *Proc., International conference on artificial intelligence and statistics*, 564-571.

Thibaux, R. (2008). "Nonparametric bayesian models for machine learning". doctoral thesis, University of California, Berkeley.

Walski, T. M., and Pelliccia, A. (1982). "Economic analysis of water main breaks." *Journal of the American Water Works Association*, 74(3), 140-147.

Wang, C.-w., Niu, Z.-g., Jia, H., and Zhang, H.-w. (2010). "An assessment model of water pipe condition using Bayesian inference." *Journal of Zhejiang University-SCIENCE A*, 11(7), 495-504, 10.1631/jzus.A0900628.

Wang, Y., Zayed, T., and Moselhi, O. (2009). "Prediction Models for Annual Break Rates of Water Mains." *Journal of Performance of Constructed Facilities*, 23(1), 47-54, 10.1061/(ASCE)0887-3828(2009)23:1(47).

Weerasinghe, D. (2018). “A Failure Analysis of Small Diameter Cast Iron Pipes in Reactive Soil Zones of Melbourne.”, doctoral thesis,Monash University, Melbourne, Australia. In preparation.

Yang, S., and De Angelis, D. (2013). "Maximum Likelihood." *Computational Toxicology: Volume II*, B. Reisfeld, and A. N. Mayeno, eds., Humana Press, Totowa, NJ, 581-595.

APPENDIX A

Table A - 1: Expected number of failures for high pressure water mains in 2013.

Total number of failures in a pipe up to 2012	Total number of pipes in the group	Total number of failures in 2013	NHPP	HBP	BSM
0	898	4	17.41	3.23	8.42
1	141	3	6.81	8.80	4.41
2	52	2	3.13	6.31	3.36
3	25	5	1.70	4.50	1.58
4	8	3	0.84	1.91	1.23
5	2	2	0.30	0.59	0.67
6	3	1	0.48	1.07	0.83
7	1	0	0.06	0.42	0.25
Total	1130	20	30.73	26.82	20.74

Table A - 2: Expected number of failures for medium pressure water mains in 2013.

Total number of failures in a pipe up to 2012	Total number of pipes in the group	Total number of failures in 2013	NHPP	HBP	BSM
0	2922	26	47.09	8.56	20.35
1	377	16	16.01	23.29	14.05
2	125	9	6.64	15.09	10.10
3	54	10	4.50	9.69	7.92
4	21	2	2.11	5.01	3.96
5	6	1	0.44	1.78	1.52
6	4	2	0.52	1.42	1.55
7	3	0	0.43	1.24	1.08
Total	3512	66	77.74	66.08	60.54

Table A - 3: Expected number of failures for low pressure water mains in 2013.

Total number of failures in a pipe up to 2012	Total number of pipes in the group	Total number of failures in 2013	NHPP	HBP	BSM
0	678	8	9.85	1.82	3.48
1	73	4	2.93	4.49	4.22
2	32	2	1.76	3.85	2.50
3	14	3	0.88	2.50	1.45
4	2	0	0.08	0.48	0.36
5	1	0	0.03	0.30	0.50
6	1	0	0.08	0.36	0.50
Total	801	17	15.62	13.8	13

APPENDIX B

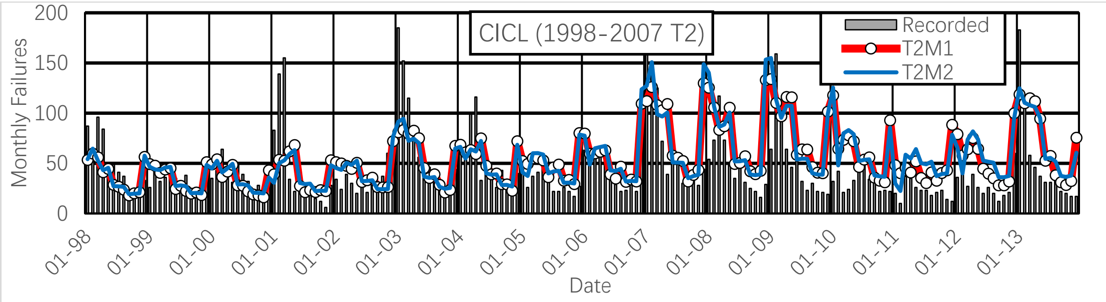

Figure B - 1: CICL dataset T2 monthly failures.

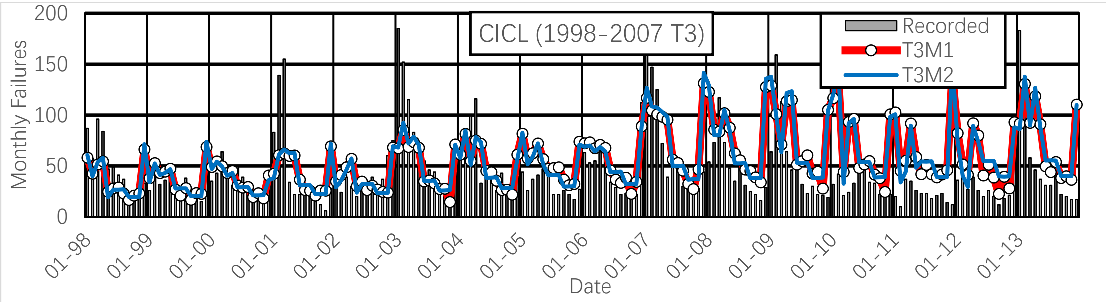

Figure B - 2: CICL dataset T3 monthly failures.

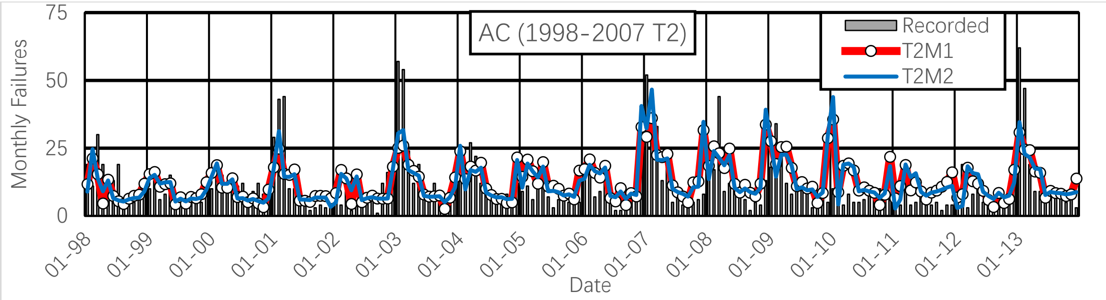

Figure B - 3: AC dataset T2 monthly failures.

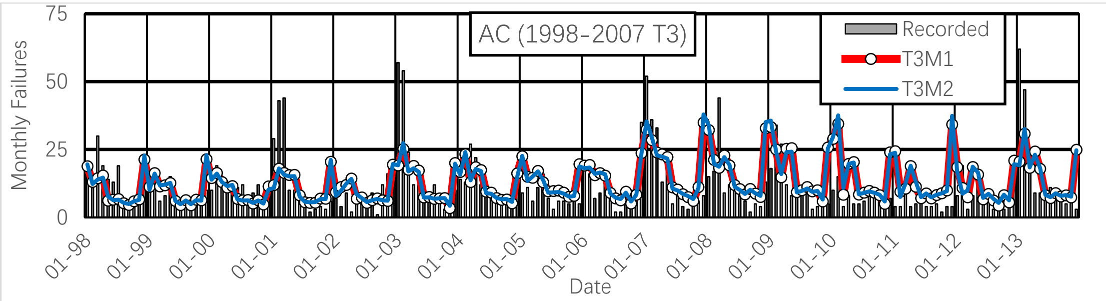

Figure B - 4: AC dataset T3 monthly failures.

APPENDIX C

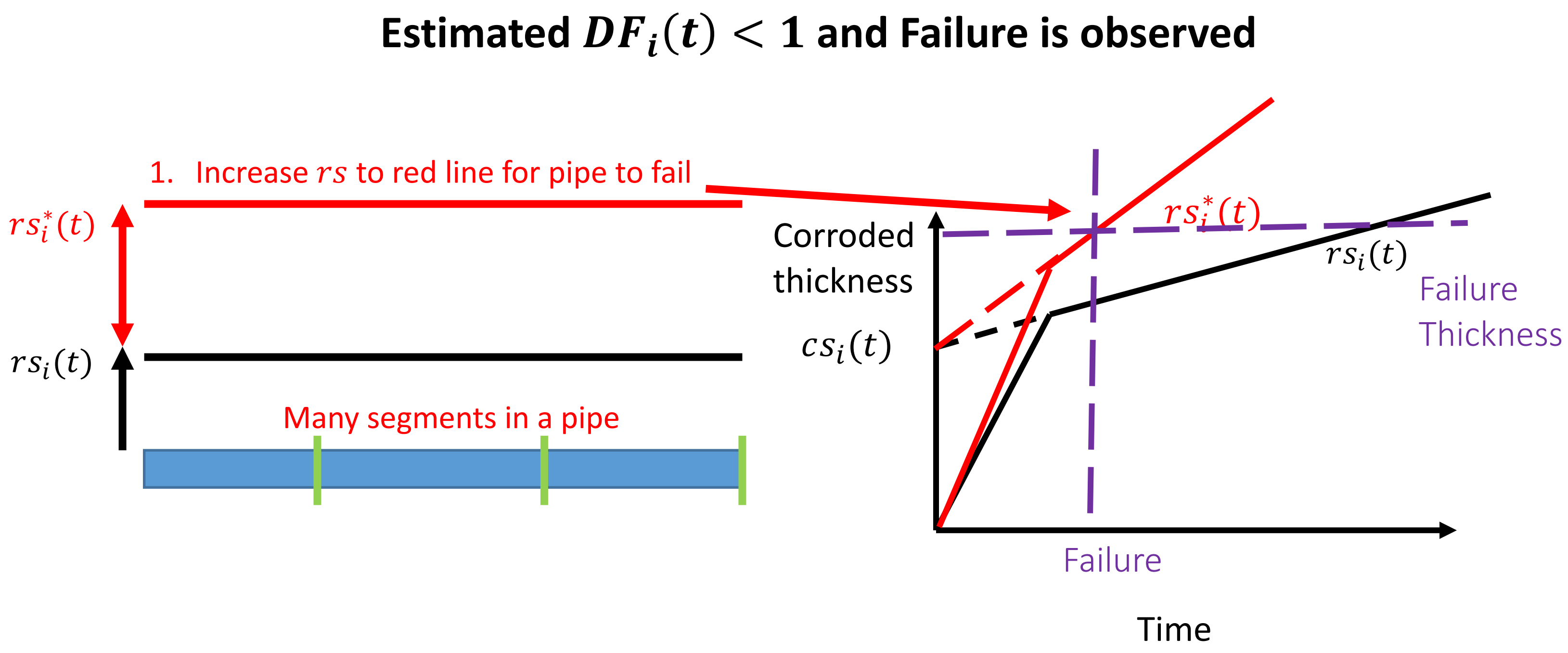

Figure C - 1: Updating corrosion parameters for $DF_i(t) < 1$ and Failure is observed for MPP-P1 model.

Estimated $DF_i(t) \geq 1$ and Failure is observed

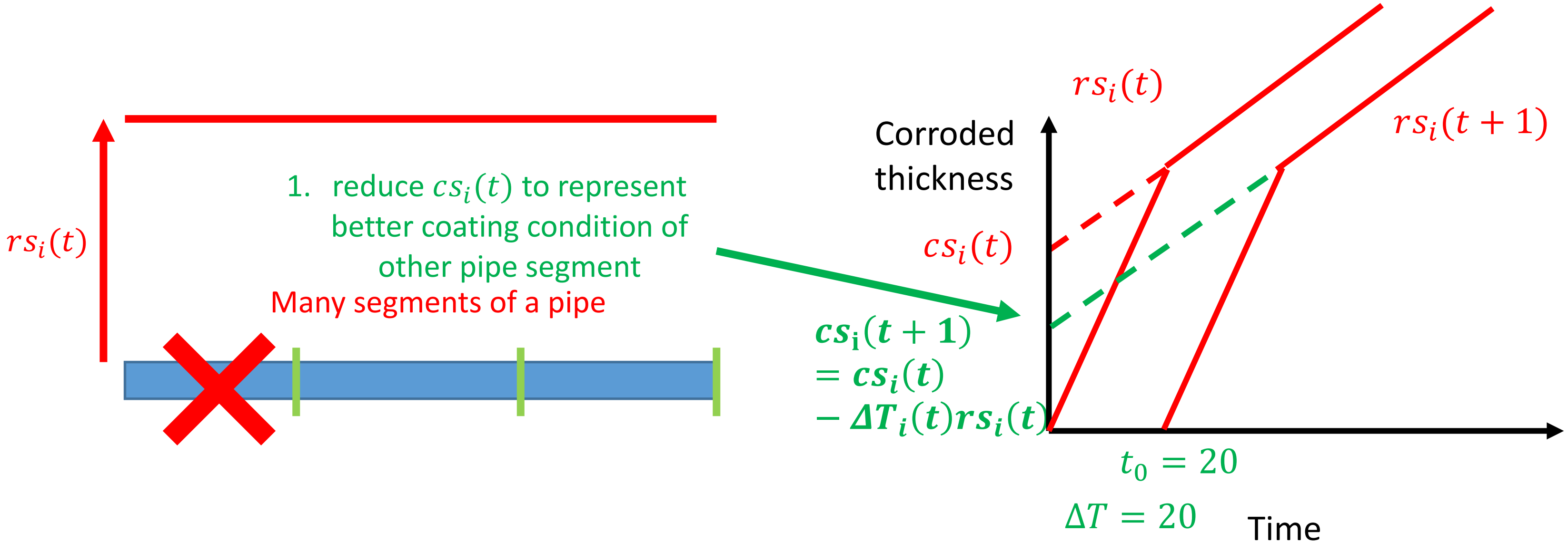

Figure C - 2: Updating corrosion parameters for $DF_i(t) \geq 1$ and Failure is observed for MPP-P1 model.

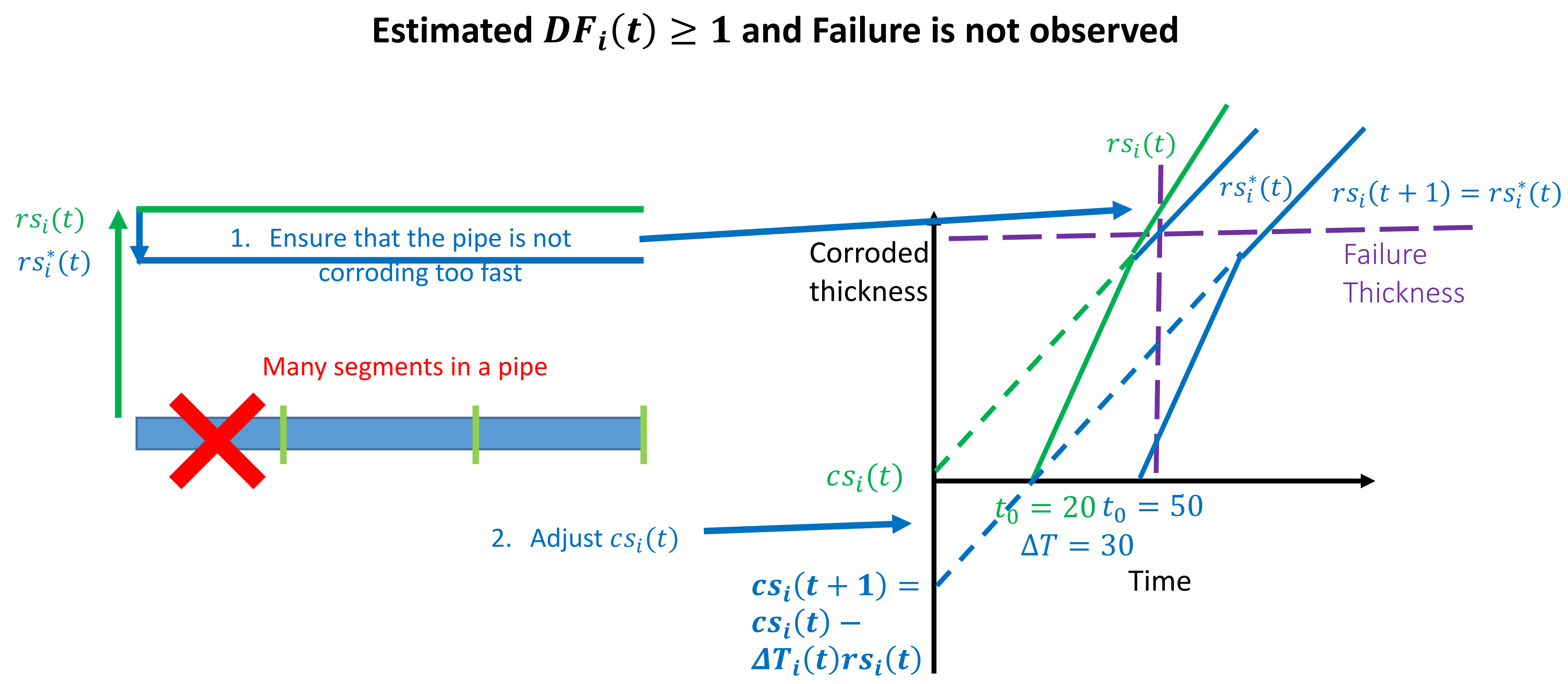

Figure C - 3: Updating corrosion parameters for $DF_i(t) \geq 1$ and Failure is not observed for MPP-P1 model.

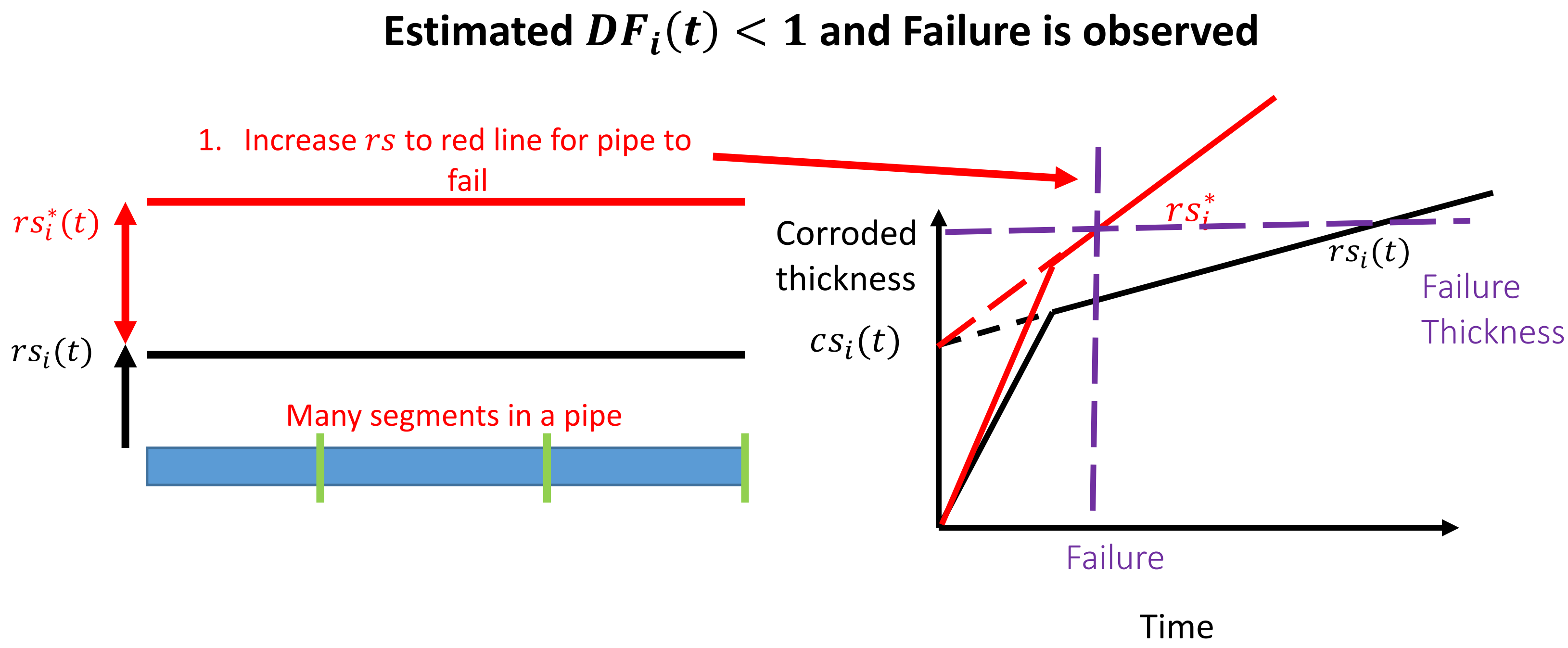

Figure C - 4: Updating corrosion parameters for $DF_i(t) < 1$ and Failure is observed for MPP-P2 model.

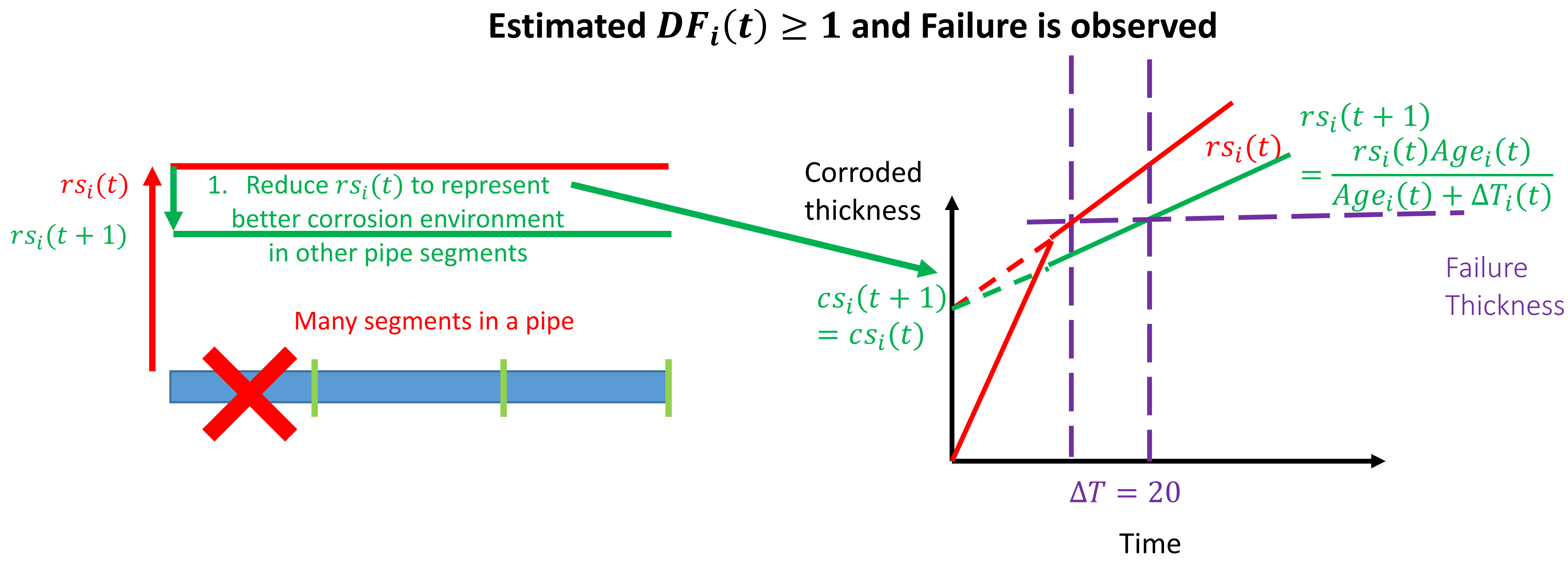

Figure C - 5: Updating corrosion parameters for $DF_i(t) \geq 1$ and Failure is observed for MPP-P2 model.

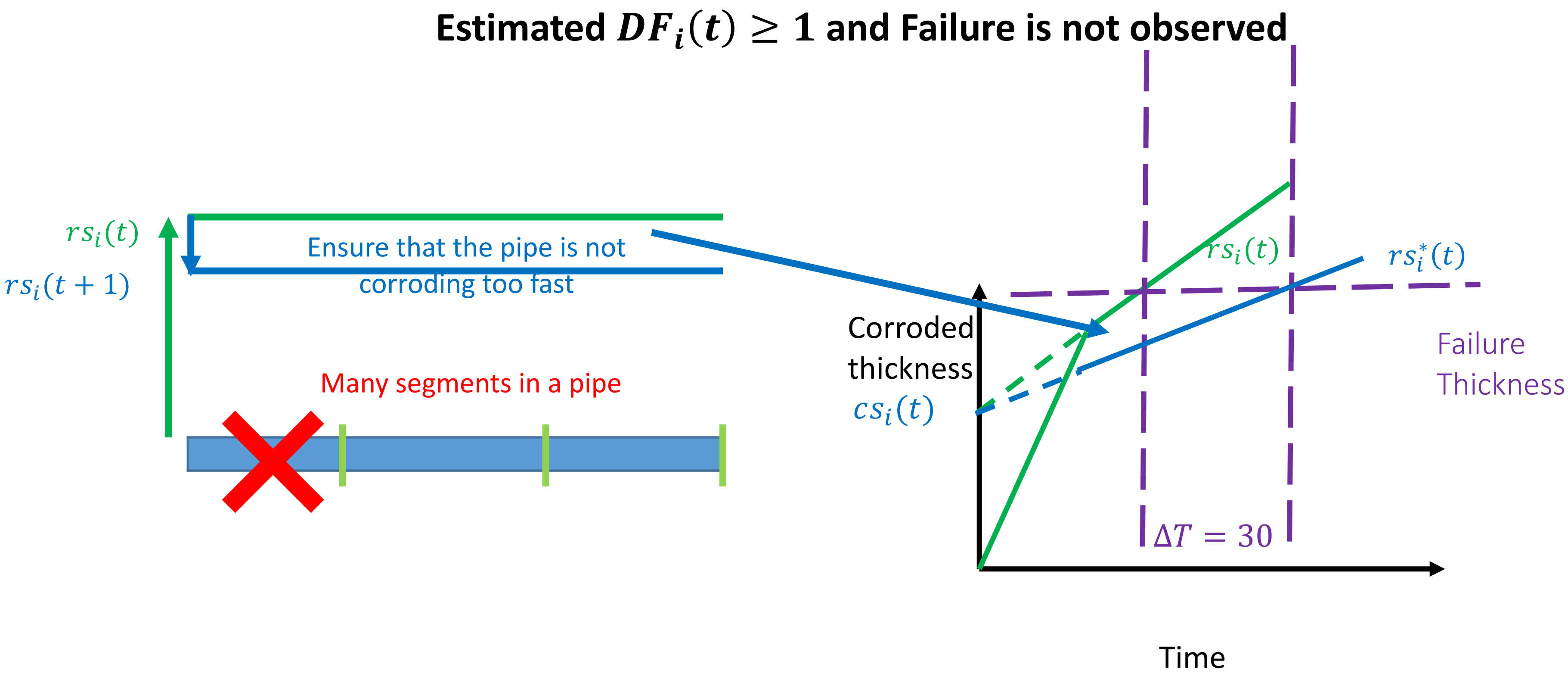

Figure C - 6: Updating corrosion parameters for $DF_i(t) \geq 1$ and Failure is not observed for MPP-P2 model.

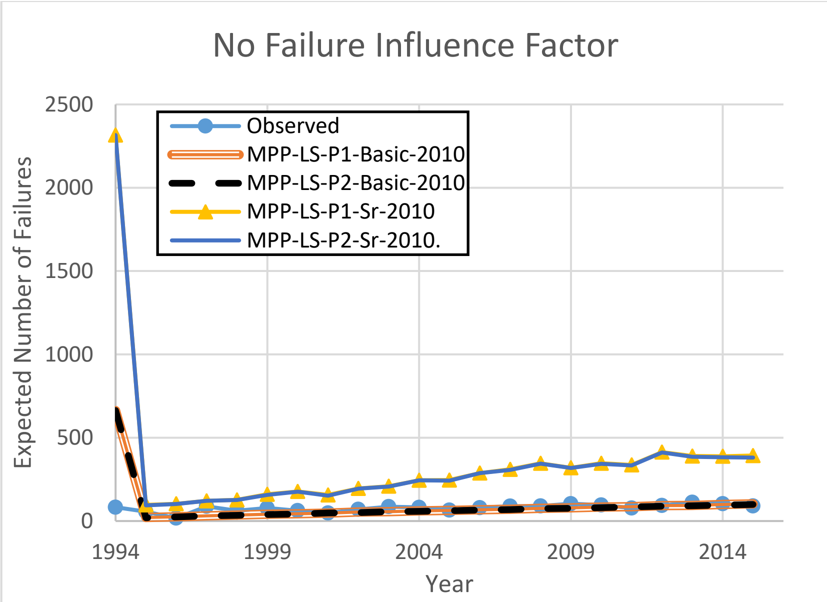

Figure C - 7: Expected number of failures estimated by the MPP model using failure data up to 2010.

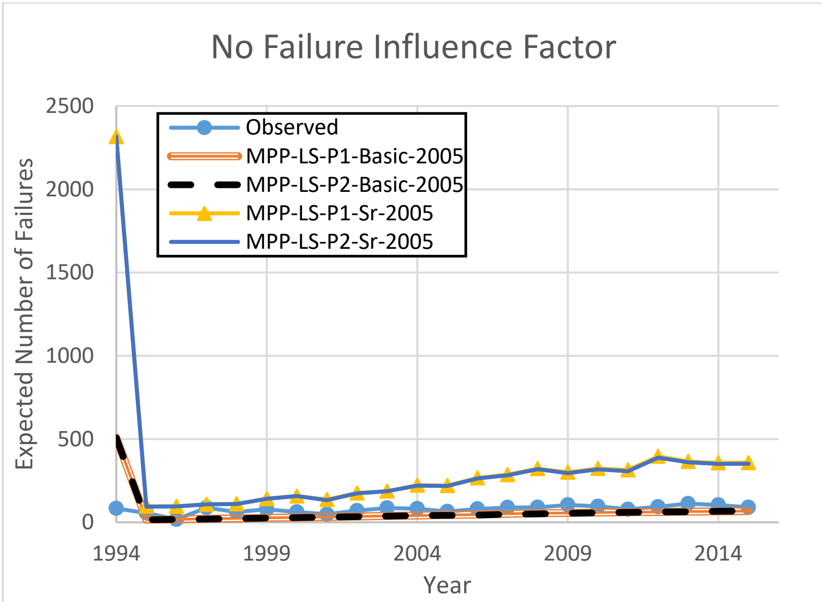

Figure C - 8: Expected number of failures estimated by the MPP model using failure data up to 2005.

Table C - 1: RMSE for MPP models (longitudinal failures) with a range of decay factors and radius of influence.

a	MPP-LS-P1-Basic								MPP-LS-P2-Basic							
	TrainYr=2010				TrainYr=2005				TrainYr=2010				TrainYr=2005			
	R500	R200	R100	R50	R500	R200	R100	R50	R500	R200	R100	R50	R500	R200	R100	R50
0.1	23.8	23.6	23.2	18.3	21.7	21.8	22.4	27.0	21.7	21.4	21.1	17.5	24.6	24.6	25.3	29.7
0.2	18.7	18.5	18.6	18.8	32.3	32.3	32.3	32.8	19.5	19.2	19.5	19.7	34.2	34.2	34.2	34.7
0.3	20.0	20.4	20.4	20.4	35.1	35.1	35.1	35.2	21.0	21.5	21.6	21.6	36.7	36.7	36.7	36.7
0.4	20.9	21.0	21.0	21.0	36.0	36.0	36.0	36.0	22.0	22.2	21.9	22.0	37.7	37.7	37.7	37.7
0.5	21.2	21.5	21.3	21.3	36.6	36.6	36.6	36.6	22.4	22.6	22.4	22.4	37.8	37.8	37.8	37.8
0.6	21.8	21.8	21.7	21.7	37.1	37.1	37.1	37.1	23.0	23.0	22.8	22.9	38.5	38.5	38.5	38.5
0.7	21.8	21.8	21.8	21.8	37.1	37.1	37.1	37.1	23.0	23.0	23.0	22.9	38.6	38.6	38.6	38.6
0.8	21.9	22.0	21.8	21.8	37.2	37.2	37.2	37.2	23.0	23.2	23.2	23.1	38.8	38.8	38.8	38.8
0.9	21.9	21.7	21.8	21.8	37.2	37.2	37.2	37.2	23.1	22.9	22.9	23.0	38.4	38.4	38.4	38.4
1	22.0	22.0	21.8	21.8	37.5	37.5	37.5	37.5	23.3	23.2	23.1	23.1	38.7	38.8	38.8	38.8
1.1	22.3	21.9	22.0	22.0	37.6	37.6	37.6	37.6	23.5	23.1	23.3	23.2	38.9	38.9	38.9	38.9
1.2	22.2	22.2	22.2	22.2	37.6	37.6	37.6	37.6	23.4	23.4	23.4	23.4	38.8	38.8	38.8	38.8
1.3	22.2	22.2	22.4	22.4	37.5	37.5	37.5	37.5	23.4	23.4	23.5	23.7	38.8	38.9	38.9	38.9
1.4	22.4	22.2	22.2	22.2	37.7	37.7	37.7	37.7	23.6	23.3	23.5	23.5	38.9	38.8	38.8	38.8
1.5	22.3	22.3	22.1	22.1	37.8	37.8	37.8	37.8	23.6	23.4	23.5	23.4	38.9	38.8	38.8	38.8
1.6	22.3	22.1	22.2	22.2	37.5	37.5	37.5	37.5	23.5	23.3	23.3	23.4	38.8	38.8	38.8	38.8
1.7	22.4	22.6	22.2	22.2	37.6	37.6	37.6	37.6	23.7	23.8	23.4	23.5	39.1	39.0	39.0	39.0
1.8	22.2	22.3	22.2	22.2	37.4	37.4	37.4	37.4	23.3	23.5	23.7	23.4	39.2	39.1	39.1	39.1
1.9	22.3	22.3	22.3	22.3	37.6	37.6	37.6	37.6	23.4	23.6	23.6	23.6	39.2	39.2	39.2	39.2
2	22.1	22.4	22.4	22.4	37.7	37.7	37.7	37.7	23.5	23.5	23.5	23.7	38.9	39.2	39.2	39.2

Table C - 2: MAE for MPP models (longitudinal failures) with a range of decay factors and radius of influence.

a	MPP-LS-P1-Basic								MPP-LS-P2-Basic							
	TrainYr=2010				TrainYr=2005				TrainYr=2010				TrainYr=2005			
	R500	R200	R100	R50	R500	R200	R100	R50	R500	R200	R100	R50	R500	R200	R100	R50
0.1	19.5	19.2	18.5	13.5	17.2	17.2	18.0	23.2	17.0	16.9	16.2	12.7	20.0	19.9	20.8	26.0
0.2	14.6	14.6	14.6	14.7	29.6	29.6	29.6	30.1	15.5	15.2	15.6	15.7	31.4	31.4	31.4	32.0
0.3	16.1	16.4	16.2	16.2	32.4	32.4	32.4	32.4	17.1	17.5	17.4	17.4	34.1	34.1	34.1	34.2
0.4	16.8	16.6	16.8	16.8	33.5	33.5	33.5	33.5	17.9	18.2	17.7	17.8	35.2	35.2	35.2	35.2
0.5	17.0	17.3	17.0	17.0	33.9	33.9	33.9	33.9	18.3	18.4	18.3	18.2	35.3	35.3	35.3	35.3
0.6	17.5	17.6	17.5	17.5	34.4	34.4	34.4	34.4	18.9	19.0	18.6	18.9	36.0	36.0	36.0	36.0
0.7	17.7	17.8	17.3	17.3	34.5	34.5	34.5	34.5	19.0	19.1	18.8	18.6	36.0	36.0	36.0	36.0
0.8	17.6	17.7	17.6	17.6	34.5	34.5	34.5	34.5	18.8	19.0	18.9	18.9	36.1	36.2	36.2	36.2
0.9	17.6	17.4	17.5	17.5	34.5	34.5	34.5	34.5	19.0	18.7	18.8	18.9	35.8	35.7	35.7	35.7
1	17.4	17.6	17.6	17.6	34.9	34.9	34.9	34.9	19.1	19.0	19.0	19.1	36.1	36.2	36.2	36.2
1.1	18.1	17.8	17.8	17.8	34.9	34.9	34.9	34.9	19.4	19.0	19.2	19.0	36.2	36.2	36.2	36.2
1.2	17.8	17.9	18.0	18.0	34.8	34.8	34.8	34.8	19.3	19.4	19.2	19.2	36.2	36.2	36.2	36.2
1.3	18.0	18.0	18.1	18.1	34.9	34.9	34.9	34.9	19.3	19.4	19.4	19.6	36.2	36.3	36.3	36.3
1.4	18.1	17.9	17.8	17.8	35.0	35.0	35.0	35.0	19.4	19.1	19.4	19.3	36.4	36.3	36.3	36.3
1.5	18.1	17.9	17.9	17.9	35.1	35.1	35.1	35.1	19.4	19.1	19.2	19.2	36.3	36.3	36.3	36.3
1.6	17.8	17.6	17.8	17.8	34.8	34.8	34.8	34.8	19.1	19.0	19.2	19.3	36.2	36.2	36.2	36.2
1.7	18.1	18.3	17.8	17.8	34.9	34.9	34.9	34.9	19.6	19.5	19.3	19.3	36.5	36.4	36.4	36.4
1.8	17.7	18.0	17.7	17.7	34.6	34.6	34.6	34.6	19.0	19.3	19.5	19.1	36.5	36.4	36.4	36.4
1.9	17.9	18.1	18.0	18.0	34.9	34.9	34.9	34.9	19.2	19.5	19.4	19.4	36.6	36.5	36.5	36.5
2	17.6	18.0	18.1	18.1	34.9	34.9	34.9	34.9	19.2	19.4	19.5	19.6	36.3	36.5	36.5	36.5

Table C - 3: Area under first 20% length of prediction curve for MPP-LS-P1-Basic-2010-R50 (longitudinal failures).

a	Year																				
	1995	**1996**	**1997**	**1998**	**1999**	**2000**	**2001**	**2002**	**2003**	**2004**	**2005**	**2006**	**2007**	**2008**	**2009**	**2010**	**2011**	**2012**	**2013**	**2014**	**2015**
0.1	0.045	0.049	0.034	0.029	0.039	0.032	0.036	0.027	0.031	0.028	0.042	0.047	0.034	0.051	0.042	0.044	0.044	0.047	0.042	0.048	0.039
0.2	0.044	0.050	0.033	0.031	0.043	0.034	0.034	0.027	0.029	0.028	0.042	0.045	0.035	0.047	0.044	0.048	0.041	0.044	0.039	0.050	0.037
0.3	0.046	0.048	0.032	0.030	0.040	0.032	0.034	0.027	0.030	0.028	0.042	0.046	0.035	0.048	0.044	0.047	0.044	0.045	0.039	0.052	0.038
0.4	0.043	0.046	0.033	0.028	0.041	0.030	0.033	0.028	0.029	0.029	0.039	0.046	0.036	0.047	0.044	0.047	0.043	0.047	0.041	0.048	0.039
0.5	0.045	0.047	0.034	0.027	0.039	0.026	0.035	0.026	0.031	0.027	0.041	0.046	0.036	0.045	0.043	0.047	0.044	0.045	0.040	0.049	0.039
0.6	0.045	0.047	0.032	0.029	0.039	0.026	0.036	0.030	0.030	0.028	0.042	0.046	0.034	0.047	0.043	0.048	0.042	0.046	0.040	0.051	0.041
0.7	0.047	0.046	0.032	0.030	0.042	0.030	0.033	0.026	0.026	0.027	0.040	0.047	0.036	0.045	0.045	0.047	0.043	0.045	0.040	0.051	0.038
0.8	0.046	0.040	0.034	0.032	0.041	0.029	0.037	0.026	0.025	0.029	0.041	0.049	0.035	0.047	0.044	0.047	0.044	0.045	0.040	0.049	0.042
0.9	0.047	0.053	0.033	0.028	0.042	0.030	0.035	0.029	0.027	0.028	0.037	0.044	0.035	0.046	0.041	0.047	0.044	0.047	0.040	0.050	0.038
1	0.044	0.050	0.034	0.031	0.041	0.032	0.034	0.027	0.027	0.028	0.040	0.044	0.033	0.046	0.043	0.047	0.043	0.045	0.041	0.050	0.036
1.1	0.044	0.043	0.033	0.031	0.042	0.033	0.039	0.029	0.030	0.029	0.033	0.044	0.033	0.047	0.043	0.048	0.043	0.043	0.041	0.050	0.036
1.2	0.046	0.049	0.034	0.029	0.041	0.031	0.036	0.029	0.027	0.028	0.042	0.046	0.033	0.050	0.044	0.045	0.041	0.044	0.039	0.049	0.039
1.3	0.046	0.044	0.033	0.028	0.042	0.034	0.034	0.027	0.028	0.029	0.040	0.044	0.033	0.050	0.046	0.048	0.043	0.044	0.041	0.050	0.040
1.4	0.045	0.045	0.033	0.031	0.040	0.034	0.039	0.029	0.028	0.028	0.039	0.048	0.033	0.048	0.044	0.048	0.045	0.044	0.040	0.051	0.038
1.5	0.046	0.043	0.034	0.027	0.041	0.031	0.033	0.025	0.029	0.027	0.039	0.045	0.034	0.047	0.045	0.048	0.042	0.046	0.040	0.047	0.039
1.6	0.044	0.049	0.033	0.028	0.045	0.028	0.035	0.026	0.030	0.026	0.040	0.044	0.036	0.045	0.043	0.047	0.043	0.046	0.042	0.050	0.041
1.7	0.044	0.051	0.036	0.031	0.041	0.029	0.034	0.029	0.032	0.029	0.039	0.048	0.034	0.044	0.044	0.049	0.044	0.045	0.041	0.049	0.038
1.8	0.043	0.046	0.033	0.028	0.041	0.027	0.035	0.029	0.029	0.026	0.038	0.047	0.034	0.049	0.045	0.049	0.042	0.044	0.041	0.050	0.040
1.9	0.046	0.050	0.035	0.033	0.042	0.033	0.036	0.025	0.029	0.027	0.037	0.044	0.033	0.049	0.042	0.050	0.042	0.045	0.040	0.049	0.038
2	0.046	0.046	0.031	0.030	0.041	0.028	0.036	0.029	0.028	0.028	0.039	0.046	0.034	0.045	0.044	0.048	0.044	0.045	0.039	0.051	0.038

Table C - 4: Area under first 20% length of prediction curve for MPP-LS-P2-Basic-2010-R50 (longitudinal failures).

a	Year																				
	1995	**1996**	**1997**	**1998**	**1999**	**2000**	**2001**	**2002**	**2003**	**2004**	**2005**	**2006**	**2007**	**2008**	**2009**	**2010**	**2011**	**2012**	**2013**	**2014**	**2015**
0.1	0.045	0.051	0.034	0.029	0.042	0.035	0.037	0.029	0.032	0.030	0.049	0.051	0.036	0.053	0.044	0.052	0.052	0.054	0.044	0.050	0.040
0.2	0.043	0.048	0.033	0.031	0.046	0.037	0.038	0.029	0.030	0.030	0.051	0.049	0.039	0.050	0.045	0.054	0.049	0.053	0.043	0.052	0.039
0.3	0.045	0.056	0.032	0.030	0.044	0.034	0.035	0.029	0.030	0.030	0.050	0.049	0.037	0.050	0.045	0.053	0.052	0.053	0.042	0.052	0.040
0.4	0.042	0.048	0.033	0.028	0.044	0.033	0.036	0.031	0.031	0.031	0.049	0.050	0.037	0.050	0.045	0.054	0.050	0.053	0.044	0.051	0.042
0.5	0.043	0.050	0.034	0.028	0.041	0.029	0.037	0.028	0.032	0.029	0.049	0.050	0.037	0.048	0.045	0.054	0.052	0.053	0.043	0.051	0.041
0.6	0.044	0.047	0.031	0.030	0.041	0.031	0.037	0.031	0.031	0.030	0.049	0.050	0.037	0.050	0.044	0.054	0.050	0.054	0.044	0.052	0.041
0.7	0.046	0.051	0.032	0.030	0.044	0.031	0.036	0.029	0.028	0.030	0.048	0.051	0.038	0.048	0.046	0.053	0.050	0.052	0.044	0.052	0.039
0.8	0.045	0.048	0.033	0.032	0.042	0.032	0.038	0.028	0.028	0.031	0.047	0.052	0.037	0.048	0.046	0.054	0.051	0.054	0.043	0.051	0.043
0.9	0.046	0.058	0.033	0.030	0.044	0.032	0.037	0.030	0.030	0.030	0.048	0.048	0.037	0.049	0.044	0.054	0.051	0.054	0.045	0.052	0.041
1	0.043	0.053	0.034	0.032	0.043	0.035	0.036	0.030	0.030	0.030	0.047	0.049	0.036	0.049	0.045	0.054	0.051	0.053	0.044	0.052	0.038
1.1	0.043	0.046	0.032	0.032	0.044	0.035	0.040	0.031	0.031	0.030	0.045	0.049	0.035	0.049	0.044	0.055	0.051	0.052	0.044	0.052	0.039
1.2	0.046	0.053	0.033	0.030	0.043	0.033	0.038	0.032	0.030	0.030	0.048	0.050	0.035	0.051	0.045	0.053	0.050	0.053	0.043	0.051	0.041
1.3	0.046	0.047	0.033	0.029	0.044	0.034	0.037	0.029	0.029	0.030	0.048	0.048	0.035	0.051	0.047	0.054	0.051	0.053	0.044	0.052	0.041
1.4	0.044	0.050	0.033	0.032	0.044	0.034	0.038	0.031	0.030	0.030	0.047	0.051	0.037	0.051	0.045	0.055	0.051	0.053	0.044	0.053	0.040
1.5	0.045	0.047	0.033	0.028	0.043	0.033	0.034	0.028	0.030	0.030	0.048	0.050	0.037	0.050	0.046	0.055	0.050	0.053	0.043	0.051	0.041
1.6	0.043	0.048	0.032	0.030	0.046	0.033	0.038	0.029	0.031	0.028	0.047	0.049	0.038	0.048	0.045	0.055	0.051	0.054	0.045	0.051	0.041
1.7	0.043	0.050	0.036	0.032	0.044	0.032	0.037	0.030	0.032	0.031	0.048	0.052	0.037	0.047	0.046	0.055	0.050	0.053	0.044	0.050	0.040
1.8	0.043	0.047	0.032	0.029	0.042	0.030	0.037	0.032	0.030	0.029	0.049	0.051	0.037	0.051	0.047	0.055	0.051	0.052	0.045	0.051	0.041
1.9	0.046	0.054	0.034	0.033	0.045	0.035	0.037	0.028	0.029	0.029	0.049	0.049	0.036	0.051	0.044	0.055	0.051	0.053	0.044	0.051	0.040
2	0.046	0.046	0.032	0.030	0.044	0.033	0.038	0.031	0.030	0.031	0.048	0.050	0.037	0.048	0.046	0.054	0.051	0.053	0.043	0.052	0.040

Table C - 5: Area under first 20% length of prediction curve for MPP-LS-P1-Basic-2005-R50 (longitudinal failures).

a	Year																				
	1995	**1996**	**1997**	**1998**	**1999**	**2000**	**2001**	**2002**	**2003**	**2004**	**2005**	**2006**	**2007**	**2008**	**2009**	**2010**	**2011**	**2012**	**2013**	**2014**	**2015**
0.1	0.048	0.035	0.037	0.025	0.040	0.031	0.033	0.029	0.031	0.027	0.039	0.046	0.030	0.049	0.041	0.044	0.045	0.037	0.034	0.044	0.037
0.2	0.045	0.046	0.032	0.029	0.040	0.031	0.035	0.027	0.032	0.028	0.039	0.044	0.031	0.047	0.041	0.045	0.048	0.038	0.035	0.043	0.037
0.3	0.044	0.046	0.032	0.028	0.041	0.031	0.035	0.029	0.030	0.029	0.040	0.044	0.033	0.047	0.037	0.043	0.046	0.034	0.034	0.044	0.035
0.4	0.043	0.047	0.034	0.028	0.043	0.030	0.037	0.030	0.029	0.027	0.037	0.045	0.033	0.049	0.040	0.046	0.046	0.037	0.034	0.044	0.038
0.5	0.048	0.044	0.034	0.028	0.041	0.032	0.034	0.029	0.029	0.028	0.037	0.043	0.029	0.045	0.041	0.044	0.046	0.037	0.034	0.044	0.034
0.6	0.044	0.046	0.036	0.028	0.039	0.032	0.036	0.032	0.029	0.027	0.036	0.045	0.029	0.045	0.040	0.046	0.045	0.036	0.033	0.044	0.034
0.7	0.045	0.041	0.036	0.028	0.039	0.033	0.032	0.027	0.028	0.028	0.038	0.043	0.030	0.048	0.039	0.045	0.045	0.036	0.034	0.043	0.036
0.8	0.047	0.045	0.036	0.030	0.041	0.030	0.035	0.029	0.029	0.029	0.036	0.045	0.032	0.050	0.040	0.045	0.048	0.037	0.034	0.045	0.037
0.9	0.044	0.045	0.034	0.027	0.040	0.032	0.034	0.028	0.029	0.026	0.037	0.046	0.031	0.047	0.040	0.046	0.046	0.035	0.034	0.042	0.036
1	0.045	0.049	0.033	0.026	0.041	0.030	0.034	0.029	0.027	0.027	0.037	0.043	0.032	0.047	0.041	0.048	0.046	0.036	0.034	0.044	0.036
1.1	0.046	0.048	0.033	0.025	0.040	0.030	0.036	0.027	0.029	0.029	0.041	0.047	0.027	0.050	0.041	0.046	0.045	0.038	0.034	0.044	0.038
1.2	0.043	0.050	0.034	0.031	0.039	0.031	0.034	0.029	0.029	0.026	0.037	0.044	0.031	0.048	0.040	0.045	0.045	0.035	0.035	0.045	0.037
1.3	0.042	0.045	0.034	0.031	0.040	0.032	0.035	0.030	0.028	0.031	0.036	0.045	0.030	0.046	0.040	0.043	0.046	0.038	0.035	0.044	0.037
1.4	0.046	0.049	0.033	0.027	0.039	0.032	0.035	0.028	0.029	0.028	0.039	0.046	0.028	0.046	0.037	0.046	0.048	0.039	0.033	0.044	0.035
1.5	0.046	0.050	0.032	0.027	0.043	0.028	0.035	0.029	0.031	0.030	0.039	0.045	0.032	0.046	0.041	0.045	0.046	0.036	0.032	0.045	0.036
1.6	0.044	0.048	0.033	0.028	0.041	0.031	0.031	0.029	0.026	0.029	0.038	0.045	0.031	0.048	0.037	0.043	0.044	0.035	0.034	0.043	0.036
1.7	0.048	0.051	0.034	0.028	0.037	0.032	0.033	0.027	0.030	0.027	0.038	0.046	0.029	0.046	0.039	0.045	0.044	0.034	0.033	0.043	0.036
1.8	0.043	0.044	0.033	0.029	0.040	0.031	0.036	0.028	0.028	0.029	0.035	0.046	0.035	0.049	0.041	0.047	0.047	0.036	0.032	0.045	0.038
1.9	0.048	0.044	0.035	0.028	0.039	0.031	0.035	0.030	0.027	0.028	0.040	0.044	0.031	0.046	0.038	0.044	0.046	0.036	0.033	0.043	0.036
2	0.046	0.040	0.035	0.030	0.039	0.031	0.033	0.028	0.026	0.030	0.036	0.044	0.030	0.048	0.040	0.044	0.047	0.035	0.031	0.044	0.038

Table C - 6: Area under first 20% length of prediction curve for MPP-LS-P2-Basic-2005-R50 (longitudinal failures).

a	Year																				
	1995	1996	1997	1998	1999	2000	2001	2002	2003	2004	2005	2006	2007	2008	2009	2010	2011	2012	2013	2014	2015
0.1	0.043	0.055	0.035	0.028	0.042	0.035	0.036	0.032	0.030	0.032	0.049	0.049	0.034	0.047	0.042	0.049	0.048	0.042	0.035	0.043	0.035
0.2	0.045	0.052	0.033	0.029	0.043	0.035	0.035	0.031	0.032	0.029	0.048	0.051	0.033	0.047	0.041	0.049	0.050	0.043	0.037	0.044	0.035
0.3	0.044	0.050	0.034	0.029	0.044	0.033	0.039	0.031	0.032	0.031	0.052	0.051	0.032	0.048	0.041	0.050	0.048	0.042	0.036	0.044	0.036
0.4	0.045	0.046	0.035	0.030	0.043	0.034	0.038	0.030	0.033	0.032	0.048	0.049	0.036	0.048	0.040	0.051	0.048	0.043	0.036	0.044	0.035
0.5	0.044	0.049	0.034	0.031	0.045	0.035	0.038	0.030	0.032	0.030	0.049	0.050	0.033	0.045	0.040	0.050	0.048	0.043	0.036	0.044	0.035
0.6	0.046	0.051	0.033	0.029	0.044	0.035	0.037	0.027	0.032	0.031	0.050	0.048	0.034	0.048	0.041	0.049	0.049	0.044	0.036	0.045	0.036
0.7	0.046	0.054	0.034	0.031	0.045	0.036	0.038	0.030	0.031	0.028	0.049	0.051	0.033	0.047	0.042	0.050	0.047	0.044	0.035	0.043	0.036
0.8	0.044	0.052	0.034	0.028	0.042	0.036	0.039	0.030	0.030	0.030	0.050	0.049	0.035	0.048	0.042	0.049	0.048	0.044	0.036	0.043	0.036
0.9	0.045	0.048	0.032	0.030	0.043	0.034	0.035	0.031	0.031	0.028	0.048	0.051	0.033	0.048	0.041	0.053	0.048	0.043	0.036	0.043	0.034
1	0.046	0.052	0.033	0.029	0.043	0.035	0.035	0.030	0.032	0.031	0.048	0.048	0.034	0.049	0.042	0.048	0.049	0.043	0.037	0.043	0.035
1.1	0.044	0.053	0.035	0.026	0.044	0.033	0.037	0.029	0.030	0.029	0.049	0.049	0.034	0.048	0.042	0.050	0.050	0.042	0.036	0.042	0.034
1.2	0.044	0.053	0.034	0.027	0.044	0.032	0.036	0.031	0.031	0.030	0.048	0.051	0.034	0.048	0.039	0.051	0.048	0.043	0.036	0.044	0.035
1.3	0.046	0.053	0.034	0.027	0.045	0.034	0.038	0.029	0.029	0.030	0.048	0.047	0.034	0.048	0.040	0.050	0.049	0.041	0.037	0.043	0.036
1.4	0.045	0.048	0.035	0.030	0.043	0.035	0.036	0.032	0.029	0.028	0.049	0.048	0.033	0.046	0.042	0.051	0.048	0.043	0.036	0.045	0.035
1.5	0.049	0.057	0.033	0.031	0.043	0.035	0.040	0.029	0.031	0.032	0.046	0.049	0.035	0.048	0.043	0.050	0.050	0.043	0.038	0.044	0.036
1.6	0.047	0.047	0.034	0.028	0.041	0.034	0.037	0.033	0.029	0.030	0.049	0.050	0.032	0.048	0.042	0.050	0.050	0.040	0.037	0.042	0.035
1.7	0.044	0.055	0.031	0.027	0.042	0.036	0.036	0.031	0.031	0.030	0.049	0.049	0.033	0.049	0.041	0.052	0.050	0.043	0.038	0.044	0.036
1.8	0.044	0.051	0.035	0.024	0.042	0.035	0.037	0.031	0.029	0.031	0.049	0.051	0.034	0.048	0.042	0.051	0.048	0.043	0.039	0.043	0.035
1.9	0.048	0.057	0.034	0.028	0.045	0.034	0.035	0.033	0.030	0.030	0.047	0.048	0.035	0.047	0.041	0.050	0.048	0.043	0.036	0.044	0.037
2	0.043	0.055	0.033	0.031	0.040	0.035	0.037	0.031	0.030	0.029	0.047	0.049	0.034	0.050	0.039	0.051	0.048	0.042	0.035	0.042	0.036

Table C - 7: RMSE for MPP models (broken back failures) with a range of decay factors and radius of influence.

a	MPP-BB-P1-Basic				MPP-BB-P2-Basic				MPP-BB-P1-Sr				MPP-BB-P2-Sr			
	TrainYr=2011		TrainYr=2009		TrainYr=2011		TrainYr=2009		TrainYr=2011		TrainYr=2009		TrainYr=2011		TrainYr=2009	
	R100	R50	R100	R50	R100	R50	R100	R50	R100	R50	R100	R50	R100	R50	R100	R50
0.1	1360.7	1341.7	1347.9	1334.1	1477.3	1458.4	1481.4	1462.2	3288.7	3286.8	3215.0	3216.8	3426.0	3425.2	3368.6	3367.5
0.2	1287.8	1288.2	1293.2	1291.3	1407.1	1404.5	1421.3	1419.3	3261.7	3260.5	3193.3	3194.0	3399.3	3399.8	3345.1	3345.5
0.3	1270.8	1272.3	1279.1	1280.6	1385.2	1384.7	1404.5	1403.4	3252.7	3254.8	3188.6	3187.7	3391.2	3391.8	3339.4	3339.4
0.4	1263.7	1259.2	1272.3	1273.9	1379.6	1377.7	1403.0	1401.0	3249.1	3249.3	3184.8	3185.3	3389.1	3387.9	3334.5	3336.6
0.5	1255.7	1254.9	1269.6	1265.6	1375.8	1375.3	1394.7	1393.5	3248.1	3248.0	3182.4	3184.3	3386.1	3387.2	3332.1	3335.0
0.6	1255.2	1255.2	1266.3	1267.1	1371.3	1368.3	1394.6	1395.3	3248.3	3245.5	3181.4	3181.5	3385.2	3383.9	3332.3	3333.8
0.7	1249.1	1252.9	1263.3	1263.8	1366.1	1367.2	1392.2	1388.7	3245.0	3243.9	3181.0	3181.4	3383.0	3384.3	3331.6	3334.0
0.8	1249.2	1250.8	1263.9	1265.5	1367.5	1364.9	1390.4	1390.2	3244.9	3242.9	3179.5	3178.9	3382.9	3381.3	3330.0	3330.3
0.9	1249.5	1250.4	1263.7	1261.5	1362.5	1364.8	1385.5	1385.8	3241.8	3241.2	3178.8	3177.5	3381.4	3380.5	3329.8	3331.7
1	1247.5	1247.0	1260.3	1263.4	1362.7	1359.6	1384.5	1384.0	3242.7	3243.5	3177.6	3177.4	3380.0	3380.4	3329.2	3328.2
1.1	1245.8	1244.9	1259.5	1259.6	1360.1	1366.0	1387.2	1386.4	3241.5	3242.4	3177.6	3176.8	3380.5	3380.8	3330.4	3329.1
1.2	1247.2	1245.3	1257.1	1259.6	1361.7	1360.4	1387.6	1390.0	3241.7	3241.0	3178.0	3179.0	3381.2	3379.4	3330.2	3329.0
1.3	1245.6	1242.7	1261.1	1257.4	1360.9	1364.9	1384.1	1383.4	3241.6	3242.4	3179.6	3177.3	3380.0	3380.1	3330.3	3329.4
1.4	1244.8	1246.5	1262.4	1261.8	1357.4	1359.9	1384.3	1388.5	3242.7	3242.2	3178.1	3175.4	3381.0	3379.0	3328.0	3327.9
1.5	1241.9	1246.2	1256.3	1257.3	1360.8	1359.8	1387.8	1381.3	3241.3	3241.7	3176.6	3178.1	3380.5	3377.6	3329.5	3329.1
1.6	1243.8	1246.5	1256.4	1262.8	1356.7	1357.6	1385.3	1384.6	3240.5	3241.0	3177.0	3178.0	3378.2	3379.4	3327.8	3328.0
1.7	1242.4	1244.2	1259.0	1260.4	1359.4	1358.1	1384.6	1382.2	3241.5	3241.0	3177.0	3177.5	3378.8	3377.5	3326.2	3326.0
1.8	1242.1	1245.1	1257.6	1258.5	1360.7	1355.0	1382.7	1379.4	3241.6	3239.7	3177.1	3176.1	3378.1	3380.6	3327.1	3328.1
1.9	1244.8	1246.5	1255.9	1258.3	1357.0	1358.7	1382.4	1382.6	3240.0	3240.0	3175.6	3177.3	3378.9	3377.8	3328.5	3327.3
2	1242.1	1245.0	1255.9	1261.8	1356.7	1358.2	1385.3	1383.0	3241.2	3242.1	3177.6	3176.7	3377.6	3378.0	3325.7	3329.8

Table C - 8: MAE for MPP models (broken back failures) with a range of decay factors and radius of influence.

a	MPP-BB-P1-Basic				MPP-BB-P2-Basic				MPP-BB-P1-Sr				MPP-BB-P2-Sr			
	TrainYr=2011		TrainYr=2009		TrainYr=2011		TrainYr=2009		TrainYr=2011		TrainYr=2009		TrainYr=2011		TrainYr=2009	
	R100	R50	R100	R50	R100	R50	R100	R50	R100	R50	R100	R50	R100	R50	R100	R50
0.1	881.1	866.5	841.4	832.4	953.2	937.8	938.5	924.3	1978.1	1977.5	1901.0	1902.5	2063.0	2062.9	1990.4	1989.5
0.2	835.9	836.1	812.7	812.1	907.8	906.2	893.1	892.5	1943.0	1942.4	1874.0	1874.0	2027.1	2027.5	1959.2	1959.9
0.3	824.5	826.7	804.5	805.7	893.2	891.9	879.4	878.3	1929.9	1931.1	1866.8	1866.7	2015.5	2015.4	1952.0	1952.3
0.4	819.9	816.1	799.7	800.9	887.5	886.5	875.7	874.0	1924.9	1924.5	1862.1	1862.8	2010.5	2009.4	1946.5	1947.2
0.5	814.6	814.2	798.2	795.6	884.5	884.8	870.9	871.1	1921.0	1920.9	1859.6	1860.5	2006.3	2006.9	1943.5	1945.0
0.6	814.5	812.9	796.1	796.1	881.6	881.0	872.6	873.7	1921.2	1919.0	1857.5	1857.9	2003.9	2003.0	1942.1	1943.3
0.7	810.1	810.9	794.3	794.7	878.4	878.7	872.7	871.4	1919.3	1918.4	1857.8	1857.4	2002.9	2003.3	1941.7	1943.2
0.8	809.3	809.9	794.2	794.7	878.1	877.3	872.7	872.5	1918.4	1917.1	1855.7	1856.0	2002.2	2001.5	1940.0	1939.8
0.9	809.8	810.0	793.3	792.4	875.8	876.7	870.7	870.9	1915.7	1914.7	1856.3	1854.9	2000.4	1999.8	1939.8	1940.8
1	808.2	807.6	792.0	794.3	875.3	873.3	870.5	870.3	1915.9	1916.0	1853.5	1853.9	2000.2	1999.3	1938.7	1938.1
1.1	807.0	806.5	792.0	791.7	874.2	876.3	872.5	871.7	1915.5	1915.6	1854.3	1852.6	2000.1	2000.6	1939.5	1937.9
1.2	807.4	807.1	790.7	792.0	874.2	872.6	873.5	874.4	1914.4	1914.1	1854.3	1854.2	1999.6	1999.7	1938.8	1937.9
1.3	805.9	804.4	792.9	789.9	873.2	875.7	871.3	871.0	1914.6	1915.0	1854.4	1853.6	1999.0	1998.0	1938.0	1938.7
1.4	806.2	806.9	793.3	792.5	871.3	872.1	871.5	873.9	1914.5	1914.5	1853.0	1851.4	1999.3	1997.1	1937.2	1937.4
1.5	803.7	806.0	789.9	789.9	874.0	872.8	873.7	870.9	1913.5	1914.0	1852.9	1853.4	1998.6	1997.0	1938.2	1937.0
1.6	805.3	806.5	789.6	793.0	871.1	871.6	873.4	872.2	1912.6	1913.5	1852.5	1852.7	1997.5	1997.7	1936.2	1935.8
1.7	804.3	804.9	790.4	791.5	872.9	871.6	872.9	871.7	1913.2	1913.6	1851.8	1852.4	1997.5	1996.3	1935.4	1936.0
1.8	804.1	806.4	789.8	790.9	873.2	870.5	872.0	870.7	1912.8	1912.5	1852.1	1851.2	1996.0	1998.2	1935.7	1936.6
1.9	805.9	806.3	789.8	791.0	870.9	872.1	871.9	871.1	1911.6	1911.7	1851.0	1852.4	1997.0	1996.2	1936.4	1936.1
2	804.1	806.1	789.6	792.7	870.9	872.1	873.9	871.6	1912.2	1912.9	1852.0	1851.8	1994.8	1996.4	1934.8	1937.2